The University Of Sheffield.

Identification of Novel Targets to Augment Temozolomide Potency in Glioblastoma

Natasha Carmell

Academic Unit of Molecular Oncology

Department of Oncology and Metabolism

University of Sheffield

Thesis submitted to the University of Sheffield for the degree of Doctor of Philosophy

December 2018

Declaration

I confirm that I shall abide by the University of Sheffield's regulations on plagiarism and that all work submitted shall be my own unless otherwise stated. Where used, material gathered from other sources will be clearly cited in the text and permission to use figures has been requested when required.

Acknowledgements

I would like to say a very big thank you to my supervisor, Spencer, who has guided, encouraged and supported me throughout these 3 years.

Katie - thank you for listening to me and answering my million and one questions, you really are the best and I will miss you.

Thank you to everyone in the Collis, Bryant and Thompson labs for making my past 3 years so fun! Especially to Clair, Charlotte and Caroline who were always available for chats and cakes, to Luke who made the best gym and drinking pal, to Emma who loves Harry Potter as much as I do, to Callum who made me laugh so much, to David for his sparkling wit, to Ola for the all the advice, teas and coffees and to Tom for his great music taste. A big thank you must also go to Connor, not only for his hard work, but all the laughs along the way!

The support from all my friends and family has definitely made my PhD possible. In particular, I would like to say thank you my parents Tina and Michael, my sister Charlotte and my boyfriend Adam. You have all been so encouraging and supportive and I couldn't have done this without you.

Finally, thank you to both The University of Sheffield and Brain Tumour Research and Support across Yorkshire for funding my PhD and allowing me this amazing opportunity.

Abstract

Brain tumours kill more children and adults under 40 than any other cancer. Approximately half of primary brain tumours are high-grade malignancies called glioblastoma multiforme (GBM). The current treatment regime for GBM combines de-bulking surgery with radiotherapy and the chemotherapeutic temozolomide. However, mean survival for patients is approximately 15 months, with less than 5% achieving 5 year survival. Unfortunately, this devastating prognosis has improved little over the last 40 years, highlighting the need for new strategies to improve the treatment of these tumours.

To identify potential novel drug targets that could augment the cytotoxicity potency of temozolomide, a dual approach was taken in temozolomide resistant T98G GBM cells; a kinome-wide siRNA screen and two small molecule repurposing drug screens. Cell viability was calculated by high-content microscopy and algorithm-based scoring of Hoechst-positive cells. Target validation studies were carried out using additional siRNA libraries and small-molecule compound dose-escalation studies in additional GBM cell lines and primary glioma stem-like cultures.

These screens identified the targeting of Extracellular Regulated Kinase 5 (ERK5) or Fibroblast Growth Factor Receptor 4 (FGFR4), as well as the use of butamben to augment temozolomide sensitivity. We also find that ERK5 is upregulated (mRNA and protein) in GBM compared to normal brain tissue, offering a potential therapeutic window for tumour specificity.

Furthermore, the combination of EKR5 inhibition and temozolomide caused an increase in DNA damage combined with a reduction in homologous recombination and an increase in non-homologous end joining, likely to be potentiated through mitotic progression, inducing chromosomal aberrations and heightened cell death.

These exciting data provide a platform for further pre-clinical and clinical investigation into these strategies as a means to improve the treatment options for GBM patients.

Oral Presentations

Novel drug targets to augment temozolomide sensitivity in high-grade brain tumours. **Carmell N**, McGarrity-Cottrell C, Myers KN, Brown S, Collis SJ. British Neuro-oncology Society Annual Meeting, Winchester UK, July 2018.

Poster Presentations

Identification of new therapeutic targets for high-grade brain tumours. **Carmell N**, McGarrity-Cottrell C, Myers KN, Brown S, El-Khamisy S, Collis SJ. University of Sheffield Medical School Annual Research Meeting, Sheffield UK, June 2017.

Identification of new therapeutic targets for brain tumours. **Carmell N**, Brown S, El-Khamisy S, Collis SJ. University of Sheffield Medical School Annual Research Meeting, Sheffield UK, June 2016.

Publications

The relationship of CDK18 expression in breast cancer to clinicopathological parameters and therapeutic response. Barone G, Arora A, Ganesh A, Abdel-Fatah T, Moseley P, Ali R, Chan SY, Savva C, Schiavone K, **Carmell N**, Myers KN, Rakha EA, Madhusudan S, Collis SJ. Oncotarget, June 2018.

CIP2A- and SETBP1-mediated PP2A inhibition reveals AKT S473 phosphorylation to be a new biomarker in AML. Lucas CM, Scott LJ, **Carmell N**, Holcroft AK, Hills RK, Burnett AK, Clark RE. Blood Advances, May 2018.

High CIP2A levels correlate with an anti-apoptotic phenotype that can be overcome by targeting BCL-XL in chronic myeloid leukaemia. Lucas CM, Milani M, Butterworth M, **Carmell N**, Scott LJ, Clark RE, Cohen GM, Varadarajan S. Leukemia, June 2016.

Abbreviations

α-KG	α-ketoglutarate
µg	Microgram
µl	Microlitre
µM	Micromolar
ɣH2AX	ɣH2A Histone Family Member X
2-HG	R(-)-2-hydroxyglutarate
3D	3 Dimensional
5-ALA	5-Aminolevulinic Acid
5-FU	5-Fluoruracil
53BP1	53 Binding Protein 1
ABC	Avidin Biotin Complex
ALK	Anaplastic Lymphoma Receptor Tyrosine Kinase
ALPK2	Alpha Kinase 2
ALPK3	Alpha Kinase 3
AML	Acute Myeloid Leukaemia
ANOVA	Analysis of Variance
APS	Ammonium Persulphate
ARTEMIS	DNA Cross-Link Repair 1C
ATCC	American Type Culture Collection
ATM	Ataxia Telangiectasia Mutated
ATP	Adenosine Triphosphate
ATR	Ataxia Telangiectasia And Rad3-Related Protein
ATRX	Alpha Thalassemia/Mental Retardation Syndrome X-Linked
BBB	Blood Brain Barrier
BCL-xl	B-cell Lymphoma-extra large
BiCNU	Carmustine
BDNF	Brain Derived Neurotrophic Factor
BCR-Abl	Breakpoint Cluster Region Abelson Leukaemia Virus
BRCA1/2	Breast And Ovarian Cancer Susceptibility Protein 1/2
BSA	Bovine Serum Albumin
BTSC	Brain Tumour Stem Cells
CALM3	Calmodulin 3
CAM2KB	Calcium/Calmodulin Dependent Protein Kinase II Beta
CaV	Voltage Gated Calcium Channel
CCNU	Lomustine
CD	Common Docking Domain
CD #	Cluster of Differentiation #
CD133	Promin 1
CDK4/6	Cyclin Dependent Kinase 4/6
CDKL3	Cyclin Dependent Kinase Like 3
CDKN2A/B	Cyclin Dependent Kinase Inhibitor 2A/B
cDNA	Complementary DNA

CED	Convection Enhanced Delivery
CHK1/2	Checkpoint Kinase 1/2
c-MET	Proto Oncogene Hepatocyte Growth Factor Receptor
CML	Chronic Myeloid Leukaemia
CNS	Central Nervous System
CO_2	Carbon Dioxide
CSC	Cancer Stem Cell
CSF	Cerebrospinal Fluid
Ct	Cycle threshold
CT	Computerised Tomography
CTLA4	Cytotoxic T-Lymphocyte Associated Protein 4
CXCR4	Chemokine Receptor Type 4
CYP3A4	Cytochrome P450 Family 3 Subfamily A Member 4
DAB	3,3'-Diaminobenzidine
DAPI	4',6-diamidino-2-phenylindole
DCLK1	Doublecortin Like Kinase 1
ddH_2O	Double Distilled Water
DDR	DNA Damage Response
DF1	DharmaFECT 1
DGKB	Diacylglycerol Kinase Beta
DHT	Dihydrotestosterone
DMEM	Dulbecco's Modified Eagle Medium
DMPK	Dystrophia Myotonica Protein Kinase
DMSO	Dimethyl Sulfoxide
DNA	Deoxyribonucleic Acid
DNA-PK	DNA-dependent Protein Kinase
DNA-PKcs	DNA-dependent Protein Kinase Catalytic Subunit
dNTP	Deoxyribonucleotide Triphosphate
D-Pen	D-Penicillamine
DSB	Double Strand Break
dT	Deoxythymidine
DTT	Dithiothreitol
DYRK1A	Dual Specificity Tyrosine Phosphorylation Regulated Kinase 1A
E+T	ERK5-in-1 + temozolomide
ECL	Enhanced Chemiluminescence
EDTA	Ethylenediaminetetraacetic acid
EGF	Epidermal Growth Factor
EGFR	Epidermal Growth Factor Receptor
EMT	Epithelial Mesenchymal Transition
ERK	Extracellular-Signal-Regulated Kinase
ERK5i	ERK5-in-1
FA	Fanconi Anaemia
FAAP24	FA Core Complex Associated Protein 24

FACS	Fluorescence-Activated Cell Sorting
FANC	Fanconi Anaemia Complementation Group
Fc	Fragment crystallisation Region
FCS	Foetal Calf Serum
FDA	Food and Drug Administration
FES	Feline Sarcoma Oncogene
FGF	Fibroblast Growth Factor
FGFR	Fibroblast Growth Factor Receptor
FITC	Fluorescein isothiocyanate
FLT3	FMS-like Tyrosine Kinase 3
FOXM1	Forkhead Box Protein M1
FRS2α	Fibroblast Growth Factor Receptor Substrate 2 α
g	Gram
G	Gravity
GABRA1	Gamma-Aminobutyric Acid Type A Receptor Alpha1 Subunit
GAPDH	Glyceraldehyde-3-Phosphate Dehydrogenase
GBM	Glioblastoma Multiforme
G-CIMP	Glioma CpG Island Methylator Phenotype
GRK6	G Protein-Coupled Receptor Kinase 6
GSC	Glioma Stem Cells
Gy	Gray
H3-K27M	Histone 3 Lysine 27 Methionine
HCC	Hepatocellular Carcinoma
HCl	Hydrochloric Acid
HER2	Human Epidermal Growth Factor Receptor 2
HGFR	Hepatocyte Growth Factor Receptor (MET)
HR	Homologous Recombination
HRP	Horseradish Peroxidase
hTERT	human Terlomerase Reverse Transcriptase
IC_{50}	Inhibitor Concentration 50
IDH-1	Isocitrate Dehydrogenase (NADP(+))1
IF	Immunofluorescence
IgG	Immunoglobulin G
IHC	Immunohistochemistry
IL	Interleukin
iMRI	Intraoperative MRI
IPPK	Inositol-Pentakisphosphate 2-Kinase
IR	Irradiation
ITH	Intratumoural Heterogeneity
JNK	JUN N-Terminal Kinase
kDa	Kilodaltons
Ku70/80	Ku heterodimer
L	Litre
LD_{10}	Lethal Dose causing 10% cell death

M	Molar
mAB	Monoclonal Antibody
MAPK	Mitogen Activated Protein Kinase
MAPKK/MEK	Mitogen Activated Protein Kinase Kinase
MAPKKK/MEKK	Mitogen Activated Protein Kinase Kinase Kinase
MDC1	Mediator Of DNA Damage Checkpoint 1
MDM2/4	Mouse Double Minute Homolog 2/4
MEF	Myocyte Enhancer Factor
MFH (FOXC2)	Forkhead Box C2
mg	Milligram
$MgCl_2$	Magnesium Chloride
MGMT	O-6 Methylguanine DNA Methyltransferase
miRNA	micro RNA
ml	Mililitre
MLH1	DNA Mismatch Repair Protein MLH1
mM	Millimolar
MMR	Mismatch Repair
MN i	Micronuclei
mRNA	messenger RNA
MRE11A	Meiotic Recombination 11 Homolog 1
MRI	Magnetic Resonance Imaging
MSH2/3/6	NA Mismatch Repair Protein MSH2/3/6
MTH1	0-2,-5-diphenyltetrazolium bromide)
MTIC	3-methyl-(triazen-1-yl)imidazole-4-carboxamide
MTT	3-(4,5-dimethylthiazol-2-yl
MYC	Myelocytomatosis Viral Oncogene
NaCl	Sodium Chloride
NaOH	Sodium Hydroxide
NADPH	Nicotinamide Adenine Dinucleotide Phosphate
NaV	Voltage Gated Sodium Channel
NBS1	Nibrin
NEFL1	Neurofilament Light
NEK4	NIMA Related Kinase 4
nl	Nanolitre
NLK	Nemo Like Kinase
NES	Nuclear Export Signal
NF1	Neurofibromatosis type 1
NGF	Nerve Growth Factor
NHEJ	Non-Homologous End Joining
NHS	National Health Service
NICE	National Institute for Health and Care Excellence
NLS	Nuclear Localisation Signal
nM	Nanomolar
nm	Nanometre

Noc	Nocodazole
NOD	Non-Obese Diabetic
NSCLC	Non Small Cell Lung Cancer
O6BG	O-6-Benzylguanine
O6MeG	O-6-Methylguanine
OD	Optical Density
OLIG2	Oligodendrocyte Transcription Factor 2
OTP	ON-TARGETplus
PABL2	Partner And Localizer Of BRCA2
PARP-1	Poly(ADP-ribose) Polymerase 1
PARP-2	Poly(ADP-ribose) Polymerase 2
PBS	Phosphate Buffered Saline
PBS-T	PBS-Tween
PD-1	Programmed Cell Death 1
PDGF	Platelet Derived Growth Factor
PDGFRα	Platelet Derived Growth Factor Receptor A
PE	Plating Efficiency
PFA	Paraformaldehyde
PFS	Progression Free Survival
PGK1	Phosphoglycerate Kinase 1
PI	Propidium Iodide
PI3K	Phosphatidylinositol-4,5-Bisphosphate 3-Kinase
PI4KA	Phosphatidylinositol 4-Kinase Alpha
PIK3CA	Phosphatidylinositol-4,5-Bisphosphate 3-Kinase Catalytic Subunit Alpha
PIK3R1	Phosphoinositide-3-Kinase Regulatory Subunit 1
PKB/AKT	Protein Kinase B
PLCɣ	Phospholipase Cɣ
PMS1/2	Postmeiotic Segregation Increased 1/2
PNCK	Pregnancy Up-Regulated Nonubiquitous CaM Kinase
PNS	Peripheral Nervous System
PP	Pyrvinium Pamoate
PR	Proline Rich
PRC2	Polycomb Repressive Complex 2
PRKAG1	Protein Kinase AMP-Activated Non-Catalytic Subunit Gamma 1
PRKAR1A	Protein Kinase CAMP-Dependent Type I Regulatory Subunit Alpha
PRKAR2B	Protein Kinase CAMP-Dependent Type II Regulatory Subunit Beta
PRKC2	Calcium-independent Protein Kinase C2
PRKCSH	Protein Kinase C Substrate 80K-H
PRKDC	Protein Kinase DNA-activated Catalytic Peptide
PTN	Pleiotrophin
PTEN	Phosphatase and Tensin Homolog
RAD50	RAD50 Double Strand Break Repair Protein
RAD51	RAD51 Recombinase
RAS	Rat Sarcome Proto-oncogene

Rb	Retinoblastoma 1
ReDo	Repurposing Drugs in Oncology
REMBRANT	Repository for Molecular Brain Neoplasia Data
RMS	Rhabdomyosarcoma
RNA	Ribonucleic Acid
RNAi	RNA Interference
RNase	Ribonuclease
ROS1	Proto-Oncogene Tyrosine-Protein Kinase ROS
Rosc	Roscivitine
RPM	Revolutions per minute
RTase	Reverse Transcriptase
qRT-PCR	Quantitative Real Time-Polymerase Chain Reaction
SAP-1	Serum Response Factor Accessory Protein 1
SCE	Sister Chromatid Exchange
SCID	Severe Combined Immunodeficiency Disease
SCYL3	SCY1 Like Pseudokinase 3
SD	Standard Deviation
SDS	Sodium Dodecyl Sulfate
SEM	Standard Error of the Mean
SF	Survival Fraction
SFM	Serum Free Media
siRNA	small interfering RNA
SOX2	Sex Determining Region Y-Box 2
STAT	Signal Transducer And Activator Of Transcription
STAT3	Signal Transducer And Activator Of Transcription 3
STK3	Serine/Threonine Kinase 3
STK16	Serine/Threonine Kinase 16
TACC	Transforming Acidic Coiled-Coil
TBS	Tris Buffered Saline
TBS-T	TBS-Tween
TCGA	The Cancer Genome Atlas
TDP1	Tyrosyl-DNA Phosphodiesterase 1
TGFβ	Transforming Growth Factor β
TP53	Tumour Protein P53
TMA	Tissue Microarray
TMZ	Temozolomide
TTF	Tumour Treating Fields
TWF2	Twinfilin Actin Binding Protein 2
UBE3B	Ubiquitin Protein Ligase E3B
UNG	Uracil DNA Glycosylase
UV	Ultraviolet
V	Volts
VEGF	Vascular Endothelial Growth Factor
VEGF-A	Vascular Endothelial Growth Factor-A

WHO	World Health Organisation
WNT	Wingless
XLF	Non-Homologous End Joining Factor 1
XRCC4	X-Ray Repair Cross Complementing 4
XRCC5	X-Ray Repair Cross Complementing 5 (Ku70)
XRCC6	X-Ray Repair Cross Complementing 6 (Ku80)

Table of Contents

Chapter 1 – Introduction

1.1 Cancer

Between 2013 and 2015 in the UK, almost 990 people were diagnosed with cancer each day and in 2016 cancer was classified as one of the top ten leading causes of death by the World Health Organisation (CancerResearchUK, 2011b, WorldHealthOrganisation, 2018b). In 2018, more than 9 million people were diagnosed with either lung, breast, colorectal, prostate, skin or stomach cancer, the most common types of cancer throughout the world (WorldHealthOrganisation, 2018a). Although cancer treatment and survival has improved vastly, with an average of 50% of all cancer patients surviving 10 years or more, there is a need for research into and identification of novel treatments that can deliver improved treatment for currently difficult to treat and incurable tumours (CancerResearchUK, 2015).

Cancer is an extremely diverse disease, however, the development of all cancers is thought to be initiated through the progressive accumulation of mutations in DNA, conferring a selective survival advantage over normal cells, inevitably causing the death of the patient if left untreated (NationalCancerInstitute, 2015). Mutations which confer the progression and growth of cancer are termed 'driver' mutations, with the exact number of such mutations differing between cancer types, as reflected by a recent study across 29 cancer types showing up to 10 mutations, 4 on average, are required to cause and sustain cancer (Martincorena et al., 2017). Driver mutations are commonly associated with tumour suppressor genes, proto-oncogenes and DNA repair genes.

Tumour suppressor genes are also known as anti-oncogenes and their role is to limit cell proliferation whereas proto-oncogenes regulate normal cell proliferation. Loss of tumour suppressor genes and gain of function in proto-oncogenes, termed oncogenes following oncogenic mutations, leads to uncontrolled cell proliferation. Examples of tumour suppressor genes are TP53 and Rb and examples of oncogenes are HER2, hTERT, MYC and RAS. However, some genes can be both proto-oncogenes and tumour suppressors, for example NOTCH which is proto-oncogenic in acute lymphoblastic leukaemia but acts as a tumour suppressor in skin cells, with loss of function resulting in spontaneous basal cell tumours in mice (Grabher et al., 2006, Nicolas et al., 2003).

DNA repair genes, such as BRCA1/2 and MGMT, maintain genomic integrity and mutations in these genes causes deficiencies in DNA damage repair leading to genetic instability and mutagenesis. These mutations may confer a selective growth advantage, driving uncontrolled cell proliferation (Stratton et al., 2009). As tumour cells proliferate the number of mutations in their DNA accumulates which

not only results in different genetic mutations in tumours between patients but also different mutations within one tumour, termed intratumoural heterogeneity (ITH) (De Grassi et al., 2010). This accumulation of mutations in oncogenic cells is called the mutator phenotype, and was first hypothesised in 1974 when the increase in DNA mutations in cancer cells compared to normal cells was connected to tumorigenesis (Loeb et al., 1974). Originally, defective DNA polymerases were thought to cause the mutator phenotype, however, mutations in DNA damage genes were later included. For example, mutations in the nucleotide excision repair pathway, such as those present in xeroderma pigmentosum, increases the risk of UV-induced skin cancer up to 10,000 times (Bradford et al., 2011, Loeb, 2016). In hyperplasic pre-cancerous cells, the DNA damage response (DDR) has been shown to be activated, detected by markers such as ɣH2AX, CHK2, 53BP1 and ATM. This dysregulation of the DDR is thought to promote proliferation, replication stress, genome instability and carcinogenesis (Bartkova et al., 2005, Gorgoulis et al., 2005).

The number of mutations within one tumour can be anywhere from around 500 in acute myeloid leukaemia (AML) and up to 100,000 in GBM, with the majority being single-nucleotide substitutions, also called single-nucleotide polymorphisms (SNPs), of which transitions from GC to AT account for more than 60% of the mutations (Loeb, 2016). SNPs can be found within exons, introns, promoter regions and also untranslated regions (UTRs), however, SNPs found in genes encoding factors with important functions within cellular metabolism and immunity, DNA mismatch repair and cell cycle progression can result in a genetic predisposition to cancer (Deng et al., 2017). Although SNPs can increase the risk of cancer, there are around 5 million which can be found throughout the human genome, and most do not affect the expression and/or function of genes (The Genomes Project et al., 2015).

Mutations within DNA can be caused by exogenous sources, such as carcinogenic chemicals, as investigated in 1918 following the identification of epidemic scrotal cancer in chimney sweeps where coal tar, containing the yet to be identified carcinogen benzopyrene, was used to induce cancer in the ears of rabbits (Loeb and Harris, 2008). Other exogenous sources such as ionising radiation, viruses and chemicals, as well as endogenous sources such as oxidative damage which occur as a result of normal metabolism, and errors in DNA replication also cause mutations in DNA (Bartkova et al., 2005, Gorgoulis et al., 2005, Mandal et al., 2011).

The accumulation of driver mutations results in the formation of cancers which all share ten established ‘hallmarks’, irrespective of their diverse complexities (Hanahan and Weinberg, 2011). The first six hallmarks included sustaining proliferative signalling, evading growth suppressors, resisting programmed cell death, enabling replicative immortality, inducing angiogenesis and activating tissue invasion and metastasis (Hanahan and Weinberg, 2000). The additional hallmarks

included downregulation of cellular energetics and avoiding immune destruction, as well the inclusion of two hallmarks, tumour promoting inflammation and genome instability, which facilitate the accumulation of other hallmarks as cancer progresses (Hanahan and Weinberg, 2011). The importance of these hallmarks has been highlighted by the development of therapeutic approaches which target each trait, for example, telomerase inhibitors to reduce replicative immortality and VEGF inhibitors to reduce angiogenesis (Hanahan and Weinberg, 2011).

1.2 DNA Damage Response

Each day, the human genome is subject to thousands of DNA lesions which can cause errors in DNA replication and if these errors are not repaired, deleterious aberrations which can effect cell viability and subsequent progeny (Jackson and Bartek, 2009). These lesions are identified and repaired by the DNA damage response (DDR), which is comprised of individual enzymes through to complex pathways, all designed to promote the repair of any lesions which could potentiate mutations, thereby ensuring the preservation of genomic integrity (Pagès and Fuchs, 2002, Rouse and Jackson, 2002).

In cancer cells, DDR pathways are often dysregulated which results in continuous genomic instability and the accumulation of mutations contributing to the progression and malignancy of the tumours e.g. mutator phenotype. In order to survive and replicate in such a highly mutagenic background, tumours can be influenced by their tumour microenvironment (TME), as seen in colorectal cancer where deficiencies in the DDR pathway mismatch repair (MMR), which subsequently effect patient survival and response to treatment, are altered in response to the microbiome surrounding the tumour (Hale et al., 2018, Nik-Zainal, 2019).

In order to continue replicating with such a high mutational load, tumours can also become dependent on certain features, such as loss of checkpoint regulation, high dependence on oncogenes, or over reliance on DDR pathways that can still be functional even within their highly mutagenic background (Nik-Zainal, 2019). These dependencies can be selectively targeted, leaving normal, healthy cells relatively unaffected by such treatments. As molecular targeting acts in a more specific manner than traditional radiotherapy and chemotherapy treatments, normal tissue toxicity is reduced and patients are able to tolerate the reduced side effects (Ke and Shen, 2017). A successful example of molecular targeting of oncogenes can be seen in chronic myeloid leukaemia (CML), where imatinib is effective at treating 95% of patients (Roskoski Jr., 2003). The fusion gene *BCR-Abl,* which is responsible for the malignancy of the disease, is inhibited by imatinib and subsequently patients

achieve remission with undetectable levels of *BCR-Abl* (de Klein et al., 1982, Roskoski Jr., 2003).

1.3 Brain Cancer

In the UK, brain cancer kills around 5,000 people every year, reducing life expectancy by 20 years (Burnet et al., 2005), and in 2014, brain cancer was classified as a cancer of unmet need by Cancer Research UK. On average 50% of all patients diagnosed with cancer will achieve at least a 10 year survival, however, for patients with brain cancer, 10 year survival is only achieved by 13.5% (CancerResearchUK, 2011a, CancerResearchUK, 2011b).

Tumours of the nervous system include both central (CNS) and peripheral nervous systems (PNS) tumours, with brain tumours arising within the CNS. Most nervous system tumours are derived from non-neural glial cells which support and protect nerve cells (figure 1.1). This is most likely due to the ability of glial cells to grow and divide in a developed and mature nervous system, unlike nerve cells which are largely non-proliferative. Glial derived tumours are called gliomas and include astrocytomas, oligoastrocytomas and oligodendrogliomas (Zhu and Parada, 2002).

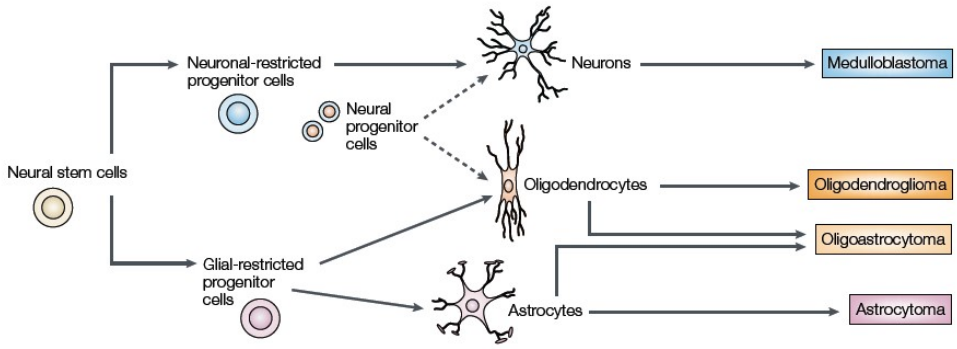

Figure 1.1: CNS Tumour Origins
Neural stem cells are believed to produce two progenitor cells: glial-restricted progenitor cells and neuronal-restricted progenitor cells. Astrocytes and oligodendrocytes are derived from glial-restricted progenitors and neurons from neuronal-restricted cells. However, there has been evidence supporting an alternative theory, whereby oligodendrocytes and motor neuron cells are derived from the same neuronal progenitor cells (Lu et al., 2002). Glial tumours of the CNS are defined by the cell from which they arise; astrocytes form astrocytomas, oligodendrocytes form oligodendrogliomas and both cell types form oligoastrocytomas. There are also CNS tumours which are formed from neural cells, such as medulloblastoma, however these generally present in children.

Figure adapted with permission from (Zhu and Parada, 2002)
License number: 4463600514905

Interestingly, there appears to be a link between immune system activity and the risk of gliomas. An increase in IgE levels, as seen with allergic disorders such as asthma, and cytomegalovirus titre are both associated with a decreased glioma risk (Bondy et al., 2008, Linos et al., 2007, Weller et al., 2015). Infection has also been associated with a decreased risk of glioma, however, conflicting reports highlight the uncertainty of this association (Weller et al., 2015). Post-operative infection has also been investigated in relation to survival in high-grade glioma patients across several studies; however, conclusive evidence showing any survival benefit has not yet been found (De Bonis et al., 2011).

Along with alterations in the immune system, genetic and epigenetic mutations have also been studied in relation to gliomas. Genome-wide analysis has enabled the identification of genetic and epigenetic changes which are found in certain types of gliomas, not only improving tumour classification, but also improving prediction of patient survival and response to treatment, all of which will positively impact the future of clinical trials and the personalisation of medicine (Reifenberger et al., 2017). These alterations are now part of the World Health Organisation (WHO) integrated diagnostic classification of gliomas, where gliomas are scored from grade I through to IV based on malignancy determined by both histopathology and the newly identified diagnostic biomarkers (Reifenberger et al., 2017, Zhu and Parada, 2002) (figure 1.2).

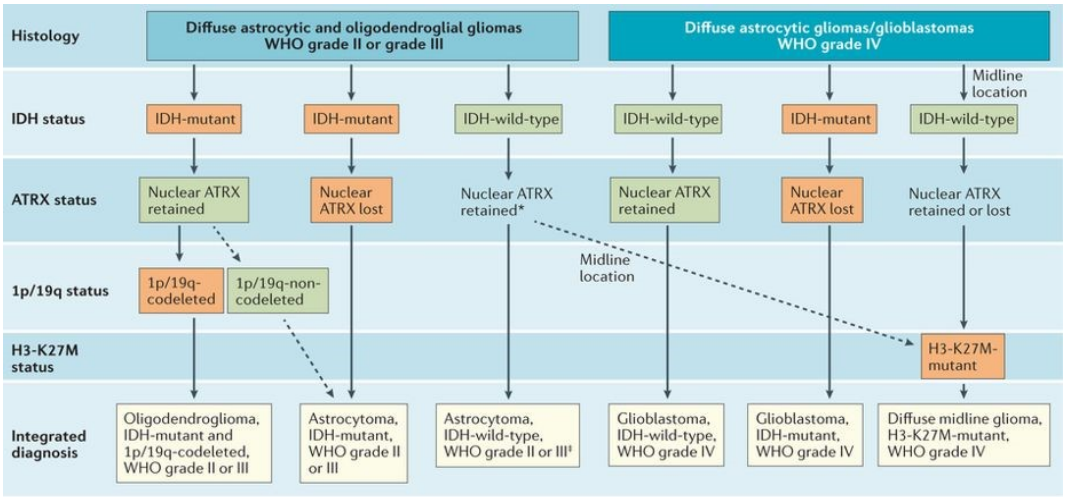

Figure 1.2: Integrated Diagnosis (Histology and Molecular Diagnostics) for WHO Grade II, III and IV Gliomas

Histological examination determines tumour type (astrocytomas, oligodendrogliaomas, glioblastomas) and grade (I - IV) which correlates with malignancy, however, molecular biomarkers have proven to be more accurate predictors of clinical outcome. IDH status, ATRX status, 1p/19q status and H3-K27M status can all be investigated in the process of classifying a tumour.

Figure copied with permission from (Reifenberger et al., 2017)
License number: 4463631369520

The biomarkers which were included by WHO as part of the integrated diagnosis pathway for gliomas include: IDH mutations, 1p/19q co-deletion and H3F3A or H3-K27M mutations, however, the biological role of some of the biomarkers, such as 1p/19q co-deletion, is not yet evident (Reifenberger et al., 2017). There are other biomarkers which may be included as requisites in future, such as ATRX loss, TERT promoter mutations and BRAF fusions/mutations (Reifenberger et al., 2017).

IDH mutant glial tumours which also have 1p/19q co-deletion and morphology similar to oligodendrocytes are predicted to have the best patient survival, with IDH mutant tumours which do not have a 1p/19q co-deletion and are astrocytic in morphology are predicted to have the next best patient survival and finally IDH wild-type tumours, found in higher grade gliomas, have the worst predicted patient survival (Weller et al., 2015). IDH mutations are important predictors of survival as these tumours are more susceptible to oxidative stress due to changes in metabolism, improving patient response to treatment, however, mutant IDH alone cannot initiate the development of gliomas (Reitman and Yan, 2010, Sasaki et al., 2012). ATRX and TP53 mutations or 1p/19q co-deletion and TERT promoter mutations are also required for the formation of astrocytomas and oligodendrogliomas respectively (Reitman and Yan, 2010). Various other genetic aberrations will also accumulate before grade II or III astrocytomas can progress in to grade IV GBMs (Reifenberger et al., 2017) (see 1.3.1).

Of all the CNS tumours which occur in adults, astrocytomas are the most common and account for around 60% of all primary brain tumours (Adamson et al., 2009). Glioblastoma multiforme (GBM), the most common glioma, is a highly malignant grade IV astrocytoma, which is characterised by disease reoccurrence and resistance to treatment (Zhu and Parada, 2002).

1.4 Glioblastoma Multiforme

GBM, the most common high-grade glioma, accounts for around half of all primary adult brain tumours (Adamson et al., 2009, Kleihues et al., 2000). GBM tumours are extremely aggressive and fast growing, with around 95% of GBM tumours arising prior to detection of a lesser grade tumour (Ohgaki and Kleihues, 2013). GBM tumours that have progressed from a less malignant astrocytoma (grade II or III) have better patient prognosis due to differences in the genetic profiles (Ohgaki and Kleihues, 2013).

Between 2007 and 2011, almost 11,000 people were diagnosed with GBM in England, with a median survival of just over 6 months and 5 year survival achieved by only 3.4% (Brodbelt et al., 2015). Currently, the most aggressive treatment for

GBM is de-bulking surgery followed by radiotherapy and chemotherapy in the form of temozolomide (TMZ) (Stupp et al., 2009). The heterogeneity and complexity of the disease biology combined with rapid treatment resistance needs to be further investigated and understood in order to improve treatment regimes and consequently patient survival.

1.4.1 Genetic Aberrations in Glioblastoma

The number of mutations within one tumour varies across tissue types, ranging from around 500 in acute myeloid leukaemia (AML) up to more than 100,000 in GBM (Loeb, 2016). In order to begin to understand this complex, highly mutated disease, The Cancer Genome Atlas (TCGA) piloted a GBM study in 2008 investigating aberrations in DNA and mRNA of 206 GBM patients (CancerGenomeAtlasResearchNetwork, 2008). This investigation was built upon and in 2013 more than 500 GBM tumours were analysed, identifying somatic mutations and transformed pathways (Brennan et al., 2013).

Around 5 to 10% of GBM cases are secondary tumours, arising from a less malignant, lower grade astrocytoma (grade II or III) (Ohgaki and Kleihues, 2013). IDH mutations are associated with the development of low grade gliomas and are often found in combination with mutations in TP53, a tumour suppressor, and ATPX, involved in gene regulation via chromatin remodelling and also telomere maintenance (Reifenberger et al., 2017). Every IDH mutant tumour has a mutation in IDH1 at amino acid 132, where arginine is replaced by histidine (R132H) (Cohen et al., 2013). IDH mutations enable cells to convert α-ketoglutarate (αKG) to R(-)-2-hydroxyglutarate (2-HG) instead of NADPH (Cohen et al., 2013). This leads to abnormal methylation of DNA and histones and eventually the formation of CpG islands, also known as the glioma CpG island methylator phenotype (G-CIMP) and the reduced NADPH production increases the susceptibility of these tumours to oxidative stress, improving patient response to treatment (Reitman and Yan, 2010). To progress to a grade IV GBM, there are various aberrations that occur; CDKN2A and CDKN2B loss (cell cycle regulation) and 19q loss. Other mutations found in IDH mutant GBM tumours include activation of the MYC and RAS/PI3K pathway (survival and proliferation), FOXM1 (cell cycle progression) and E2F2 (transcription factor controlling cell cycle progression and tumour suppressors), as well as silencing of PRC2 (chromatin modifications) (Reifenberger et al., 2017). The outlook for patients with secondary mutant IDH GBM is better than that of those with primary GBM, with a median survival of 31 months (Ohgaki and Kleihues, 2013). This is due to several factors including prevalence of mutant IDH GBM tumours in younger adults (20-50 years) and a higher proportion of MGMT promoter

methylation (90% compared to 40%) (Reifenberger et al., 2017). This renders the tumours more sensitive to the cytotoxic effects of the mainstay chemotherapeutic alkylating agent temozolomide.

GBM IDH wild type (WT) tumours also have associated genomic aberrations including: PTEN mutations or deletions (tumour suppressor), CDKN2A and CDKN2B loss, TERT promoter mutations (telomere maintenance), gain of chromosome 7, loss of chromosome 10 and amplification in EGFR (growth, survival, and proliferation). There are also several mutations, which are less prevalent, including those in the tumour suppressor TP53 and several proteins involved in survival and proliferation e.g. PIK3CA, PIK3R1 and NF1. There are also some less common amplifications including: MDM2 and MDM4 which are inhibitors of TP53 activity and CDK4 and CDK6 which regulate cell cycle progression. Receptor amplification is also seen in a subset of IDH WT tumours and includes PDGFRα and HGFR, which both have roles in cell survival and proliferation (Reifenberger et al., 2017) and amplification in EGFR is found in around 50% of all GBM cases diagnosed. Around half of the EGFR mutations which occur have a deletion of exons 2 to 7 and this generates the EGFR variant III (EGFRvIII), a constitutively active receptor which has no ligand binding domain (Aldape et al., 2015). EGFR mutations have been shown to be insignificant in determining overall survival (Hartmann et al., 2013). A combination of EGFR amplification, combined with two of the following 3 mutations: TERT promoter, gain of chromosome 7 or loss of chromosome 10 is sufficient to diagnose a IDH WT GBM tumour (Stichel et al., 2018).

1.4.2 Molecular Classification of Glioblastoma Subtypes

As well as investigating genomic aberrations, gene expression data has been used to subtype GBM tumours based on dominant gene expression or mutations. TP53, RB1 and receptor tyrosine kinases have previously been identified as being mutated in a high proportion of GBM tumours and have therefore been implicated in the development of GBM, however, further investigation into molecular classification has identified four sub-groups: proneural, neural, classical and mesenchymal (figure 1.3) (CancerGenomeAtlasResearchNetwork, 2008, Verhaak et al., 2010).

Of the 4 subtypes, the proneural group was found to have the best survival due to the presence of IDH mutations and a lower overall age at diagnosis, encompassing secondary GBMs which progress from lesser grade astrocytomas. Proneural GBM subtypes were also shown to have amplification of PDGFRA and neural stem cell genes such as SOX2. Neural subtypes were found to express nerve associated genes such as NEFL1 and GABRA1. Classical subtypes had chromosome7 amplification and chromosome 10 loss combined with high levels of EGFR

amplification, and although TP53 is the most commonly mutated gene in GBM, this mutation was not found in the classical subtype. Mesenchymal subtypes had a significant increase in NF1 deletions, as well as PTEN co-mutations (Verhaak et al., 2010). The subtyping of GBMs will likely be important therapeutically as different subgroups may require different targeted approaches in order to treat patients effectively and maximise their chance of survival.

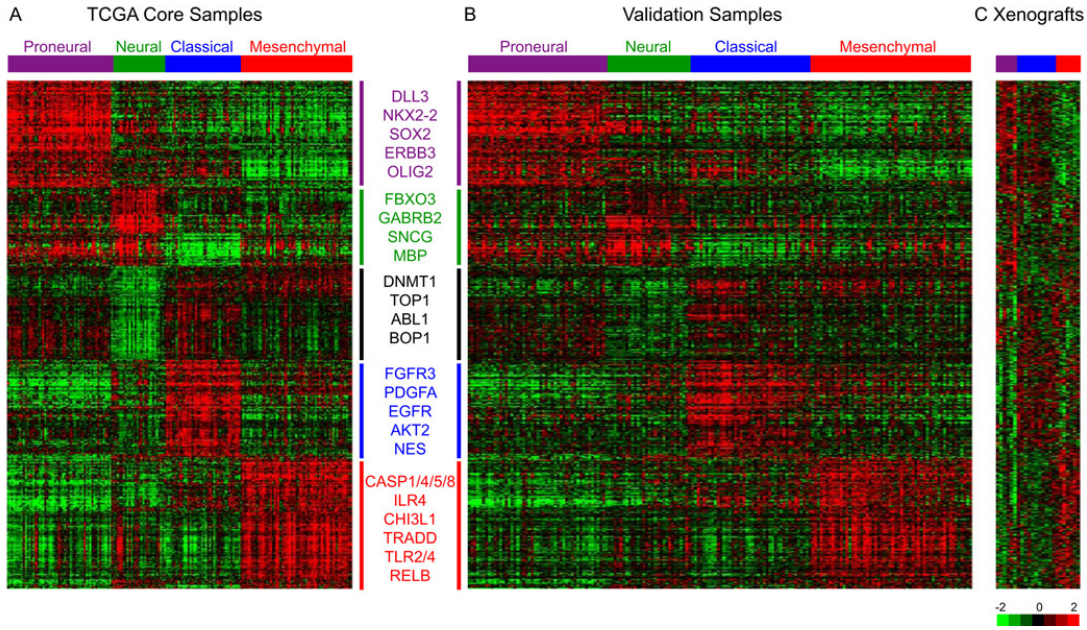

Figure 1.3: Molecular Classification of Glioblastoma Subtypes
Gene expression from 200 GBM tumours and 2 normal brain samples were analysed across 3 platforms, with 840 genes identifying 4 sub-groups of GBM: proneural, neural, classical and mesenchymal. This molecular selection data was then validated using publicly available data sets (A and B) and glioblastoma xenografts established from patient specimens implanted after surgery (C). Validation showed GBM subtyping to be reproducible across the three datasets.

Figure adapted with permission from (Verhaak et al., 2010)
License number: 4464810890816

1.5 Multimodal Treatment of GBM

1.5.1 De-bulking Surgery

The standard treatment for GBM involves de-bulking surgery to remove the majority of the malignant tumour, followed by radiotherapy and concomitant and adjuvant chemotherapy, in the majority of cases this is the DNA alkylating agent temozolomide. The importance of de-bulking surgery is reflected by a multivariate analysis study which showed removal of less than 98% of the tumour can significantly reduce survival from a median of 13 months to 8.8 months (Lacroix et al., 2001). However, tumour margins are extremely difficult to accurately identify

due the limited imaging techniques and the migratory nature of GBM cells which have been discovered up to 6cm away from CT imaged tumour margins. MRI is also unable to identify GBM tumour margins effectively with tumour cells identified 2.5cm away from the imaged boundaries (Price and Gillard, 2014). This inability to image the tumour margin accurately inhibits complete resection of the tumour, enabling the disease to recur. The extent of tumour removal that can be achieved by surgery is also highly influenced by the location of the tumour, as surgery could potentially cause damage to or removal of healthy brain tissue. For example, patients with frontally located tumours were found to have a longer median survival compared to those with tumours located elsewhere (101 weeks compared to 47 weeks) (Jeremic et al., 1994).

There have been various innovations in order to improve the outcome of surgical removal of brain tumours including the use of intraoperative MRI (iMRI) and 5-aminolevulvinic acid hydrochloride (5-ALA) which enables surgeons to identify tumour cells as they fluoresce (Kuhnt et al., 2011, Teixidor et al., 2016). However, even with these advances, GBM is a highly migratory and infiltrative disease making it still extremely difficult to remove all traces of the cancer cells without compromising eloquent brain tissue (Teixidor et al., 2016).

1.5.2 Radiotherapy

Treating GBM by postoperative radiotherapy has been the standard procedure for almost half a century, with a comparison study in 1980 expressing the efficacy of radiotherapy in prolonging survival post-surgery whilst also highlighting the need to 'continue the search for an effective chemotherapeutic' (Walker et al., 1980). Radiotherapy uses ionizing radiation in the form of high energy x-rays to cause DNA damage and eventually cell death within the precise tumour location. The central nervous system, however, is formed of tissues that are highly resistant to radiotherapy meaning a higher dose is often needed to cause cell death (Cassidy et al., 2015).

In the 1970s, 60Gy of whole brain radiotherapy was shown to increase survival by 2.3 times in GBM patients compared to ≤45Gy and is still the dose used today, however, now GBM patients receive 60Gy in once daily fractions of 2Gy for 30 days post-surgery (Gzell et al., 2017). Hyper-fractionated radiotherapy (60Gy over 30 days in more fractions i.e. twice daily) was shown to have adverse effects on GBM patient survival (Barani and Larson, 2015).

Intensity-modulated radiotherapy (IMRT) and volumetric-modulated arc therapy (VMAT) are the techniques used to treat GBM patients today. IMRT enables the x-

rays to be targeted more directly at the tumour resulting in less toxicity to the surrounding eloquent brain tissue but does rely heavily on MRI. There are few studies regarding VMAT in GBM, however, it is a dynamic radiotherapy which is able to specifically target the tumour giving a similar dose to IMRT but in a shorter period of time (Gzell et al., 2017).

Magnetic Resonance Linear Accelerators (MR Linac) are a relatively new technology, with the UK's first scan taking place in a healthy volunteer in November 2017. The MR Linac is able to 'precisely locate tumours, tailor the shape of X-ray beams in real time and accurately deliver doses of radiation to moving tumours', aiming to limit radiation damage to healthy tissues and maximise the dose to the tumour (TheRoyalMarsden, 2017). It will therefore be interesting to see if clinical implementation of these new and emerging imaging techniques will be bought into treatment of GBMs in the near future.

1.5.3 Chemotherapy

In 1987, a meta-analysis used randomised trial data to determine the effect of adjuvant nitrosoureas chemotherapy on GBM patient survival when compared to treatment with radiotherapy alone (Stenning et al., 1987). Nitrosoureas chemotherapeutics are drugs (e.g. carmustine and lomustine) which are able to cross the blood brain barrier and cause alkylation damage to both DNA and RNA (Schabel, 1976). Their findings showed a 9% increase in 1 year survival when patients were treated with both radiotherapy and adjuvant chemotherapy, however, due to the small data set their conclusions were tentative (Stenning et al., 1987). Published nearly two decades later, a larger meta-analysis which compared randomised trial data from 3004 patients found similar results; a modest 6% increase in one year survival (GMTGroup, 2002). Although the effects of nitrosoureas chemotherapy still remain unclear, implants in the form of carmustine (BiCNU) wafers are used by the NHS to treat GBM patients following de-bulking surgery, however, they are associated with increased complications and are therefore used infrequently (Bregy et al., 2013, NICE, 2007).

Synthesised in the 1980s, temozolomide is a cytotoxic alkylating agent which causes methylation of DNA, and is now used as an adjuvant and concomitant chemotherapeutic to treat GBM. When exposed to the slightly alkaline pH of the blood, temozolomide is metabolised to 3-methyl-(triazen-1-yl)imidazole-4-carboxamide (MTIC), which is further metabolised into a methyldiazonium ion. Methyldiazonium methylates DNA at several places, however, O-6-methylguanine is believed to be the most cytotoxic adduct yet only accounts for less than 8% of all lesions caused by temozolomide (Kaina et al., 2007, Newlands et al., 1997).

O-6-methylguanine adduct is directly repaired by the enzyme O-6-methylguanine DNA methyltransferase (MGMT) (Agarwala and Kirkwood, 2000, Newlands et al., 1997). MGMT repairs the damage by transferring the methyl group from O-6-methylguanine to itself, permanently inactivating the enzyme and leading to its degradation. If the level of methylation exceeds the level of MGMT enzyme and the damage cannot be repaired, O-6-methylguanine can be paired with dT (deoxythymidine) causing transition mutations from a GC pairing to O-6-methylG T pairing. The inability of the mismatch repair pathway (MMR) to repair the damage is potentially why this lesion is so cytotoxic. The transition mutation causes a futile cycle of base excision and base insertion which results in perpetual single strand breaks in DNA. Replication forks can stall when they reach these lesions and this may result in reduced replication rates or fork collapse and generation of DNA double strand breaks (continued under Associated DSB Repair Pathways) and subsequent apoptotic mechanisms are activated (figure 1.4). If cells have a deficient mismatch repair (MMR) pathway they can continue through the cell cycle with methylated DNA bases (Harris et al., 2015, Noonan et al., 2012). Translesion synthesis (TLS) polymerases can also be activated in order to bypass the O-6-methylguanine lesion, allowing the cell to tolerate the damage and continue DNA replication. However, this mechanism is less faithful in its replication abilities and can result in point mutations (Fu et al., 2012).

N-3-methyladenine and N-7-methylguanine are the most common DNA lesions caused by temozolomide treatment; however, these are readily repaired by the Base Excision Repair (BER) pathway and were initially believed to play no role in temozolomide resistance in GBM (see 1.7.2).

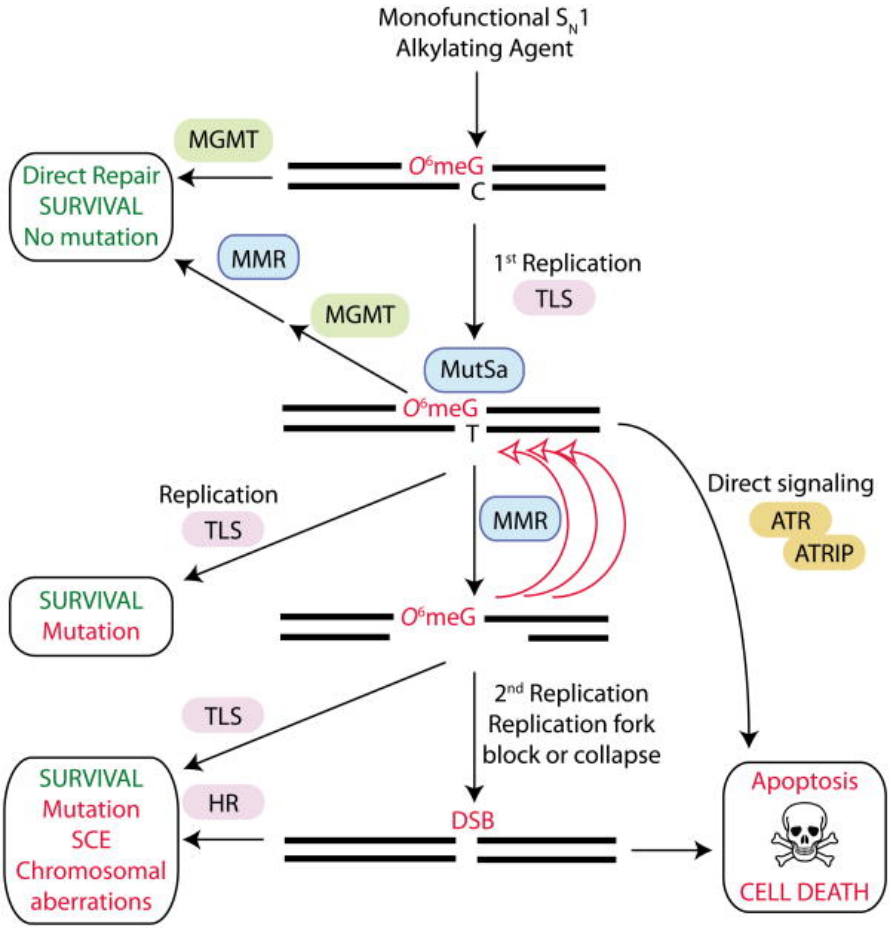

Figure 1.4: Processing of TMZ induced O-6-methylguanine Lesions
O-6-methylguanine is directly repaired by MGMT, however, if the level of methylation exceeds the level of MGMT enzyme, unrepaired O-6-methylguainine will be incorrectly paired with thymine and TLS polymerases can be activated to bypass this lesion enabling replication to continue. The incorrect base pairing is detected by the mismatch repair (MMR) pathway which recognises the damage, resulting in futile cycles of MMR causing single strand gaps or breaks in DNA. In the subsequent cycle of replication, replication fork collapse can cause double strand DNA breaks (DSB). DSBs can be repaired by HR or NHEJ; however, mutations can occur as a result of these pathways or alternatively apoptosis is induced. Initial detection of the O-6-methylguanine lesions can also immediately induce apoptosis by activation of ATR-ATRIP pathway.

Figure adapted with permission from: (Fu et al., 2012)
License number: 4474130220785

Before approval for treatment of GBM, promising preclinical data for temozolomide showed anti-tumour activity in mouse models of various cancers, an excellent oral bioavailability of 98%, rapid activation and the ability to infiltrate the blood brain barrier (BBB) (Newlands et al., 1997). Important data from a randomised trial were published in 2005, showing that treatment with both radiotherapy and adjuvant temozolomide for newly diagnosed GBM patients significantly increased survival by 2.5 months when compared to radiotherapy alone. An increase in 2 year survival of

GBM patients from 10.4% to 26.5% lead to temozolomide being NICE (National Institute of Health and Care Excellence) approved, and in 2007, patients diagnosed with primary brain tumours in the UK could receive this treatment (Arney, 2013, Stupp et al., 2005). A further study comparing survival of patients treated with radiotherapy combined with carmustine and those treated with adjuvant temozolomide showed the later treatment to be superior, with a higher median value of 15.9 months compared to 11.5 months (Vinjamuri et al., 2009). Both 1 and 2 year survival post diagnosis were also higher for patients treated with adjuvant temozolomide by 20% and 27% respectively. However, on average the patients treated with adjuvant carmustine had larger tumours and there was also no difference in progression free survival. This could mean temozolomide may not be more beneficial in halting disease progression but as it has a much lower toxicity than carmustine, it may be a better treatment choice (Vinjamuri et al., 2009).

The current treatment regime for newly diagnosed patients with GBM is de-bulking surgery followed by concomitant temozolomide (75mg/m^2 for 42 days) and radiotherapy (60Gy over 30 fractions) 4 weeks post-surgery. 4 weeks after concomitant temozolomide chemo-radiotherapy finishes, 6 28 day cycles of adjuvant temozolomide are given (100-200mg/m^2 on days 1-5 depending on haematological tolerance) (ClinicalTrials.gov, 2018).

1.5.4 Tumour Treating Fields

Tumour Treating Fields (TTF) are low intensity alternating current fields which disrupt tumour cell proliferation by acting as an anti-mitotic agent (Gzell et al., 2017). A randomised phase III trial between July 2009 and 2014 investigated the effect of TTF in combination with adjuvant temozolomide in almost 700 patients with GBM. In a report published at the end of 2017, median progression free survival was significantly improved by 2.7 months (6.7 months: 4.0 months TTF+TMZ: TMZ) and overall survival was also significantly improved by 4.9 months (20.9 months: 16.0 months TTF+TMZ: TMZ). Importantly, the combination of TTF with adjuvant temozolomide was tolerated well and there was no increase in adverse effects when compared to patients who received temozolomide only. However, the device must be worn on a shaved scalp for >18 hours every day, which of course could create issues for some patients and it is unfortunately not yet NICE approved so would cost a patient upwards of £18,000 per month (Stupp et al., 2017). Currently, NICE do not endorse the use of TTF for patients who have been newly diagnosed with GBM as ‘they are not an efficient use of NHS resources’ (NICE, 2018a).

1.5.5 Proton Beam Therapy

Proton bean therapy (PBT) utilises beams of protons which cause DNA damage via ionising radiation, however, PBT is a more accurate alternative to traditional x-ray radiotherapy (Jäkel, 2007). The energy of the protons can be adjusted in order to target tumours deeper within the body, making it preferable for harder to reach tumours such as those in the CNS, sarcomas and cancers of the head and neck (Frisch and Timmermann, 2017). Due to the limited side scatter of protons, normal tissue toxicity is also reduced which is desirable for paediatric patients as the irreversible side effects of traditional x-ray based radiotherapy are well established and include both physical and mental defects (Armstrong et al., 2010, Paulino et al., 2000). There is currently a phase II clinical trial recruiting newly diagnosed GBM patients in order to investigate whether there is any survival benefit for patients who receive PBT in combination with temozolomide to both IMRT and traditional radiotherapy, a trial which is now feasible in England due to the NHS commission of two PBT centres (ClinicalTrials.gov, 2018, NHSEngland).

1.6 Blood Brain Barrier

One key issue with treating GBM tumours is the blood brain barrier (BBB). The BBB is formed by endothelial tight junctions and it is vital in maintaining brain homeostasis. The protective role of the BBB makes it difficult for systemically delivered drugs to pass into the brain and target brain tumours (Ballabh et al., 2004). Unlike many drugs, temozolomide is lipophilic and has a relatively low molecular weight, meaning it is readily able to cross the BBB (Kelly et al., 2005). Aiming to improve drug delivery to the brain, drugs such as mannitol that cause a short term disruption of the BBB have been trialled; however, the results were not promising and there were many dangerous side effects including neurological toxicity (Siegal et al., 2000). Drug efflux transporters within the central nervous system also contribute to brain homeostasis, pumping nutrients into and toxins out of the brain. Inhibition of these transporters has been shown to increase the ability of a drug to pass into the brain without damaging the integrity of the BBB. However, little development has occurred following disappointing clinical trial results (Siegal et al., 2000, Van Tellingen et al., 2015).

Delivery of drugs directly into the brain is one way to overcome the BBB without the risks of BBB disruption, however, there are still many issues associated with methods of direct delivery. An intraventricular catheter, such as an Ommaya reservoir, allows drugs to be delivered directly into cerebral spinal fluid (CSF) which surrounds the entire CNS. As the drugs are delivered directly into the CSF, they are now contained within the CNS by the BBB and therefore will have reduced systemic

toxicity. Once the drugs are delivered, their ability to diffuse is ultimately affected by their size. Small molecules diffuse quickly resulting in a reduced drug concentration, conversely, large molecules have extremely poor diffusion abilities (less than 1 mm over 72 hours), both resulting in reduced treatment efficacy. To overcome the inability of large molecules to diffuse, convection-enhanced delivery (CED) stents have been developed to deliver drugs over a continuous pressure gradient allowing a more even distribution of drugs throughout the brain tissue (Zhou et al., 2012). The PRECISE trial, which compared the use of CED stents to deliver bacterial toxins to treatment with carmustine wafers, showed no difference in patient survival. However, this could be due to a variety of factors including drug efficacy and variation in stent positions (Kunwar et al., 2010).

Even if effective drug delivery into the brain could be achieved, it will not necessarily be able to effectively target GBM due to the recurrent and highly invasive nature of the tumour. The tumour blood brain barrier has been shown to be compromised in GBM tumours detectable on MRI scans, however, the more invasive tumour cells which are outside the compromised tumour blood brain barrier and are migrating into healthy brain tissue have an intact and effective barrier against drugs. These malignant cells would be able to evade exposure to drug treatments, continue to proliferate and cause recurrence of GBM (Van Tellingen et al., 2015).

1.7 Resistance to Treatment

1.7.1 MGMT Promoter Methylation and Mismatch Repair

Resistance to treatment is a characteristic of GBM tumours which leads to the recurrence of the tumour and consequently patient death. Treatment resistance is extremely complex; however, advances will need to be made in order to improve patient response and survival. Methylation of the MGMT promotor is one factor known to be beneficial for GBM patient survival as these tumours are sensitive to temozolomide chemotherapy.

Methylation downregulates MGMT expression meaning tumours with MGMT promoter methylation are more responsive to temozolomide treatment as O-6-methylguanine bases are left unrepaired, leading to futile MMR cycles and eventually apoptosis of the GBM tumour cells (figure 1.5) (Xie et al., 2016). This induction of apoptosis by temozolomide relies on a proficient MMR pathway (Hickman and Samson, 2004).

As MGMT is able to directly repair the toxic lesions caused by temozolomide, inhibitors of this enzyme have been tested in GBM clinical trials as potentiators of

temozolomide cytotoxicity. O-6-benzylguanine (O6-BG) irreversibly inhibits MGMT repair activity via the transfer of a benzyl group to the active site of MGMT (Konduri et al., 2009). In a phase I trial combining O6-BG with temozolomide, haematological toxicity, particularly myelosuppression, was a major limitation. The dose of O6-BG to inhibit MGMT activity for 48 hours and the maximum tolerated dose (MTD) of temozolomide in combination with O6-BG was established. The regime established from the phase I trial was as follows: 1 hour IV infusion of 120mg/m^2 O6-BG followed immediately by a 30mg/m^2 O6-BG infusion for 48 hours. Oral temozolomide, at a maximum tolerated dose of 472mg/m^2, was given within 60 minutes of completing the initial O6-BG infusion (Quinn et al., 2005). This regime was tested in a phase II clinical trial in patients with GBM and anaplastic gliomas (anaplastic astrocytoma and anaplastic oligodendrogliomas). Combination treatment was able to re-sensitise anaplastic gliomas to temozolomide, however, this was not seen in GBM cases. As haematological toxicity was an issue with the combination treatment, the temozolomide dose was reduced by 50% which may partially explain this lack of sensitivity observed in this trial (Quinn et al., 2009), however, even this reduced dose is above the 100-200mg/m^2 recommended as part of standardised care.

High grade brain tumours can also become resistant to temozolomide treatment very quickly, and almost 90% of patients with recurrent GBM have tumours that have a complete lack of response to a second cycle of temozolomide (Oliva et al., 2010). This is not due to a change in MGMT promotor methylation status, as when patients who are initially sensitive to temozolomide treatment (methylated MGMT promoter) become resistant; their methylation status remains unchanged (Felsberg et al., 2011, Maxwell et al., 2008). The constantly mutating and evolving tumour genome results in massive intratumoural heterogeneity (ITH) and consequently treatment failure and disease recurrence (Qazi et al., 2017).

Patients with mutations in the MMR pathways within their tumours have an increased resistance to temozolomide treatment. Their ineffective repair pathway and lack of MRR induced apoptosis means they have a tolerance for mismatched base pairs and lesions in DNA. This causes an increase in mutagenic properties resulting in many changes, including resistance to chemotherapy. Loss of MLH1 has been shown to confer temozolomide resistance in GBM cell lines and loss of MSH6 protein has been shown to be a driver in the development of GBM (Forsström et al., 2017, Stritzelberger et al., 2018). However, mutations in MMR pathway are not believed to be important in resistance to temozolomide treatment in GBM due to the minimal detection of microsatellite instability (MSI), a marker of MMR deficiency (Maxwell et al., 2008).

Cells can overcome depletion of MSH6 (a key MMR protein) by forming a dimerised MSH2-MSH3 complex (MUTSβ), enabling the MMR pathway to re-establish its repair activity (Maxwell et al., 2008). As MSH3 expression is less than that of MSH6, the formation of MUTSβ complexes reaches a saturation point resulting in limited MMR repair which may be insufficient to repair multiple mismatched bases, generating an increase in the number of somatic mutations (Marsischky et al., 1996, Maxwell et al., 2008). Interestingly, an increase in mRNA expression of MMR genes MSH6, MSH3, MSH6 and PMS1 was detected in GBM patients following treatment with temozolomide. The only patient who did not have a significant increase in MSH6 mRNA post temozolomide treatment survived the longest, suggesting an increase in MMR gene expression may play a role in temozolomide resistance (Sun et al., 2018). In addition to gliomas, high MSH6 expression has been correlated with worse survival in melanoma and osteosarcoma (Alvino et al., 2014, Jentzsch et al., 2014, Liang et al., 2017). This dysregulation of MMR proteins could possibly result in defective interaction between MMR proteins resulting in an incompetent DNA repair pathway, a tolerance for mismatched base pairs and lesions in DNA and an increase in the mutagenic potential of the tumour cell (Sun et al., 2018).

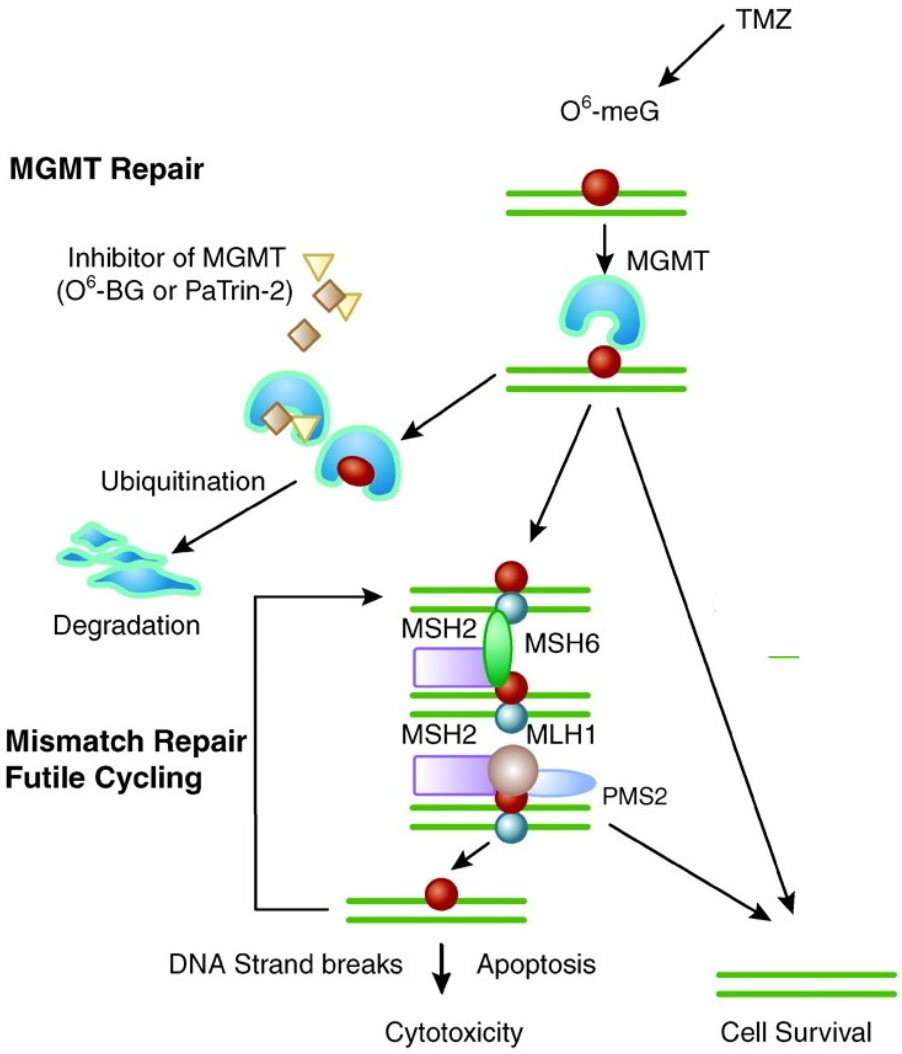

Figure 1.5: O-6-methylguanine Repair: MGMT and Mismatch Repair

O-6-methylguanine damage (red circle) is directly repaired by MGMT, which accepts the methyl group and is then ubiquitinated and degraded leaving the DNA repaired (A). This enzyme is inactivated and degraded in a similar mechanism by accepting a benzyl group from O-6-benzylguanine (O^6-BG) or PaTrin-2. However, if the level of methylation exceeds the level of MGMT enzyme, unrepaired O-6-methylguainine will be incorrectly paired with thymine (blue circle). This incorrect base pairing is detected by the mismatch repair (MMR) pathway which recognises the damage. This pathway begins with the dimerization of both MSH2 and MSH6 (MUTSα complex) and MLH1 and PMS2 (MUTLα complex) which recognise the mismatched pairing and go on to recruit the exonuclease EXO1 to remove the newly paired thymine on the daughter strand of DNA. The methylated base is then re-paired with thymine by DNA polymerase and Ligase I. This results in a futile cycle of MMR causing single strand gaps or breaks in DNA. In the subsequent cycle of replication, replication fork collapse can causing double strand DNA breaks (DSB) and eventually cell death (Liu and Gerson, 2006, Friedman et al., 2000). In order for a cell to undergo apoptosis as a result of O-6-methylguanine induced futile MMR cycling, the MUTSα complex must be present (Hickman and Samson, 2004).

Figure adapted with permission from (Liu and Gerson, 2006).
License number: 4465320276281

1.7.2 APNG and Base Excision Repair

Higher MGMT expression positively correlates with resistance to temozolomide chemotherapy; however, alkylpurine–DNA–N-glycosylase (APNG) has also been shown to play a role in in resistance to temozolomide in GBM patients, with high expression conferring poorer overall survival (Agnihotri et al., 2012).

APNG is a DNA repair protein which is part of the Base Excision Repair (BER) pathway which easily repairs the majority of lesions caused by temozolomide: N-3-methyladenine and N-7-methylguanine (Lee, 2016). shRNA depletion of APNG is able to sensitise previously resistant primary orthotopic xenograft GBM cells (which are heterogonous and express MGMT) to temozolomide. Temozolomide resistant T98G cells are also sensitised following APNG silencing by siRNA, with both depleted primary and immortalised GBM cells exhibiting reduced cell viability, increased DNA damage and apoptosis in response to temozolomide treatment (Agnihotri et al., 2012).

Inhibition of the BER pathway has therefore been targeted in order to attempt to sensitise resistant tumour cells to temozolomide. By using methoxyamine which binds to the abasic site inhibiting BER, tumour cells are sensitised to alkylation damage caused by temozolomide (Fishel et al., 2007, Taverna et al., 2001).

Interestingly, when APNG protein expression was investigated in MGMT positive GBM tumours from patients who received either radiotherapy or radiotherapy and temozolomide, those without detectable APNG protein had significantly improved overall survival. However, when patients who received only radiotherapy were selected, there was no difference in survival in relation to APNG expression (Agnihotri et al., 2012). However, a more recent study, which excluded healthy cells from the analysis, has shown high expression of APNG confers better survival in GBM patients (Fosmark et al., 2017). It is speculated that high APNG protein levels could cause dysregulation of the downstream BER pathway increasing the burden on the subsequent repair proteins, particularly on the rate limiting step including polymerase β, resulting in cytotoxic levels of 5'dRP and ultimately apoptosis (Fosmark et al., 2017, Trivedi et al., 2008).

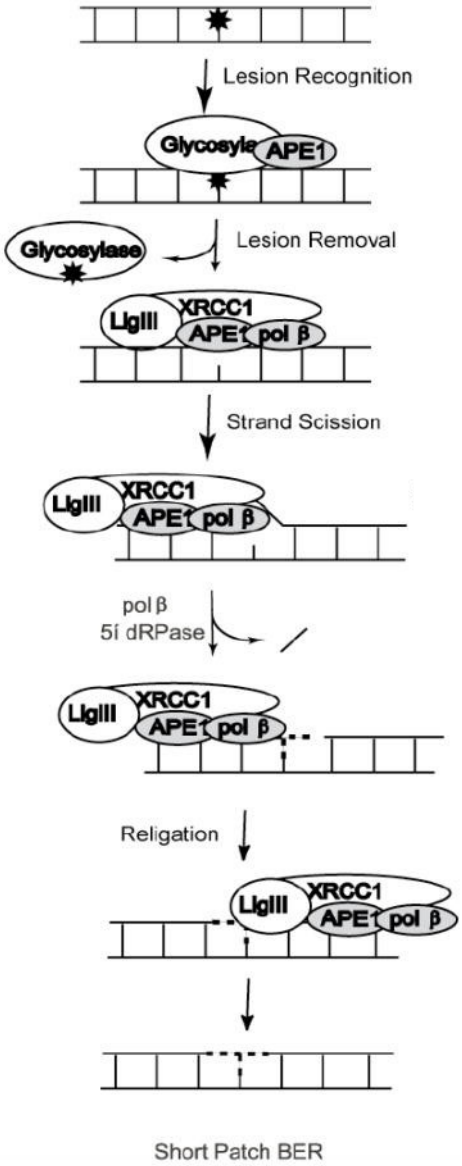

Figure 1.6: Short Patch Base Excision Repair

Short patch base excision repair (BER) pathway is the main DNA repair pathway involved in repairing lesions more commonly caused by temozolomide resulting in N-3-methyladenine and N-7-methylguanine. DNA glycosylase and AP endonuclease 1 (APE1) process the damaged DNA base, removing the lesion and creating a nick in the DNA. DNA polymerase β (polβ) identifies the single nucleotide gap in the DNA acting to remove 5' sugar phosphate and incorporating a single nucleotide into gap to the 3' end before recruiting XRCC1 and DNA ligase IIIα (LigIIIα) for the final ligation.

Figure adapted with permission from (Almeida and Sobol, 2007)
License number: 4473630988720

1.7.3 Associated DSB Repair Pathways: Homologous Recombination

Homologous recombination (HR) is a highly faithful repair mechanism for double strand breaks in DNA (DSB). HR uses the homologous sister chromatid to carry out repair of DSB breaks and can therefore only occur when a cell is in S-phase or G2-phase of the cell cycle (Branzei and Foiani, 2008). Although not used to directly repair lesions caused by temozolomide, HR may be employed to repair the DNA DSBs subsequently generated by replication cycles.

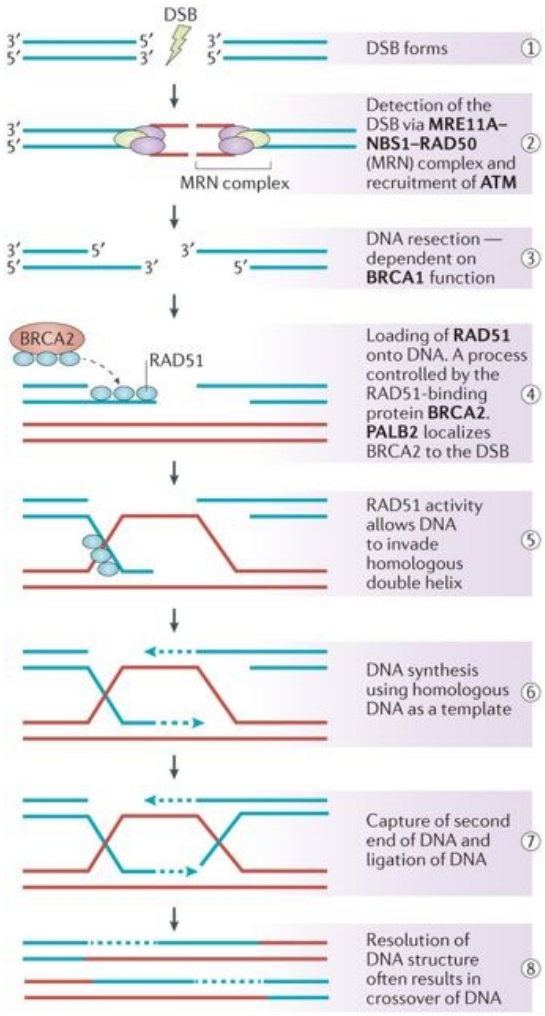

Figure 1.7: Homologous Recombination Repair

Homologous recombination (HR) pathway is involved in the repair of DNA damage causing stalled forked and DSBs. HR resolves the damage in a way that restores the DNA back to its original sequence. HR repairs damaged in a sequence of steps reliant on a many proteins, including tumour suppressors highlighted in bold. Following a DSB (1), a complex of MRE11-NBS1-RAD50 detects and binds to the break and recruits ATM, initiating repair (2). DNA is resected on the 5' ends of both strands, requiring BRCA1 activity (3). PALB2 recruits BRCA2 to the DSB, then BRCA2 sequesters RAD51 to the resected single strand DNA (4). RAD51 complexed to DNA invades homologous double strand DNA (red) (5). New DNA is synthesised using the homologous DNA as a guide, DNA polymerases to synthesis the nucleotides and the ssDNA as the primer (6). DNA is ligated and cleaved before the break is completely restored (7 & 8). Crossover of DNA into the homologous chromosome is a common occurrence.

Figure adapted from (Lord and Ashworth, 2016)
License number: 4554770634745

1.7.4 Associated DSB Repair Pathways: Non-homologous End Joining

Non-homologous End Joining (NHEJ) acts largely in G1-phase and is also involved in the repair of DSBs. Ku70 and Ku80 dimerise to form the Ku complex which recognises the DSB. NHEJ, although it will resolve the DSB, can result in the loss of genetic information and the breaks will be simply be ligated back together (Branzei and Foiani, 2008). Similarly to HR, NHEJ is not used to directly repair lesions caused by temozolomide but may be used to repair the DNA DSBs subsequently generated by replication cycles.

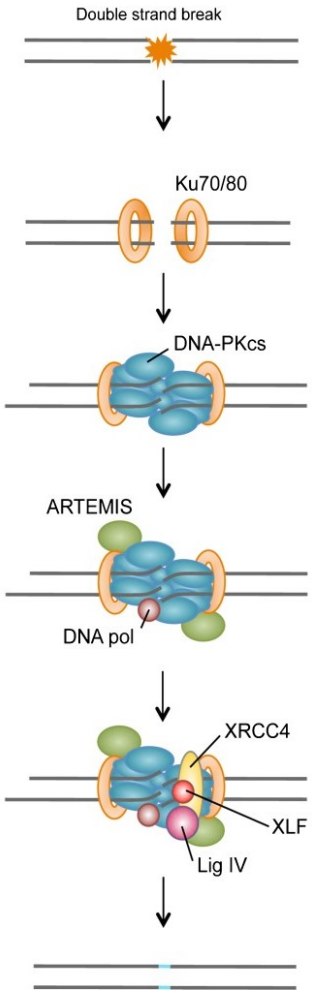

Figure 1.8: Non-homologous End Joining Repair

Non-homologous end joining (NHEJ) is another pathway involved in the repair of DSBs. NHEJ is much less faithful in its repair mechanism, simply ligating broken ends of DNA together which can result in loss of genetic material and translocations. The Ku complex of Ku70 and Ku80 recognises the DSB and recruits other NHEJ proteins. DNA-PKcs are recruited to the Ku heterodimer bound to DNA forming the DNA-PK complex. Active DNA-PK recruits NHEJ proteins such as ARTEMIS, DNA polymerase, XRCC4, XLF and DNA Ligase IV, as well as γH2AX a well-established marker of DSBs which also recruits further DSB repair proteins. Several cycles of additions and deletions of nucleotides can occur before NHEJ is complete.

Figure adapted with permission from (Brochier and Langley, 2013)
License number: 4466611036385

1.7.5 Heterogeneity, Tumour Microenvironment and Glioma Stem Cells

As previously mentioned, GBM tumours have been classified into 4 subtypes based on gene expression and mutations (figure 1.4); however prognosis for 3 subtypes is similar with recurrence after 8-9 months of treatment and an average survival of 15 months (Verhaak et al., 2010). Only mutant IDH tumours classified as proneural GBMs have a better prognosis (Verhaak et al., 2010). Although GBM tumours have now been subtyped, this may be an oversimplification of this extremely complex disease, as even within individual tumours there is massive morphological and phenotypical heterogeneity, including changes in gene expression, cell metabolism, proliferation, angiogenesis, immunogenicity, motility and metastasis, as well as evidence supporting heterogeneous glioma stem cell and tumour propagating populations (Patel et al., 2014, Piccirillo et al., 2009, Piccirillo et al., 2015, Sottoriva et al., 2013, Qazi et al., 2017). Intratumoural heterogeneity (ITH) is most likely driven by a combination of factors including genetic instability, tumour microenvironment (TME) and heterogenic cancer stem cells (CSCs) (Marusyk and Polyak, 2010). As such, this constantly mutating and evolving tumour can become resistant to multi-modal treatment resulting in disease recurrence and subsequent death of the patient (Qazi et al., 2017).

The TME has roles in initiation, propagation and metastasis of cancer and includes the vasculature, immune cells, fibroblasts, signalling molecules and extracellular matrix which surround the tumour (Wang et al., 2018b). Tumour cells are able to change their phenotype in response to signals from their microenvironment, for example, injecting teratocarcinoma into mice blastocysts resulted in the development of healthy mice with cells from different lineages derived from the injected tumour cells (Mintz and Illmensee, 1975). As the TME is not homogeneous, the tumour will have differences in vasculature and immunity and will be surrounded by ECM of varying compositions, all of which will result in altered signalling throughout the TME and consequently phenotypic heterogeneity throughout the tumour (Marusyk and Polyak, 2010).

Similarly to the TME, CSCs are also implicated in ITH and were first isolated in 1997 from patients with acute myeloid leukaemia (AML), whereby CD34+ and CD38- cells were able to induce AML in non-obese diabetic and severe combined immunodeficiency disease (NOD/SCID) mice across multiple transplantations (Dick, 1997). CD34 is a transmembrane phosphoglycoprotein which binds to l-Selectin, a cell adhesion molecule on leukocytes and binds to Crkl, a protein which also regulates cell adhesion, however, little is known about the function of CD34 (Sidney et al., 2014). CD38 is also a transmembrane glycoprotein which is usually found on the surface of immune cells; however, loss of this marker is associated with haematopoietic precursors identified from embryonic stem cells (Lu et al., 2004).

Cell surface markers CD44 (positive) and CD24 (negative) were then used to identify CSCs from the first solid tumour (breast cancer) in 2003 (Al-Hajj et al., 2003). CD24 and CD44 both have roles in cell adhesion, CD44 is a hyaluronic acid receptor and CD24 is a heat stable antigen and both are expressed in many tumour cells (Agnihotri et al., 2012). However, it is unclear whether CD44+/CD24- cells are true CSCs due to conflicting reports (Abraham et al., 2005, Jang et al., 2016).

Glioma cancer stem-like cells (GCSc) have also been identified and have the following properties: 'self-renew in culture, propagate phenotypically similar tumours upon *in vivo* secondary transplantation and give rise to neurons and glia-like differentiated progenies both *in vivo and in vitro*' (Ahmed et al., 2013). Prominin 1, also called CD133, is a transmembrane glycoprotein which is normally located on embryonic stem cells or localised to plasma membrane protrusions such as microvilli (Li, 2013b). CD133 was used as a marker to isolate high grade primary medulloblastoma cells which could differentiate *in vitro* into phenotypically similar cells to those seen in the primary tumour. These cells were termed brain tumour stem cells (BTSCs) (Singh et al., 2003). CD133 positive cells, purified from both GBM patient samples and GBM patient derived xenograft tissues, recover from ionising radiation induced DNA damaged significantly more quickly than CD133 negative cells (Bao et al., 2006). This is achieved through increasing the activation of DNA damage checkpoint genes, CHK1 and CHK2, and an enhanced ability to repair DNA damage leading to a greater survival in response to DNA damage (Ahmed et al., 2015, Bao et al., 2006). Cells isolated from primary cultured GBM cells which are CD133 positive and upregulate other CSC markers (nestin, CD44, CXCR4) are more resistant to temozolomide and also over-express MGMT (Liu et al., 2006). Furthermore, recurrent GBM tumours also have higher CD133 expression compared to the primary GBM tumour. Additionally grade III glioma patients with >1% CD133+ cells have a significantly reduced survival and an increased chance of tumour recurrence (Liu et al., 2006, Zeppernick et al., 2008). However, it has been shown that CD133- cells are also able to initiate tumour formation in immunocompromised mice (Beier et al., 2007, Ogden et al., 2008). A combination of CD133 positive cells and other neural stem cell markers are now used to identify GSC populations more accurately (Ahmed et al., 2015). Examples of such markers include nestin and OLIG2 (Ahmed et al., 2013). Nestin is upregulated during CNS development and is involved nerve cell mitosis, however, expression is usually downregulated as cells differentiate into glial- or neuronal-derived cells (Suzuki et al., 2010). OLIG2 is a transcription factor which is predominantly expressed in the CNS and is also important in the development of motor neurons and oligodendrocytes (Tsigelny et al., 2016).

As GSCs are quiescent, they have an increased resistance to both radio- and chemotherapy which selectively target highly proliferative cells (Rich and Bao,

2007). Once proliferative tumour cells have been killed, remission of disease is achieved and then treatment stops which enables previously quiescent GSCs to re-initiate tumour regrowth. As GSCs have increased MGMT expression; recurrent tumours are more likely to be resistant to temozolomide chemotherapy, however, some GBM tumours have MGMT negative GSCs which are still resistant to temozolomide chemotherapy (Ahmed et al., 2013, Liu et al., 2006). There is still a lot to learn about GSCs, importantly whether the heterogeneous GSCs are derived as a consequence of intratumoural heterogeneity or whether they are the drivers of this complex microenvironment.

1.8 Novel Therapies and Current Targets in Clinical Trials

Out of 36 completed phase III or IV trials listed on a clinical trials database (https://clinicaltrials.gov/), 10 trials (28%) currently have published results. Of these, only 3 were investigating targeted therapy in combination with the standard treatment of radiotherapy and temozolomide, one trial was investigating pain management and another was investigating neurological side effects of radiotherapy (confusion, tiredness etc.), therefore 8 trials are included in table 1.1.

Table 1.1: Completed Phase III and IV GBM clinical trials

Trial Number	Therapeutic	IR	Chemotherapy	Diagnosis	Phase	Improved OS
689221	Cilengitide	Yes	TMZ	New	III	No
777153	Cediranib	No	CCNU	Recurrent	III	No
943826	Bevacizumab	Yes	TMZ	New	III	No
686725	TMZ	Yes	Early post-surgery TMZ	New	IV	Yes
154375	Imatinib	No	HU	Recurrent	III	No
884741	Bevacizumab	Yes	TMZ	New	III	No
00482677	TMZ	Yes	TMZ in Elderly (65 yrs)	New	III	Yes
304031	TMZ	Yes	Increased Adjuvant TMZ	New	III	No

Table 1.1 *- There were no improvements in overall survival with the addition of novel therapeutics to the treatment regime. Early-post surgery temozolomide and temozolomide treatment for the elderly did improve overall survival.*

Two trials of the three trials combined standard treatment with bevacizumab, a monoclonal antibody which binds to and inhibits VEGF-A – an important pro-angiogenic protein overexpressed in GBM (Chinot et al., 2014, Gilbert et al., 2014, Stupp et al., 2014). The remaining trial combined cilengitide, an αvβ3 and αvβ5 integrin inhibitor, with standard temozolomide chemo-radiotherapy treatment. Integrins are found on the cell surface enabling binding to the extracellular matrix,

they are abundant in GBM tumours and tumour vasculature (Bello et al., 2001). In a phase II trial, cilengitide had more effective anti-cancer activity as a mono- and combined therapy in patients with MGMT promoter methylation (Stupp et al., 2014). Neither bevacizumab nor cilengitade was able to improve overall survival; however, progression free survival did increase by 3-4 months in both bevacizumab trials (Chinot et al., 2014, Gilbert et al., 2014). Since the addition of the chemotherapeutic temozolomide, treatment for GBM has remained unchanged for around a decade, highlighting a lack of translation from research findings to clinical trials through to patients. Aside from a selection of various chemotherapeutics (temozolomide, carmustine/BiCNU, lomustine/CCNU and everolimus) bevacizumab is the only other FDA approved treatment for brain tumours, however, it is not endorsed by NICE for the treatment of patients with newly diagnosed GBM (NationalCancerInstitute, 2018, NICE, 2018b).

Asunercept is a fusion protein combining the Fc domain from an IgG fused to the cell surface receptor CD95 (CD95-Fc) (Wick et al., 2014). Asunercept inhibits the CD95 ligand binding to its receptor CD95, reducing migration and invasion of GBM tumour cells and in a phase II trial showed an improved 6 month progression free survival in combination with radiotherapy when compared to radiotherapy alone (20.7% v 3.8%) (Kleber et al., 2008, Wick et al., 2014). Asunercept has been undergoing NICE technology appraisal for the treatment of GBM since August 2017 in order to determine the cost benefit of the drug to the NHS (NICE, 2017a).

Depatuxizumab mafodotin (ABT-414) has also been undergoing NICE technology appraisal since March 2017 as a potential treatment for patients newly diagnosed with GBM that have EGFR amplifications. However, investigation into the use of this treatment by the NHS for recurrent EGFR amplified GBM has been suspended as of January 2018 (NICE, 2017b). ABT-414 is an EGFR monoclonal antibody conjugated to the antimitotic drug monomethyl auristatin F. ABT-414 is able to target both amplified EGFR and mutant EGFRvIII and is currently being investigated in a phase III clinical trial in combination with temozolomide chemo-radiotherapy treatment in newly diagnosed patients (ADCReview, ClinicalTrials.gov, 2018).

Nivolumab is a monoclonal antibody which binds to PD-1 receptors on the surface of T-cells thereby activating an immune response. However, as a phase III trial comparing nivolumab alone to bevacizumab alone in patients with recurrent GBM showed no survival benefit, nivolumab was withdrawn from NICE technology appraisal (NICE, 2016b). Nivolumab is currently in phase III in clinical trials for patients with newly diagnosed GBM, however, patients with a methylated MGMT promoter will receive nivolumab in addition to temozolomide and radiotherapy (checkmate-548) and those with an un-methylated and active MGMT promoter will

receive either nivolumab and radiotherapy or temozolomide and radiotherapy (checkmate-498) (ClinicalTrials.gov, 2018).

DCVax®-L is a cell based immunotherapy which uses lysates from the patient's GBM tumour and immature dendritic cells taken from the patient's blood to activate the dendritic cells to raise an immune response targeting the tumour. Both phase I and phase II trials which combined DCVax®-L with temozolomide chemo-radiotherapy showed promising results in newly diagnosed patients, with a median survival of 3 years and a 10 year survival achieved by 2 patients. A phase III trial is currently underway in 348 newly diagnosed GBM patients (NorthwestBiotherapeutics, 2018). DCVax®-L was undergoing NICE technology appraisal, however, this was suspended as of September 2018 due to lack of evidence from the company (NICE, 2016a).

1.9 Hypothesis and Project Aims

siRNA screens have been used previously to identify novel targets to improve treatment for patients with GBM. For example, an siRNA screen identified SGK1 as an important gene in maintaining GSCs, a genome-wide siRNA screen identified genes important for tumour migration and chemo-resistance and a kinome-wide siRNA screen which showed depletion of PLK1 radio-sensitises GBM cells (Kulkarni et al., 2018, Tandle et al., 2013, Yang et al., 2013a).

The hypothesis for this project was 'inhibition of yet to be identified targets or pathways will enhance the cytotoxic effect of temozolomide in GBM'.

The aim of this project was to identify and validate novel molecular targets and/or druggable pathways that confer an increase in sensitivity to the NICE approved and extensively used GBM chemotherapeutic agent temozolomide. Targets identified from these proof-of-concept data could then be developed into future adjuvant therapies to improve the outcome for GBM patient survival.

The objectives were to:

1. Carry out a kinome wide siRNA and small molecule drug re-purposing screens in the temozolomide resistant immortalised GBM cell line T98G.
2. Validate and refine primary hits from the siRNA screen using an alternative pooled siRNA library and siRNA pool deconvolution into individual siRNA. Determine whether targets confer an increase in temozolomide sensitivity in a panel of GBM cell lines.
3. Validate any targets by determining their expression (mRNA and protein) in brain tumours compared to healthy brain tissue.

4. Validate and refine primary hits from small molecule drug screens by dose-response curves in a panel of GBM cell lines.
5. Investigate mechanism(s) by which GBM cells are sensitised to temozolomide using functional assays investigating DNA damage, proliferation and apoptosis.

Chapter 2 – Materials and Methods

2.1 Materials

2.1.1 General Laboratory Equipment, Plastics and Consumables

Table 2.1: General Laboratory Equipment, Plastics and Consumables.
Airstream ESCO Class II Biological Safety Cabinet
Agar Granulated, Melford
Applied Biosystems 7900 Real-Time PCR
BD FACSCalibur™
BD Plastipak™ 10ml Syringe
BD FACSCalibur™
Bio-Rad mini-PROTEAN Tetra Cell
Bio-Rad S1000 Thermal Cycler
Bio-Rad PowerPac™ Basic Power Supply
Biosphere® Filter Tips 0.1-10µl, 2-20 µl, 2-100 µl, 100-1000 µl
BioTek Elx405 Select CW Plate Washer
Cellstar ® Cell Culture Dishes 100x20mm
Corning 50ml Reagent Reservoir
Costar 96 Well Tissue Culture Treated Plates
CytoOne Multiwell Plate, 6 well
Eppendorf Centrifuge 5430
Eppendorf Centrifuge 5810 R
Eppendorf Centrifuge S415 R
Epson Expression 1680 Pro Scanner
Fisher Scientific FB15-12 TopMix
Fisher Scientific MH-214 Analytical Balance
Fisher Scientific SG-607 Analytical Balance
FisherBrand™ 5 ml, 10 ml and 25 ml Disposable Serological Pipettes
Fisherbrand™ Electric Pipet Controller
Fujifilm Fuji Medical X-ray Film Super RX
GE NanoVue Plus
Gilson P10, P20, P200 Multichannel Pipettes
Gilson P2, P10, P20, P200 and P1000 Pipettes
Grant JB Aqua 18 Plus
Hawksley AC1000 Improved Neubauer Haemocytometer

Jenway 3510 pH Meter
Konica Mibolta SRX101A Film Processor
Life Technologies Countess II
Microplate 384 well PP PCR with skirt, Greiner Bio-one
Millex-GP Syringe Filter Unit, 0.22 µm, polyethersulfone, 33 mm, gamma sterilized
Molecular Devices ImageXpress Micro High Content Microscope
Nanodrop ND 1000 Spectrophotometer
Nikon Eclipse TE200 Fluorescent Microscope
PlateLoc Velocity 11
Sanyo MCO-19AIC (UV)
Sarstedt Cell Scraper 25 cm
Sarstedt CryoPure 1.8 ml White
Sarstedt P200, P1000 Pipette Tips
SLS 15ml/50ml polypropylene tubes
Star Lab 8-strip PCR Tubes, 0.2 ml & Caps
Sterilin Universal Tubes
Stuart® Mini Gyro-rocker
Techne Dri-Block® DB-2D
Thermo Fischer Immu-Mount
Thermo Megafuge 40
Thermo Multidrop 384
Thermo Multiskan FC
Thermo Nunc™ EasYFlask™ 25 cm^2 Nunclon™ Delta Surface
Thermo Nunc™ EasYFlask™ 75 cm^2 Nunclon™ Delta Surface
Thermo Scientific Multidrop Combi
Walker Safety Cabinet Class II MSC (Model TDA-2G)
Welch 2515C-75 REV A
XCell SureLock™ Mini-Cell Electrophoresis System

2.1.2 Reagents

Table 2.2: Reagents
1,4-dithiothreitol (DTT): Sigma DTT-RO
30% acrylamide mix: Geneflow
Acetic Acid, Glacial: Fisher Scientific, A38-212
Ammonium Persuphate (APS), Fisher

Benzonase Nuclease: Novagen, 70664-3
Biotinylated Goat Anti-Mouse IgG Antibody: Vector Laboratories, BA9200
BioRad Protein Assay Dye Reagent Concentrate: BioRad, 500-0006
Bovine Serum Albumin (BSA): Sigma, A2153
Calcium Chloride: Sigma 499609
DAB Peroxidase (HRP) Substrate Kit: Vector Laboratories SK-4100
Dako Target Retrieval Solution, Citrate pH 6 (x 10): Agilent, S2369
DharmaFECT 1: GE Healthcare, □ T-2001-01
Dimethyl Sulfoxide (DMSO): Fisher Chemical, D/4120/PB08
DPX Mountant: Sigma 06552
Dulbecco's Modified Eagle Medium (DMEM): Lonza, BE12-604F
Ethylenediaminetetraacetic Acid (EDTA): Sigma, 1233508
Ethanol: Fisher Scientific, AC615090010
Foetal Calf Serum: Lonza, BE12-60F4
Goat Serum Blocking Solution: Vector Laboratories, S-1000
Glycerol: Sigma, G5516
Hoechst 33342 Trihydrochloride, Trihydrate: Life Technologies, H3570
Hydrochloric Acid (HCL) 37%: Fisher Sceintific A144-500LB
Hydrogen Peroxide: Sigma, 95321
Isopropanol: Fisher Scientific, A416-4
Lipo 2000: ThermoFisher,11668019
Lipofectamine RNAiMAX Transfection Reagent: Life Technologies, 13778030
Magnesium Chloride: Sigma, M8266
Marvel Milk Powder
Methanol: Fisher Scientific, A452SK-4
Methylene Blue: Sigma Aldrich, M9140
MTT (3-(4,5-dimethylthiazol-2-yl)-2,5-diphenyltetrazolium bromide): Sigma, M2128
NuPAGE® LDS Sample Buffer (4X): ThermoFisher, NP007
NuPAGE® MOPS SDS Running Buffer (20X): ThermoFisher, NP001
NuPAGE® Transfer Buffer (20X): ThermoFisher NP0006
NuPAGE™ 4-12% Bis-Tris Protein Gels, 1.5 mm, 10 well: ThermoFisher, NP0335BOX
NuPAGE™ 4-12% Bis-Tris Protein Gels, 1. 5mm, 15 well: ThermoFisher, NP0336BOX
Oxoid PBS tablet: Thermo Scientific, Cat. No. BR0014
Paraformaldehyde (PFA) solution 4% in PBS: Sanat Cruz, SC-281692
Phosphatase Inhibitor: Sigma, P5726
PIB: Sigma, P2714

Pierce ECL Western Blotting Substrate: Thermo Scientific, 32106
Potassium Chloride: Sigma, P9333
Protran Nitrocellulose Membrane: VWR, 732-4016
Propidium Iodide, Sigma P4864
QAIshredder (50): Qiagen, 79654
Qiagen Rneasy Mini Kit: Qiagen 74104
RNase A: Sigma
SeeBluePlus2 Prestained Standard: ThermoFisher, LC5925
5X siRNA Buffer: Dharmacon, B-002000-UB-100
Sodium Chloride: Sigma, S7653
Sodium Citrate: Sigma, 1613859
Sodium Dodecyl Sulphate (SDS): Sigma, L3771-500G
Sodium Hydroxide (NaOH) Pellets: Sigma, 1.06462 EMD
Sucrose: Sigma, S7903
SYBR® Gold Nucleic Acid Gel Stain: Thermo Scientific, S11494
TaqMan™ Reverse Transcription Reagents: Applied Biosystems, N8080234
TaqMan™ Universal PCR Master Mix No AmpErase UNG: Applied Biosystems, 4324018
Tris Base: Sigma, TRIS-RO
Tris Hydrochloride: Sigma 10812846001
Triton™ X-100: Sigma, X100 SIGMA-ALDRICH
Trypsin (0.5g/l trypsin, 0.2g/l versene (EDTA)): Lonza, 17-161E
TWEEN® 20: Sigma, P1379
VECTASTAIN® ABC Kit: Vector Laboratories, PK-4000
Visualiser™ Western Blot Detection Kit: Fisher Scientific, 10553414
Xylene: Sigma, 247642
β-Mercaptoethanol: Fisher, M/P200/05

2.1.3 Inhibitors and Cytotoxic Agents

Table 2.3: Cytotoxic Agents

Item	Mechanism of Action	Solvent	Company
BIX 02189	MEK5 inhibitor	Ethanol	Selleckchem (S1531)
BLU554	FGFR4 inhibitor	DMSO	Selleckchem (S8503)
Butamben	Anaesthetic	DMSO	Selleckchem (S4583)
ERK5-IN-1	Inhibits EGFR-induced ERK5 auto-phosphorylation	DMSO	Tocris (5393)

D-Penicillamine	Anti-rheumatic Chelating agent (Wilson's disease)	Water	Simga (P4875)
Nocodazole	Anti-mitotic agent	DMSO	Sigma (M4104)
O6-Benzylguanine	AGT inhibitor	Methanol	Sigma (B2292)
Pyrvinium Pamoate	Androgen receptor inhibitor	DMSO	Sigma (P0027)
Roscovitine	Cyclin-dependent kinase inhibitor	DMSO	Sigma (R7772)
Temozolomide	Methylation of DNA	DMSO	Sigma (T2577)
XMD8-92	ERK5 inhibitor	DMSO	Selleckchem (S7525)

Purified Water

Ultra-pure deionised water (ddH_2O) was obtained by a Purite Prestige Labwater 250 purification system.

Sterilisation

Glassware was washed in RBS detergent and rinsed in cold water followed by ddH_2O before being dried in a hot air oven at 80 °C. Glassware was then autoclaved for 15 minutes at 120 °C and 100 kPa in a MP24 Rodwell autoclave (Scientific Laboratory Supplies).

2.1.4 Antibodies

Table 2.4: Primary Antibodies

Primary Antibody	Raised In	Company	Protein Size (kDa)	Dilution
Anti-53BP1	Rabbit	Abcam (ab368823)	214	1:500
Anti-β-Actin	Mouse	Abcam (ab8226)	42	1:2000
Anti-β-Tubulin	Mouse	Abcam (ab7797)	50	1:2000
Anti-pDNAPKcs (s2056)	Rabbit	Abcam (ab18192)	460	1:1000
Anti-ERK5	Mouse	Santa Cruz (sc-398015)	89	1:1000
Anti-FANCD2	Mouse	Abcam (ab12450)	166	1:1000
Anti-FGFR4	Rabbit	Cell Signalling (2894)	89	1:500
Anti-MGMT	Mouse	Abcam (ab39253)	22	1:1000

Anti-O-6-Methyl-2'-deoxyguanosine	Mouse	Axxora (SQX-SQM003.1)		1:100
Anti-RAD51	Rabbit	Santa Cruz (sc-8349)	37	1:500

Table 2.5: Secondary Antibodies

Secondary Antibody	Company	Dilution
Alexa Fluor ® 488 Goat Anti-Mouse	Life Technologies (A-11304)	1:1000
Alexa Fluor ® 488 Goat Anti-Rabbit	Life Technologies (A-11034)	1:1000
Alexa Fluor ®594 Goat Anti-Rabbit	Life Technologies (A-11012)	1:1000
Polyclonal Goat Anti-Mouse IgG, HRP-Linked	Dako (P0447)	1:1000
Polyclonal Swine Anti-Rabbit IgG, HRP Linked	Dako (P0399)	1:1000
Biotinylated Goat Anti-Mouse IgG, HRP linked	Vector Labs (BA9200)	1:200

2.1.6 siRNA Sequences

Table 2.6: siRNA Sequences

Library	Gene	Sequence
ON-TARGET plus	MGMT siRNA # 1	GGUUGUGAAAUUCGGAGAA
ON-TARGET plus	MGMT siRNA #2	GAUGGAUGUUUGAGCGACA
ON-TARGET plus	MGMT siRNA #3	AAAUAAAGCUCCUGGGCAA
ON-TARGET plus	MGMT siRNA #4	UGGCCGAAACUGAGUAUGU
siGENOME	MGMT siRNA # 1	GAAAUUCGGAGAAGUGAUU
siGENOME	MGMT siRNA # 2	CCAGACAGGUGUUAUGGAA
siGENOME	MGMT siRNA # 3	CAAGGAUUGUGAAAUGAAA
siGENOME	MGMT siRNA # 4	GCCCGAGGCUAUCGAAGAG
ON-TARGET plus	PARP-1 siRNA # 1	GAUUUCAUCUGGUGUGAUA
ON-TARGET plus	PARP-1 siRNA # 2	GAAAACAGGUAUUGGAUAU
ON-TARGET plus	PARP-1 siRNA # 3	GUUCUUAGCGCACAUCUUG
ON-TARGET plus	PARP-1 siRNA # 4	CCAAUAGGCUUAAUCCUGU
ON-TARGET plus	TDP-1 siRNA # 1	CCACAAAUCUGGAGAGUCG
ON-TARGET plus	TDP-1 siRNA # 2	GACCAUAUCUAGUAGUGAU
ON-TARGET plus	TDP-1 siRNA # 3	GGACCAGUUUAGAAGGAUA
ON-TARGET plus	TDP-1 siRNA # 4	GUGAUAAGCGAGAGGCUAA
siGENOME	FANCD2 siRNA # 1	GGUCAGAGCUGUAUUAUUC
siGENOME	FANCD2 siRNA # 2	GAUAAGUUGUCGUCUAUUA

siGENOME	FANCD2 siRNA # 3	GAUCAACUCUCCUAAAGAU
siGENOME	FANCD2 siRNA # 4	GAACAAAGGAAGCCGGAAU
siGENOME	GRK6 siRNA # 1	GAGCUUGGCCUACGCCUAU
siGENOME	GRK6 siRNA # 2	CGAACACGGUGCUACUCAA
siGENOME	GRK6 siRNA # 3	UGGUGAAGAAUGAACGGUA
siGENOME	GRK6 siRNA # 4	UGGCGGUGGAAAUCGCAAA
siGENOME	PI4KA siRNA # 1	GUGAAGCGAUGUGGAGUUA
siGENOME	PI4KA siRNA # 2	CCACAGGCCUCUCCUACUU
siGENOME	PI4KA siRNA # 3	GCAGAAAUUUGGCCUGUUU
siGENOME	PI4KA siRNA # 4	CCAACAUGACUGAGCGCGA
siGENOME	CAMK2B siRNA # 1	GGACGAGGACCAGCACAAG
siGENOME	CAMK2B siRNA # 2	GGACACCGUCACUCCUGAA
siGENOME	CAMK2B siRNA # 3	GCAAGCCUGUGGACAUCUG
siGENOME	CAMK2B siRNA # 4	CGGCCUAGCUAUCGAGGUG
siGENOME	DYRK1A siRNA # 1	UAAGGAUGCUUGAUUAUGA
siGENOME	DYRK1A siRNA # 2	GCUAAUACCUUGGACUUUG
siGENOME	DYRK1A siRNA # 3	AAACUCGAAUUCAACCUUA
siGENOME	DYRK1A siRNA # 4	CUUUGAACCUAACACGAAA
siGENOME	PNCK siRNA # 1	AGAAACACACGGAGGACAU
siGENOME	PNCK siRNA # 2	GCAGUGCUCCGUAGGAUCA
siGENOME	PNCK siRNA # 3	AAGAAACACACGGAGGACA
siGENOME	PNCK siRNA # 4	GAUUUGAGGGUGUGGCGCA
siGENOME	SCYL3 siRNA # 1	GAACAUUGGUGGAAAGUUU
siGENOME	SCYL3 siRNA # 2	GAGCUGAACUGGGAAGAUA
siGENOME	SCYL3 siRNA # 3	UUAAAGAGCUAUACACUGA
siGENOME	SCYL3 siRNA # 4	CAACAGACCUUGCACUCAA
siGENOME	DGKG siRNA # 1	GAAUAUUCCUCCAAGAAGA
siGENOME	DGKG siRNA # 2	CAGCGCAGAUACUAAUAUA
siGENOME	DGKG siRNA # 3	CACAUGAGCCGAUUAGCUA
siGENOME	DGKG siRNA # 4	GCAGCCAUGUUGCACGAUU
siGENOME	PIK3C2B siRNA # 1	GCCGGAAGCUUCUGGGUUU
siGENOME	PIK3C2B siRNA # 2	CAAGAGCUCUGGCCGAAUC
siGENOME	PIK3C2B siRNA # 3	GCUGAGACCCUGCGUAAGA
siGENOME	PIK3C2B siRNA # 4	GCUACCAGCUAUGAAGAUU
siGENOME	PRKAR1A siRNA # 1	CGAGACAGCUAUAGAAGAA
siGENOME	PRKAR1A siRNA # 2	GAUAAUGAGAGAAGUGAUA
siGENOME	PRKAR1A siRNA # 3	UACGGUAGCUGAUGCAUUG
siGENOME	PRKAR1A siRNA # 4	GUGGGAACGUCUUACGGUA
siGENOME	STK16 siRNA # 1	GAGGUACGCUGUGGAAUGA
siGENOME	STK16 siRNA # 2	CGACAUGCAUCGCCUCUUC
siGENOME	STK16 siRNA # 3	GGUACGCUGUGGAAUGAGA
siGENOME	STK16 siRNA # 4	UGAAGCGAAUCCUGUGUCA
siGENOME	DMPK siRNA # 1	GCACUUCGCCUUCCAGGAU
siGENOME	DMPK siRNA # 2	GCGGAGACCUAUGGCAAGA
siGENOME	DMPK siRNA # 3	UGAAGAUCAUGAACAAGUG

siGENOME	DMPK siRNA # 4	GCUUGAGCCACACGUGCAA
siGENOME	PDGFRB siRNA # 1	GAAAGGAGACGUCAAAUAU
siGENOME	PDGFRB siRNA # 2	GGAAUGAGGUGGUCAACUU
siGENOME	PDGFRB siRNA # 3	CAACGAGUCUCCAGUGCUA
siGENOME	PDGFRB siRNA # 4	UGACAACGACUAUAUCAUC
siGENOME	PRKDC siRNA # 1	GCAAAGAGGUGGCAGUUAA
siGENOME	PRKDC siRNA # 2	GAGCAUCACUUGCCUUUAA
siGENOME	PRKDC siRNA # 3	GAUGAGAAGUCCUUAGGUA
siGENOME	PRKDC siRNA # 4	GCAGGACCGUGCAAGGUUA
siGENOME	ALPK3 siRNA # 1	UAGAUUCCCUGAAGAACUA
siGENOME	ALPK3 siRNA # 2	CCAAAGACCUGCUGAAAGC
siGENOME	ALPK3 siRNA # 3	GCAAGCCCCUGGAGUCUUA
siGENOME	ALPK3 siRNA # 4	GAACAUGAGUCGGGAGUAC
siGENOME	FGFR4 siRNA # 1	GCACUGGAGUCUCGUGAUG
siGENOME	FGFR4 siRNA # 2	CCUCGAAUAGGCACAGUUA
siGENOME	FGFR4 siRNA # 3	AUAACUACCUGCUAGAUGU
siGENOME	FGFR4 siRNA # 4	GCAUUCGGCUGCGCCAUCA
siGENOME	PRKAG1 siRNA # 1	GGACAUCUACUCCAAGUUU
siGENOME	PRKAG1 siRNA # 2	GAUGCUGUCUCUUCAUUAA
siGENOME	PRKAG1 siRNA # 3	CAACAUCGAUCACAUUACU
siGENOME	PRKAG1 siRNA # 4	AAGCAGAGGUUCACCGACU
siGENOME	MAP3K3 siRNA # 1	GAUAGAAGCUCAAGCAUGA
siGENOME	MAP3K3 siRNA # 2	AAACUCAGCUUUAUGACAA
siGENOME	MAP3K3 siRNA # 3	CCAAGCAGGUCCAAUUUGA
siGENOME	MAP3K3 siRNA # 4	GCAAACGCCUGCAGACGAU
siGENOME	IPPK siRNA # 1	GCAAGAUCGUCAACUAUUA
siGENOME	IPPK siRNA # 2	UAACGAAGGUGCAGCAGUA
siGENOME	IPPK siRNA # 3	CGUCAACUAUUAUUCAAAG
siGENOME	IPPK siRNA # 4	AGAUGGGCCUUAUGAUGAA
siGENOME	CALM3 siRNA # 1	GGGAGAAGCUGACCGAUGA
siGENOME	CALM3 siRNA # 2	GGAUGGAGAUGGCACUAUC
siGENOME	CALM3 siRNA # 3	GGACAGAACCCCACUGAAG
siGENOME	CALM3 siRNA # 4	GAGAUGGCCAGGUCAAUUA
siGENOME	STK3 siRNA # 1	GCCCAUAUGUUGUAAAGUA
siGENOME	STK3 siRNA # 2	ACAAGUACCUGUUGAAUCA
siGENOME	STK3 siRNA # 3	CCACAAGCACGAUGAGUGA
siGENOME	STK3 siRNA # 4	CGGUCAAGUUGUCGCAAUU
siGENOME	PRKAR2B siRNA # 1	GAACAUCGCUACCUAUGAA
siGENOME	PRKAR2B siRNA # 2	GAACGAACAUGGAUAUUGU
siGENOME	PRKAR2B siRNA # 3	GUUCAAUGCUCCAGUAAUA
siGENOME	PRKAR2B siRNA # 4	GAAAGUAGUAGAUGUGAUA
siGENOME	PGK1 siRNA # 1	CAAAAUUGAUGAUCCAUUA
siGENOME	PGK1 siRNA # 2	UUGAUGAUCCAUUAAGUAA
siGENOME	PGK1 siRNA # 3	GCACAGCAUCUCAGCUCAU
siGENOME	PGK1 siRNA # 4	GAAGCGGGUCGUUAUGAGA

siGENOME	FES siRNA # 1	CGAGGAUCCUGAAGCAGUA
siGENOME	FES siRNA # 2	AGGAAUACCUGGAGAUUAG
siGENOME	FES siRNA # 3	CAACAGGAGCUCCGGAAUG
siGENOME	FES siRNA # 4	GGUGUUGGGUGAGCAGAUU
siGENOME	NEK4 siRNA # 1	GAACAAACAUCAUCAAAGU
siGENOME	NEK4 siRNA # 2	GGAGGUAUAUGCAGUAUUU
siGENOME	NEK4 siRNA # 3	GAAGAAAGGCCGUCUGUGA
siGENOME	NEK4 siRNA # 4	AAACAGGACUUGAGCAAUA
siGENOME	PRKCZ siRNA # 1	GAACGAGGACGCCGACCUU
siGENOME	PRKCZ siRNA # 2	GACCAAAUUUACGCCAUGA
siGENOME	PRKCZ siRNA # 3	GGUUGUUCCUGGUCAUUGA
siGENOME	PRKCZ siRNA # 4	CGUCAAAGCCUCCCAUGUU
siGENOME	CDKL3 siRNA # 1	GUAUAGAGCUCCCGAAUUA
siGENOME	CDKL3 siRNA # 2	GAACAGUCAUGAAAUGUAA
siGENOME	CDKL3 siRNA # 3	UGUAAUGGCUUGAAAGAAA
siGENOME	CDKL3 siRNA # 4	GAUAGUGGCCAUUAAGAUA
siGENOME	ALPK2 siRNA # 1	GCAACAAGCUGAAGAUUAU
siGENOME	ALPK2 siRNA # 2	CAACAUACCUGACAAUUUC
siGENOME	ALPK2 siRNA # 3	GGACAAAGCAGAAUUGAUU
siGENOME	ALPK2 siRNA # 4	GACCUUCAUUGAUCAGUUU
siGENOME	PRKCSH siRNA # 1	UGAAGAAGAUCCUUAUUGA
siGENOME	PRKCSH siRNA # 2	GGUCAACGAUGGUGUUUGU
siGENOME	PRKCSH siRNA # 3	GGAGUUUGCUUACCUGUAC
siGENOME	PRKCSH siRNA # 4	UCACCAAUCAUCACUUCUA
ON-TARGET plus	PNCK siRNA # 1	GCAGUGCUCCGUAGGAUCA
ON-TARGET plus	PNCK siRNA # 2	AGAAACACACGGAGGACAU
ON-TARGET plus	PNCK siRNA # 3	CAUCGUCGCUCUGGAGGAU
ON-TARGET plus	PNCK siRNA # 4	CAGCAGCGUCUACGAGAUC
ON-TARGET plus	DMPK siRNA # 1	GUACGUGGCCGACUUCUUG
ON-TARGET plus	DMPK siRNA # 2	GGGACGACUUCGAGAUUCU
ON-TARGET plus	DMPK siRNA # 3	GAAAUGUUCUAUGGGCAGA
ON-TARGET plus	DMPK siRNA # 4	GAACUUCGCCAGUCAACUA
ON-TARGET plus	FGFR4 siRNA # 1	CCUCGAAUAGGCACAGUUA
ON-TARGET plus	FGFR4 siRNA # 2	AUAACUACCUGCUAGAUGU
ON-TARGET plus	FGFR4 siRNA # 3	GCACGAGGCUCCAUGAUCG
ON-TARGET plus	FGFR4 siRNA # 4	GAUUACAGGUGACUCCUUG
ON-TARGET plus	MAP3K3 siRNA # 1	GAGCACAAAUGGCGAGAAC
ON-TARGET plus	MAP3K3 siRNA # 2	GAUCUACAUUACAUGAACA
ON-TARGET plus	MAP3K3 siRNA # 3	GAACCGACGUCACCGGAUG
ON-TARGET plus	MAP3K3 siRNA # 4	GAUAGAAGCUCAAGCAUGA
ON-TARGET plus	FES siRNA # 1	CGAGGAUCCUGAAGCAGUA
ON-TARGET plus	FES siRNA # 2	GGUGUUGGGUGAGCAGAUU
ON-TARGET plus	FES siRNA # 3	GAAGAGUGGUGUUGUCCUG
ON-TARGET plus	FES siRNA # 4	GAAAGUGGAUGGCCCAGCG
ON-TARGET plus	PRKCSH siRNA # 1	GGUCAACGAUGGUGUUUGU

ON-TARGET plus	PRKCSH siRNA # 2	GCUACGAGCUCACCACCAA
ON-TARGET plus	PRKCSH siRNA # 3	GAGAAGGGCCGUAAGGAGA
ON-TARGET plus	PRKCSH siRNA # 4	GCGAGUACCUCAUGGAGCU
ON-TARGET plus	TWF2 siRNA # 1	CCAUUGAGCUGGUGCACAC
ON-TARGET plus	TWF2 siRNA # 2	UUAACGAGGUGAAGACAGA
ON-TARGET plus	TWF2 siRNA # 3	GGGUACAAGUGCAGCAUCA
ON-TARGET plus	TWF2 siRNA # 4	GAGCAGGACUUCCAUCUGG

Table 2.7: siTOOLS™ siRNA Sequences

Gene	Sequence
ERK5 siRNA#1	TCAAAGACTTGAGCAGGGC
ERK5 siRNA#2	ATCCTGGAACTAGGTCTAC
ERK5 siRNA#3	AGACTGGTTTAAGAATTCC
ERK5 siRNA#4	TCTACTGTGGCAGCAAGGC
ERK5 siRNA#5	TTGGTACAGGAAGTAGCGC
ERK5 siRNA#6	AACATCTGGACAGCCAGGC
ERK5 siRNA#7	ATGCCATGGCCTTCGAGCC
ERK5 siRNA#8	AATCACGGCTGGTGATGGG
ERK5 siRNA#9	TATCGGCAGGGTTCATGCC
ERK5 siRNA#10	AGTCAGCAAGCAGGGAGGC
ERK5 siRNA#11	TAAGGCTGAAAGGTGGGTC
ERK5 siRNA#12	TTTGAGAATGCTCCCATGG
ERK5 siRNA#13	AATTTCAGCCACAATGGCC
ERK5 siRNA#14	TATAGGCCCGCACCCTCTC
ERK5 siRNA#15	TACTGATGTTCAGCGGGCG
ERK5 siRNA#16	ATTCCTCCAGGTCAAAGCC
ERK5 siRNA#17	TGAGGAGTGGATGATCTGG
ERK5 siRNA#18	TGACATGGAAGACTGAGGG
ERK5 siRNA#19	AAAGTCACCAATCTTGAGC
ERK5 siRNA#20	AATGGTGTCAGGTGCAGGG
ERK5 siRNA#21	ACTGGTAGGTTGGACTGGG
ERK5 siRNA#22	AAAGGCAAAGTCAAAGGGC
ERK5 siRNA#23	ATACTCAGTCATGAAGTAC
ERK5 siRNA#24	AATGGCCTCCTTAATGCGC
ERK5 siRNA#25	TAGAGCCCGCAGATTGTGG
ERK5 siRNA#26	TTGGCTCGTTCTTGCCGCC
ERK5 siRNA#27	TGTGCCTGAGAACACAGGG
ERK5 siRNA#28	TGAACCTGCAGAATAATCC
ERK5 siRNA#29	ATCTCTGAGCCGGCTCCTC
ERK5 siRNA#30	TCAGGATCATGGTACTTGG
FGFR4 siRNA #1	TTGACTTGCCGGAAGAGCC
FGFR4 siRNA #2	TAGGGTCCGAAGGTCAGGC
FGFR4 siRNA #3	TCATCATCGTTGCTGGAGG
FGFR4 siRNA #4	ATGACGATGTGCTTCAGCC
FGFR4 siRNA #5	AACCTCCTGCTGGTATTGG

FGFR4 siRNA #6	ATGCCAAAGGCCTCTGCAC
FGFR4 siRNA #7	TAGTCAATGTGGTGGACGC
FGFR4 siRNA #8	ATAGCAGCTCTCCAGCCAG
FGFR4 siRNA #9	TCAAGCTCCACTTCCTCAG
FGFR4 siRNA #10	AAACCGTCGGCTCCGAAGC
FGFR4 siRNA #11	TTAGGACTTGCACATAGGG
FGFR4 siRNA #12	TACACTTCCGGGACTCCAG
FGFR4 siRNA #13	TGACATTTGGGCCATCAGG
FGFR4 siRNA #14	AAGCTGGCAATCTCTAGGC
FGFR4 siRNA #15	TACAGGACCTCCACCTCTG
FGFR4 siRNA #16	AATGCTCCCGTCAAGACGC
FGFR4 siRNA #17	ACGCATCAGCCCGTACAGC
FGFR4 siRNA #18	AGGACTGGGAAGGAGAGCG
FGFR4 siRNA #19	TCTAGCAGGTAGTTATAGC
FGFR4 siRNA #20	TATAGCGGATGCTGCCCAC
FGFR4 siRNA #21	TCTGAGCTATTGATGTCTG
FGFR4 siRNA #22	ACACGTTCCGCAGGTACAG
FGFR4 siRNA #23	ATTCTGCAGGACGATCATG
FGFR4 siRNA #24	ATTTGCTCCTGTTTTCGGC
FGFR4 siRNA #25	AGACTGGTAGGAGAGGCCG
FGFR4 siRNA #26	TAACTGTGCCTATTCGAGG
FGFR4 siRNA #27	AGGCTCAGCCAAACCCGGG
FGFR4 siRNA #28	TAATCAAGGTGAGATTCTG
FGFR4 siRNA #29	AGAGACGGCCAGCAGGACC
FGFR4 siRNA #30	TCATGGAGCCTCGTGCCAG

2.1.7 TaqMan™ Gene Expression Probes for Quantitative PCR

Table 2.8: TaqMan™ Gene Expression Probes

Gene	Assay ID	Company	Fluorescent Reporter Dye
DMPK	Hs0104329_m1	ThermoFisher	FAM
FES	Hs01120751_m1	ThermoFisher	FAM
FGFR4	Hs01106910_g1	ThermoFisher	FAM
GAPDH	Hs02758991_g1	ThermoFisher	FAM
MAP3K3	Hs00176747_m1	ThermoFisher	FAM
MGMT	Hs01037698_m1	ThermoFisher	FAM
PNCK	Hs00736137_m1	ThermoFisher	FAM
PRKCSH	Hs00160457_g1	ThermoFisher	FAM
TWF2	Hs00911870_g1	ThermoFisher	FAM

2.1.8 Standard Solutions

Alkaline Unwinding Solution 4g NaOH pellets and 2.5ml 20mM EDTA (included in comet assay kit) made up to 500ml with ddH_2O

Comet Electrophoresis Buffer 8g NaOH pellets and 2ml 500mM EDTA made up to 1000ml with ddH_2O

10% APS 1g APS dissolved in 10ml ddH_2O

5% BSA 25g BSA dissolved in 500ml PBS

1M DTT 1.54g DTT dissolved in 10ml ddH_2O

500mM EDTA 146.12g EDTA dissolved in 1000ml ddH_2O

70% Ethanol 700ml ethanol and 300ml ddH_2O

5% Marvel Milk 10g Marvel milk powder dissolved in 200ml PBS-T

70% Methanol 700ml methanol and 300ml ddH_2O

Methylene Blue (0.4%) 2g methylene blue dissolved in 500ml 70% or 100% methanol

5M NaCl 146g NaCl dissolved in 500ml ddH_2O

NuPAge MOPS SDS Running Buffer 25ml NuPage MOPS SDS Running Buffer (20X) in 475ml ddH_2O

NuPage Transfer Buffer 50ml NuPage Transfer Buffer (20X), 750ml ddH_2O and 200ml methanol

PBS 1 Oxoid PBS tablet dissolved in 100ml ddH_2O and sterilised by autoclaving

PBST 500µl TWEEN 20 dissolved in 500ml PBS

10% SDS 50g SDS dissolved in 500ml ddH_2O

10X TBS 24.2g Tris-Base and 80g NaCl dissolved in 300ml ddH_2O. HCl was added until pH 7.6 was reached and ddH_2O made the solution up to 1000ml

TBST 500µl TWEEN 20 dissolved in 500ml TBS

1.0M Tris pH 8.0 131.14 g tris base dissolved in 600ml ddH_2O. HCl was added until pH 8.0 was reached. ddH_2O made the solution up to 1000ml.

2.2 Methods

2.2.1 Mammalian Cell Culture

Passaging Cells

T98G cells, U-87 cells and LN-18 cells were purchased from American Type Culture Collection (ATCC) and U-138 cells were taken from lab stocks originally purchased from ATCC. U-251 cells were a gift from Professor Susan Short (Leeds Institute of Cancer and Pathology). All mammalian cell lines were cultured in T75 flasks in Dulbecco's Modified Eagle Medium (DMEM) supplemented with 10% foetal calf serum (FCS). Cells were incubated at 37°C with 5% CO_2. .

For general maintenance, cells were passaged as follows upon reaching 80-90% confluence. Media was removed and cells were washed twice in 10ml PBS. 1ml of trypsin was added to the flask which was incubated at 37°C with 5% CO_2 until the cells had detached. Cells were pelleted at 1200 RPM for 3 minutes. Supernatant was removed and the pellet was re-suspended in 10ml 10% FCS in DMEM. A fraction of this suspension was used to re-seed a new flask containing 10% FCS DMEM, typically 1:10 for all cell lines.

All cell lines were routinely tested for mycoplasma infection and were only passaged 20 times in order to avoid phenotypic drift.

Table 2.9: GBM Cell Line Derivation

Cell Line	Source	MGMT Status	Other	Reference
LN-18	65 year old male	Positive	Mutant & WT TP53	(Diserens et al., 1981)
T98G	61 year old male	Positive	Mutant TP53	(Stein, 1979)
U-87	male	Negative	WT TP53	(Ponten and Macintyre, 1968)
U-138	47 year old male	Positive	FA deficient WT TP53	(Beckman et al., 1971)
U-251	75 year old male	Negative	Mutant TP53	(Ponten and Macintyre, 1968)

Table 2.9 *- Immortalised GBM cell lines used throughout the studies. Cell lines have various genetic differences including MGMT and TP53 status and FA pathway proficiency.*

Cryopreservation

After trypsinising and centrifuging cells at 1200 RPM for 3 minutes, the pellet was re-suspended in 10% FCS DMEM with 10% DMSO. An 80% confluent flask was re-suspended in 2700µl of 10% FCS DMEM and 300µl of DMSO was added slowly. 1ml

aliquots were placed in cryovials, stored at -80 °C for 24 hours and then transferred to liquid nitrogen.

Thawing Cells

Cells were rapidly thawed in a 37°C water bath, transferred to a falcon tube and 9ml of 10% FCS DMEM was added. After spinning at 1200 RPM for 3 minutes, the supernatant was removed and the pellet re-suspended in 10ml 10% FCS DMEM. The cells were transferred to a T25 flask and incubated at 37°C with 5% CO_2.

2.2.2 Reverse siRNA transfection

siRNA stocks

ON-TARGET plus and siGENOME siRNAs, all purchased from Dharmacon, were diluted in RNase free water and 5X siRNA buffer to make a stock of 20mM.

6 well plate transfections

3µl of 20µM siRNA was added to 250µl of DMEM and 4µl of RNAiMAX was added to 250µl of DMEM. These were left to incubate for 5 minutes at room temperature. RNAiMAX-DMEM mix was added to the siRNA-DMEM mix and these were left to complex for 30 minutes at room temperature. This complex was pipetted to the bottom of the well before adding cells. 200,000 cells were seeded in 1ml of 10% FCS DMEM and a further 500µl of 10% FCS DMEM added. The total well volume was 2ml. The final siRNA concentration was 30nM in each well. The plate was left to incubate for 24/48/72 hours at 37°C with 5% CO_2, before harvesting for a western blot.

96 well plate transfections

For each column on a 96 well plate, 1.9 µl of 20µM siRNA was added to 125µl of serum free SFM and 3µl of RNAiMAX was added to 125µl of SFM. These were left to incubate for 5 minutes at room temperature. RNAiMAX-SFM mix was added to the siRNA-SFM mix and these were left to complex for 30 minutes at room temperature. 25µl of this complex was pipetted to the bottom of the well. Cells were seeded in 100µl of 10% FCS DMEM. The final siRNA concentration was 30nM/well. The plate was left to incubate for 48 hours at 37°C with 5% CO_2, before the addition of various drugs as specified in results. Cytotoxicity was then analysed using 3-(4,5-Dimethylthiazol-2-yl)-2,5-Diphenyltetrazolium Bromide (MTT) and an average was taken across 6 inner wells in a column.

384 well plate transfections

1.25µl of 20µM siRNA was diluted in 8.75µl of RNase free water, giving a concentration of 2.5µM. 9µl of 2.5µM siRNA was added to 141µl of RNase free water to give a siRNA concentration of 150nM. 5µl of 150nM siRNA was added to

each well of a 384 well plate, followed by 0.06µl of RNAiMAX in 5 µl of SFM. This mix was left to complex for 30 minutes at room temperature. 400 T98G cells in 15µl of 10% FCS DMEM were seeded in each well of the plate which was then left at room temperature for 60 minutes in order to reduce edge effects . The plate was incubated for 48 hours at 37°C with 5% CO_2. 25µl of 10% FCS DMEM was added to each well to dilute out the siRNA and 50µM temozolomide was added where necessary. Cells were then incubated for a further 5 days, before fixing and staining ready for imaging.

2.2.3 siRNA and Drug Screen Timings

Both the siRNA and small molecule drug screens were 7 day assays conducted in 384 well plates as outlined in figure 2.1. Following a 48 hour transfection or drug treatments, cells were then incubated with temozolomide for 5 days (Patil et al., 2014).

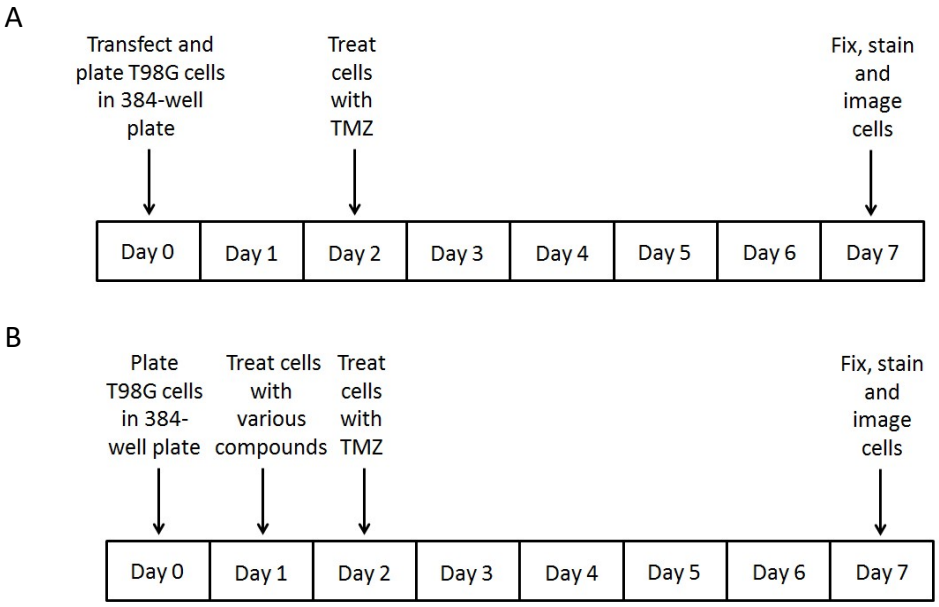

Figure 2.1: siRNA and Drug Screening procedure

Cells were reverse transfected with siRNA and plated on day 0. Following a 48 hour knock down, RNAi was diluted and TMZ was added for 5 days. Cells were then fixed in 4% PFA with 5µg Hoescht/ml, imaged and analysed (A).

Cells were plated on day 0. 24 hours later, cells were then treated with various compounds using a LabCyte Echo 500 machine. 24 hours after the first treatment TMZ was then added using a LabCyte Echo 500 machine for 5 days. Cells were fixed in 4% PFA with 5µg Hoescht/ml, imaged and analysed (B).

2.2.4 384 Well Plate Fixing, Staining and Imaging

384 well plates were washed 3 times in 50µl of PBS/well using a ELx405 Select Deep Well Washer. Cells were fixed and stained in 5µg of Hoescht/ml in 4% PFA for 20 minutes in the dark at room temperature. Plates were washed 3 times in 50µl of PBS/well, with the final 50µl remaining in the well. Plates were then sealed using a PlateLov Velocity 11 and imaged on a Molecular Devices ImageXpress Micro high content microsope at a 2X objective. One image was taken per well and a Multi Wavelength Cell Scoring application on MetaXpress was used to analyse the images.

2.2.5 RNA Studies

RNA Extraction

Qiagen RNeasy Mini Kit was used to extract RNA from cultured cells. Media was removed and cells were washed in PBS before 350µl of RLT Buffer was added to each well of a 6 well plate. The cells were scraped off the well and placed into a QIAshredder before being centrifuged for 2 minutes. 350µl of 70% ethanol was added to the supernatant which was then transferred to an RNeasy minispin column and centrifuged for 15 seconds. 700µl of RWI buffer was added to the column which was centrifuged for a further 15 seconds. This was repeated twice with 500µl of RPE buffer with the final centrifugation step being 2 minutes. Finally the RNA was eluted with 50µl RNase free water. Total RNA levels in each sample were quantified using the Nanodrop ND 1000 Spectrophotometer.

Reverse Transcription

RNA samples were reverse transcribed using the TaqMan™ Reverse Transcription Reagents (table 2.10) ready for qPCR. Each sample was made up to 25µl with 200ng of RNA and ddH_2O. These samples were then amplified on a PCR machine, making cDNA from the extracted RNA (table 2.11).

Table 2.10: TaqMan™ RT-PCR Master Mix

Reagent	Quantity
dNTPs	5.5µl
$MgCl_2$	5µl
Random Hexamers	1.25µl
RNase Inhibitor	0.5µl
Multiscribe RTase	0.625µl
10X Buffer	2.5µl

Table 2.11: RT-PCR Programme for cDNA		
Step	**Temperature (°C)**	**Minutes**
1	25	5
2	48	60
3	95	5
4	4	-

RT-qPCR - Relative mRNA Expression

cDNA samples generated from extracted RNA were run in triplicate on a 384 well PCR plate. Each reaction was made up of: 2µl of cDNA, 5µl of TaqMan™ Universal PCR Mastermix, 2.5µl of ddH_2O and 0.5µl of probe (table 2.7). GAPDH was run as a control for each sample. After sealing, the plate was run on a 7900 Real Time-PCR machine with FAM filter and 40 repeats settings. Double delta Ct ($2^{-\Delta\Delta CT}$) analysis was used to determine gene expression and calculate siRNA knockdown using an average Ct value from the triplicate runs.

Example:

$\Delta\Delta CT = \Delta CT$ (Target Probe $_{\text{target siRNA transfected}}$ – GAPDH Probe $_{\text{target siRNA transfected}}$) – ΔCT (Target Probe $_{\text{non-targeting siRNA transfected}}$ – GAPDH Probe $_{\text{non-targeting siRNA transfected}}$)

Fold change = $2^{-\Delta\Delta CT}$

% Knockdown = $(1-(2^{-\Delta\Delta CT}) *100$

2.2.6 Western Blotting

Protein Extraction and Quantification

Cells previously transfected and seeded in a 6 well plate were washed twice in PBS and 100µl of lysis buffer (table 2.12) was added to each well. Cells were harvested from the plate using a cell scraper and transferred to an eppendorf, vortexed and then left to lyse for 30 minutes on ice. The cells were centrifuged at 15,000G for 15 minutes at 4°C and the supernatant was then transferred into fresh eppendorfs. 4X NuPage LDS Loading Buffer and 5mM DTT were added to the lysates which were boiled for 5 minutes at 95°C and then stored at -20°C until required.

Table 2.12: Lysis Buffer		
Reagent	**Stock**	**Amount for 5ml**
50mM Tris pH 8.0	1M	250 µl
200mM NaCl	5M	200 µl
1% Triton X-100	100%	50 µl
1mM DTT	1M	5 µl
1mM EDTA	500mM	10 µl
Benzonase	25U/ml	10 µl
PIB	10x	500 µl
Phos. Inhibitors	100x	50 µl
ddH2O	-	3.97 ml

39µl of ddH_2O and 1µl of protein lysate were added to a well of a 96 well, in triplicate. 200µl of Protein Assay Dye Reagent Concentrate (BioRad), diluted 1:5, was then added to the wells. Optical Density (OD) was read at 595nm on a Multiskan FC, Thermo Scientific spectrophotometer. The protein standard curves, which were made using bovine serum albumin (BSA), were used to quantify protein concentration by solving the linear quadratic equation y = mx + c, where m is the slope gradient and c is the y-intercept.

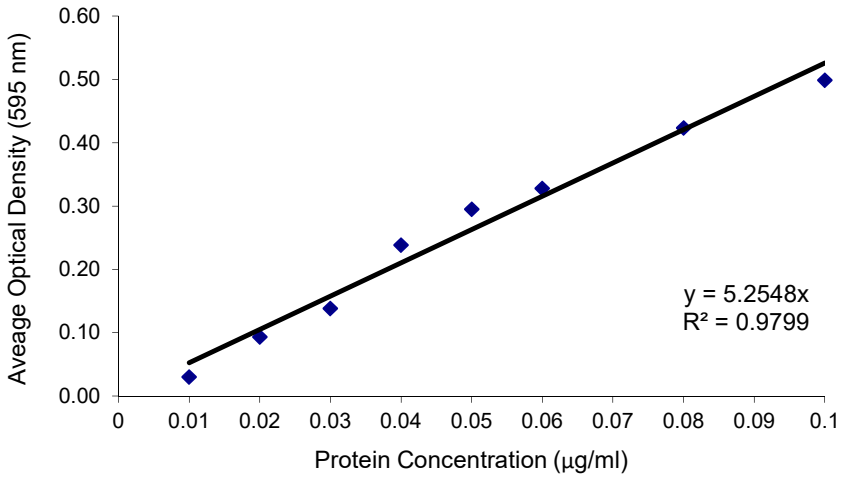

Figure 2.2: BSA titration standard curve
The standard curve created from BSA standards was used to calculate protein concentration.

SDS-PAGE and Western Blotting

10 or 15 well NuPAGE 4-12% Bis-Tris gels were used for western blotting. 50µg of protein and 4X NuPage LDS Loading Buffer were loaded on to the gels. 5µl of 1X SeeBluePlus2 Prestained Standard was also loaded beside the protein samples as a molecular weight reference. Any empty wells were loaded with 5µl of 4X NuPage LDS Loading Buffer. The samples were electrophoresed in Mini PROTEAN Tetra Cells, using 1X NuPage Running Buffer, at 150V for 90-120 minutes. Protein from the gels was transferred to nitrocellulose membranes at 100V for 120 minutes in Mini PROTEAN Tetra Cells, using 1X NuPAGE transfer buffer. Membranes were blocked for 60 minutes in 5% milk dissolved in PBS-T. Membranes were incubated with primary antibodies overnight at 4°C. After 3 washes in PBS-T, membranes were incubated with secondary antibodies conjugated to HRP at a concentration of 1:1000. Membranes were again washed 3 times in PBS-T and then visualised using Pierce ECL western blotting substrate. The membrane were developed using medical x-ray film and a Konica SRX 101A Processor.

2.2.7 Clonogenic Survival Assay

Cells were seeded at various densities in 10cm plates in 10ml of 10% FCS DMEM. After a 24 hour incubation period which enabled the cells to adhere, each plate was either drug or DMSO treated in triplicate, as specified in the results.

The cells were grown for 21 days before the media was removed and methylene blue (0.4%) was used to stain the colonies. Following 30 minutes incubation, methylene blue was removed and any excess was washed from the plates in warm water. The colonies were counted and the plating efficiency (PE) was calculated by the average number of colonies counted on the DMSO treated control plates divided by the number of cells plated. The survival fraction (SF) was then calculated by the number of colonies counted/ number of colonies plated multiplied by the PE.

2.2.8 3-(4,5-Dimethylthiazol-2-yl)-2,5-Diphenyltetrazolium Bromide (MTT) Cytotoxicity Assay

If un-transfected, cells were plated in 100µl of 10% FCS DMEM per well of a 96 well plate or in 125µl of 10% FCS DMEM per well of a 96 well plate if siRNA transfected. The seeding densities had previously been optimised to yield a linear relationship between OD_{540} and cell number. Cells were incubated for 24 hours or 48 hours prior to the addition of various drugs at different concentrations (6 wells/concentration), as specified in results. 6 or 7 days after plating (as specified in results), 50µl of

3mg/ml MTT diluted in PBS, was added to the cells. Following a 3 hour incubation period, media was removed using a pipette and the purple formazan precipitate dissolved in 200µl of DMSO. OD values were read at 540nm on a Multiskan FC plate reader. The survival fraction was calculated from an average taken from 6 replicates compared to DMSO treated or DMSO treated and non-targeting siRNA transfected controls.

2.2.9 Flow Cytometry

Annexin V and Propidium Iodide (PI)

Annexin V and PI are used as a dual stain to determine whether cells are apoptotic, necrotic or healthy. Healthy cells have an intact membrane and do not take up either dye. Annexin V has a high affinity for phosphatidylserine which is relocated to the outer membrane of a cell during early apoptosis. If annexin V is conjugated to a fluorescent marker such as FITC (fluorescein isothiocyanate) then apoptotic cells can be detected using fluorescent activated cell sorting (FACS). PI is naturally fluorescent and intercalates in between base pairs of double strand DNA. If a cell is necrotic it does not have an intact membrane and therefore PI is able to access the DNA where it can bind. This can also be detected using FACS (ThermoFisherScientific, 2018). After cells were plated in 10cm dishes and drug treated in triplicate, they were collected at various time points specified in results. Media was removed and cells were washed twice in PBS before 2ml of trypsin was added. Both media and PBS washes were retained. Following detachment, cells were collected in 5ml of PBS which was added to the media and PBS washes. This was then centrifuged at 1,200 rpm for 3 minutes. Following removal of the supernatant, the cell pellet was washed in 10ml of PBS. Cells were re-suspended in 100µl of 1x annexin V binding buffer before 5µl of both annexin V and PI were added. Cells were left to incubate for 15 minutes. 400µl of 1x DNA binding buffer was added to each sample before being analysed on the FACSCalibur. FITC Annexin V apoptosis detection kit (BD Biosciences, 556547) was used. FlowJo was used to analyse the results.

2.2.10 Immunofluorescence

Immunofluorescence (IF) was used to detect DNA damage within the cells via markers such as: 53BP1, DNA-PKcs (s2056) and RAD51. Cells were seeded (20,000 in 500µl of 10% FCS DMEM) on glass coverslips in 24 well plates in triplicate. Following 24 hours for the cells to adhere, they were treated with various drugs as specified in the results. Following drug treatment, cells were permeablised in

Triton-X100 for 1-3 minutes before being fixed in 4% PFA for 10 minutes. Cells were then blocked in 10% FCS for 1-2 hours. Primary antibodies diluted in 2% FCS were added to each well and left over-night at 4°C. The following day, cells were washed thoroughly with PBS before the secondary Alexa-Fluor antibodies (made in 2% FCS) were added for 1-2 hours at room temperature in the dark. The cells were washed in PBS alone, washed in DAPI made up in PBS (1µg/ml) and washed again in PBS alone. Cells were then washed in ddH_2O before being mounted using immu-mount (Thermo). Slides were imaged on a Nikon Eclipse TE200 Fluorescent Microscope. Images were scored by counting the foci of around 100 nuclei for each condition in an experimental repeat or as a percentage of total cells visible in each field of view over multiple fields across each slide.

IF was also used to detect methylation of guanine at O6 using O-6-methyl-2'-deoxyguanosine antibody. Following seeding and drug treatment, cells were washed in PBS before being fixed in 4% PFA for 10 minutes. Cells were washed and then 2.5M HCl was used to denature the DNA for 30 minutes. Cells were washed and then permeablised in 0.5% Triton-X100 in PBS for 15 before being blocked in 3% BSA made in PBS for 1-2 hours. Cells were incubated with primary antibody (1:100) over-night at 4 °C. Day 2 followed the same protocol as the standard IF above.

2.2.11 Alkaline Comet Assay

Alkaline comet assays are used to detect single strand DNA breaks. Following lysis which leaves DNA unharmed, a current is applied to the DNA suspended in agarose. The more breaks in the DNA, the further it will migrate through the agarose (negatively charged DNA migrates to positive cathode). Once a nucleotide stain is applied, the DNA 'tails' can be visualised using fluorescent microscopy (Ostling and Johanson, 1984). A Trevigen comet assay kit was used and instructions were followed. Cells were suspended in agarose, lysed in lysis buffer provided (triton-X100 and 2.5M NaCl) for an hour at 4°C. The lysis buffer enables the DNA to form supercoiled loops which appeared as the heads of the comets. The DNA nucleoids were then exposed to alkaline unwinding buffer before the gels were run at 21V for 30 minutes in an electrophoresis buffer. Slides were dipped in 70% ethanol before being dipped in ddH_2O and left to dry. SYBR Gold (1:30000) nucleotide stain was used to stain the DNA. 50 cells in each condition were imaged using FITC channel and 20x lens on a Nikon Eclipse TE200 Fluorescent Microscope. Tail moment, calculated by TriTek Comet Score software, was used as a measure of DNA damage severity, combining tail length and intensity of DNA within the tail (AMSBiotechnology, 2010).

2.2.11 Immunohistochemistry

Fixing and Embedding cell pellets

To prepare a cell line pellet for immunohistochemistry (IHC), cells were reverse transfected as before (2.2.2 Reverse siRNA transfection) however, transfections were scaled up into a T75 flask. Control or ERK5 siRNA from siTOOLS™ was used over a 48 hour transfection, and each flask had a final concentration of 10nM siRNA. Following transfection, cells were washed with PBS, detached using 2ml of trypsin EDTA, re-suspended in PBS and pelleted at 1200 RPM for 2 minutes in a 50ml falcon tube. Cells were then washed twice with 10ml of PBS before being pelleted again. 1ml of 4% PFA was used to re-suspend and then fix the cells for 10 minutes at room temperature. Cells were then pelleted in a 1.5ml eppendorf before PFA was removed. The cell pellet was then encased in molten 2% agarose before being stored in 70% ethanol until processing. The following steps were all completed by Maggie Glover (Technician in the Department of Oncology and Metabolism within the University of Sheffield). Leica TP 1020 tissue processor was used to automatically process the pellets. An alcohol concentration gradient was used to dehydrate the cells, xylene was used to clear the cells and finally molten wax under vacuum was used to fill the cells. Processed cell pellets were then embedded in wax using a Leica EG1150 wax embedder before being sectioned at 5 microns using a Leica RM2245 Microtome.

IHC staining protocol

Both cell pellets and commercial tissue microarrays (TMAs) underwent the following IHC staining protocol.

Slides were submerged in xylene for 10 minutes followed by 100% ethanol for 10 minutes. Slides were then placed in 95% ethanol for 3 minutes. 30ml hydrogen peroxide in 270ml of 100% methanol was then added to the slides for 30 minutes in order to exhaust the samples of natural peroxidases. Slides were then placed in Dako Target Retrieval Solution (pH 6) made up 1:10 in ddH2O in a pressure cooker for a 20 minute heat cycle, in order to break methylene bonds formed during formalin fixing and make the epitopes available again for antibody binding. Slides were then washed in PBS-T before being blocked in 10% goat serum made up in 1% BSA Triton-X100 in PBS for an hour. Primary antibody (anti-ERK5) made up in 2% goat serum was added to the slides which were left to incubate over-night at 4°C. Slides were washed in PBS-T before the secondary antibody (biotinylated goat anti-mouse) was added to the slides 1:200 made up in 1% BSA in PBS-T for 1 hour. Slides were washed with PBS-T and then Avidin-Biotin Complex (ABC) (Vector Laboratories) was added to the slides for 30 minutes. ABC contains tetravalent avidin and biotinylated HRP, which are complexed in equal ratios prior to being added to the slides, resulting in 3 HRP molecules bound to 1 avidin molecule at the

site of the biotinylated secondary antibody. This is used to intensify the target antigen signal. DAB substrate (3,3'-diaminobenzidine)(Vector Laboratories), along with hydrogen peroxide, was added to the slides for 30 seconds. DAB is oxidized by hydrogen peroxide and catalysed by HRP resulting in a brown insoluble precipitate at the site of the antibody-HRP complex. A secondary antibody alone was used as a negative control. Tap water was used to stop the DAB reaction and slides were then dehydrated in alcohol before being cleared in xylene and then mounted using DPX Mountant (sigma).

The following human paraffin embedded TMAs were purchased from US Biomax: GL481, BS17016b and BS17016c.

2.2.12 Statistical Analysis

Statistical analysis was performed using Microsoft Excel or GraphPad Prism 7, however, Dr Stephen Brown, who analysed the results from the siRNA screen, used R. Means and standard deviation were calculated from 3 experimental repeats where possible. Non-parametric tests were used to analyse the data: Mann-Whitney U Tests (t-test) or Kruskal-Wallis H Tests (one way ANOVA) with Dunn's correction for pairwise comparison for individual p-values were used.

Chapter 3 – siRNA Kinome Screen in Temozolomide resistant GBM cells

3.1 Introduction

In 2004, 291 mutated genes were identified as 'cancer genes'. Protein kinases were predicted to make up only 2.16% of the oncogenic genes identified, however, they were found to make up 9.28%, more than four times the original prediction (Futreal et al., 2004). Not only have protein kinases have been shown to be causal in cancer development, they also have enzymatic activity which requires ATP binding to an active site in order to function, making them attractive drug targets (Bhullar et al., 2018).

Imatinib was the first protein kinase inhibitor to be FDA approved for treating cancer in humans. Imatinib is a tyrosine kinase inhibitor used to treat patients with chronic myeloid leukaemia (CML), a blood cancer causing uncontrolled division of white blood cells (Roskoski Jr., 2003). The fusion gene *BCR-Abl,* which characterises CML, is formed when Abelson Leukaemia Virus (ABL) kinase is translocated to Breakpoint Cluster Region (BCR) on chromosome 22, generating the shortened Philidelphia chromosome (de Klein et al., 1982). Imatinib is effective at treating patients with CML as it inhibits *BCR-Abl* kinase activity, a mutation which is present in 95% of patients (Roskoski Jr., 2003). Since this initial approval for Imatinib, 37 protein kinase inhibitors targeting cancer have been approved by the FDA (Bhullar et al., 2018). It is not only the 'druggability' of kinases which makes them attractive targets, inhibition of master regulator kinases also unlocks the potential to target subsequent downstream signalling pathways which may be fundamental to the development and progression of cancer (Manning, 2009).

Given this previous success and the potential to target complex signalling networks combined with the fact GBM patient survival has remained unchanged for decades (Manning, 2009, Stupp et al., 2005), a kinome-wide siRNA screen was chosen to investigate the hypothesis 'inhibition of yet to be identified targets/pathways will enhance the cytotoxic effects of temozolomide in Glioblastoma Multiforme'.

Data from a previous siRNA screen conducted in GBM cells was published by another research group in 2012, who investigated synthetic lethality in GBM using a combination of siRNA and temozolomide, with a focus on resistance to alkylation damage (Svilar et al., 2012). Temozolomide resistant GBM cells, were reverse transfected with targets from the Ambion Silencer Druggable Genome siRNA Library (Version 1.1) (final conc. 20nM) for 5 hours, incubated for a further 48 hours (in fresh media) to allow knock-down of targets and finally treated with 1mM temozolomide for 24/48 hours. Cell viability was assessed by a redox reaction.

Bacteria, yeast and human cells were used to try to identify novel targets important in resistance to alkylation. A ubiquitin ligase (E3B) and DNA repair protein (UNG) showed interesting results, however, some initial findings in yeast did not translate into human cells (Svilar et al., 2012). A previous siRNA screen investigating GBM survival genes was also conducted by the same group and published prior to their temozolomide screen. Here they identified 55 genes which also showed a particular enrichment in proteasomes and the ubiquitin degradation pathways (Thaker et al., 2009).

Temozolomide causes methylation damage to several DNA bases, however, the most toxic O-6-methylguanine lesion accounts for less than 8% of the total lesions formed (Kaina et al., 2007). Methylation of O-6 guanine is either directly repaired by MGMT or if unrepaired, the methylated guanine can be incorrectly paired with thymine. Mismatch repair (MMR) recognises this incorrect pairing and removes the newly paired base on the complementary strand so O-6-methylguanine remains on the parental strand of DNA. The methylated base is then re-paired with thymine and the futile cycle of MMR continues resulting in single strand gaps or breaks in DNA eventually causing apoptosis. Second round synthesis can also result in GC to AT transitions when the mispaired T is used as a template (Friedman et al., 2000). GBMs rapidly become resistant to temozolomide treatment, reflected by the complete lack of response to a second cycle of temozolomide in more than 90% of recurrent GBM cases (Oliva et al., 2010). Resistant cells can have increased MGMT expression or may have inactivating mutations in MMR proteins (e.g. mutS homolog 6) limiting MMR induced apoptosis (Cahill et al., 2007, Sarkaria et al., 2008). However, a trial inhibiting MGMT activity did not show promising results in a Phase II trial; failing to increase sensitivity to temozolomide and causing haematological toxicities (Quinn et al., 2009).

Therefore, to provide novel, relevant and potentially druggable hits, an siRNA screen was carried out in the temozolomide resistant T98G cell line using the Dharmacon™ On-TARGETplus (OTP) Protein Kinase SMARTpool siRNA Library.

3.2 RNAi Screen Optimisation

3.2.1 Temozolomide Sensitivity in GBM Cells

T98G cells are a GBM cell line resistant to temozolomide treatment. These cells have an un-methylated MGMT promoter (MGMT +ve), resulting in an increase in levels of the enzyme MGMT which facilitates efficient repair of toxic lesions caused by temozolomide. Patient tumours with an un-methylated MGMT promoter are also temozolomide resistant and account for up to 45% of malignant glioma cases

(Thon et al., 2013). The initial siRNA screen was conducted in T98G cells, however, pan-GBM clinical applicability of candidate genes was ensured by additional validation studies in the temozolomide sensitive GBM cell lines U-87 (MGMT –ve) and U-251 (MGMT –ve) and TP53 mutant GBM cell line LN-18 (MGMT +ve) (figure 3.1A).

To determine a non-toxic dose of temozolomide to be used in the siRNA screen, T98G cells were treated with increasing doses and cell viability was assessed by MTT cytotoxicity assays 5 days after the addition of temozolomide (figure 3.1B). Combining both a non-toxic dose of temozolomide (50µM) and non-toxic siRNA would ideally enable us to detect any potential hits more easily as the cells treated with temozolomide or siRNA alone would have cell viability comparable to control siRNA treated cells e.g. synthetic lethality/induced cytotoxicity.

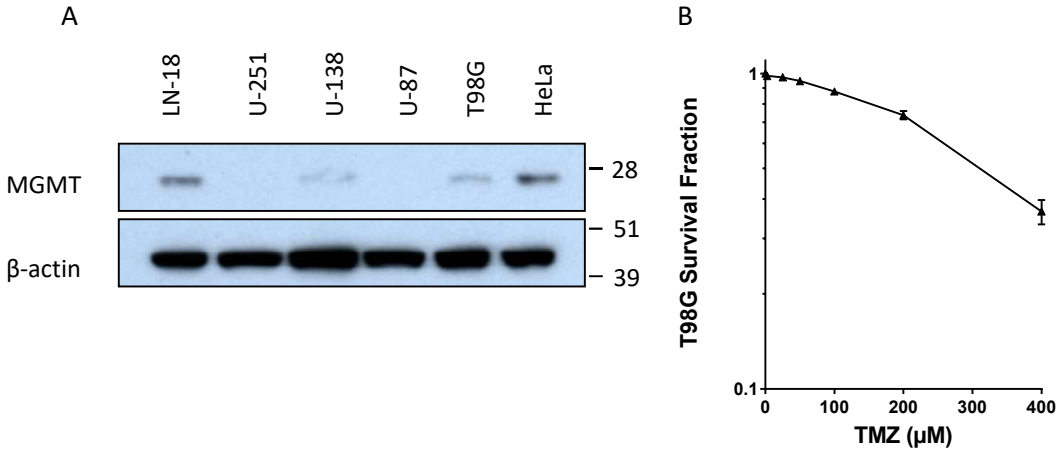

Figure 3.1: MGMT status of cell lines and cytotoxicity curves in TMZ treated T98G cells

Cells were plated and allowed to adhere for 24 hours. Untreated cells were collected for western blotting (A). Western blotting showed T98G, LN-18, U-138 and HeLa cells express varying amounts of MGMT. β-actin was used as a loading control. Following plating, T98G cells were treated with a range of doses of TMZ (0-400µM) prior to incubation for 5 days before an MTT assay was performed (B).

Data shown is the average surviving fraction (normalised to DMSO treated control) +/- standard deviation derived from three independent biological repeat experiments.

Western blot was completed by Connor McGarrity-Cottrell, 2nd Year Undergraduate Student from Sheffield Hallam University.

To transfect T98G cells within the Collis Lab, the transfection reagent RNAiMAX is used, however, the Sheffield RNAi Screening Facility (SRSF) recommends the use of Dharmafect 1 (DF1) for all cell lines. In order to determine which of these reagents was most efficient, FANCD2 was depleted over 24 and 48 hours using previously validated siRNA complexed with either transfection reagent. Inhibiting the Fanconi Anaemia (FA) pathway has previously been shown to increase the sensitivity of

GBM *in vitro* to treatment with temozolomide, with over-expression of FANCD2 protein seen in HGGs (Patil et al., 2014).

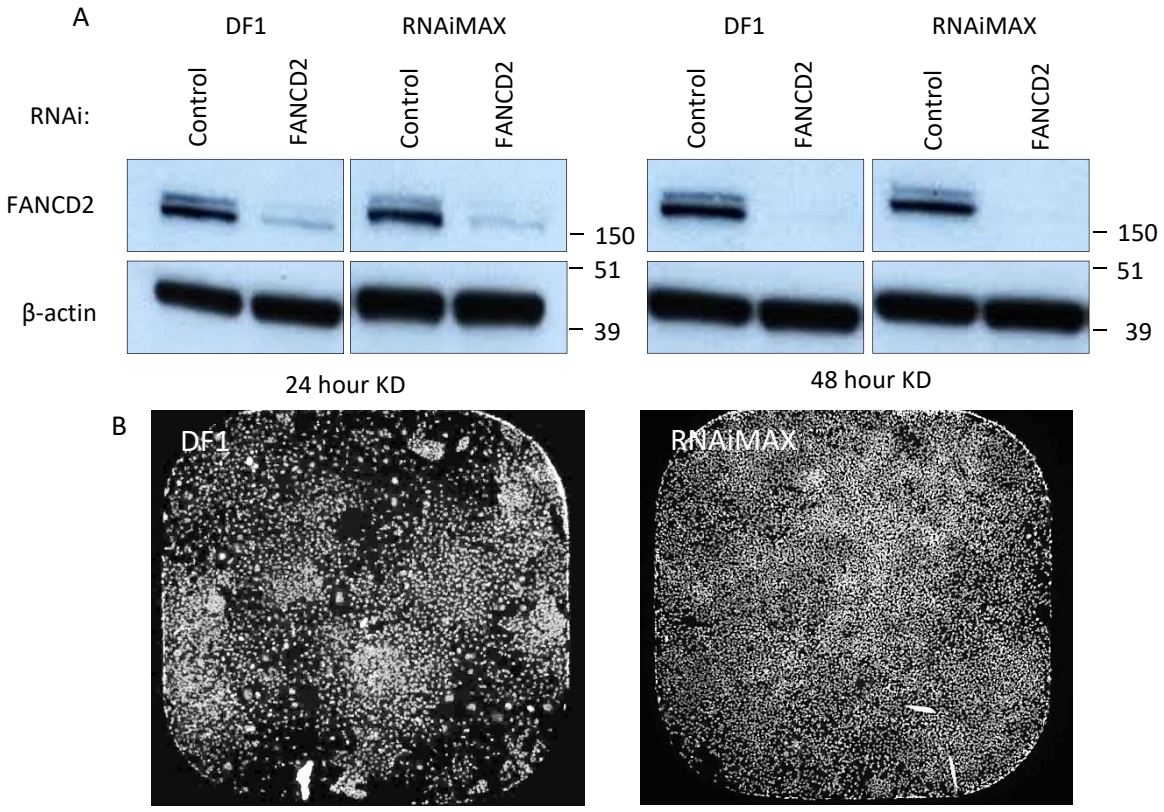

Figure 3.2: FANCD2 depletion and cell viability using DF1 and RNAiMAX
Effective knock-down of FANCD2 protein in T98G cells can be seen using both RNAiMAX and DF1 as transfection reagents over 24 and 48 hours via western blot. β-actin was used as a loading control (A). T98G cells were reverse transfected with control siRNA in a 384 well plate. 48 hours later, cells were fixed in PFA and stained with Hoechst and wells were imaged on a 2x objective (B).

From the western blots (figure 3.2A) both RNAiMAX and DF1 equally depleted cells of FANCD2 protein, with a 48 hour transfection generating a more effective knock down. Images taken from a 384-well plate (figure 3.2B) of T98G cells transfected with non-targeting siRNA showed an increased in cytotoxicity when DF1 was used and therefore RNAiMAX was determined to be the best transfection reagent for T98G cells and was selected for use in the siRNA screen.

3.2.3 Positive and Negative Controls

Experimental controls are needed to ensure that the results generated are due to the variable being tested. A negative control, in this case the non-targeting siRNA, was used to generate a reference point showing little or no effect, to which all

other results could be compared to. Dharmacon™ recommends the use of On-TARGETplus (OTP) siRNA over siGENOME (Dharmacon™, 2018). OTP non-targeting negative control siRNAs have been shown to have reduced off target effects compared to 'scrambled' control siRNA following microarray analysis 24 hours post-transfection, which is thought to be due to seed-region optimisation and dual strand modifications (Dharmacon™, 2018). SRSF also recommends completing the first siRNA screen using OTP as it is less toxic in the majority of cell lines when compared to siGENOME, therefore giving the best chance of identifying potential hits.

The non-targeting negative control siRNA is made up of a pool of 4 different combinations of siRNA and occasionally one of these 'non-targeting' siRNAs can have an off target cytotoxic effect. To test the effect of these siRNAs on T98G cells, the pool was deconvolved so any potential cytotoxic effects would be highlighted. As there was no significant difference in the number of cells counted for the control pool when compared to each individual siRNA (figure 3.3), the pool of non-targeting negative control siRNA was chosen for use in the siRNA screen.

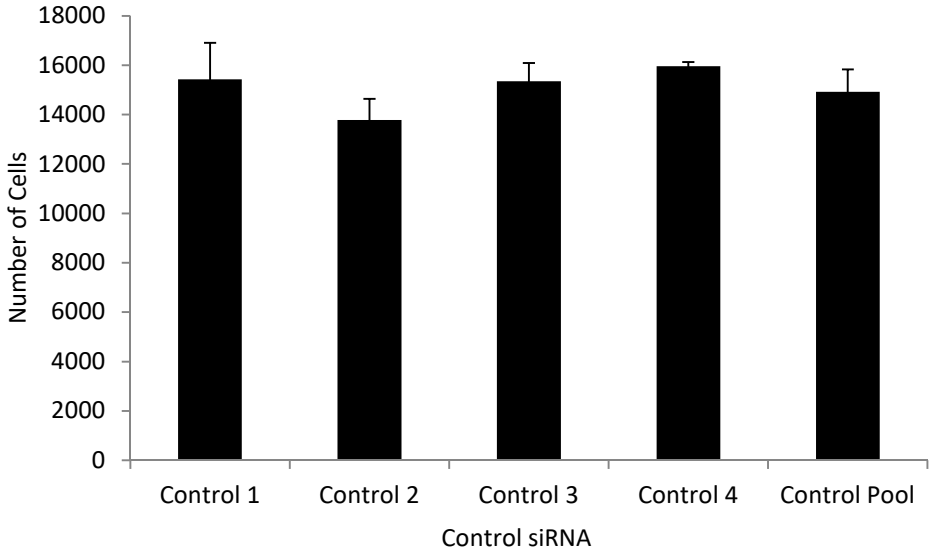

Figure 3.3: Effect of 4 individual non-targeting negative control siRNAs and non-targeting negative control pool siRNA

T98G cells were reverse transfected with non-targeting negative control siRNA for 48 hours in a 384-well plate. Following dilution of the siRNA, the cells were then incubated for a further 5 days. Cells underwent staining, fixing and imaging and wells were analysed using a Multi Wavelength Cell Scoring application on MetaXpress which counted cells based on minimum and maximum microns and intensity above background.

There was no significant difference in the number of cells counted for each individual non-targeting negative control siRNAs compared to each individual control siRNA and the pool (Kruskal-Wallis H Test).

Data shown is the average surviving fraction +/- standard deviation derived from three independent biological repeat experiments.

A positive control shows a positive result can be generated using the experimental method, and any negative results are not due to the experimental procedure, but other factors.

In order to identify a suitable positive control, potential targets were selected based on previously published data (Alagoz et al., 2013, Liu et al., 2008, Newlands et al., 1997, Patil et al., 2014). Depleting cells of PARP-1, TDP-1 and FANCD2 significantly sensitised T98G cells to treatment with 50µM temozolomide (figure 3.4). MGMT, however, when used in combination with temozolomide caused a much more significant increase in cell death and was therefore chosen as a robust positive control.

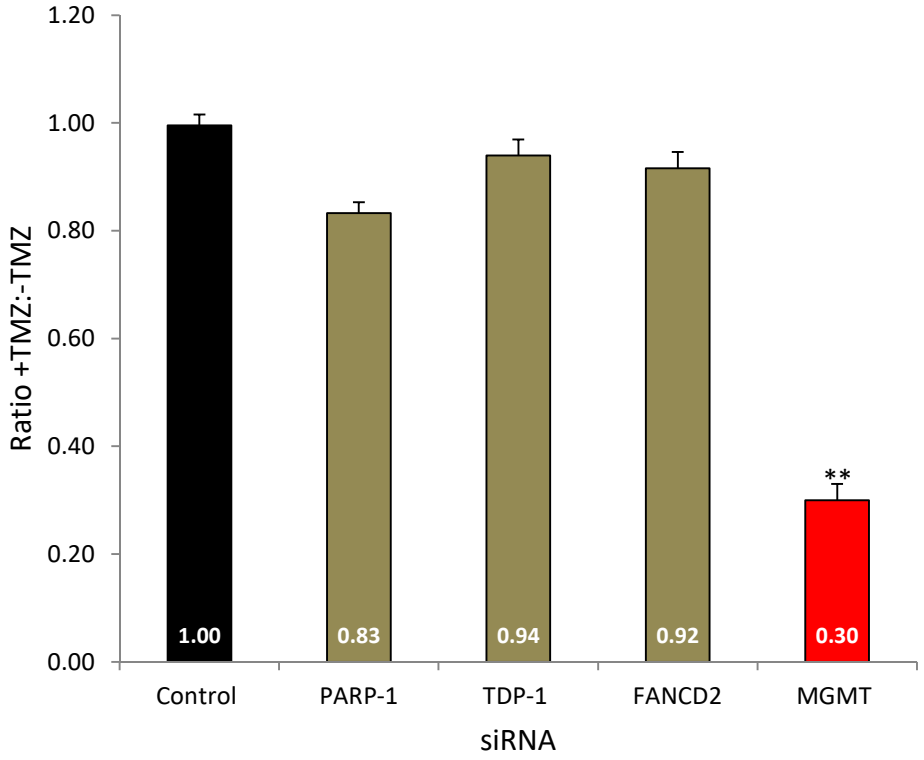

Figure 3.4: Identification of a positive control for the TMZ sensitisation screen in T98G cells
T98G cells were reverse transfected with non-targeting negative control siRNA or a potential positive control siRNA for 48 hours in a 384-well plate (PARP-1, TDP-1, FANCD2, MGMT). Following dilution of the siRNA, half of the wells were then treated with 50µM TMZ or DMSO for 5 days. Cells underwent staining, fixing and imaging and wells were analysed using a Multi Wavelength Cell Scoring application on MetaXpress which counted cells based on minimum and maximum microns and intensity above background.

PARP-1, TDP-1 and FAND2 sensitised T98G cells to treatment with 50µM TMZ, however, MGMT caused a significant increase in cell death and was therefore chosen as the positive control.

Data shown is the average surviving fraction (normalised to control siRNA) +/- standard deviation derived from three independent biological repeat experiments.
***=P<0.005 using a Mann-Whitney U Test.*

The use of PARP-1 inhibitors in combination with temozolomide are currently being investigated in clinical trials for patients with both newly diagnosed and recurrent GBM (ClinicalTrials.gov, 2018), therefore PARP-1 siRNA was a rational positive control target. However, as PARP-1 inhibitors are most effective at killing cells when they are able to trap PARP-1 and not just inhibit the enzyme activity (Murai et al., 2014), the limited cell death induced by PARP-1 siRNA in combination with temozolomide was not too surprising. There is also evidence to support redundancy between PARP-1 and PARP-2, which also may have contributed to the limited death induced by PARP-1 siRNA in combination with temozolomide (Ronson et al., 2018).

Inhibiting the FA pathway has previously been shown to increase the sensitivity of GBM *in vitro* to treatment with temozolomide, with over-expression of FANCD2 protein seen in HGGs (Patil et al., 2014). Depleting cells of FANCD2 did show a trend towards sensitisation, however, not to the extent needed for a positive control. This discrepancy may be due to pan-FA inhibitors being used previously which most likely have unidentified off target effects.

In T98G cells, knocking- down TDP-1 using siRNA has proved effective at increasing the sensitivity of the cells to treatment with temozolomide (Alagoz et al., 2013), however, the increase in cell death was not large enough to be used as a positive control for the siRNA screen.

MGMT encodes for the enzyme O-6-methylguanine-DNA methyltransferase which repairs the DNA damage induced by temozolomide (Agarwala and Kirkwood, 2000, Newlands et al., 1997). Depleting cells of MGMT caused the largest decrease in the number of cells per well and therefore the biggest increase in cell death, hence its selection as the positive control siRNA for the screen. A western blot, (figure 3.5) was conducted to confirm these results were due to the cells being depleted of MGMT.

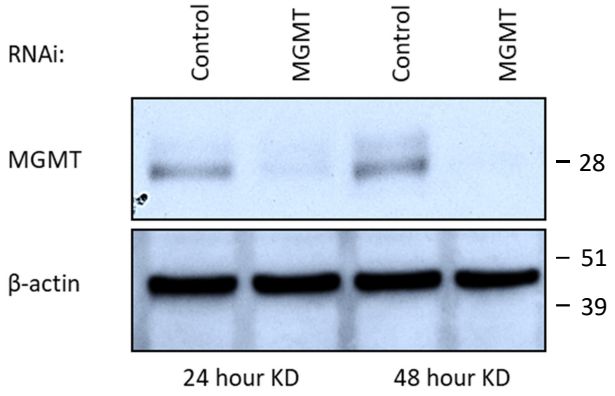

Figure 3.5: Western Blot of 24 and 48 hour knock-down of MGMT using siRNA
T98G cells were reverse transfected and plated in a 6-well plate. Cells were harvested and lysed 24 and 48 hours later. Following western blotting, effective knock-down of MGMT protein was seen at 48 hours. β-actin was used as a loading control.

The z-prime calculation was then used to determine the robustness of the assay using MGMT as the positive control and non-targeting siRNA as the negative control. A z-prime value of greater than 0.5 reflects excellent robustness and reproducibility of the assay. A z-prime score of 0 – 0.5 reflects an acceptable assay and a score of less than 0 is a poor assay, likely to generate many false positive results (Bray and Carpenter, 2017). A z-prime of greater than 0.5 was achieved consistently after automation of cell plating and a general improvement of cell maintenance (figure 3.6).

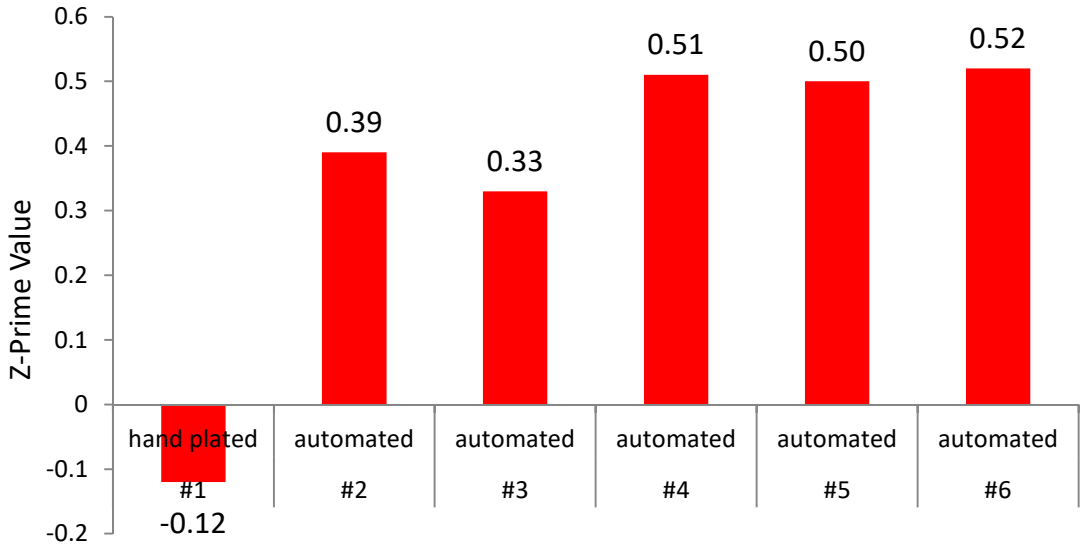

Figure 3.6: Z-prime scores

T98G cells were reverse transfected with non-targeting negative control siRNA or MGMT siRNA for 48 hours in a 384-well plate. Following dilution of the siRNA, all of the cells were then treated with 50µM TMZ for 5 days. Cells underwent staining, fixing and imaging and wells were analysed using a Multi Wavelength Cell Scoring application on MetaXpress which counted cells based on minimum and maximum microns and intensity above background.

Hand-plating cells caused a larger SD between control cells, resulting in a poor z-prime. As plating moved towards automation, the z-prime improved, eventually reaching 0.51.

The z-prime was calculated as $1 - \frac{3(SD\ control\ siRNA\ values * SD\ MGMT\ siRNA\ values)}{mean\ control\ siRNA\ values - mean\ MGMT\ siRNA\ values}$

A z-prime value of ≥ 0.5 was achieved 3 consecutive times (n=3).

3.3 On-TARGETplus Kinome Screen

OTP pooled siRNA was used for the kinome screen which was repeated 3 times in T98G cells transfected with either siRNA alone (to determine any inherent siRNA-mediated cytotoxicity) or siRNA with 50μM temozolomide. The z-prime was calculated for each plate that was treated with temozolomide and all were ≥0.5 (figure 3.7).

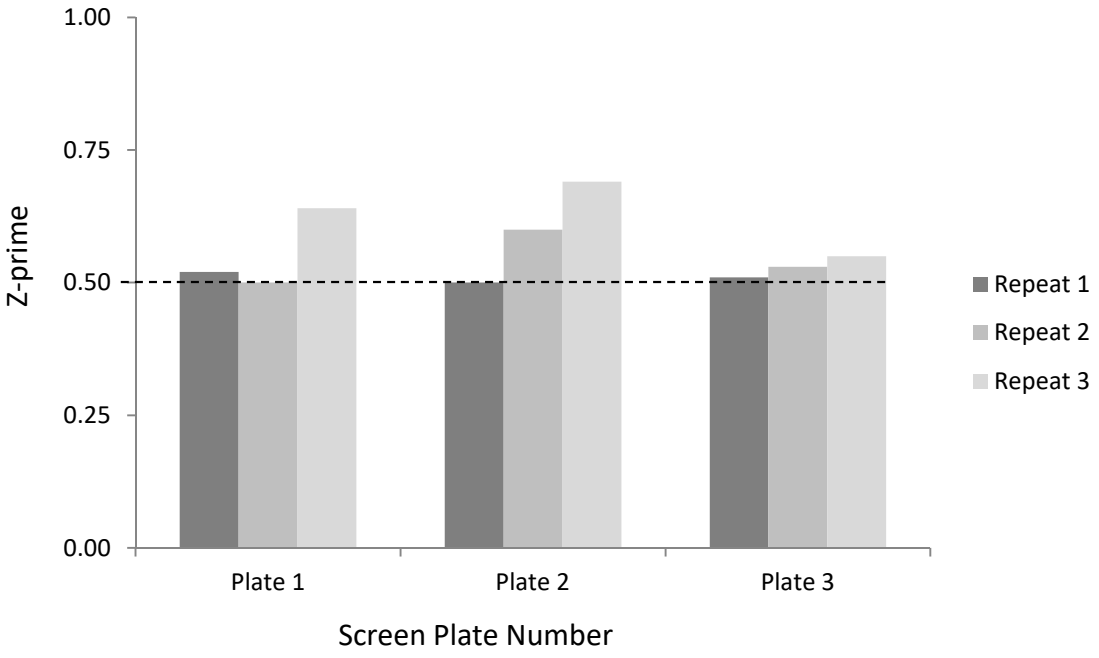

Figure 3.7: Z-prime scores for the TMZ treated plated in the Kinome Screen
A z-prime value of ≥ 0.5 was achieved in all 3 plates when MGMT siRNA was used the positive control for T98G cells treated with TMZ across the 3 repeats (n=3).

The z-prime was calculated as: $1 - \frac{3(SD\ control\ siRNA\ values * SD\ MGMT\ siRNA\ values)}{(mean\ control\ siRNA\ values - mean\ MGMT\ siRNA\ values)}$

Z-scores were generated, by Dr Stephen Brown from the SRSF using R software, for every siRNA target both with and without temozolomide. Wells were each normalised to the appropriate controls on the same plate and then median values were used to generate the z-scores, eliminating the effects any outliers would have if the mean values were used. Z-scores are directly related to standard deviation (SD) and if data are normally distributed, 95.45% will have a z-score of -2 to +2 (Bray and Carpenter, 2017). This enabled us to identify potential hits which were relatively non-toxic alone but when combined with temozolomide the number of viable cells significantly decreased and they generated a z-score close to 0. To be

more stringent with the results, a cut off of <-2.2 was therefore used when the siRNA was combined with temozolomide.

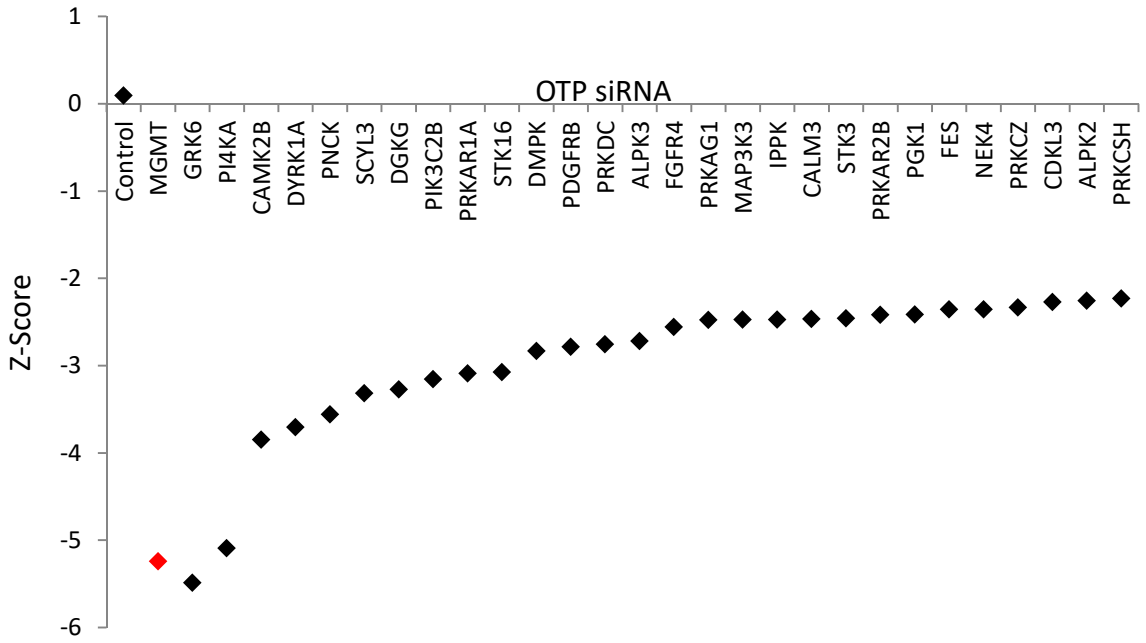

Figure 3.8: Z scores for hits identified in the Kinome Screen

The graph shows the median z-score for the negative and positive controls and potential hits when T98G cells were reverse transfected with siRNA and then treated with 50μM TMZ 48 hours later. Cells underwent staining and fixing following 5 days incubation before wells were imaged and analysed using a Multi Wavelength Cell Scoring application on MetaXpress. This application counted cells based on minimum and maximum microns and intensity above background.

The MGMT positive control generated a z-score of -5.25 (red diamond), which was a lower z-score than all but one of the potential hits. Potential hits were selected based on a z-score of <-2.2 when treated with siRNA and TMZ and >-2 when treated with siRNA alone.

3.4 Hit Validation

3.4.1 Hit Validation – siGENOME Pooled siRNA

siGENOME siRNA was used to validate potential hits that sensitised T98G cells to temozolomide using OTP pooled siRNA. siGENOME siRNA is synthesised differently to OTP siRNA and consists of different target regions within the mRNA, therefore any targets that had the ability to sensitise cells to temozolomide using both siRNAs would have an increased chance of being a 'real' hit and would then be validated further using deconvoluted OTP siRNA.

OTP MGMT siRNA was used in this mini-screen as siGENOME MGMT siRNA was unable to generate a z-prime of >0.5 and could only be used as a weak positive control (figure 3.9). siGENOME MGMT siRNA combined with temozolomide did show a trend towards increased cell death but this did not reach significance (p=0.07). Unfortunately, all of the hits treated with a combination of temozolomide and siGENOME siRNA did not cause a significant increase in cell death when compared to the DMSO treated controls; however, several targets did show a trend of increased death.

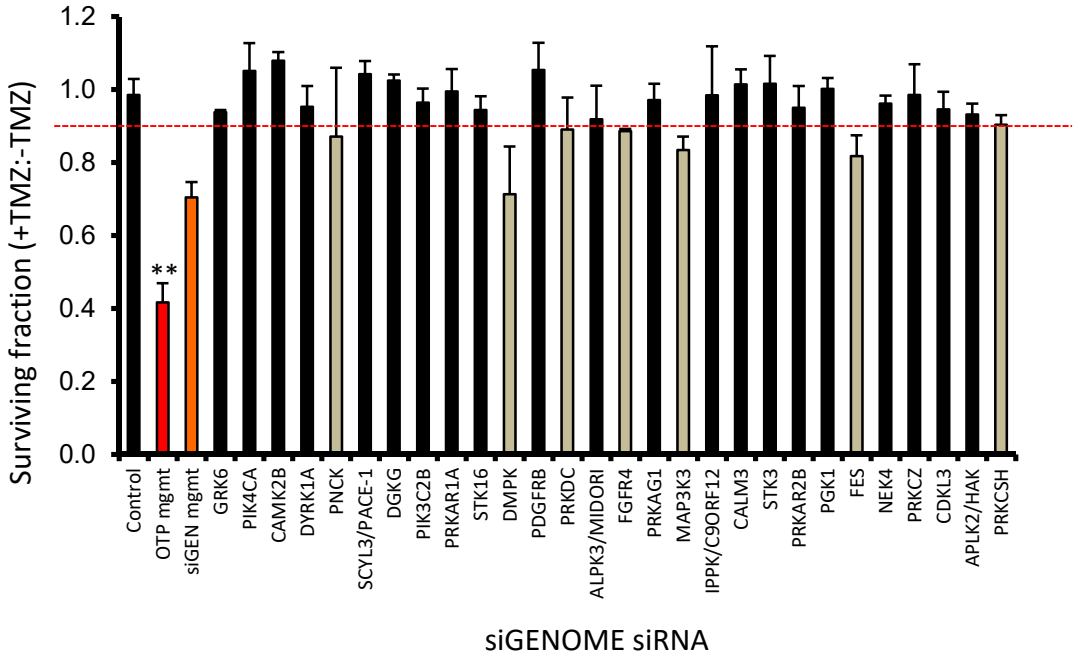

Figure 3.9: Survival Fraction of T98G cells treated with siGENOME siRNA +/- TMZ

T98G cells were reverse transfected with siRNA and then treated with 50μM TMZ 48 hours later. Cells underwent staining and fixing following 5 days incubation. Wells were imaged and analysed using a Multi Wavelength Cell Scoring application on MetaXpress. This application counted cells based on minimum and maximum microns and intensity above background. OTP MGMT siRNA was the only siRNA which caused a significant reduction in the survival fraction (p=0.009). Survival fractions of <90%, shown in the grey bars, were taken forward as positive results.

Data shown is the average surviving fraction (normalised to control siRNA) +/- standard deviation derived from three independent biological repeat experiments.
***=p<0.01 using a Mann-Whitney U Test.*

3.4.2 Hit Validation – OTP siRNA

When combined with siGENOME siRNA and temozolomide, targets which were able to achieve less than 90% survival were taken forward as potential hits for further validation. These were PNCK, DMPK, FGFR4, MAP3K3, FES and PRKCSH.

PRKDC siRNA did reduce survival by more than 10% when combined with temozolomide; however it was not taken forward as a potential hit. PRKDC is the gene that encodes for DNA-PKcs. It has previously been shown that inhibition of this target using a small molecule inhibitor (KU0060648) is able to sensitise GBM cells to temozolomide (Lan et al., 2016) and it was therefore discarded from further analyses.

Initially, further validation of the targets was to be investigated using 4 individual OTP siRNAs to each target. However, to show that comparable temozolomide sensitisation could be seen with the original OTP siRNAs, the 4 individual siRNAs were pooled together and used in combination with temozolomide. The only target to show any sensitisation in combination with temozolomide was MAP3K3 (Mitogen-Activated Protein Kinase Kinase Kinase 3, also known as MEKK3), which achieved a survival fraction of just over 80% (figure 3.10).

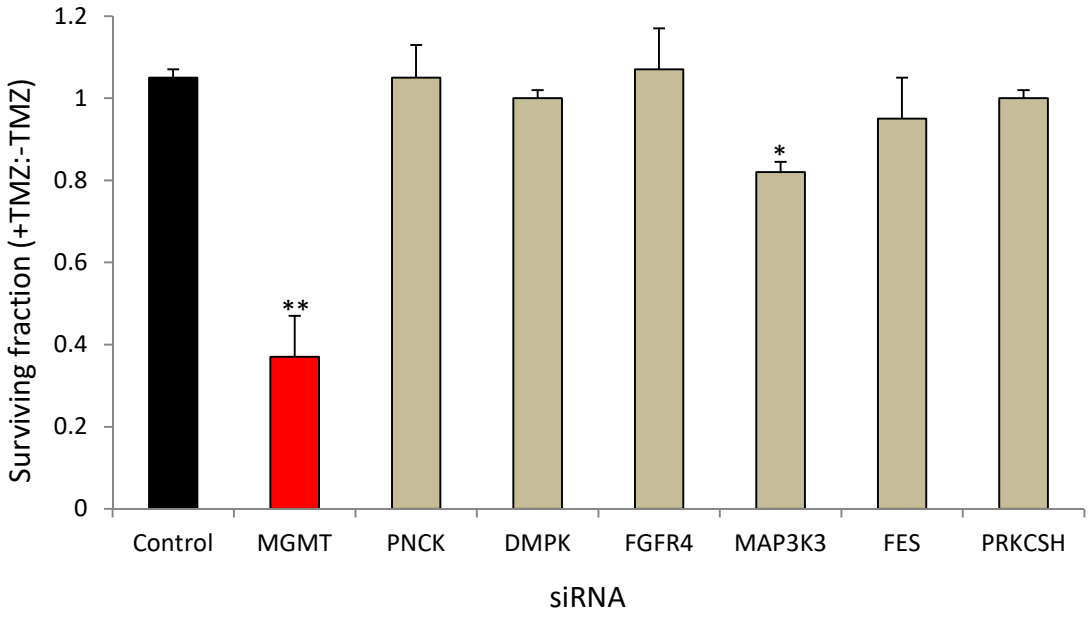

Figure 3.10: Survival Fraction of T98G cells treated with Pooled OTP siRNA +/- TMZ

T98G cells were reverse transfected with siRNA and then treated with 50μM TMZ 48 hours later. Cells underwent staining and fixing following 5 days incubation. Wells were imaged and analysed using a Multi Wavelength Cell Scoring application on MetaXpress. This application counted cells based on minimum and maximum microns and intensity above background.

Data shown is the average surviving fraction +/- standard deviation derived from three independent biological repeat experiments.
**=p<0.05 **=p<0.01 using a Mann-Whitney U Test.*

As this result was unexpected, reverse transcription polymerase chain reaction (RT-PCR), also known as quantitative PCR (qPCR), was used to determine the gene expression of each gene following 48 hour knock down using OTP pooled siRNA (figure 3.11). Both OTP and siGENOME MGMT siRNA caused greater than 80% reduction in the expression of their target gene. More than 80% reduction in gene expression was only seen only in MAP3K3 and PRKCSH pooled OTP siRNA samples. This may explain why MAP3K3 was able to show a trend towards increased cell death when combined with temozolomide (figure 3.11). PRKCSH gene expression was effectively depleted by siRNA; however, it did not result in a decreased survival fraction so is likely to be a false positive result. The use of another housekeeping gene, such as 18S, would further improve confidence in this qRT-PCR data, as off target effects of siRNA could have altered GAPDH expression, subsequently affecting ΔΔCT calculations and generating incorrect values which could account for the variable knock-down success seen using OTP siRNA (figure 3.11).

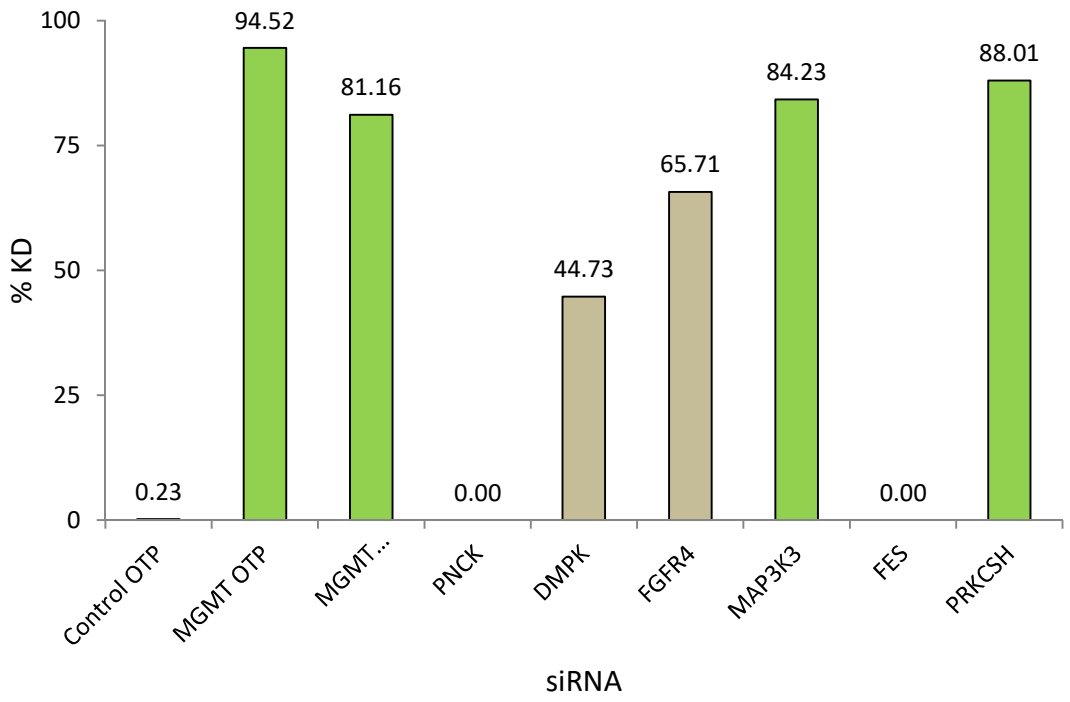

Figure 3.11: Gene Expression of T98G cells treated with Pooled OTP for 48 hours

T98G cells were reverse transfected with siRNA and cells were harvested for RNA extraction 48 hours later. Following RNA extraction, cDNA was made and qRT-PCR was performed.

Green bars represent a knock down of >80%. MGMT, MAP3K3 and PRKCSH siRNA were all able to generate sufficient knock down of their targets. GAPDH was used as a house keeping gene to normalise samples.

Fold change was calculated by $2^{-\Delta\Delta CT}$

% Knockdown was calculated by $(1-2^{-\Delta\Delta CT}) * 100$

(n=1)

As MAP3K3 (MEKK3) pooled siRNA had shown optimum knock-down of gene expression (figure 3.11), qRT-PCR was used to determine gene knock-down using the individual siRNAs, and again the use of another housekeeping gene, such as 18S, would further improve confidence in this qRT-PCR data.

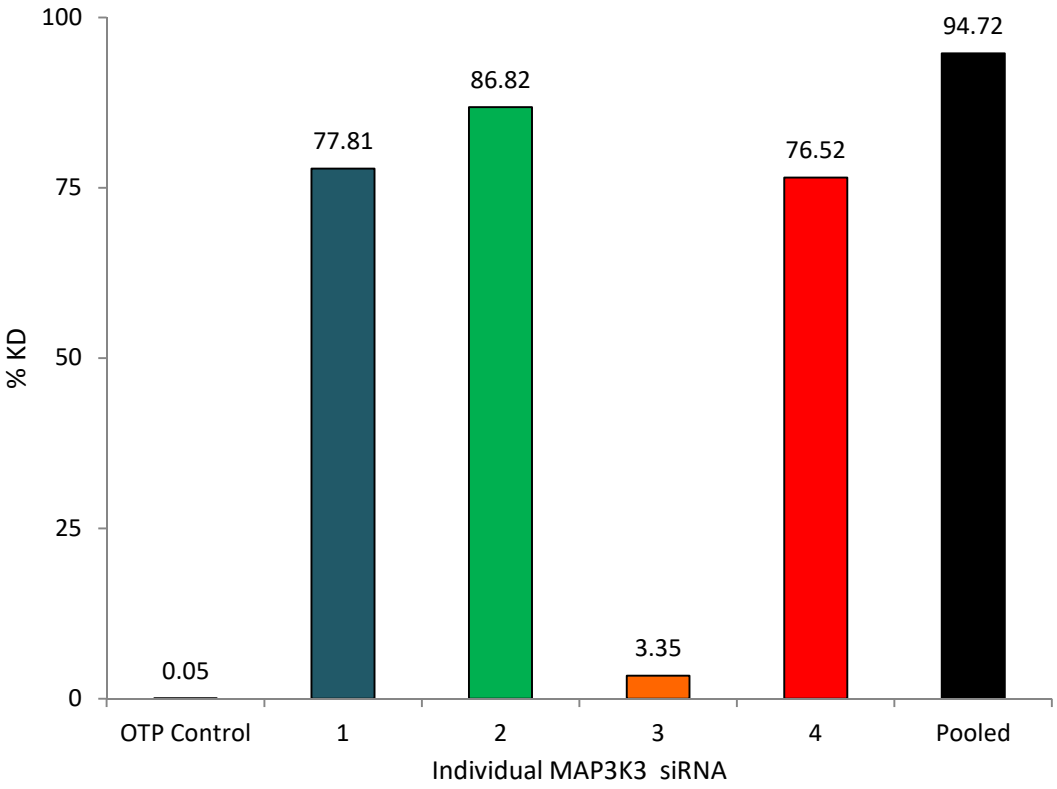

Figure 3.12: Gene Expression in T98G cells treated with Individual MAP3K3 OTP siRNA for 48 hours

T98G cells were reverse transfected with siRNA and cells were harvested for RNA extraction 48 hours later. Following RNA extraction, cDNA was made and qRT-PCR was performed.

siRNA sequence 1, 2, 4, and pooled siRNA were all able to generate sufficient knock down of their targets (>75%). GAPDH was used as a house keeping gene to normalise samples.

Fold change was calculated by $2^{-\Delta\Delta CT}$

% Knockdown was calculated by $(1-2^{-\Delta\Delta CT}) * 100$

(n=1)

siRNAs 1, 2, and 4 were able to sufficiently deplete T98G cells of MAP3K3 expression (figure 3.12). siRNA 3, however, did not show sufficient knock-down. These results from the qRT-PCR are reflected in clonogenic survival data from LN-18 cells (figure 3.13). Following a 48 hour reverse transfection, LN-18 cells were re-plated into 10cm dishes, allowed to adhere for 24 hours and then treated with a

range of temozolomide doses, 0 - 400µM. After 12 days incubation, a clonogenic survival assay showed a modest increase in sensitivity to temozolomide could be achieved using 3 out of 4 siRNAs when compared to OTP Control siRNA also treated with temozolomide (figure 3.13). siRNA 3 which was shown to be ineffective at depleting cells of MAP3K3 expression (figure 3.12) was unable to sensitise LN-18 cells to temozolomide in the clonogenic survival assay (figure 3.13).

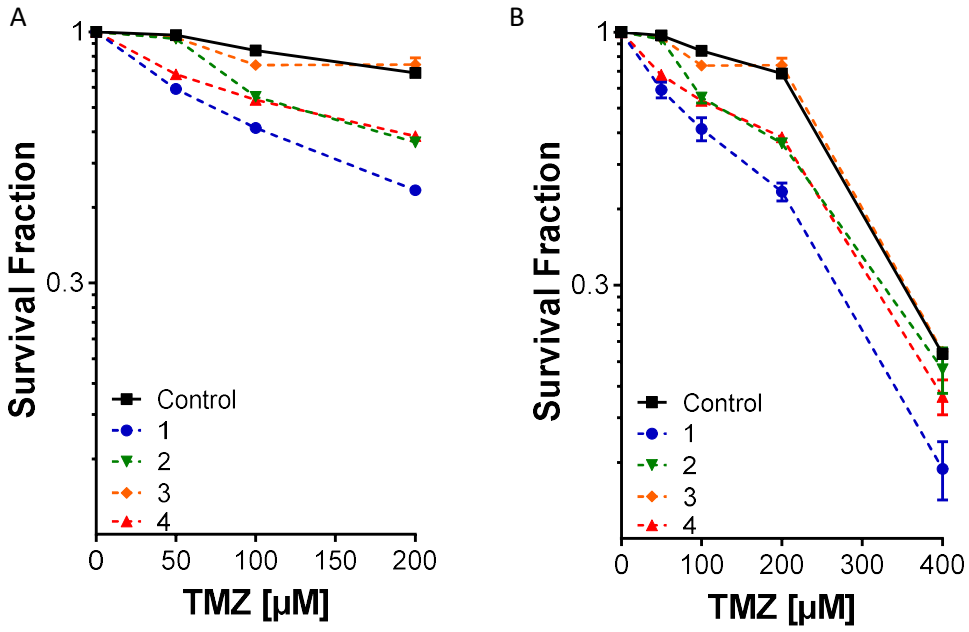

Figure 3.13: Cytotoxicity curves of GBM cells treated with MAP3K3 siRNA and TMZ

LN-18 cells were reverse transfected with the indicated siRNA for 48 hours. Cells were re-plated into 10cm dishes and left to adhere for 24 hours. They were treated with a range of TMZ doses (0 - 400µM) and left to incubate for a further 12 days, allowing colonies to form. Cell colonies were fixed in 0.04% methylene blue in 100% ethanol for 30 minutes at room temperature. >50 cells were counted as a colony. siRNAs 1, 2, and 4 were able to sensitise cells to temozolomide.

Survival fraction (A) shows LN-18 cells treated with a maximum dose of 200µM TMZ.
Survival fraction (B) shows LN-18 cells treated with a maximum dose of 400µM TMZ.
A and B show the same data plotted against a different x-axis.

Data shown is the average surviving fraction (normalised to control, 1, 2, 3 or 4 siRNA treated cells) +/- standard deviation derived from two independent biological repeat experiments.

3.5 Small Molecule Inhibitors – MAP3K3 and FGFR4

As siRNA cannot be used in patients, the next step was to identify any inhibitors for the 6 potential hits as this would increase the likelihood of potential clinical translation of these findings, and these inhibitors could be used to further validate the initial siRNA hits. There can, however, be phenotypic differences between

siRNA depletion and catalytic inhibition of kinases, most likely due to differences in protein-protein interactions. siRNA reduces protein expression by targeting mRNA for degradation, however, catalytic inhibition will not affect protein expression, allowing protein-protein interactions and any biologically important scaffold roles of the protein to continue (Weiss et al., 2007).

In 2015, BLU9931, created by Blueprint Medicines, was published as the first selective fibroblast growth factor receptor 4 (FGFR4) inhibitor. This inhibitor is designed to inhibit active FGFR4 pathways in hepatocellular carcinoma (Hagel et al., 2015). This inhibitor is commercially available, however, during the course of this study, another inhibitor (BLU554) made by the same company was launched into clinical trials and was also commercially available. BLU554 was therefore purchased from Selleckchem (Catalogue Number S8503).

There are, however, currently no selective inhibitors that are commercially available for any of the other hits; however, mitogen-activated protein kinase kinase kinase 3 (MAP3K3/ MEKK3) pathway has inhibitors available to downstream targets. Mitogen-activated protein kinase kinase 5 (MAP2K5/MEK5) and extracellular signal-related kinase 5 (ERK5) are found downstream of MAP3K3 and can be inhibited using a commercially available inhibitors, BIX 02189 and ERK5-in-1. These inhibitors were also purchased from Selleckchem (Catalogue Numbers S1531 and S7334). ERK5 generated a z-prime of -1.92 from siRNA screen results (cut off was -2.2), however, MEK5 generated a z-prime close to 0. Therefore, both the MAP3K3 and FGFR4 pathways were taken forward into further validation studies (see chapters 4 and 5 respectively).

3.6 Discussion

It was hypothesised that inhibition of yet to be identified kinase(s)/signalling pathways would enhance the cytotoxic effects of temozolomide in GBM. To investigate this hypothesis, a kinome-wide siRNA screen was completed both with and without temozolomide.

MGMT depletion was successfully used as a positive control for the kinome-wide siRNA screen, generating the second highest z-score. MGMT depletion using O-6-benzylguanine has been explored in phase I and II clinical trials in patients with recurrent GBM, however, it was poorly tolerated resulting in haematological toxicity, a subsequent reduction in temozolomide treatment and no improvement to overall patient survival (Quinn et al., 2005, Quinn et al., 2009). MGMT is the enzyme responsible for repairing DNA base adducts which occur following methylation, catalysing the removal of methyl groups from DNA to itself. This

enzyme is important for both protection against mutagenesis and defence against the cytotoxicity of alkylating agents (Konduri et al., 2009), therefore, it may not be too surprising that the depletion of this enzyme following O-6-benzylguanie treatment was poorly tolerated in patients. However, almost a third of newly diagnosed GBM patients and almost a quarter of recurrent GBM patients who have failed temozolomide therapy do not express high levels of MGMT and 97% of these patients have tumours with proficient MMR pathways, indicating alternative temozolomide resistance pathways independent of MGMT and MMR proteins (Maxwell et al., 2008). These findings therefore highlight both the heterogeneity of GBM tumours and the need for novel and well-tolerated targets to improve the potency of existing treatment regimes such as temozolomide.

There are, however, limitations to using siRNA including the variability of mRNA depletion and off-target effects resulting in downregulation of other mRNAs. One example is a screen which was investigating ABT-737 sensitivity, an anti-cancer drug which inhibits a selection of anti-apoptotic proteins in the BCL-2 family (BCL-2, BCL-xl and BCL-w) without inhibiting other family members (MCL-1, BCL-B, BFL-1). The 3 best hits involved in ABT-737 sensitivity were all a result of off target effects acting on MCL-1 as opposed to their intended target (Lin et al., 2007). However, Dharmacon™ recommends the use of OTP siRNA as it has a 'dual strand modifications pattern to reduce off-target effects by 90%' (Dharmacon™, 2018).

One problem that arose during validation of potential hits from the initial OTP screen was the loss of reproducibility when the siRNA pools were deconvoluted. This could be due to a number of factors including ineffective transfection, poor siRNA quality, incorrect dilution of lyophilised siRNA, transfection into non-replicating cells and many more; all would result in ineffective knock-down of the intended target. The positive control siRNA MGMT was purchased as 4 deconvoluted sequences alongside the other siRNAs identified as potential hits. Deconvoluted MGMT siRNA was reconstituted, transfected, stored identically to all other deconvoluted siRNAs yet it was effective at depleting cells of the intended target, sensitising GBM cells to temozolomide. This would suggest the lack of reproducibility was not due to the reconstitution, dilution, transfection processes. The ineffective depletion of target mRNA caused a problem in the progression of the project and disappointingly Dharmacon only guarantee a knock-down of more than 75% in 3 out of 4 siRNA sequences if a final concentration of 100nM is used. Therefore it was decided that the targets which had available inhibitors would be taken forward and validated using either effective individual OTP siRNA (MAP3K3) or using alternative siRNA from siTOOLs (ERK5 and FGFR4) (chapter 4.4 and chapter 5.3).

Another criterion to take hits forward to further validation studies was evidence of pathway dysregulation in human cancers. Both MAP3K3/ERK5 and FGFR4 pathways have previously been shown to be dysregulated in cancer.

MAP3K3 is over-expressed in almost two thirds of ovarian carcinomas (where expression is correlated with both grade and response to chemotherapy), and has also been shown to be amplified in up to 20% of breast cancers, with shRNA depletion increasing sensitivity to both doxorubicin and 5-FU (Fan et al., 2014, Jia et al., 2016). Overexpression of MAP3K3 in GBM cell lines enhances NF-κB activation, increasing cell survival and resistance to both doxorubicin and camptothecin (Samanta et al., 2004). Although the inhibition of MAP3K3 would subsequently inhibit a whole pathway of downstream targets and signalling pathways, there currently no successful specific inhibitors reported. Examples of downstream targets of MAP3K3 include MEK5/ERK5 (chapter 4), ERK1/2, JNK, p38 and NF-κB (Johnson and Lapadat, 2002, Yang et al., 2001). Interestingly, temozolomide has been shown to activate both JNK and p38 signalling in GBM cells, and following pharmacological inhibition of JNK, GBM cells become sensitised to temozolomide (Vo et al., 2014). The same trend is seen with p38 inhibition, however, to a lesser extent than following JNK inhibition (Vo et al., 2014). ERK1/2 activation, a downstream target of MAP3K3, has also been shown to be both positively and negatively regulated in GBM cells following temozolomide treatment (Wang et al., 2016, Xu et al., 2018a).

Once ERK5, downstream of MAP3K3, is activated, it has many roles within normal cells including survival, proliferation, differentiation and migration, as well as anti-apoptotic functions (Drew et al., 2012, Wang and Tournier, 2006). An siRNA screen has identified the MEK5-ERK5 pathway to be involved in the EMT of breast cancer cells, driven by MEF2B and TGFβ activation by ERK5 (Pavan et al., 2018). Hepatocellular carcinoma (HCC) and osteosarcoma have also been shown to have ERK5 gene amplification and over-expression which correlates with worse prognosis due to increased disease aggression and metastasis (Rovida et al., 2015, Tesser-Gamba et al., 2012). More recently, ERK5 has been shown to be activated in the development of lung cancer, activating CHK1 and the subsequent DNA damage response pathways in response to radiation (Jiang et al., 2019). Additionally, ERK5 together with a member of the H2A histone family (H2AFJ), has also been linked in chemo- radio-resistance in colorectal cancer through a gene set enrichment analysis (Wang et al., 2018c).

FGFs and FGFRs are thought to play a role in oncogenesis as dysregulation of the associated pathways (proliferation, survival, angiogenesis, epithelial-mesenchymal transition and migration) is associated with increased tumorigenicity. For example, driver mutations in the FGF and FGFR signalling pathways are present in over 90%

of melanoma cases (Flippot et al., 2015). FGFR4 is a target for patients with HCC as FGF19, which binds to FGFR4 in normal physiological conditions, is both amplified and over-expressed in these tumours (Sawey et al., 2011, Wu et al., 2011).

Of the remaining 26 kinases identified, 3 targets were shown to be linked to either calcium or calmodulin signalling. These were Calmodulin 3 (CALM3), Calcium/Calmodulin Dependent Protein Kinase II Beta (CAMK2B), Calcium/Calmodulin-Dependent Protein Kinase Type 1B (PNCK). Calcium Modulated Protein or calmodulin has previously been shown to be important for the growth of rat glioblastoma cells (C6 cells), with increasing inhibition of calmodulin correlating with reduced tumour cell growth and is discussed further in chapter 6.6 (Lee and Hait, 1985). However, when an anti-psychotic and calmodulin inhibitor (trifluoperazine) was combined with chemotherapy (bleomycin) in 17 GBM patients in a Phase II trial, there was unfortunately no improvement with the combination. Although trifluoperazine is lipophilic and readily crosses the blood brain barrier, bleomycin is amphipathic and therefore potentially ineffective at treating GBM; possibly explaining why there was no sensitisation observed (Hait et al., 1990, Kristiansen et al., 1981). More recently, data has been published showing that trifluoperazine decreases tumour growth and metastasis in both flank and orthotopic xenograft models of GBM specifically through reactivation of the calcium channel IP_3R (Kang et al., 2017). By identifying the associated mechanism of action, this could be developed as a novel target to enhance the cytotoxicity of temozolomide in order to potentially improve GBM patient survival.

G-Protein Coupled Receptor Kinase 6 (GRK6) generated the highest z-score from the OTP screen with a value of -5.49, lower than that of MGMT. Overexpression is associated with worse overall survival for patients with colorectal cancer and hepatocellular carcinoma (HCC) and better overall survival for patients with lung adenocarcinomas (Li, 2013a, Tao et al., 2018, Yao et al., 2016). Increased GRK6 mRNA expression is also correlated with higher glioma grades and increased proliferation *in vitro*, furthermore when U-251 cells which highly express GRK6 were depleted of GRK6 using siRNA, their temozolomide sensitivity was increased (Xu et al., 2017). These data therefore provide a good positive control for the screen, furthermore, dysregulation of GRK6 has recently been shown to be a therapeutic target in several cancer types, increasing the likelihood of inhibitors being developed and investigated in clinical trials (Che et al., 2018, Li, 2013a, Tao et al., 2018, Xu et al., 2017).

Other targets have also been previously linked to gliomas, for example Dual Specificity Tyrosine Phosphorylation Regulated Kinase 1A (DYRK1A), a kinase involved in both cell proliferation and neuronal development, as well as an array of signalling pathways (Neumann et al., 2018). Inhibition of DYRK1A decreases

primary glioma cell survival and proliferation, particularly in cells which over-express Epidermal Growth Factor Receptor (EGFR) and more recently, this target has been identified as a positive regulator of angiogenesis in endothelial cells (Pozo et al., 2013, Rozen et al., 2018). DYRK1A, located on chromosome 21, is overexpressed in patients with trisomy 21/Down syndrome and is also dysregulated in Alzheimer's disease (Neumann et al., 2018). Developing a successful inhibitor with the ability to cross the BBB could therefore benefit a huge population of patients beyond oncology. Interestingly, epigallocatechin gallate, an inhibitor of DYRK1A, is currently being investigated in clinical trials for Down syndrome (ClinicalTrials.gov, 2018).

Phosphatidylinositol-4-Phosphate 3-Kinase Catalytic Subunit Type 2 Beta (PIK3C2B) is a member of the phosphoinositide 3-kinase (PI3K) family. PI3K signalling has many roles including cell proliferation and survival, as well as oncogenic potential. However, in non-small cell lung cancer (NSCLC) where PI3K signalling dysregulation is frequent, mutations targeting the kinase domain of PIK3C2B have been shown to have no overall effect on PI3K signalling and therefore it is believed PIK3C2B has little involvement in tumorigenesis (Kind et al., 2017). Contrastingly, PIK2C2B over-expression is correlated with breast cancer grade, with depletion using shRNA targeting PIK3C2B leading to reduced cell proliferation in 3D tumour models as well as reducing tumour growths by 55% *in vivo* when shRNA silenced PIK3C2B cells were injected into mammary fat pads of nude mice. However, this difference was not significant *in vivo*, possibly due to a large range in tumour size (Chikh et al., 2016). In GBM patients, increased PIK3C2B expression, detected by cDNA microarrays, has been identified as a potential cause of resistance to the EFGR inhibitor erlotinib, however, EGFR inhibitors are yet to gain NICE approval for treating patients with GBM (Loew et al., 2008, NICE, 2018a).

Platelet Derived Growth Factor Receptor β (PDGFRβ) is important in development *in utero* but also for cell proliferation, survival, migration and many more. PDGFRβ shRNA depletion inhibited xenograft growth and cell proliferation *in vitro,* sensitising rat C6 GBM cells to radiotherapy (Hong et al., 2017). Unfortunately, a PDGFRβ inhibitor tandutinib was unsuccessful in a phase II trial in GBM patients failing to improve overall survival but this treatment was not combined with temozolomide or radiotherapy and was not enriched for PDGFRβ over-expression which may account for the trial failure (Batchelor et al., 2017). An alternative PDGFR inhibitor, AG1295, has also been shown to reduce both proliferation and migration of rat C6 GBM cells *in vitro*, however, this compound has not yet reached clinical trials (Singh et al., 2018). ERK1/2, downstream targets of PDGFR, may play a role in temozolomide resistance in GBM which could provide rationale for PDGFR inhibitors being trialled in combination with standard GBM chemo-radiotherapy regimes (Singh et al., 2018, Wang et al., 2016, Xu et al., 2018a). However, when

sorafenib, an inhibitor of tyrosine kinases PDGFR and VEGFR and an inhibitor the RAF/MEF/ERK pathway, was trialled in combination with adjuvant temozolomide in GBM patients, there was no improvement to either progression free or overall survival (Hainsworth et al., 2010), possibly indicating limited potential for PDGFR inhibitors in treating patients with GBM.

Serine/Threonine Kinase 3 (STK3) is a pro-apoptotic kinase which acts to restrict proliferation and is also part of the Hippo signalling pathway, which has been shown to be involved in both tumour development and maintenance (Moroishi et al., 2015). High levels of STK3 mRNA (taken from TGCA database) in GBM patients have shown a reduced overall median survival to 12.4 months compared to 14.7 months for patients with low mRNA expression (Varghese et al., 2016). Furthermore, STK3 has also been identified as a potential therapeutic target for a subset of AMLs as both shRNA depletion and small molecule inhibition of STK3 leads to decreased proliferation in a some but not all immortalised and patient derived AML cell lines (Camgoz et al., 2018). This finding reinforces the heterogeneity of cancer and the need for disease sub-typing in order to drive the personalisation of medicine and reduce the reliance on generalised treatment regimes.

Phosphoglycerate Kinase 1 (PGK1) phosphorylation is dysregulated and over-expressed in in many cancers, increasing proliferation and tumorigenesis of cells, and has been shown to increase resistance to radiotherapy in astrocytomas (Yan et al., 2012). Furthermore, phosphorylation of PGK1 at threonine 243, regulated by M2 macrophages secreting IL-6, has been shown to correlate with prognosis in GBM. When stratified into low and high PGK1 phosphorylation, patients with high levels of phosphorylation had a 7.5 month reduction in survival time (13.5 months high v 20 months low), highlighting the importance of macrophages in driving changes in gene expression effecting response to treatment and ultimately survival (Zhang et al., 2018c).

Other targets have also been previously linked to cancer, for example Protein Kinase cAMP-Dependent Type I Regulatory Subunit Alpha (PRKAR1A) and Protein Kinase CAMP-Dependent Type II Regulatory Subunit Beta (PRKAR2B) which normally act to regulate cAMP dependent protein kinase (PKA). Mutations in PRKAR1A protein can cause Carney Complex (CNC) which results in pigmentation of the skin as well as benign and cancerous tumours (Iliopoulos et al., 2009). PRKAR1A is dysregulated in many cancers with increased protein expression resulting in a poorer response to radiotherapy in patients with prostate cancer and depletion using siRNA has been shown to reduce cholangiocarcinoma (bile duct cancer) cell proliferation (Loilome et al., 2011, Pollack et al., 2009). PRKAR2B has also been linked to prostate cancer, with over-expression resulting in increased EMT and

tumour metastasis *in vivo (Sha et al., 2018)*. Data from an shRNA screen investigating temozolomide sensitivity in GBM cells has also identified PRKAR1B as a potential target, however, this was not further investigated as hits were selected based on currently available small molecule inhibitors (Johannessen et al., 2018). However, this could indicate a potential role for cAMP and PKA signalling in temozolomide sensitivity. This is particularly interesting as ion channels are frequently mutated in GBM with more than 90% of GBM patients exhibiting mutations in genes related to ion transport (Joshi et al., 2011).

Little is known about Serine/Threonine Kinase 16 (STK16) in comparison to other identified targets; however, it is known to be involved in secretory pathways and regulation of VEGF. A selective STK16 inhibitor has been developed; however, it was only able to reduce proliferation in one cell line tested (MCF-7) but increasing doses of the inhibitor did induce apoptosis in both MCF-7 cells and He-La cells, also enhancing the potency of chemotherapeutic doxorubicin, indicating a possible target to enhance the potency of other DNA damaging chemotherapeutics (Liu et al., 2016).

Protein Kinase AMP-Activated Non-Catalytic Subunit Gamma 1 (PRKAG1) is a regulatory subunit of AMP-activated protein kinase (AMPK) which is activated in response to metabolic stress. Depleting colon cancer cells (HCT-116) of PRKAG1 using siRNA has been able to reduce cell viability and increase apoptosis (Fisher et al., 2015). Interestingly, when AMPK was depleted using siRNA or inhibited using a small molecule, GBM cells became more resistant to temozolomide treatment, which may indicate AMPK activity is required for temozolomide-induced cell death (Zhang et al., 2010).

Cyclin Dependent Kinase Like 3 (CDKL3) is part of a family of proteins which are important for cell cycle progression, Cyclin Dependent Kinases (CDK). Curcumol which has both anti-proliferative and anti-inflammatory properties has been shown to deplete cells of CDKL3 at both mRNA and protein level. Both shRNA and curcumol were able to decrease growth and migration of cholangiocarcinoma cells potentially via G1 arrest and subsequent apoptosis (Zhang et al., 2018b).

Protein Kinase C Zeta (PRKCZ) is a known tumour suppressor in CRC and when lost causes microRNA 200 dysregulation. This depletion of microRNA 200 causes increased EMT leading to liver metastases in around 70% of CRC patients (Shelton et al., 2018). However, in a model of breast cancer stem cells, over-expression of PRKCZ and MAPK3, both acting upstream of STAT3, are believed to confer resistance to chemotherapeutic doxorubicin and PRKCZ has been shown to be upregulated (2-fold) in GBM cells compared to normal brain tissue, and to promote increased proliferation (Moreira et al., 2018, Seto and Andrulis, 2015). Interestingly, STAT3 dysregulation has also been linked to both MEK-ERK5 and

FGFR4 signalling pathways, both targets which have been selected for further investigation. MEK5 has been shown to be upregulated (22-fold) in benign cells following transformation by expression of a constitutively active oncogene STAT3 (Song et al., 2004) and activating mutations within FGFR4 in rhabdomyosarcoma has been shown to increase in both total and phosphorylated STAT3 (Taylor VI et al., 2009). Potentially the inhibition of PRKCZ could therefore lead to the dysregulation of various signalling pathways which activate STAT3.

siRNA depletion of Never In Mitosis Gene A (NIMA)-Related Kinase 4 (NEK4) is able to reduce migration of lung cancer cells, with *in vivo* studies showing reduced metastases in mice treated with NEK4 depleted cells (Ding et al., 2018). NEK4 has also been implicated in the DDR, as NEK4 siRNA depleted cells have an impaired NHEJ response to double strand DNA damage mediated by DNA-PKcs, potentially highlighting a mechanism by which temozolomide potency could be enhanced. Furthermore, shRNA depletion of NEK4 resulted in increased cell proliferation, which could also potentiate the cytotoxic effects of temozolomide when combined with defective DNA damage pathways (Nguyen et al., 2012). However, targeted therapy which enhances the proliferation rate of cancer cells would be far from ideal, particularly in cancer as aggressive and mutational as GBM.

In summary, 28 targets were identified from the OTP siRNA screen and 7 of these were also able to sensitise resistant GBM cells to temozolomide using siGENOME siRNA. From the targets which could be validated using siRNA or from previously published data (MAP3K3, FGFR4, PRKDC, GRK6, PRKCSH), only one (PRKCSH) failed to sensitise GBM cells to temozolomide treatment. MAP3K3/ERK5 and FGFR4 were taken forward for future studies as small molecule inhibitors were available, however, several of the other targets which could not be validated post OTP screening would also make interesting targets for further investigation. Furthermore, as many of the targets identified by the siRNA screen have been linked to cancer or GBM previously and siGENOME siRNA targeting MGMT was not able to significantly sensitise cells to temozolomide treatment ($p=0.07$), if funding and time were no object, it may have been prudent to re-test all initial hits using a different pooled siRNA (e.g. siTOOLs™). An example of this is GRK6, which was initially identified as a target from the OTP screen and was subsequently not identified by the siGENOME validation. However, GRK6 has recently been validated by a publication which showed depleting GRK6 in cells expressing high levels sensitised them to temozolomide (Xu et al., 2017).

Chapter 4 – Validating Extracellular Signal-Related Kinase 5 as a novel Temozolomide sensitising factor.

4.1 Mitogen-Activated Protein Kinase (MAPK) Signalling

Mitogen-activated protein kinases (MAPKs) are a diverse range of conserved proteins which enable a cell to transform extracellular stimuli into signalling cascades needed to activate or inhibit various pathways. These three-tiered cascades are involved in pathways ranging from cell survival and apoptosis, to cell differentiation and migration, and are tightly regulated through phosphorylation cascades. Following the activation of a receptor, the conventional MAPK phosphorylation cascade initiates with MAP kinase kinase kinase (MAPKKK) phosphorylating a MAP kinase kinase (MAPKK/MEK) which in turn phosphorylates a MAP kinase (MAPK), such as ERK5. Activated MAP kinases continue the signalling cascade by phosphorylating serine or threonine and then proline on various targets (Dhillon et al., 2007, Goldsmith and Dhanasekaran, 2007) (figure 4.1).

There are 7 established human MAP kinase pathways, 4 of which are classified as conventional: extracellular signal-related kinase 1/2 (ERK1/2), extracellular signal-related kinase 5 (ERK5), c-Jun N-terminal kinases 1, 2, 3 (JNK1/2/3) and p38α/β/ɣ/δ. These kinases are activated by upstream MAPKKs through phosphorylation of both threonine and tyrosine in their activation loop. Between threonine and tyrosine sits an amino acid which varies depending on the MAPK family: glutamic acid for ERK, proline for JNK and glycine for p38 (Cargnello and Roux, 2011, Nithianandarajah-Jones et al., 2012).

Unconventional MAP kinases, extracellular signal-related kinase 3/4 (ERK3/4) and Nemo-like kinase (NLK), have either glycine or glutamine in place of tyrosine and extracellular signal-related kinase 7 (ERK7), although it does have the threonine and tyrosine present in its activation loop, is not considered to be conventional as it is activated by auto-phosphorylation as opposed to phosphorylation by a MAPKK. The biological role of unconventional MAPKs are yet to be discovered (Cargnello and Roux, 2011).

Dysregulation of MAP kinases occurs in a spectrum of diseases including polycystic kidney disease, diabetes and Alzheimer's. Dysregulation of MAP kinase signalling has also been identified in cancer, with ERK1/2 signalling is estimated to be abnormal in 33% of all human cancers (Mebratu and Tesfaigzi, 2009). The ERK5 signalling pathway is not as well studied as the ERK1/2 pathway; however it has recently been reported to have an important role in cancer development and resistance to treatment (Simões et al., 2016); see section 4.3 for further details.

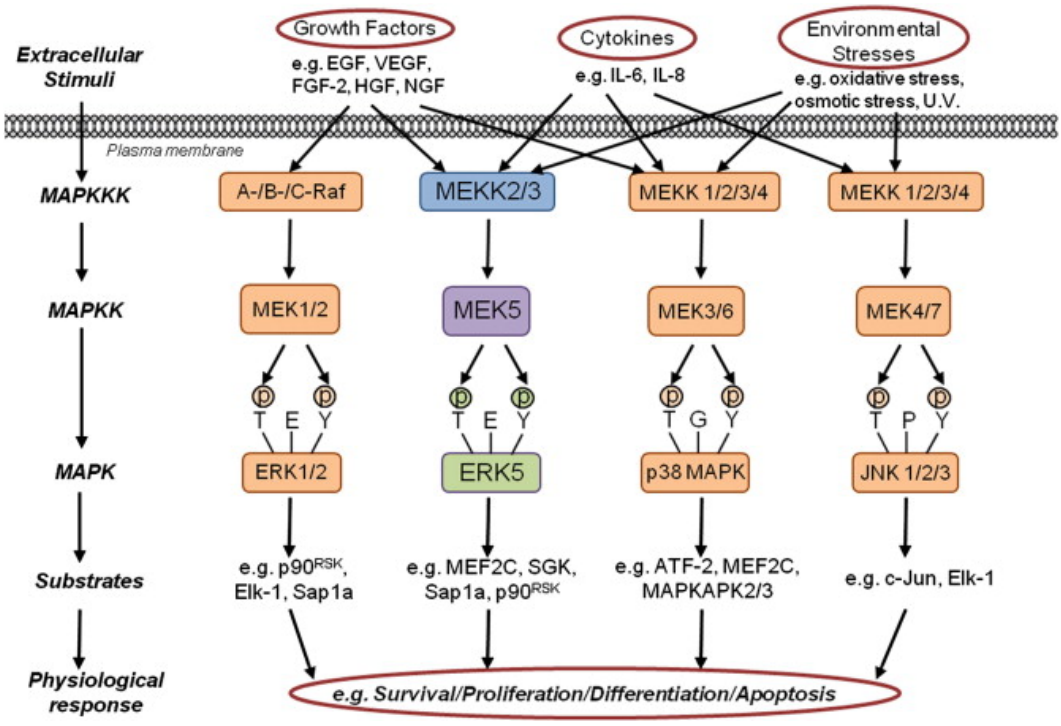

Figure 4.1: MAPK Signalling
Growth factors, cytokines and environmental stresses are all activators of the 4 classical MAPK signalling pathways: ERK1/2, ERK5, p38 and JNK1/2/3. Pathway activation causes a phosphorylation cascade activating downstream targets. Active MAP kinase kinase kinases (MAPKKK/MEKK) phosphorylate MAP kinase kinases (MAPKK/MEK) which in turn phosphorylate MAP kinases (MAPK). Activated MAPKs continue the signalling cascade, effecting survival, proliferation, differentiation and apoptosis.

Legend adapted from (Nithianandarajah-Jones et al., 2012)
Figure copied with permission from (Nithianandarajah-Jones et al., 2012)
License number: 4450740151251

4.2 Extracellular Signal-Related Kinase 5 Signalling

ERK5 is the newest member of the MAP kinase family and was first identified as Big Mitogen-like Kinase 1 (BMK1) in 1995 (Lee et al., 1995). ERK5, much larger than other MAP kinases, has a kinase domain located in its N-terminal which is phosphorylated at threonine 218 and tyrosine 220 by MEK5 (figure 4.2). Inactive ERK5 is folded to allow the N- and C-terminals to interact, tethered to in the cytoplasm by Hsp90 and cdc37 (Erazo et al., 2013, Honda et al., 2015). This conformational interaction is thought to potentially act as a nuclear export signal (NES), inhibiting the nuclear localisation signal (NLS) allowing ERK5 to accumulate in the cytoplasm (Nithianandarajah-Jones et al., 2012). The C-terminal of ERK5 is auto-phosphorylated following activation by MEK5 causing dissociation of ERK5-

cdc37 from Hsp90, activating the nuclear localisation signal (NLS) resulting in the translocation of ERK5 in to the nucleus (Erazo et al., 2013, Simões et al., 2016).

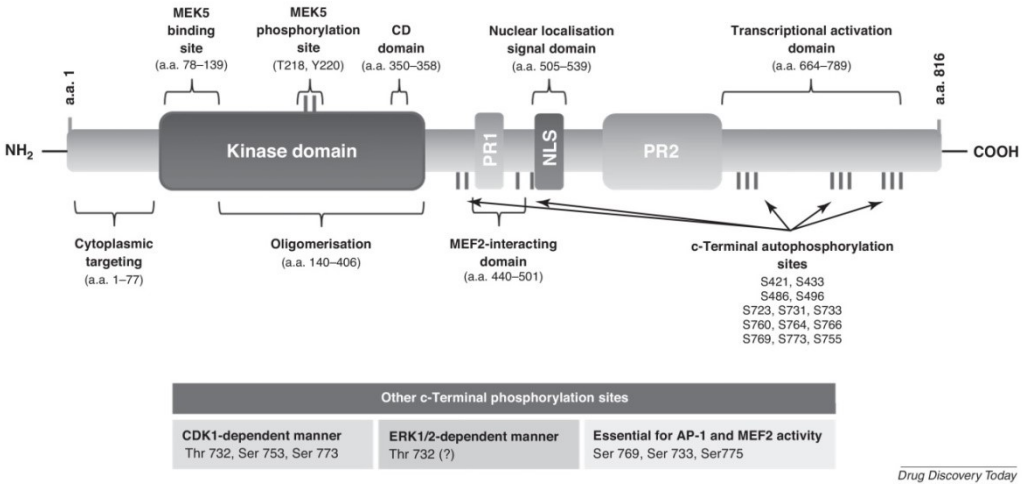

Figure 4.2: ERK5 Diagram

ERK5 comprises of 816 amino acids and is highly homologous to ERK1/2 (66% homology). The N-terminal contains the kinase domain with MEK5 binding and phosphorylation sites, a common docking (CD) domain and cytoplasmic localisation domain. The C-terminal contains the nuclear localisation signal (NLS) between two proline-rich (PR1/2) domains, a MEF2-interacting domain and auto-phosphorylation sites.

Legend adapted from (Simões et al., 2016)
Figure copied with permission from (Simões et al., 2016)
License number: 4323220889024

Previous work used a yeast two-hybrid screen that identified both MEKK2 and MEKK3; MAPKKKs which share 94% sequence homology, as activators of MEK5 signalling. Both were able to phosphorylate MEK5 in response to stimulation with epidermal growth factor (EGF) and hydrogen peroxide oxidative stress, however, MEKK2 bound to and activated MEK5 more strongly than MEKK3 (Chao et al., 1999, Sun et al., 2001, Kato et al., 1998). Alongside oxidative stress and EGF, there are several other known activators of the ERK5 pathway including: vascular endothelial growth factor (VEGF), fibroblast growth factor 2 (FGF2), platelet-derived growth factor (PDGF), brain-derived neurotrophic factor (BDNF), nerve growth factor (NGF) and several cytokines an example of which is interleukin 6 (IL-6) (Carvajal-Vergara et al., 2005, Cavanaugh et al., 2001, Finegan et al., 2009, Nithianandarajah-Jones et al., 2012).

ERK5 is also known to be activated by substrates other than MEK5. ERK1/2 has been shown to phosphorylate threonine 732 in the C-terminal of ERK5, translocating ERK5 to the nucleus without the dual phosphorylation of the threonine and tyrosine bases in its kinase domain (Honda et al., 2015). Another MEK5 independent activation of ERK5 occurs during mitosis, when ERK5 is

responsible for ensuring an appropriate G2-M phase transition. Here, ERK5 is activated by cyclin-dependent kinases (CDKs) phosphorylating its C-terminal (Iñesta-Vaquera et al., 2010).

Once ERK5 is activated it has many roles within normal cells including survival, proliferation, differentiation and migration, as well as anti-apoptotic functions (Drew et al., 2012, Wang and Tournier, 2006). To affect these pathways, ERK5 interacts with and enhances transcription of many targets including: MEF2, c-MYC, SAP-1, cFOS (English et al., 1998, Yang et al., 1998, Kamakura et al., 1999). ERK5 activates its substrates via phosphorylation of serine or threonine next to proline (Nimesh et al., 2003). ERK5 has also been shown to act upstream of PKB/AKT via FGFR2, PDGFβ, FLT3 (Lennartsson et al., 2010, Razumovskaya et al., 2011, Roberts et al., 2010).

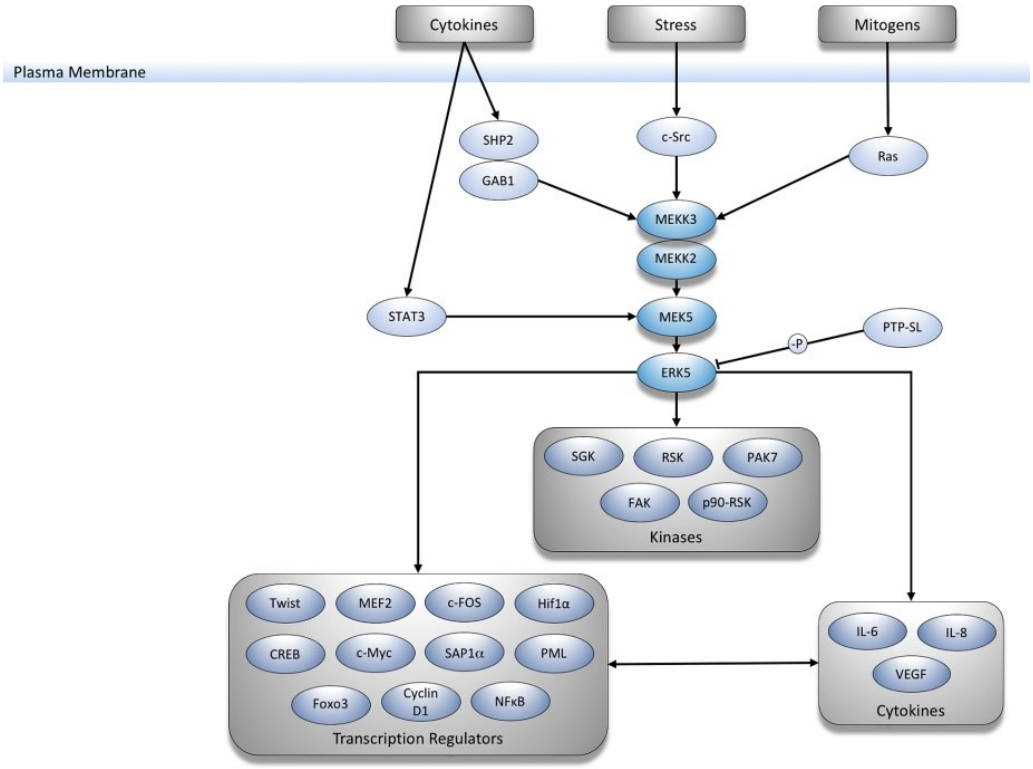

Figure 4.3: ERK5 Signalling
ERK5 has many downstream targets such as SAP1, c-Myc and MEF2 which are phosphorylated as a result of ERK5 activation, influencing survival, apoptosis and proliferation. ERK5 also phosphorylates kinases and cytokines such as SGK and IL-6. However, ERK5 can also auto-phosphorylate its C-terminus which results in translocation from the cytoplasm to the nucleus where it may act as a transcription factor.

Legend adapted from (Drew et al., 2012)
Figure copied with permission from (Hoang et al., 2017)
License number: 4450910077831

As well as the roles previously described, ERK5 is also physiologically vital during the course of development. In embryos, the role of ERK5 signalling has been shown to be essential for cardiovascular development, with knock out mice dying at around 9-11 days *in utero* due to complications in heart development, poor development of vasculature in both the embryo and placenta, as well as increased endothelial cell death (Regan et al., 2002, Sohn et al., 2002, Yan et al., 2003). Adult mice with an inducible ERK5 knock out also died 2-4 weeks after ERK5 depletion due to increased endothelial cell death which caused their vasculature to become 'leaky' resulting in massive haemorrhage (Hayashi et al., 2004). The importance of ERK5 in maintaining vasculature integrity potentially highlights problems developers might face if ERK5 inhibitors are trialled in humans.

4.3 MEK5 and ERK5 in Cancer

The MEK5/ERK5 pathway has been shown to be increasingly important in both cancer development and disease progression. Over-expression of ERK5 in breast cancer is associated with reduced disease free survival time (Montero et al., 2009). Furthermore, an RNAi screen has identified this pathway in epithelial-mesenchymal transition (EMT) of breast cancer cells, driven by MEF2B and TGFβ activation by ERK5. It was noted that both constitutively active MEK5 and over-expression of ERK5 was not able to induce EMT alone, however, depletion of MEK5 or ERK5 reduced the growth of metastatic lung tumours in orthotopic breast cancer mice models (Pavan et al., 2018). Not only is the MEK5-ERK5 pathway important in EMT, MEK5 has been shown to be upregulated (22 fold increase) in response to benign cells being transformed by constitutively active oncogene STAT3, potentially implicating the MEK5-ERK5 signalling pathway in oncogenesis when combined with aberrant STAT3 signalling (Song et al., 2004).

Both constitutively active MEK5 and ERK5 over-expression have been identified in prostate cancer, conferring a more progressive and metastatic disease (Mehta et al., 2003, Simões et al., 2015). Downregulation of miRNA-143, which acts to downregulate ERK5 mRNA expression, has also been identified in prostate cancers and is associated with increased tumorigenicity (Akao et al., 2006). Furthermore, inhibition of ERK5 using the small molecule inhibitor XMD8-92 increased the sensitivity of colon cancer cells to the chemotherapeutic fluorouracil (5-FU), a thymidine synthesis inhibitor, reducing xenograft growth by 70% (Pereira et al., 2016).

Hepatocellular carcinoma (HCC) and osteosarcoma have also been shown to exhibit ERK5 gene amplification and over-expression, both correlating with worse prognosis due to increased disease aggression and metastasis (Rovida et al., 2015,

Tesser-Gamba et al., 2012). Additionally, there are several other cancers in which ERK5 is dysregulated and this also confers worse prognosis. These diseases include pancreatic cancer, lung cancer, malignant mesothelioma, neuroblastoma, leukaemia, bladder cancer and squamous cell carcinoma (Simões et al., 2016).

Based on the results from the siRNA kinome screen (chapter 3), this chapter focuses on validation of ERK5 as a novel target in sensitising GBM cell to temozolomide treatment.

4.4 Depletion and inhibition of ERK5 increases GBM cell death in response to Temozolomide

siRNA was used to deplete GBM cells of MAP3K3 which sensitised them to treatment with temozolomide (chapter 3, figure 3.13), however, as there are no small molecule inhibitors to MAP3K3, downstream targets were selected for further target validation studies. siTOOLS Biotech have developed siPOOLS™ siRNA which comprises a pool of 30 different sequences of siRNA to the target gene. As the concentration of each of the siPOOLS™ siRNA sequences are used at picomolar, compared to nanomolar concentrations when using standard pooled (4 sequences) or individual siRNAs, the possibility of any off target effects on other genes is reduced, increasing the specificity and reliability (Hannus et al., 2014, siTOOLsBiotechGmbH, 2018).

A range of 1nM to 10nM of siRNA was suggested by siTOOLS™ as the working concentrations to initially test for effective depletion of the target using siPOOLS™. Western blotting shows a successful knock-down of ERK5 was achieved and 10nM depleted GBM cells of ERK5 most effectively (figure 4.4). A final siRNA concentration of 10nM is lower than 30nM as recommended for siRNA screening by the SRSF screening facility, and as previously mentioned, Dharmacon will only guarantee a knock-down of more than 75% in 3 out of 4 siRNA sequences if a final concentration of 100nM is used, highlighting the successful knockdown of ERK5 was completed using a relatively low siRNA concentration (Dharmacon™, 2018). Due to the homology between MAPK family members, particularly ERK1/2 and MEK5, it would have been good practise to investigate the specificity of the ERK5 siRNA, for example, probing for ERK1/2 and MEK5 expression via western blot following siRNA knock-down of ERK5.

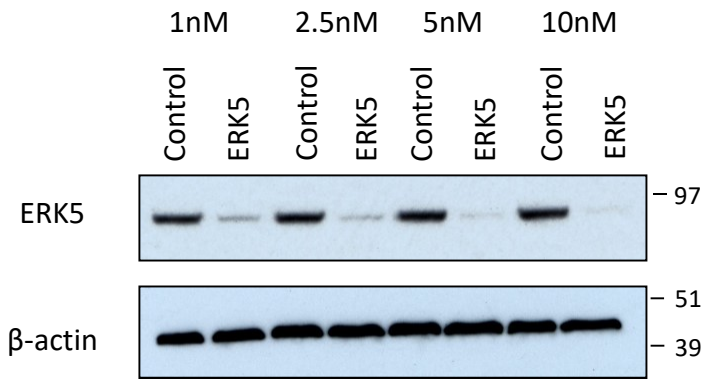

Figure 4.4: Expression of ERK5 in T98G cells treated with ERK5 siPOOLS siRNA for 48 hours
T98G cells were reverse transfected with the indicated siRNA at varying concentrations (1-10nM) before harvesting for protein lysis 48 hours later. Cells were lysed, protein was quantified and samples were run on a western blot.
siRNA concentration of 10nM generated the best knock down of ERK5 and β-actin was used as a loading control.

As 10nM siRNA showed the most robust depletion of ERK5, it was selected for further experiments. To validate ERK5 as a target that can sensitise GBM cells to temozolomide, multiple MGMT +ve and MGMT -ve GBM cell lines were reverse transfected with ERK5 siRNA for 48 hours in 96 well plates. Cells were treated with doses of temozolomide ranging from 0-400μM, and following 5 days incubation, an MTT assay was performed.

Depletion of ERK5 increased sensitivity to temozolomide in 4 GBM cell lines (figure 4.5), which contributes to the validation of the MAP3K3 pathway as a putative drug target. Both MGMT positive (T98G and LN-18) and MGMT negative (U-87 and U-251) cell lines showed an increased sensitivity which bodes well for pan-GBM clinical applicability of ERK5 inhibition as it does not select for one population of patients. However, as ERK5 has been shown to localise in and affect the function of mitochondria, it would be important to validate these findings using a non-metabolic assay, such as crystal violet, which can be used to infer cell viability where the staining is proportional to cell number and is independent of mitochondrial function (Charni et al., 2010).

However, as patients cannot be treated with siRNA, small molecule drug-like inhibitors of ERK5 were next investigated for further validation (inhibition vs mRNA/protein depletion) and to develop proof-of-concept data. As previsouly mentioned, there can be phenotypic differences between siRNA depletion and catalytic inhibition of kinases, most likely due to differences in protein-protein interactions. siRNA reduces protein expression by targeting mRNA for degradation, however, catalytic inhibition will not affect protein expression, allowing protein-

protein interactions and any biologically important scaffold roles of the protein to continue (Weiss et al., 2007).

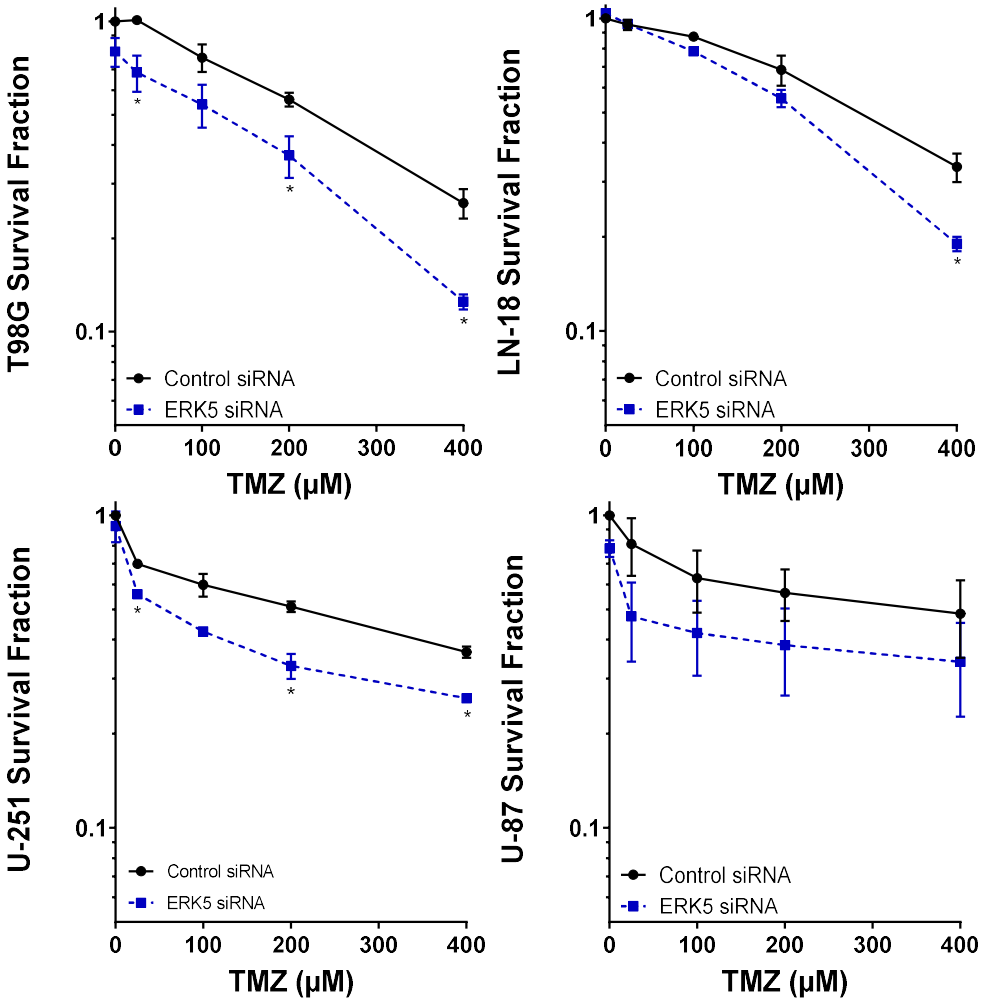

Figure 4.5: Cytotoxicity curves of GBM cells treated with Control or ERK5 siRNA

Cells were reverse transfected with the indicated siRNA and then treated with a range of TMZ (0-400μM) 48 hours later. Following 5 days incubation an MTT assay was performed. ERK5 siRNA alone showed range of toxicities in the different cell lines, being least toxic in LN-18 cells and most toxic in U-87 cells. All cell lines showed a reduced survival fraction when treated with TMZ in comparison to control cells, showing a modest increase in sensitivity to TMZ irrespective of their MGMT status (T98G and LN-18 are MGMT +ve and U-251 and U-87 are MGMT –ve).

Data shown is the average surviving fraction (normalised to DMSO treated control siRNA) +/- standard deviation derived from 2 independent biological repeat experiments.
**=p<0.05 using a Mann-Whitney U Test.*

There are currently no ERK5 or MEK5 inhibitors in clinical trials; however, there are commercially available inhibitors (table 4.1). ERK5-in-1 was purchased from Selleck (S7334) as a selective ERK5 inhibitor, however, a recent paper has shown off-target inhibition of BRD4 at IC_{50} values only slightly higher than those for ERK5 (Deng et al.,

2013, Wang et al., 2018a). There is another ERK5 inhibitor available, XMD8-92, which has been historically used to target ERK5, however, this compound also targets DCLK1 with similar IC_{50} values to those for ERK5 and also targets BD4 at higher doses (Sureban et al., 2014, Wang et al., 2018a, Yang et al., 2010). XMD8-92 was purchased from Sigma Aldrich (SML1382). There are 2 inhibitors for MEK5, BIX02188 and BIX02189, which were purchased from Selleck (S1530 and S1531). However, as BIX02188 and BIX02189 were discovered from the same high-throughput screen and BIX02189 has a lower IC_{50} value for MEK5 (Tatake et al., 2008), this was selected over BIX02188 for future work.

Table 4.1: IC_{50} of MEK5/ERK5 inhibitors

Inhibitor	Target	IC_{50}(nM)
ERK5-in-1	ERK5	162
	BRD4	217/618
XMD8-92	ERK5	364
	BRD4	2343/3465
	DCLK-1	97
BIX01288	MEK5	4.3
	ERK5	810
BIX01289	MEK5	1.5
	ERK5	59

Table 4.1 *- Commercially available MEK5 and ERK5 inhibitors with a range of IC_{50} values. Both XMD8-92 and ERK5-in-1 also inhibit bromodomain-containing proteins (BRD4s) (Tatake et al., 2008, Wang et al., 2018a, Yang et al., 2010).*

BIX02189 is a MEK5 inhibitor and at higher concentrations an ERK5 inhibitor (Tatake et al., 2008). As this inhibitor has an IC_{50} value of 1.5nM for MEK5 and 59nM for ERK5, a dose response ranging from 0-1µM in combination with temozolomide (50µM) was carried out. There was, however, no difference in survival (data not shown). The concentration was further increased up to 10µM of BIX02189; however, this resulted in more cell death from BIX02189 alone but there was no increase in temozolomide sensitivity (50µM) (data not shown). A clonogenic assay was completed at a dose of 1µM in LN-18 cells, again with no increase in sensitisation (data not shown). However, this may not be surprising as several published studies use at least 10µM for inhibition of kinase activity in cell lines (Belkahla et al., 2018, Su et al., 2014). As ERK5-in-1 has off-targets effects on BRD4, the lack of sensitisation seen when using MEK5 inhibitors could potentially indicate that BRD4 inhibition is important in temozolomide sensitivity rather than the loss of ERK5 catalytic activity. Bromodomain inhibition has previously been shown to decrease the proliferation of GBM cells, also resulting in additive cell death when

cells were treated in combination with temozolomide (Lam et al., 2018, Pastori et al., 2014).

ERK5-in-1 was tested in combination with temozolomide in GBM cells. Initially a western blot was used to detect inhibition of ERK5 activity using a range of doses of ERK5-in-1 (ERK5i) (figure 4.6A); however, phosphorylation of ERK5 could only be detected following stimulation of the pathway using EGF. ERK5i was able to sensitise T98G cells to temozolomide when both drugs were used in combination (figure 4.6B). 0.25µM ERK5i was selected for future experiments as it was able to inhibit ERK5 phosphorylation and sensitise T98G cells to temozolomide most significantly (p=<0.0001) whilst causing with little cell toxicity when used alone (survival fraction 0.9).

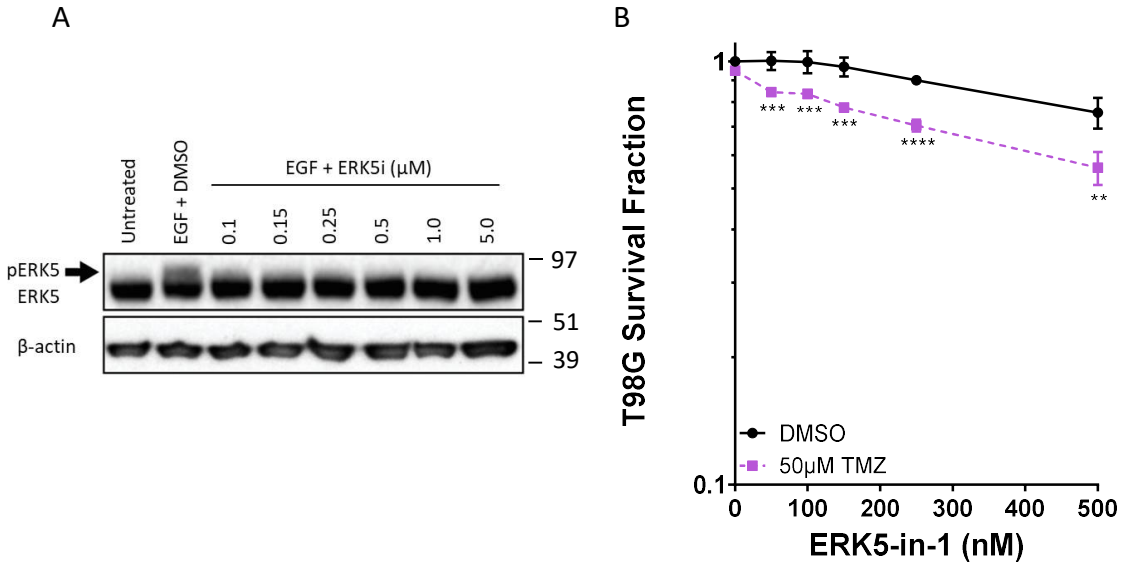

Figure 4.6: Inhibition of ERK5 activity using ERK5i in GBM cells

Cells were plated and allowed to adhere for 24 hours. Cells were treated with a range of doses of ERK5i (0-500nM) before being treated with EGF or TMZ 1.5 hours later. Cells were collected for western blotting 30 minutes after EGF treatment (A) or were incubated for 5 days with TMZ before an MTT assay was performed (B). ERK5i was able to inhibit ERK5 phosphorylation and sensitise T98G cells to TMZ when used in combination. The most significant decrease in survival fraction was using a combination of 250nM ERK5i and 50µM TMZ.

Data shown is the average surviving fraction (normalised to DMSO treated controls) +/- standard deviation derived from 5 independent biological repeat experiments.
***=p<0.005 ***=p<0.001 ****=p<0.0001 using a Mann-Whitney U Test.*

ERK5i was then combined with increasing doses of temozolomide in a panel of GBM cell lines and was able to sensitise them irrespective of MGMT status (figure 4.7). Combination treatment did not sensitise U-251 cells significantly to temozolomide, however, there was a trend in decreased survival. All other cell lines had a significant decrease in survival with at least one concentration of temozolomide

used, with variability in sensitivity possibly due to differences in ERK5 protein expression across the cell lines.

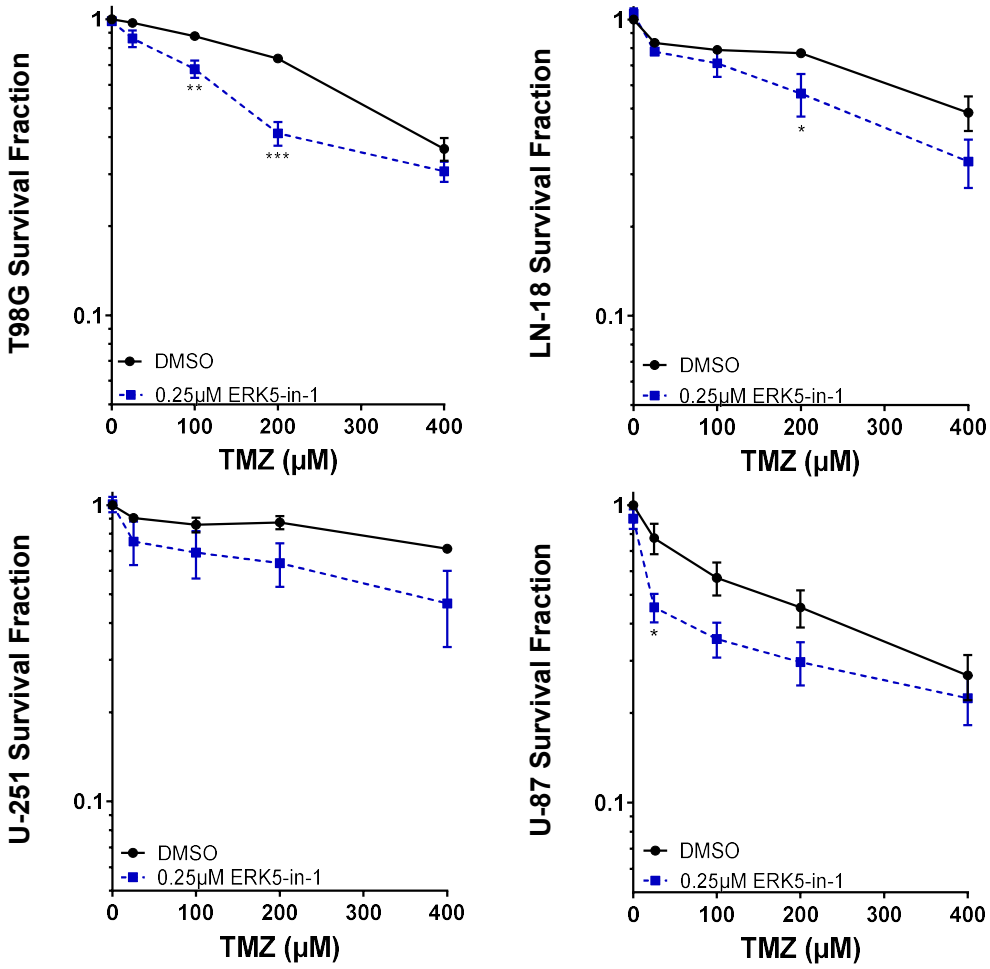

Figure 4.7: Cytotoxicity curves of GBM cells treated with ERK5i and TMZ

Cells were plated before being treated with 0.25μM ERK5i 24 hours later. A range of doses of TMZ (0-400μM) were added 90 minutes later. Following 5 days incubation an MTT assay was performed. ERK5i showed little toxicity alone, however, all cell lines showed a reduced survival fraction when treated with the combination of ERK5i and TMZ in comparison to TMZ alone.

Data shown is the average surviving fraction (normalised to DMSO treated controls) +/- standard deviation derived from 2 independent biological repeat experiments.
**=p<0.05 **=p<0.005 ***=p<0.001 using a Mann-Whitney U Test.*

Clonogenic survival assays are more sensitive compared to MTT assays, as they are a more accurate measure of growth and survival as opposed to metabolism. Clonogenic survival assays are not reliant on mitochondrial function therefore the results generated cannot be modulated by any possible changes which could be caused to mitochondria following ERK5i drug treatment. To determine the

temozolomide potentiating effects of ERK5i, clonogenic assays were completed in LN-18 and U-251 cells in combination with ERK5i and/or temozolomide. ERK5i was able to dramatically sensitise both cell lines to temozolomide at the sub-micro molar dose of 250nM (figure 4.8).

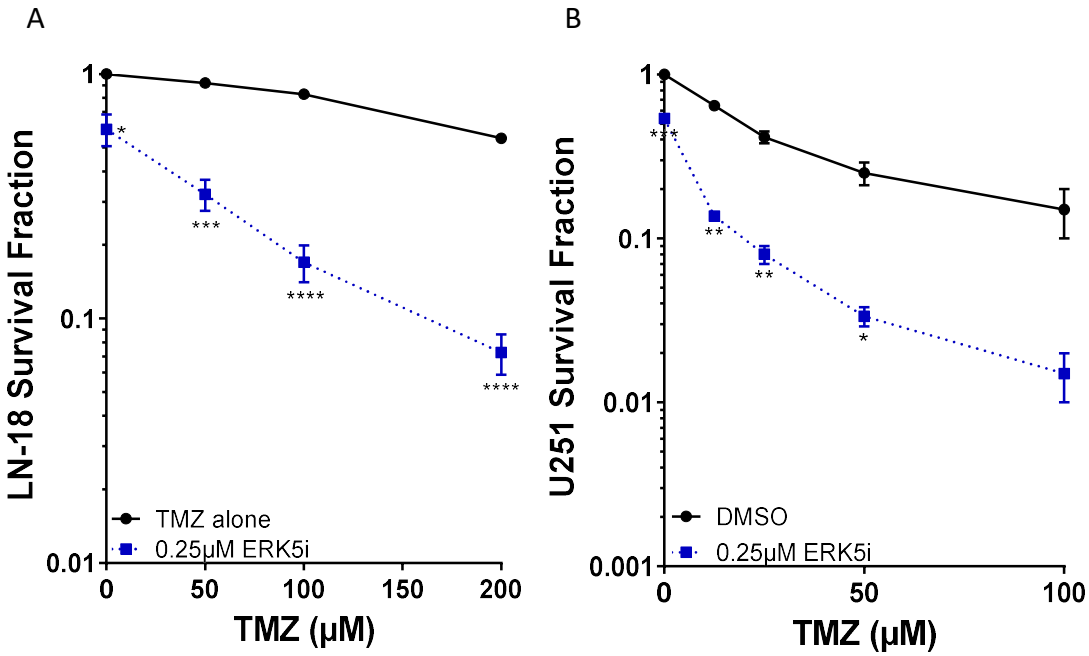

Figure 4.8: Cytotoxicity curves of GBM cells treated ERK5i and TMZ

Cells were plated before being treated with ERK5i 24 hours later. Following a 90 minute incubation a range of doses of TMZ were added. 0-400μM TMZ was added to LN-18 cells (MGMT +ve) and 0-100μM was added to U-251 cells (MGMT -ve). Cells were incubated for 12 days allowing colonies to form. Cell colonies were fixed in 0.04% methylene blue in 100% ethanol for 30 minutes at room temperature. >50 cells were counted as a colony. Both cell lines were sensitised to TMZ, however, U-251 cells are more sensitive so lower doses were used.

Data shown is the average surviving fraction (normalised to DMSO treated controls) +/- standard deviation derived from 5 independent biological repeat experiments.
A x-axis – 0.0001 B x-axis 0.001
**=p<0.05 **=p<0.005 ***=p<0.001 ****=p<0.0001 using a Mann-Whitney U Test.*

U-251 experiments were completed by Connor McGarrity-Cottrell, 2nd Year Undergraduate Student from Sheffield Hallam University.

Due to the variation in temozolomide sensitivity observed across GBM cell lines following ERK5 inhibition (figure 4.7, figure 4.8), total and phosphorylated ERK5 protein were investigated using western blotting (figure 4.9). As previously seen with T98G cells, other GBM cell lines also express un-phosphorylated ERK5 under normal conditions and may therefore be more reliant on total protein levels as opposed to catalytic activity. Although there are small changes in ERK5 expression between the cell lines, this does not reflect the variability seen in temozolomide sensitivity following treatment with ERK5i, perhaps indicative that off-target BRD4 inhibition is important here.

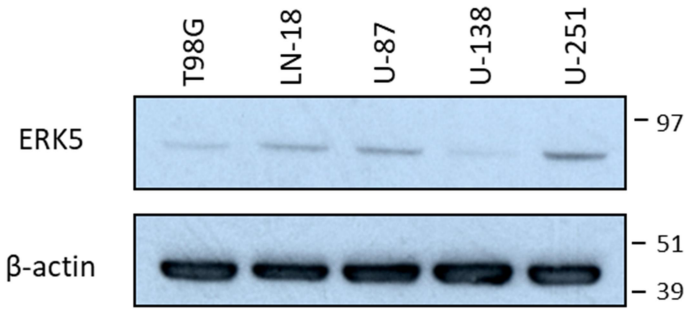

Figure 4.9: Expression of ERK5 in GBM Cell Lines

Cells were plated and allowed to adhere for 24 hours before being collected for western blotting. Samples were probed for ERK5 expression and β-actin was used as a loading control for the western blot. There is a small difference in ERK5 expression between GBM cell lines, however, ERK5 remains un-phosphorylated under normal conditions.

Western blot was completed by Connor McGarrity-Cottrell, 2nd Year Undergraduate Student from Sheffield Hallam University.

To ensure this was not a drug specific effect, XMD8-92 was also used in combination with temozolomide in a clonogenic survival assay. XMD8-92 was able to sensitise GBM cells to temozolomide, however, this effect was less than that of ERK5i (figure 4.10). XMD8-92 was used at a concentration 10 times higher than that of ERK5i in order to establish any sensitisation, however, although the IC_{50} for XMD8-92 is double the IC_{50} for ERK5-in-1, XMD8-92 is an inhibitor of BRD4 at higher concentrations (1-2μM) had to be used in order to generate sensitisation to temozolomide (table 4.1). These data could therefore be a result of off-target effects of XMD8-92 on BRD4.

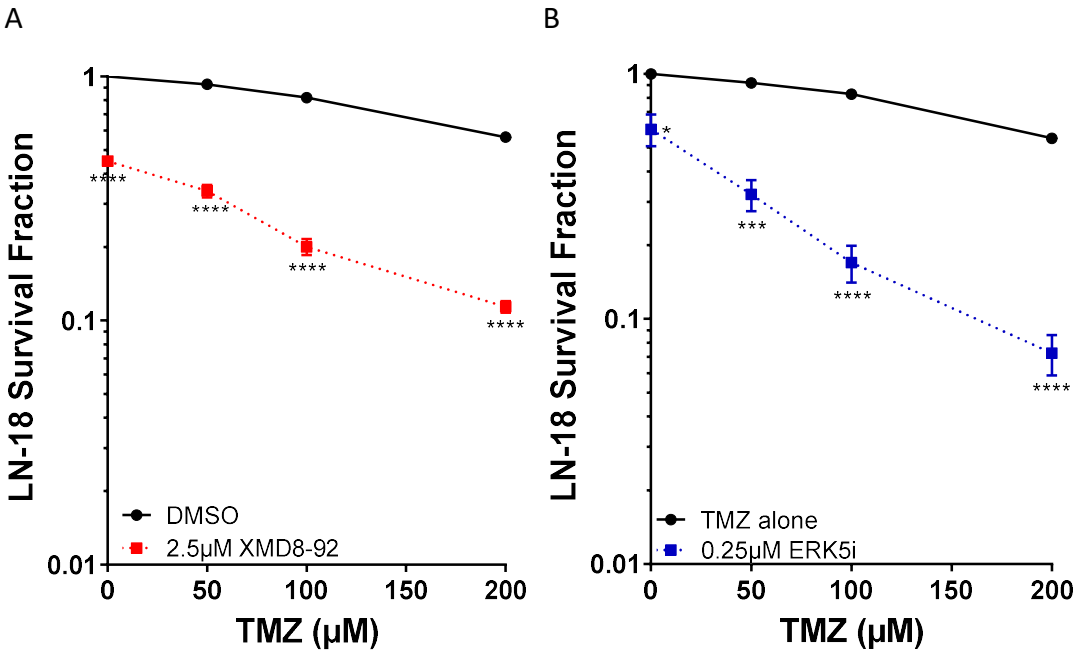

Figure 4.10: Cytotoxicity curves of GBM cells treated with XMD8-92 or ERK5i and TMZ

Cells were plated before being treated with XMD8-92 (A) or ERK5i (B) 24 hours later (data taken from figure 4.8A). Following a 90 minute incubation a range of doses of TMZ were added (0-200μM). Cells were incubated for 12 days allowing colonies to form. Cell colonies were fixed in 0.04% methylene blue in 100% ethanol for 30 minutes at room temperature. >50 cells were counted as a colony. Survival fraction (A) shows LN-18 cells treated with 2.5μM of XMD8-92. This sensitised cells to TMZ, however, ERK5i (0.25μM) was able to sensitise cells more effectively to TMZ, shown by the increased reduction in survival fraction (B)

Data shown is the average surviving fraction (normalised to DMSO treated controls) +/- standard deviation derived from 3 independent biological repeat experiments.

**=p<0.05 **=p<0.005 ***=p<0.001 ****=p<0.0001 using a Mann-Whitney U Test.*

Combination treatment was also able to sensitise patient derived Glioma Stem Cells (GSCs) to temozolomide, however, this was not as large an effect as seen in immortalised cell lines (figure 4.11). It is important to note, however, that in order to maintain the stem properties of GSCs; they are cultured in EGF and FGF. As EGF is known to activate the ERK5 pathway at doses as low as 0.1ng/ml, the reduced effect in sensitisation may be due to increased pathway activation likely requiring re-optimisation and an increase in the concentration of ERK5i used (Kato et al., 1998).

ERK5 protein levels were also detected in both primary derived glioma stem cells and the corresponding 'bulk' cells (figure 4.12). The 'bulk' population do not express stem cell markers and are not grown in EGF or FGF; however, no difference was observed in either ERK5 phosphorylation or total protein expression between the two populations. There appears to be slightly more ERK5 protein in both GBM2

stem and bulk samples but very little difference in sensitivity to temozolomide following ERK5 inhibition was observed, however, as this experiment was completed once under different conditions compared to the data generated from immortalised cells, it is difficult to draw any firm conclusions until repeated experiments with optimised conditions are established.

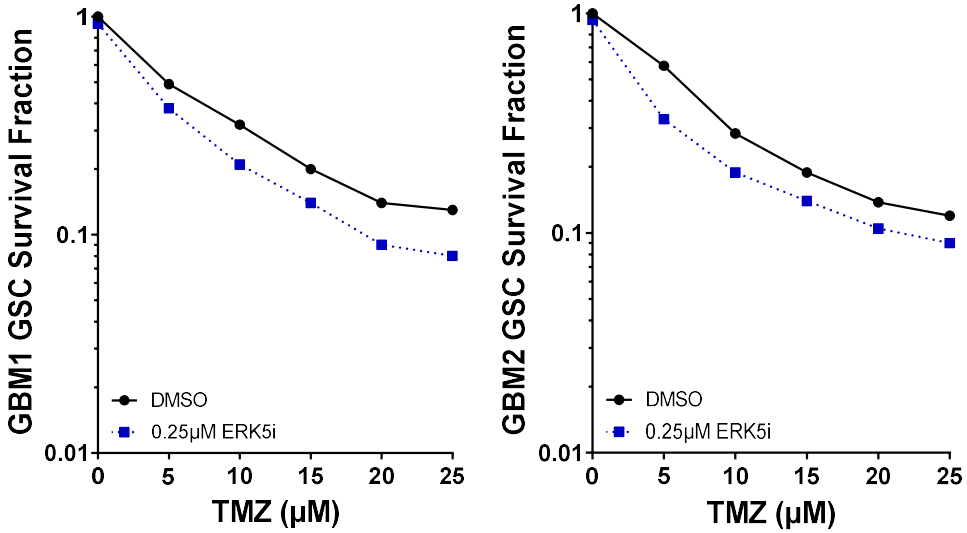

Figure 4.11: Cytotoxicity curves of Glioma Stem Cells treated ERK5i and TMZ

Cells were cultured with 20ng/ml EGF and 10ng/ml FGF to maintain stemness, before being plated on matrigel coated plates 24 hours before the addition of ERK5i. Following a 90 minute incubation a range of doses of TMZ were added (0-25μM TMZ). Cells were incubated for 3 days before media was replaced. Cells were incubated for a further 17 days allowing colonies to form. Cell colonies were fixed in 0.04% methylene blue in 100% ethanol for 30 minutes at room temperature. >50 cells were counted as a colony. The combination of ERK5i and temozolomide caused a reduction in survival fraction compared to temozolomide alone in 2 populations of Glioma Stem Cells.

Data shown is the average surviving fraction (normalised to DMSO treated controls) from 1 independent biological experiment.
These experiments were completed by Mr Ola Rominiyi, a clinical PhD student in the Collis laboratory.

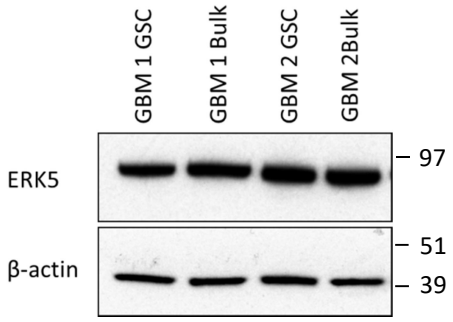

Figure 4.12: Expression of ERK5 in Patient Derived GBM Cells

Primary cells taken from GBM tumours during surgery were cultured in standard media ('bulk') or media supplemented to select for stem-like cells. After 6 weeks cells were harvested and lysed for western blotting. Samples were probed for ERK5 expression and β-actin was used as a loading control for the western blot. There is little difference in ERK5 expression between both the stem and 'bulk' populations, with ERK5 remaining un-phosphorylated.

Of the multiple GBM cell line tested, there was only one cell line (U-138) which was not sensitised to temozolomide with either ERK5 siRNA or ERK5i (figure 4.13). U-138 cells did express the least total ERK5 protein compared to the other GBM cell lines, and ERK5 was also un-phosphorylated under normal conditions (figure 4.9).

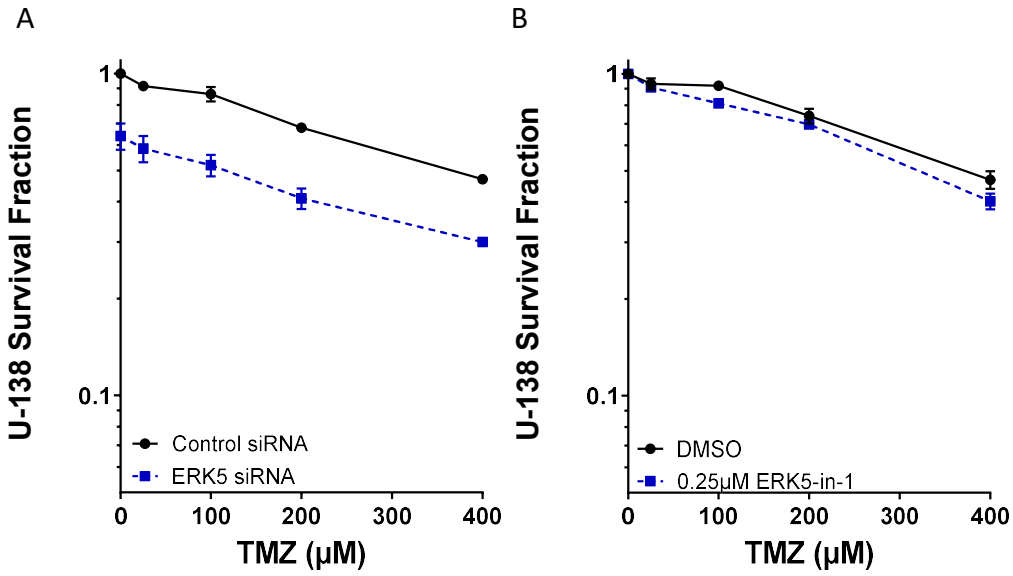

Figure 4.13: Cytotoxicity curves of GBM cells treated with ERK5 siRNA or ERK5i

Cells were reverse transfected with indicated siRNA and then treated with a range of TMZ (0-400μM) 48 hours later (A) or cells were plated before being treated with 0.25μM ERK5i 24 hours later and then range of doses of TMZ (0-400μM) were added 90 minutes later (B). Following 5 days incubation an MTT assay was performed. Both siRNA and ERK5i were unable to sensitise U-138 cells to treatment with temozolomide. However, ERK5 siRNA alone did cause a significant decrease in survival fraction compared to control siRNA alone (p=0.03).

Data shown is the average surviving fraction (normalised to DMSO treated controls) +/- standard deviation derived from 2 (A) or 5 (B) independent biological repeat experiments.

Obviously there are numerous genetic and epigenetic differences between all the GBM cell lines used in this study. However, one known difference in U-138 cells, also known as HTB-16 cells, is that they are deficient in the Fanconi Anaemia (FA) DNA repair pathway, which is known to affect cellular sensitivity to temozolomide (Chen et al., 2007). To investigate further whether the presence of an intact FA pathway is required for ERK5i-mediated sensitisation to temozolomide, the FA-proficient LN-18 cells were depleted of the key FA pathway subunit FANCD2 using siRNA and then treated with ERK5i and temozolomide both individually and in combination. Depleting cells of FANCD2 caused varying results; two biological repeats showed FANCD2-depleted cells were still sensitised to temozolomide by ERK5i, whilst another two biological repeats showed FANCD2-depleted cells were less sensitive to temozolomide sensitisation by ERK5i, with no significant difference between combination treatment and temozolomide alone (figure 4.14).

Combination treatment was always significantly different to DMSO treated controls in all repeats. This variability meant that no firm conclusions could be drawn and it is unknown at present if FANCD2 proficiency is key to ERK5i sensitisation.

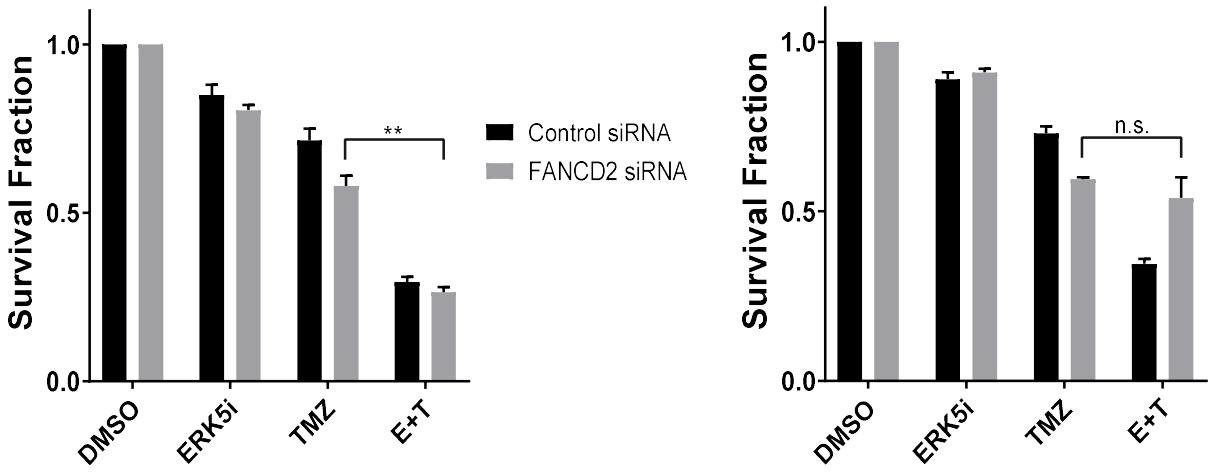

Figure 4.14: Cytotoxicity curves of GBM cells treated with control or FANCD2 siRNA ERK5i and TMZ

Cells were reverse transfected with the indicated siRNA and then treated with 0.25μM ERK5i 48 hours later. Following a 90 minute incubation cells were treated with 50μM TMZ. Following 5 days incubation an MTT assay was performed. For 2 repeats FANCD2 depletion did not affect ERK5i sensitisation of GBM cells to TMZ, with combination treatment significantly reducing survival compared to TMZ alone (p=0.009) (A). FANCD2 depletion reduced the efficacy of this sensitisation in another 2 repeats, with no significant difference between combination treatment and TMZ alone (B). Control and FANCD2 siRNA combined with ERK5i and TMZ resulted in a significant increase in cell death when compared to DMSO treated controls in all repeats (p=<0.001).

Data shown is the average surviving fraction (normalised to DMSO treated control or FANCD2 siRNA) +/- standard deviation derived from 2 independent biological repeat experiments.
***=p<0.005 using a Kruskal-Wallis H Test.*

MTT assays and clonogenic survival assays are used to determine cell growth and survival; however, annexin V and PI staining are used to identify dead, apoptotic and necrotic cells (ThermoFisherScientific, 2018), and were therefore used to investigate the mode of increased cell death observed with ERK5i in combination with temozolomide. Annexin V and PI staining showed a decrease in live cells (no stain) and an increase in dead cells (annexin V and PI positive) with the combination of ERK5i and temozolomide over a time course in T98G and U-251 cells (figure 4.15). Interestingly, the percentage of dead cells and reduction in live cells was more than additive in the combination treatment 96 hours and 120 hour post treatment in T98G cells and 120 hours post treatment in U-251 cells, suggesting a potentially induced lethality/synergistic phenotype. At 120 hours, the percentage of live T98G and U-251 cells treated with the combination of ERK5i and temozolomide was significantly different when compared to untreated cells (p-

value 0.049). Dead cell values did not quite reach significance (p-values 0.086); however, a trend of increased cell death can be seen with combination treatment. In U-138 cells which were not sensitive to the combination of ERK5i and temozolomide (figure 4.13), there were no significant changes over the time course (figure 4.16).

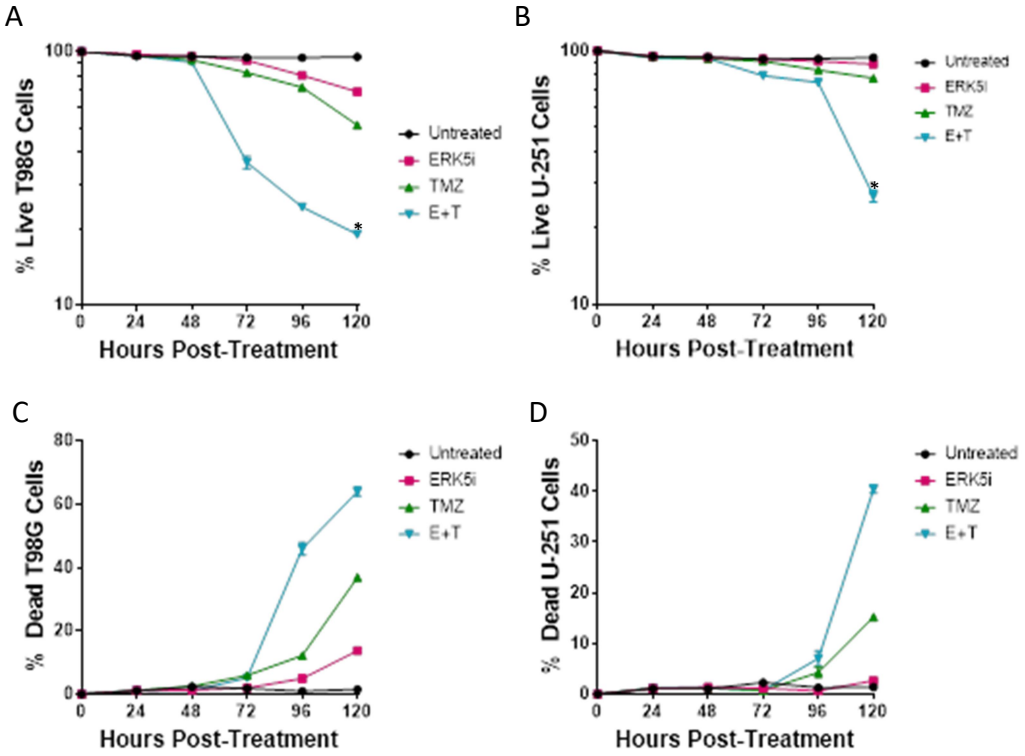

Figure 4.15: Percentage of live and dead GBM cells after treatment

T98G cells (A & C) or U-251 cells (B & D) were plated in 10cm dishes before being treated with ERK5i (0.25µM) 24 hours later. Following a 90 minute incubation 200µM TMZ was added. Cells were collected for FACS at various time points, before being stored at -20°C in 70% ethanol prior to processing. Cells were incubated with annexin V and PI as per the protocol and then analysed on the FACSCalibur. Unstained cells were used to determine the gates for annexin V, PI or dual stained cells. Combination of ERK5i and TMZ caused a significant decrease in live cells at 120h post treatment in both cell lines (p=0.009), however, dead cells showed an increasing trend almost reaching significance (p=0.086).

Data shown is the average (normalised to DMSO treated controls) from 2 independent biological repeat experiments.
**=p<0.05 using a Mann-Whitney U Test.*

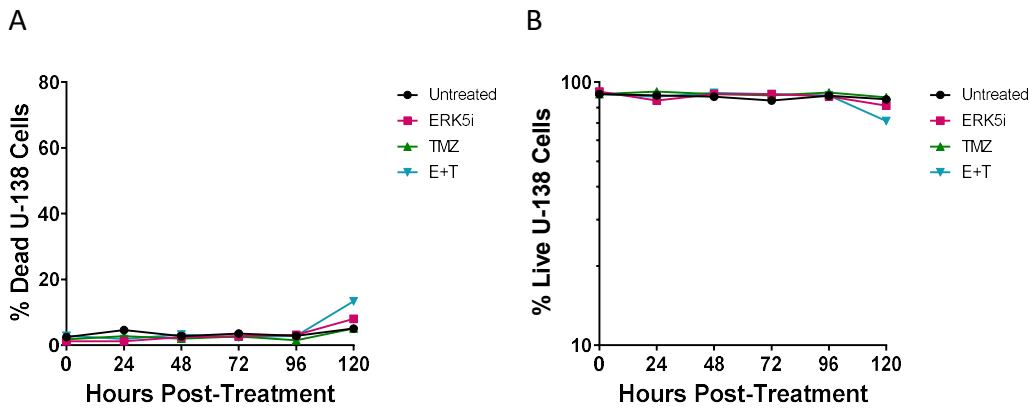

Figure 4.16: Percentage of live and dead U-138 cells after treatment

U-138 cells were plated in 10cm dishes before being treated with ERK5i (0.25μM) 24 hours later. Following a 90 minute incubation 200μM TMZ was added. Cells were collected for FACS at various time points, before being stored at -20°C in 70% ethanol prior to processing. Cells were incubated with annexin V and PI as per the protocol and then analysed on the FACSCalibur. Unstained cells were used to determine the gates for annexin V, PI or dual stained cells. Combination of ERK5i and TMZ did not cause a significant increase in dead cells (A) or a significant decrease in live cells (B) at any time points.

Data shown is the average (normalised to DMSO treated controls) from 2 independent biological repeat experiments.

Collectively, these data confirm ERK5 to be a credible drug target to augment the efficacy of temozolomide cytotoxicity effects on GBM cells, and provide compelling proof-of-concept data to warrant further investigation into the mechanism behind this.

4.5 MGMT and ERK5 levels are unchanged by combination treatment

As previous blots have shown ERK5 to be un-phosphorylated in GBM immortalised and primary cells under normal conditions, the effect of temozolomide on ERK5 activity was investigated at increasing concentrations, however, this showed no change, suggesting that ERK5 is not observably activated in cells following temozolomide treatment (figure 4.17A).

MGMT is known to play a critical role in sensitivity to temozolomide (Kaina et al., 2007); the effect of ERK5i on MGMT levels was therefore investigated at various time points using western blotting to ascertain if the temozolomide sensitisation conferred by ERK5i was a consequence of altered MGMT levels. There was no detectable change in MGMT levels following treatment with ERK5i (figure 4.17B).

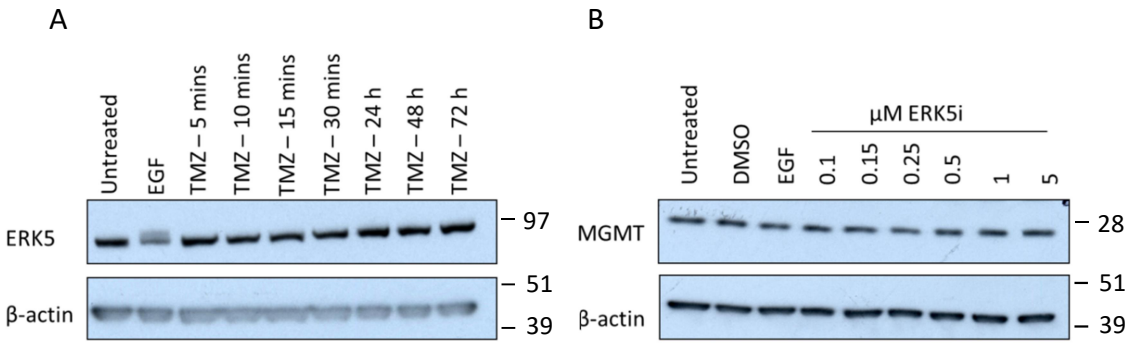

Figure 4.17: Effect of TMZ and ERK5i on ERK5 and MGMT protein expression
T98G cells were plated before being treated with either 50μM TMZ (A) or ERK5i (B). Cells were harvested, lysed and protein was quantified before being loaded on to a gel. Membranes were probed with ERK5 primary antibody (A) or MGMT primary antibody (B). β-actin was used as a loading control.
There was no change in expression of ERK5 or MGMT with the addition of TMZ or ERK5i.

4.6 Combination treatment causes more DNA damage and Genomic Instability

The DNA damage response (DDR) of GBM cells treated in combination with ERK5i and temozolomide was next investigated. Previous experiments have used 50μM temozolomide over a 5 day period; however, as these next studies were conducted over 24 hours, an increased dose of temozolomide was used (200μM) with the aim of enhancing any effects seen.

Firstly, an increase in DNA damage was investigated using 53BP1. 53BP1 is used as a marker of double strand breaks in DNA (Schultz et al., 2000). The number of foci per nucleus were counted in around 100 cells except the positive irradiation (IR) control. The score from each nucleus was combined to give an average number of foci for each condition (figure 4.18). LN-18 cells treated with ERK5i and temozolomide in combination (E+T) had a more than additive number of 53BP1 foci/nucleus when values from ERK5i and temozolomide conditions alone were added together. U-251 cells, however, did not exhibit a comparable phenotype, although combination of ERK5i and temozolomide did result in more DNA damage (figure 4.18).

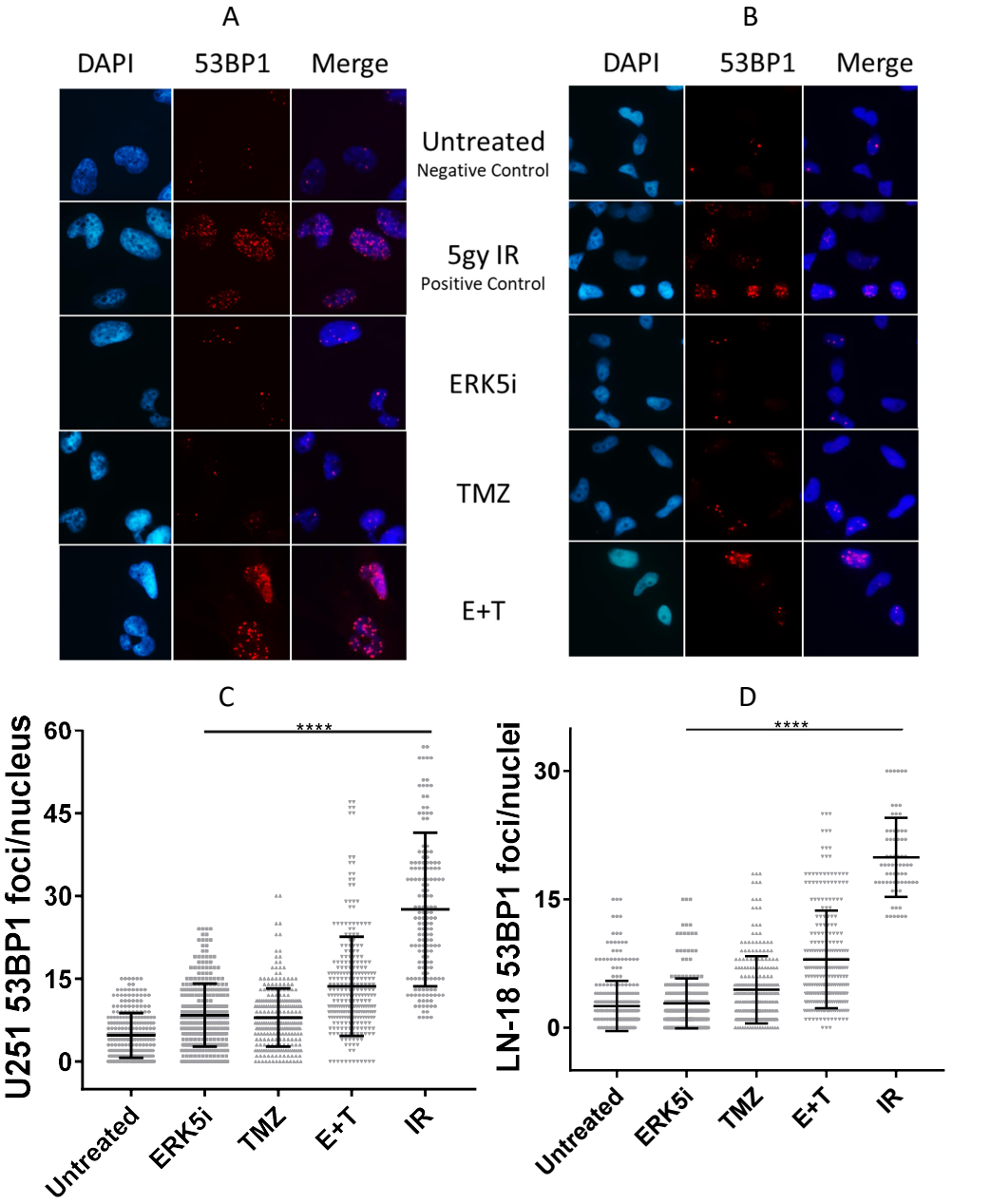

Figure 4.18: 53BP1 foci in GBM cells 24 hours after treatment

U-251 cells (A) or LN-18 cells (B) were plated on coverslips before being treated with ERK5i (0.25μM) 24 hours later. Following a 90 minute incubation 200μM TMZ was added. 24 hours later cells were fixed ready for IF processing. Cells were imaged at 20x objective on a Nikon Eclipse TE200 Fluorescent Microscope and the numbers of foci were counted and averaged. LN-18 cells treated with E+T had a slightly more than additive average compared to the value of ERK5i and TMZ drug alone combined (8.00 v 7.28) (D). U-251 cells treated with the combination E+T did not have more than an additive average number of foci (C). All conditions were significantly different from untreated cells and each other.

*****p=<0.0001 (n=≥2) using a Kruskal-Wallis H Test.*

Comet assays are used to measure and visualise breaks in DNA, as opposed to IF which uses only markers of DNA damage. Following lysis which leaves DNA unharmed, an electric current is applied to the DNA suspended in agarose. The more breaks in the DNA, the further it will migrate through the agarose (negatively charged DNA migrates to positive cathode). Once a nucleotide stain is applied, the DNA 'tails' can be visualised using fluorescent microscopy (Ostling and Johanson, 1984). The alkaline comet assay was used for these studies, enabling all DNA damage (both single and double stranded DNA breaks) to be visualised and quantified. Tail moment, calculated by TriTek Comet Score, is used as a measure of DNA damage severity, combining tail length and intensity of DNA within the tail (AMSBiotechnology, 2010).

Both T98G and U-251 cells had a significant increase in tail moment in temozolomide and combination (E+T) treated cells when compared to untreated cells ($p=<0.0001$). There was also a significant difference between temozolomide treated and combination (E+T) treated cells ($p=<0.0001$). Average tail moment for T98G cells was 34.29 for temozolomide compared to 57.06 for combination treatment (E+T), and in U-251 values were 69.65 compared to 136.78. In both cell lines, the combination treatment resulted more than additive DNA damage (figure 4.19).

U-138 cells were not sensitive to the combination of ERK5i and temozolomide treatment. These cells were also investigated via a comet assay. There was a significant increase in tail moment in temozolomide and combination (E+T) treated cells when compared to untreated cells, however, there was no significant difference between these two treatments (figure 4.20), which is consistent with the survival data.

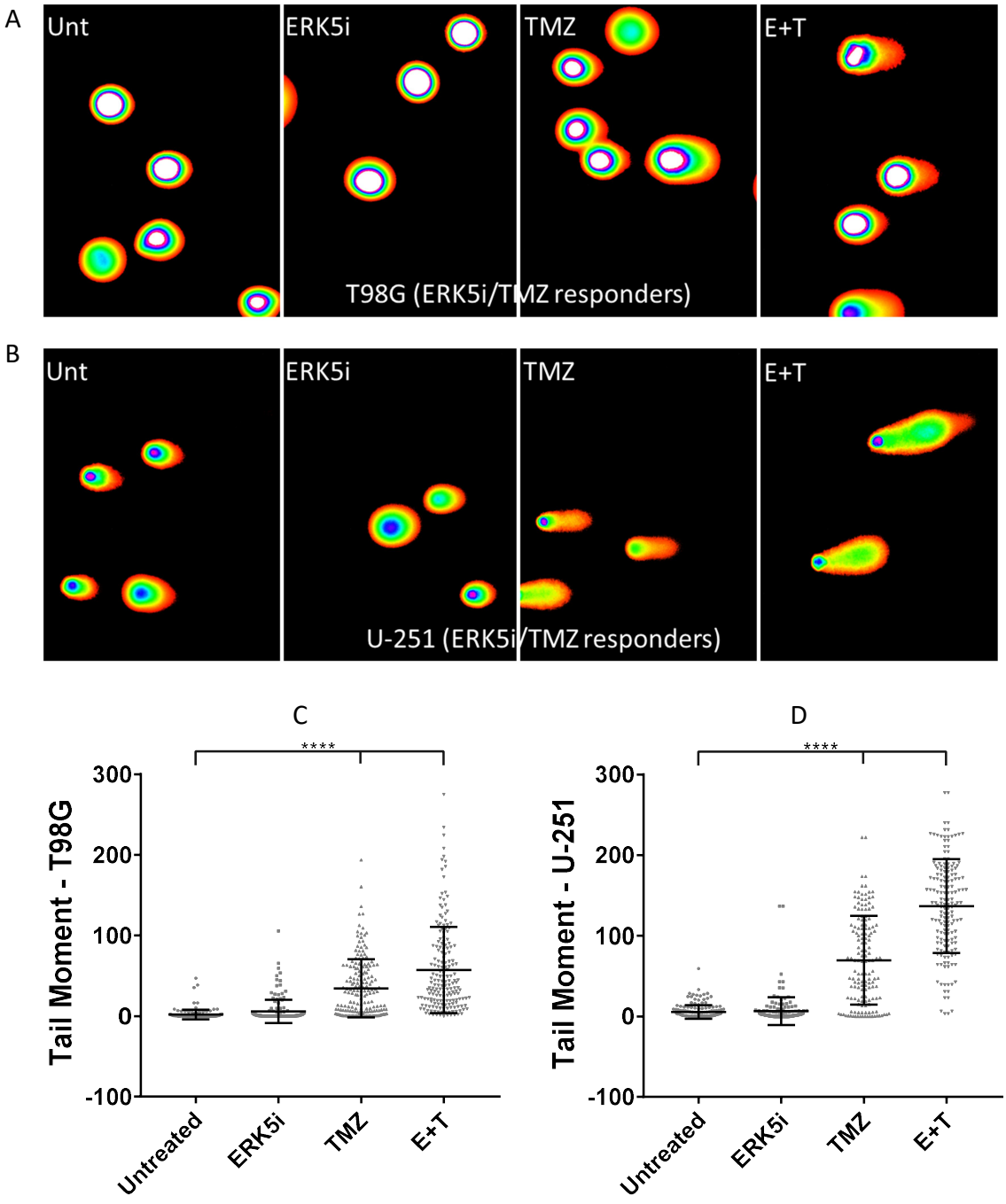

Figure 4.19: DNA damage in GBM cells 24 hours after treatment

T98G cells and U-251 cells were plated 24 hours before being treated with ERK5i (0.25µM). Following a 90 minute incubation 200µM TMZ was added and a further 24 hours later cells were harvested for comet assay. Images are representative of T98G cells (A) and U-251 cells (B) visualised on Comet Score after various treatments. Tail moment was calculated for around 50 cells per condition for each repeat. Cells were imaged at 20x objective on a Nikon Eclipse TE200 Fluorescent Microscope after being stained with SYBR Gold. Combination treatment of ERK5i and TMZ caused the largest tail moment with values of 57.06 and 136.78 for T98G and U-251 respectively (C & D) (p=<0.0001).

*****p=<0.0001 using a Kruskal-Wallis H Test.*
(n=3)

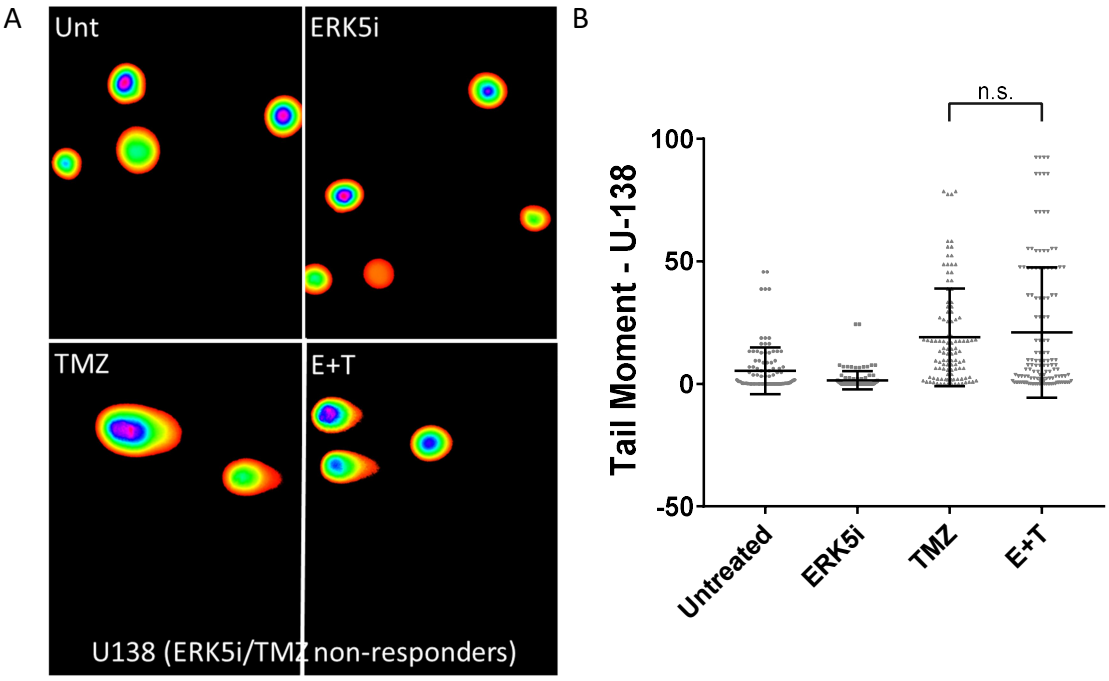

Figure 4.20: DNA damage in GBM cells 24 hours after treatment

U-138 cells were plated 24 hours before being treated with ERK5i (0.25µM). Following a 90 minute incubation 200µM TMZ was added and a further 24 hours later cells were harvested for comet assay. Images are representative of U-138 cells (A) visualised on Comet Score after various treatments. Tail moment was calculated for around 50 cells per condition for each repeat. Cells were imaged at 20x objective on a Nikon Eclipse TE200 Fluorescent Microscope after being stained with SYBR Gold. Combination treatment of ERK5i and TMZ caused no more damage than TMZ alone (B).

(n=2)

As both 53BP1 IF and comet assays showed an increase in DNA damaged caused by combination treatment, levels of O-6-methylguanine, NHEJ and HR-related damage were then investigated in order to try and ascertain a greater understanding of how such damage is being generated and what DNA repair pathways are being activated in response.

O-6-methylguanine lesions are the most toxic damage caused by temozolomide. These were first investigated by immunofluorescence (IF). 1mM temozolomide was used as a positive control. Both cells treated with the combination of ERK5i and 200µM temozolomide and the positive control had a significant increase in detectable lesions (p-value <0.0001) compared to untreated cells. Temozolomide alone also had a significant increase in the percentage of positive cells; however, this increase was slightly less significant (p-value 0.002). One unexpected finding was that ERK5i alone was responsible for a modest increase in O-6-methylguanine lesions, however, this increase was not significant (p-value 0.84) (figure 4.21). Unlike the trends in DNA damage visualised by the comet assay, there was no significant difference between cell treated with 200µM temozolomide and those with combination treatments. Additionally, the percentage of positive cells in the combination treatment are likely due to an additive effect of both ERK5i and temozolomide individually, suggesting that O-6-methylguanine lesions are unlikely to be the mechanism by which more breaks are being generated in cells following combination treatments.

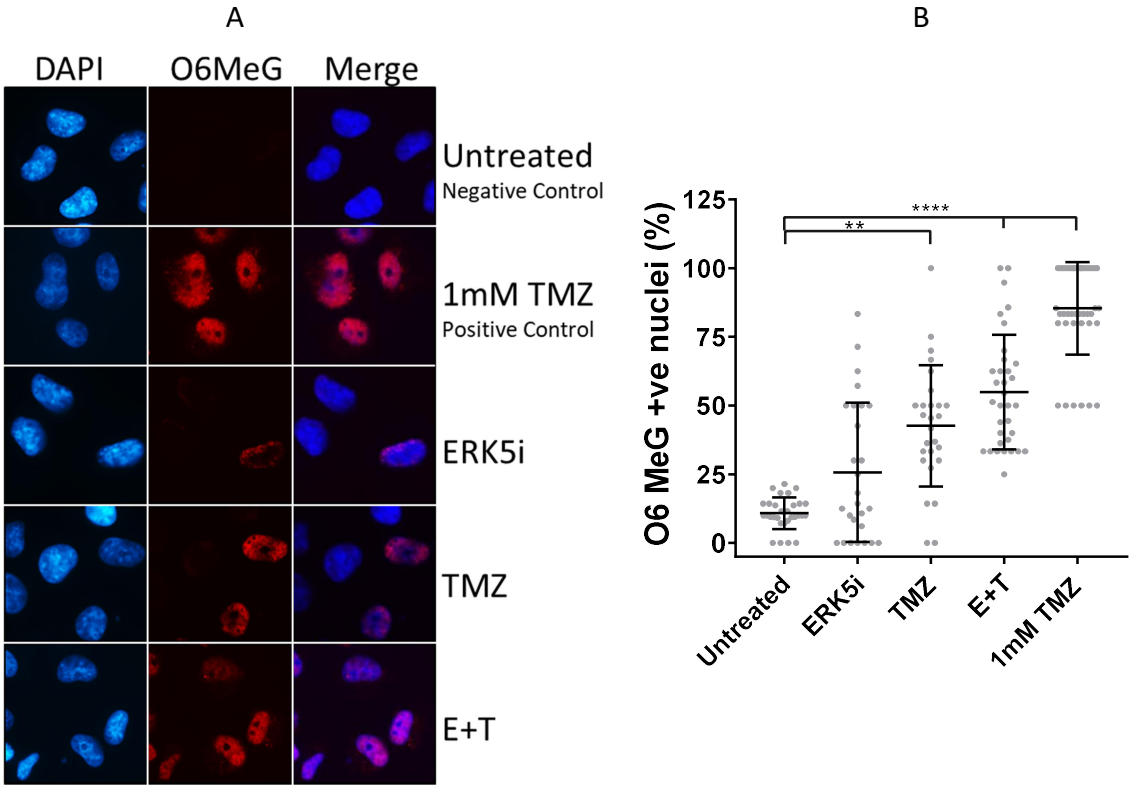

Figure 4.21: O-6-methylguanine positive GBM cells 24 hours after treatment

LN-18 cells were plated on coverslips before being treated with ERK5i (0.25µM) 24 hours later. Following a 90 minute incubation 200µM TMZ was added. 24 hours later cells were fixed ready for IF processing. Cells were imaged at 20x objective on a Nikon Eclipse TE200 Fluorescent Microscope. Images are representative of each condition (A). The numbers of positive cells were counted and averaged (B). LN-18 cells treated with E+T and the 1mM TMZ positive control were the most significantly different to the untreated cells (p<0.0001). TMZ alone was also significantly different to untreated cells but to a lesser extent.

***p=<0.005 ****p=<0.0001 using a Kruskal-Wallis H Test.*
(n=2)

DNA-PKcs is used to detect double strand DNA breaks that will be primarily repaired by non-homologous end joining (NHEJ) (Meek et al., 2008). DNA-PKcs activation was investigated using phosphorylation of serine 2056. Unfortunately, the number of foci could not be accurately counted in these cell lines as the stain was very speckled so as an alternative, the number of DNA-PKcs positive cells were scored. Results were generated as a percentage of total cells visible in each field of view over multiple fields across each slide within individual experimental repeats (figure 4.22). Both MGMT positive and MGMT negative GBM cell lines exhibited more DNA-PKcs positive cells when treated with the combination of ERK5i and temozolomide. This percentage was more than additive when compared to the value generated by ERK5i and temozolomide alone in both cell lines. All conditions except for ERK5i alone were significantly different to untreated cells in LN-18, however, combination treatment and positive IR control generated the most

statistically significant results (p<0.0001). Both combination of ERK5i and temozolomide and the positive IR control were significantly different to untreated cells in U-251 generating p values of 0.0009 and <0.0001 respectively.

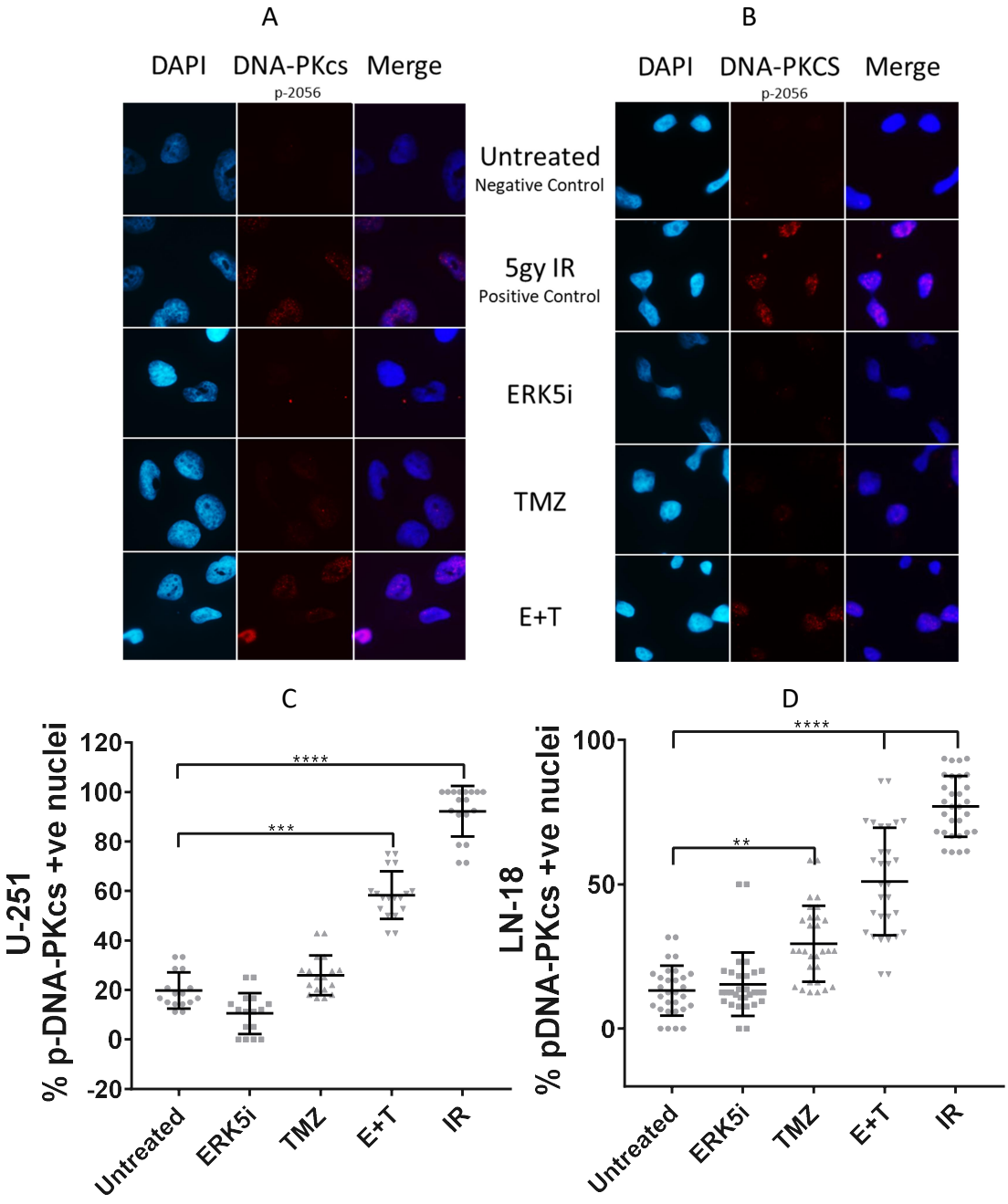

Figure 4.22: phospho-DNA-PKcs (s2056) positive GBM cells 24 hours after treatment

U-251 cells (A) or LN-18 cells (B) were plated on coverslips before being treated with ERK5i (0.25μM) 24 hours later. Following a 90 minute incubation 200μM TMZ was added. 24 hours later cells were fixed ready for IF processing. Cells were imaged at 20x objective on a Nikon Eclipse TE200 Fluorescent Microscope and the numbers of positive cells were counted and averaged. Both U-251 cells (C) and LN-18 cells (D) treated with E+T had more than additive percentage of positive cells compared to the value of ERK5i and TMZ drug alone combined, 58.37% v 36.45% for U-251 and 50.98% v 44.69% for LN-18.

***p=<0.005 ****p=<0.0001 using a Kruskal-Wallis H Test.*
(n=≥2)

RAD51 is also used in repairing double strand breaks in DNA; however, it is associated with the homologous repair (HR) pathway, particularly within the S-G2 phases of the cell cycle (Krejci et al., 2012). When RAD51 was investigated in LN-18 cells treated with ERK5i and temozolomide in combination, there was a no significant difference in RAD51 positive cells when compared to untreated cells. Both temozolomide alone and positive IR control were significantly different to untreated cells (figure 4.23).

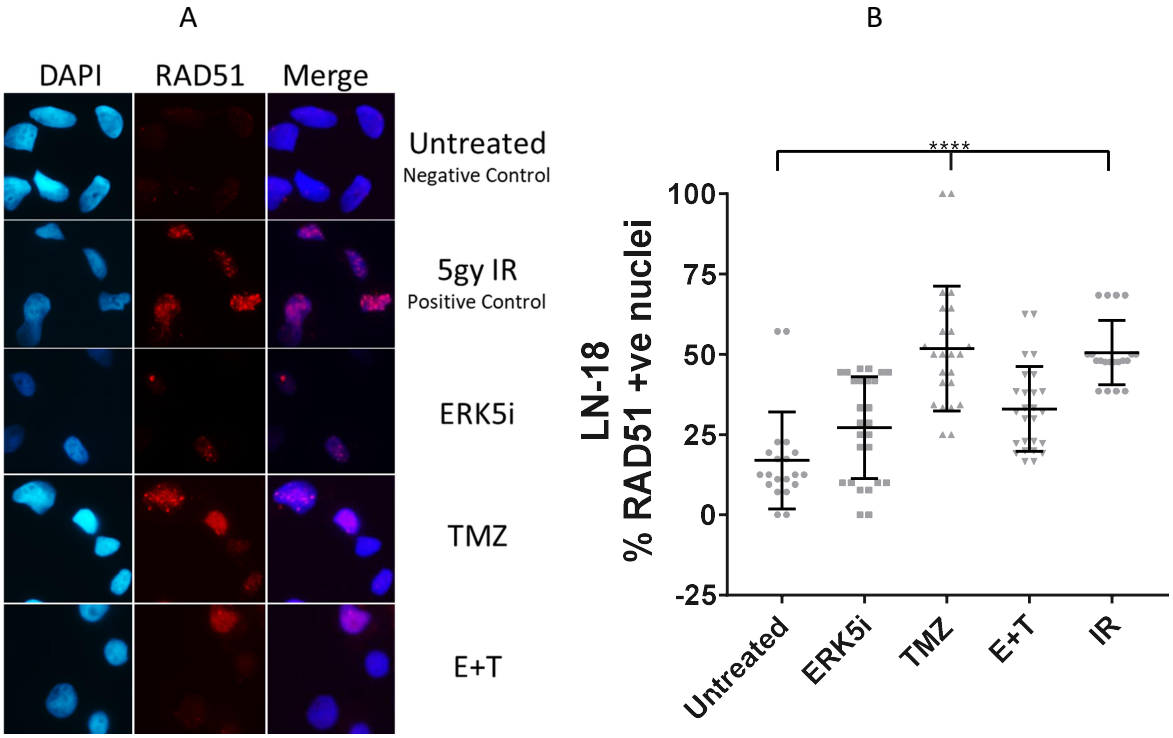

Figure 4.23: RAD51 positive GBM cells 24 hours after treatment

LN-18 cells (A) were plated on coverslips before being treated with ERK5i (0.25µM) 24 hours later. Following a 90 minute incubation 200µM TMZ was added. 24 hours later cells were fixed ready for IF processing. Cells were imaged at 20x objective on a Nikon Eclipse TE200 Fluorescent Microscope and the numbers of positive cells were counted and averaged. LN-18 cells treated with TMZ and IR had the highest percentage of positive cells (51.77% and 50.50% respectively) (B). Both conditions had a p value <0.0001. Combination treatment was not significantly different to untreated cells (33.01%).

*****p=<0.0001 using a Kruskal-Wallis H Test.*
(n=2)

Micronuclei (MNi) are formed during mitosis (anaphase) when a chromosome or a fragment of chromosome is not incorporated into daughter nuclei. MNi are only formed in a dividing population of cells, particularly if there is significant DNA damage present as cells enter mitosis, and are therefore used as a marker of genetic instability (Fenech, 2000). Combination of ERK5i and temozolomide caused an increase in the percentage of MNi compared to untreated cells in both cell lines (p-value 0.0135 for T98G cells and 0.0136 for LN-18 cells) (figure 4.24).

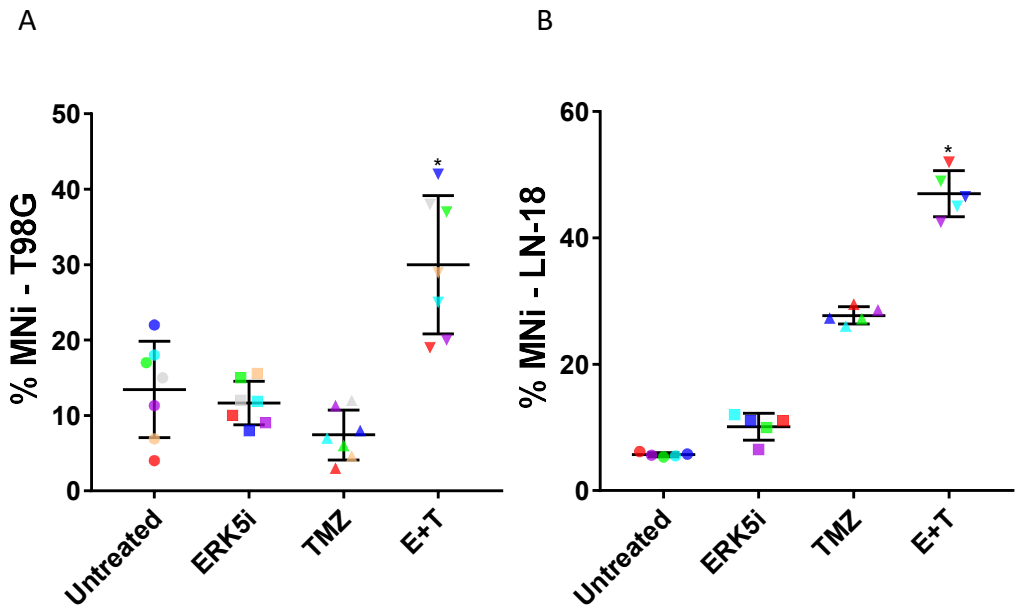

Figure 4.24: Micronuclei in GBM cells 24 hours after treatment

T98G cells (A) and LN-18 cells (B) were plated on coverslips before being treated with ERK5i (0.25µM) 24 hours later. Following a 90 minute incubation 200µM TMZ was added. 24 hours later cells were fixed ready for IF processing. Cells were imaged at 20x objective on a Nikon Eclipse TE200 Fluorescent Microscope and the numbers of MNi were counted as a percentage of total cells. E+T combination treatment was the only condition significantly different to untreated cells (p-value 0.0135 and 0.0136 for T98G and LN-18 cells respectively).

***p=<0.05 using a Mann-Whitney U Test.*
(n=≥5)

4.7 Cell Cycle Arrest - Nocodazole and Roscovitine

Nocodazole is an anti-mitotic agent that inhibits the formation of microtubules by binding to β-tubulin, inhibiting microtubule polymerisation. This inhibition causes an accumulation of cells in mitosis as cells are unable to form metaphase spindles and cannot divide (Zieve et al., 1980). Roscovitine is a cyclin-dependent kinase (CDK) inhibitor targeting CDK1, 2, 5, 7 and 9 by competing with ATP-binding. Acute exposure to roscovitine is an established method to prevent entry of cells into S-phase of the cell cycle (Cicenas et al., 2015).

GBM cells were treated with nocodazole in combination with ERK5i and temozolomide for 24 hours. Consistent with previous data the combination treatment of ERK5i and temozolomide caused the largest tail moment, significantly different to temozolomide alone (64.03 v 43.02). Interestingly, the addition of nocodazole reduced the amount of DNA damage levels to those seen in temozolomide + nocodazole (T+N) levels, suggesting that this damage is mainly derived during mitotic progression (figure 4.24). This is consistent with the dramatic increase in MNi observed in cells treated with ERK5i and temozolomide (figure 4.25).

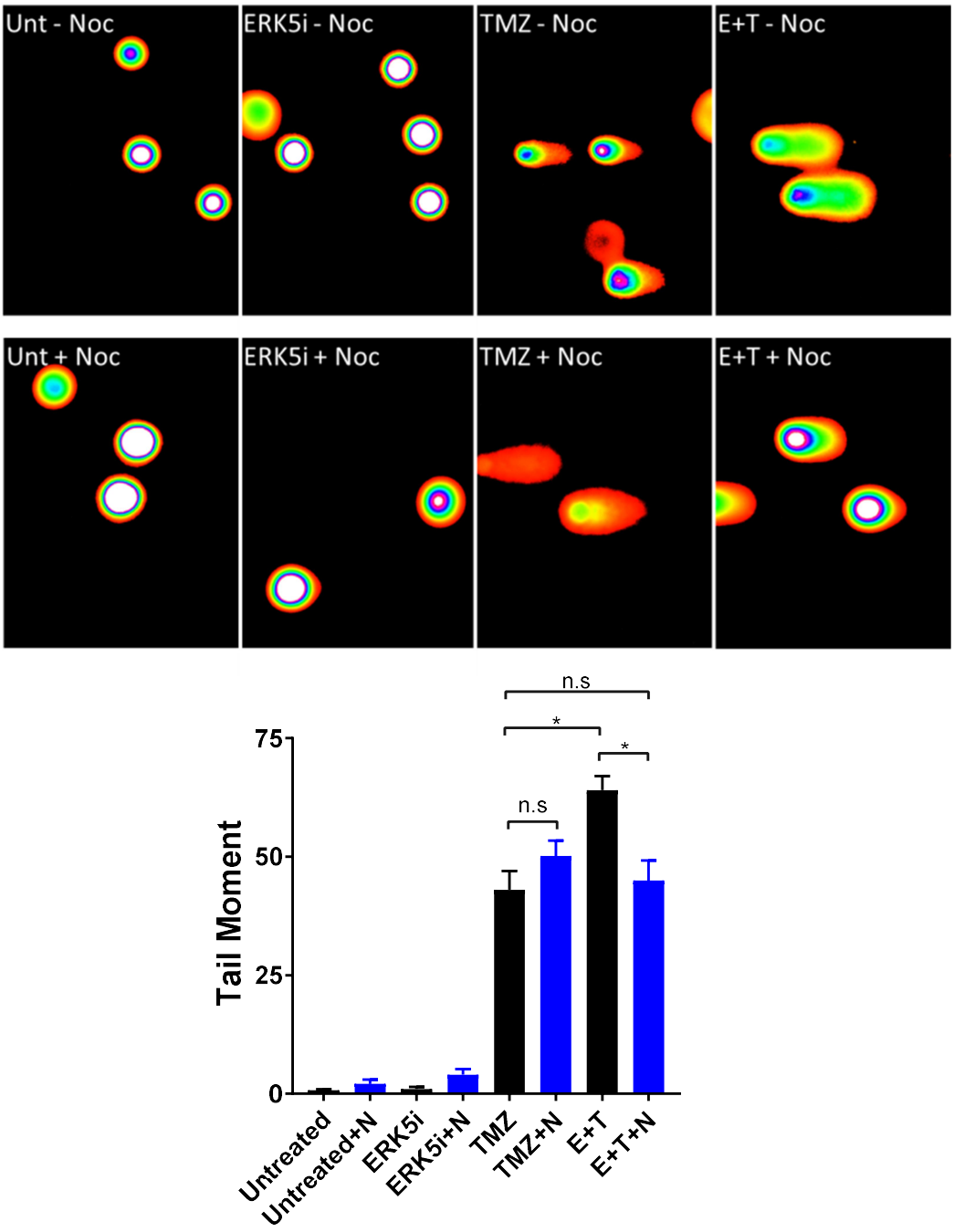

Figure 4.25: DNA damage in GBM cell treated with Nocodazole

T98G cells were plated 24 hours before being treated with ERK5i (0.25µM). Following a 90 minute incubation 200µM TMZ and 1ng/ml nocodazole was added and a further 24 hours later, cells were harvested for comet assay. Images are representative of T98G cells visualised on Comet Score after various treatments. Tail moment was calculated for around 50 cells per condition for each repeat. Cells were imaged at 20x objective on a Nikon Eclipse TE200 Fluorescent Microscope after being stained with SYBR Gold. E+T caused a significant increase in tail moment when compared to TMZ alone (p-value 0.04), however, this was significantly reduced with the addition of nocodazole (E+T v + E+T+N p-value 0.03). Nocodazole increased tail moment slightly in other drug treatments, however, not significantly. TMZ and E+T were significantly different to untreated cells +/- nocodazole.

**p=<0.05 using a Kruskal-Wallis H Test.*
(n=2)

GBM cells were also treated with roscovitine, for 4 hours, following the addition of ERK5i and temozolomide. Unlike nocodazole, the addition of roscovitine caused no difference in tail moment and did not alter 53BP1 foci expression (figure 4.26, 4.27).

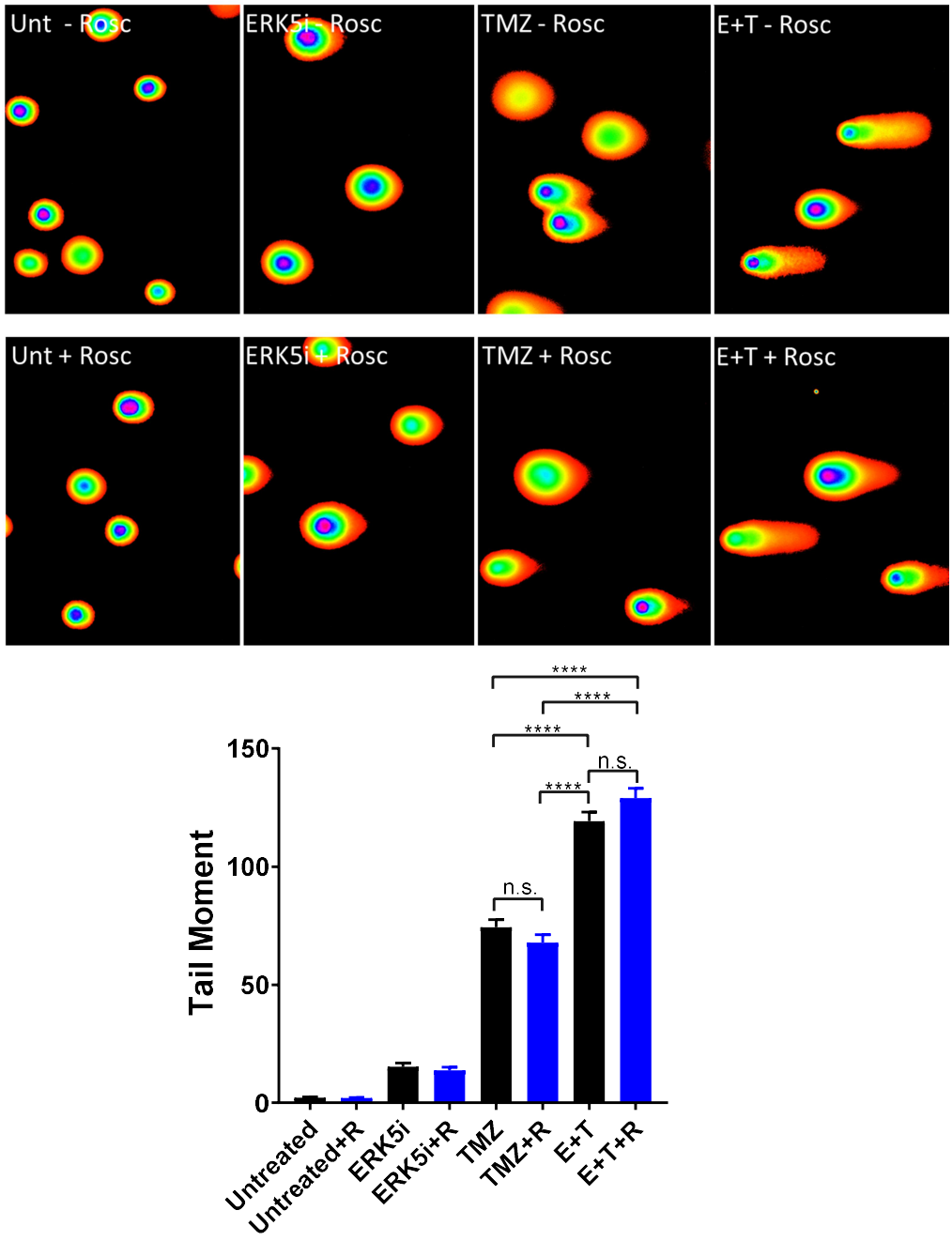

Figure 4.26: DNA damage in GBM cell treated with Roscovitine

T98G cells were plated 24 hours before being treated with ERK5i (0.25µM). Following a 90 minute incubation 200µM TMZ was added and a further 20 hours later 10µM roscovitine was added for 4 hours. Cells were then harvested for comet assay and images are representative of cells visualised on Comet Score after various treatments. Tail moment was calculated for around 50 cells per condition for each repeat. Cells were imaged at 20x objective on a Nikon Eclipse TE200 Fluorescent Microscope after being stained with SYBR Gold. E+T caused a significant increase in tail moment when compared to TMZ alone (p-value <0.0001), unchanged by treatment with roscovitine.

*****p=<0.0001 using a Kruskal-Wallis H Test.*
(n=2)

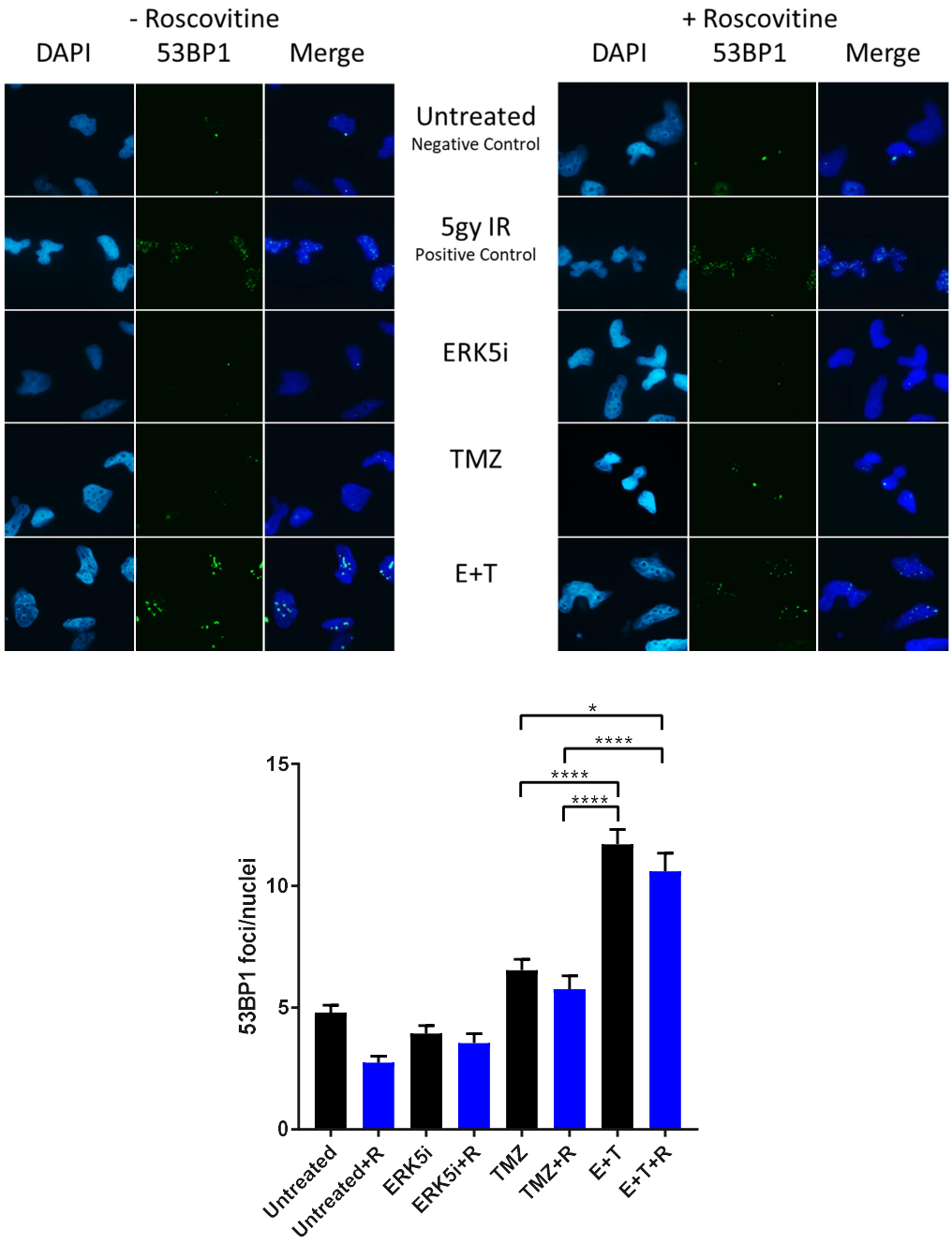

Figure 4.27: 53BP1 foci in GBM cells following Roscovitine treatment

T98G cells were plated on coverslips before being treated with ERK5i (0.25µM) 24 hours later. Following 90 minutes incubation 200µM TMZ was added and a further 20 hours later 10µM roscovitine was added for 4 hour. Cells were fixed ready for IF processing. Cells were imaged at 20x objective on a Nikon Eclipse TE200 Fluorescent Microscope and the numbers of foci were counted and averaged. Images are representative of conditions. T98G cells treated with roscovitine had no significant change in the number of foci for the identical drug treatment E+T caused the highest average foci/nuclei, significantly different to TMZ alone(p<0.0001 (B).

**p<0.05 ****p=<0.0001 using a Kruskal-Wallis H Test.*
(n=3)

Taken together, these findings suggest the combination of ERK5i and temozolomide causes an increase in DNA damage which is generated during mitosis and ultimately leads to cell crisis/death. The damage generated primarily activates the NHEJ pathway (as the HR pathway may be inhibited by ERK5i), which is particularly active in the G1 phase of the cell cycle. However, it has also been reported by several groups that deleterious activity of the NHEJ pathway outside of G1 can lead to DNA damage and chromosomal aberrations (Adamo et al., 2010, Pace et al., 2010).

4.8 Validating ERK5 as a target in GBM

As ERK5 inhibition is able to sensitise GBM cells to temozolomide, the expression of ERK5 within GBM tumours is vital for the combination to work, particularly if a therapeutic window is to offer selectivity of tumour cells over normal brain tissue. Even though ERK5 has been implicated in several cancers, there has been little investigation into ERK5 as a target for treating patients with GBM.

Initially, ERK5 mRNA expression in GBM was investigated using publically available expression data. This revealed a significant increase in relative mRNA expression in GBM compared to normal brain tissue (figure 4.28)

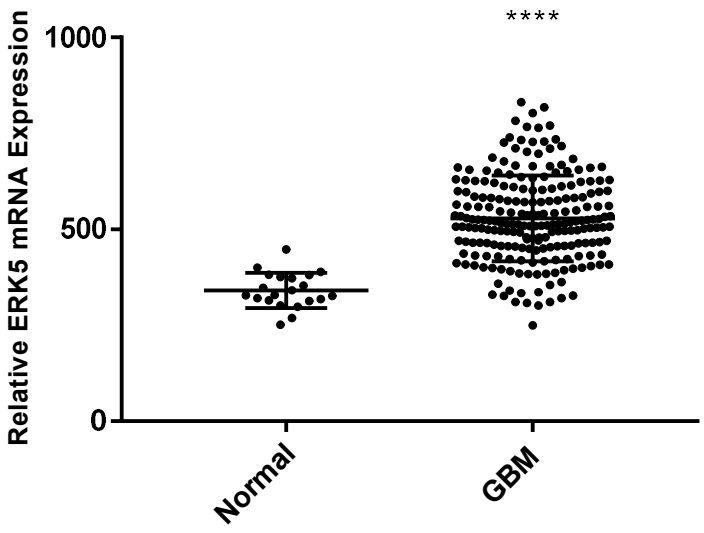

Figure 4.28: Relative ERK5 mRNA Expression

Relative mRNA expression of ERK5 was calculated using information from the REpository for Molecular BRAin Neoplasia DaTa (REMBRANT). There was significant increase in relative mRNA expression in GBM samples when compared to normal samples. The expression values were 341.07 for normal brain (n=20) and 528.77 for GBM (n=215).

*****p-=<0.0001 using a Mann-Whitney U Test.*

To further validate ERK5 as a target in GBM, ERK5 protein expression was investigated using immunohistochemistry (IHC). The ERK5 antibody chosen for IHC was able to detect ERK5 protein expression via western blotting in GBM cells shown throughout this chapter and it has also been used to detected ERK5 expression via IHC in melanoma tissue microarrays (TMAs) (Tusa et al., 2018b). To establish a suitable primary antibody dilution for ERK5 staining of FFPE sections, slides containing FFPE cell pellet sections formed from cells treated with either control or ERK5 siRNA were used. These were processed, sectioned and mounted by Maggie Glover, a histology technician within the Department of Oncology and Metabolism at the University of Sheffield.

Once an appropriate primary antibody dilution was identified (1:4000) there was a clear difference observed in ERK5 staining when ERK5 siRNA treated cells were compared to control siRNA treated cells (figure 4.29). Previously published methods investigating ERK5 expression in melanoma by IHC used an antibody dilution of 1:100 (Tusa et al., 2018b). The antibody dilution selected for the staining of ERK5 in GBM cores was 40 times less, reducing the chances of non-specific antibody binding and false positive results. However, this was very difficult to quantify in cell pellets due to the varied dispersion of cells throughout the pellet and was therefore judged qualitatively by two independent people. A secondary antibody alone was used as a negative control and haematoxylin was not used as a counter stain as it masked the brown DAB staining making it very difficult to assess ERK5 expression.

Following primary antibody optimisation (see above and figure 4.29), a selection of TMAs were stained. These included 28 normal brain cores, 111 astrocytoma cores (grade 1: 16 cores, grade 2: 64 cores, grade 3: 31 cores) and 51 GBM cores (grade 4).

Intensity of ERK5 staining observed at 20x objective was quantified for each stained core. As ERK5 is expressed in vasculature, cores which only showed vasculature staining were classified as ‘0’ intensity. All cores were scored with numerical value ranging from 0 to 3 (table 4.2) (figure 4.30). Dr Malee Fernando, a Consultant Histopathologist at the Royal Hallamshire Hospital, generously donated her time and expertise to score the cores as an external expert.

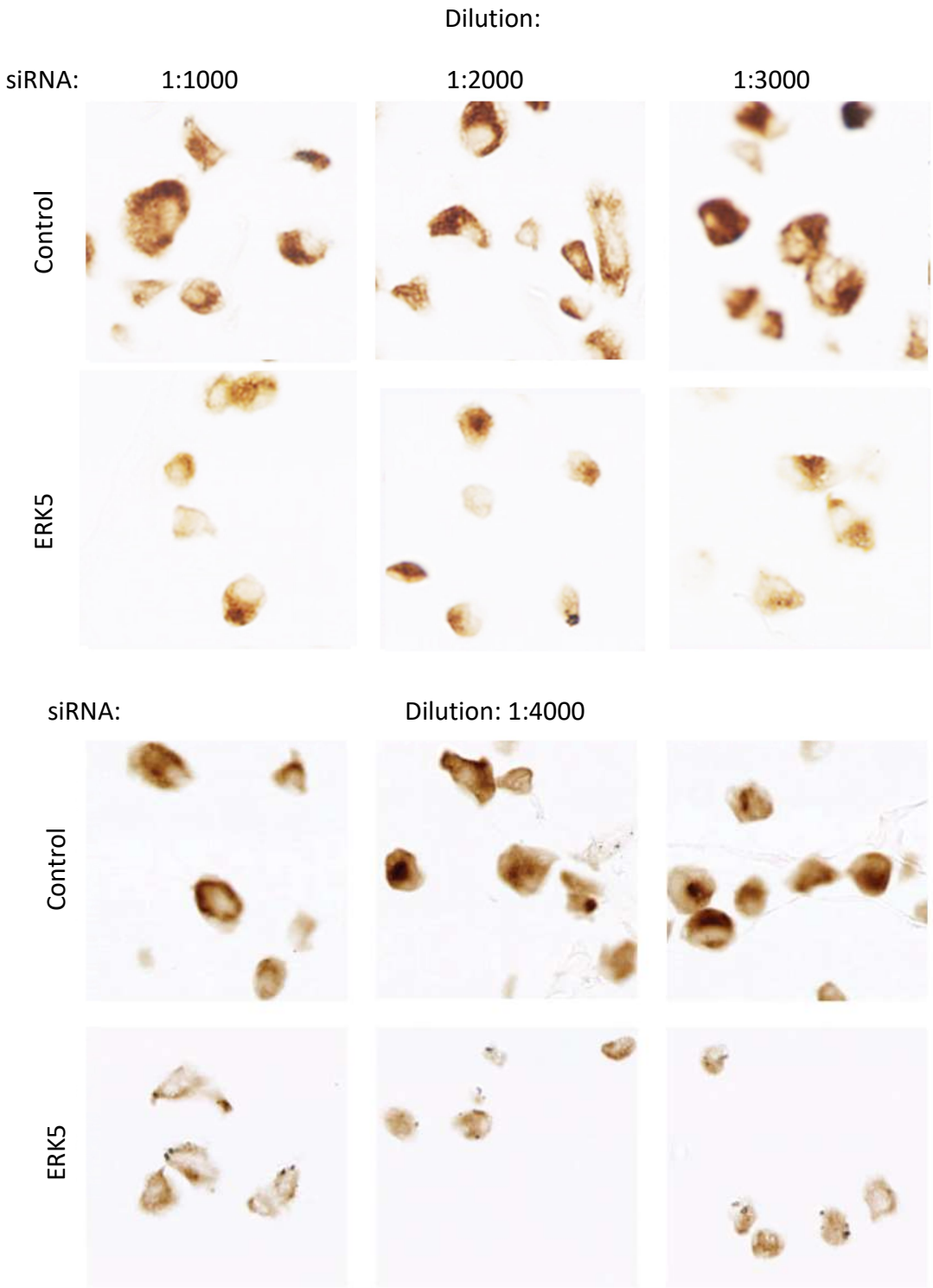

Figure 4.29: ERK5 antibody optimisation

T98G cells were reverse transfected with control or ERK5 siRNA in a T75 flask. Following a 48 hour incubation cells were harvested for fixing in 4% PFA. Cells were re-suspended in an agarose pellet. Pellets were processed and sectioned before being mounted on coverslips ready for IHC staining. A range of dilutions of antibody were tested (1:100 to 1:5000), however, 1:4000 was selected as it showed the largest difference in DAB staining between control and ERK5 siRNA treated cells.

Images were taken at 20x magnification.

Table 4.2: Classification of Staining	
Intensity	**Definition**
0	Vasculature only
1	Some but not all cells stained
2	Low intensity pan stain
3	High intensity pan stain

Table 4.2 *- Intensity scale from 0-3 enabled quantification of ERK5 staining for each TMA core. Each core was scored independently by two people before the results were compared and analysed.*

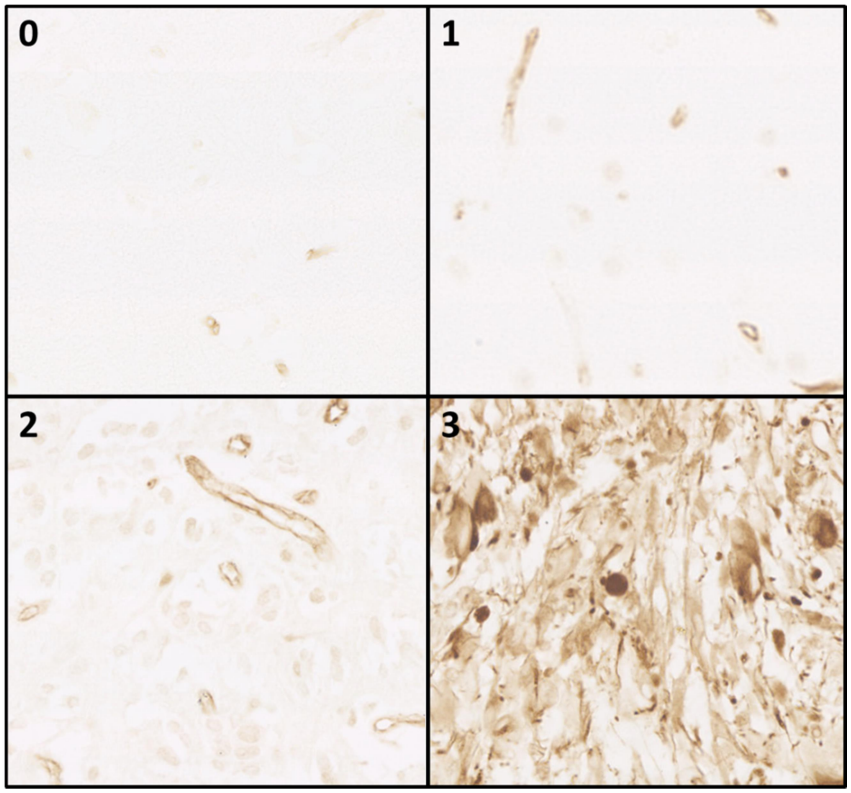

Figure 4.30: Examples of scoring grades
0, 1, 2 and 3 are representative images of cores. Vasculature was discounted as ERK5 is expressed in vessels (grade 0). Grade 3 has a highly intense pan stain, grade 2 has a pan stain of varying intensity and grade 1 has a few cells stained but not all.

T98G cell pellet sections and TMA cores showed ERK5 localisation to be both cytoplasmic and nuclear, and as expected, ERK5 was present in endothelial cells, subsequently staining vasculature in normal and astrocytoma cores. Following siRNA depletion of ERK5 and staining with an AB dilution of 1:4000, ERK5 localisation appeared to become absent from the nucleus in a large number of cells (figure 4.29).

Following independent scoring of the cores, an average was taken across each grade (figure 4.31). All grades exhibited significantly differential ERK5 expression scoring compared to normal brain tissue and the average score increased with grade, with grade 4 GBM exhibiting the highest average of 2.70. However, there was no significant difference between grade 1 compared to 2 and grade 3 compared to 4. GBM cores had the highest percentage of cores classified as 3 (79%), followed by grade 3 (61.4%), grade 2 (16.7%) and finally grade 1 (12.5%) and normal brain tissue was mostly classified as 0 (82.6%) (figure 4.32). The increased ERK5 expression in GBM tumour cells contributes to the validation of ERK5 as a viable target and highlights a potentially exploitable therapeutic window for the use of ERK5 inhibitors.

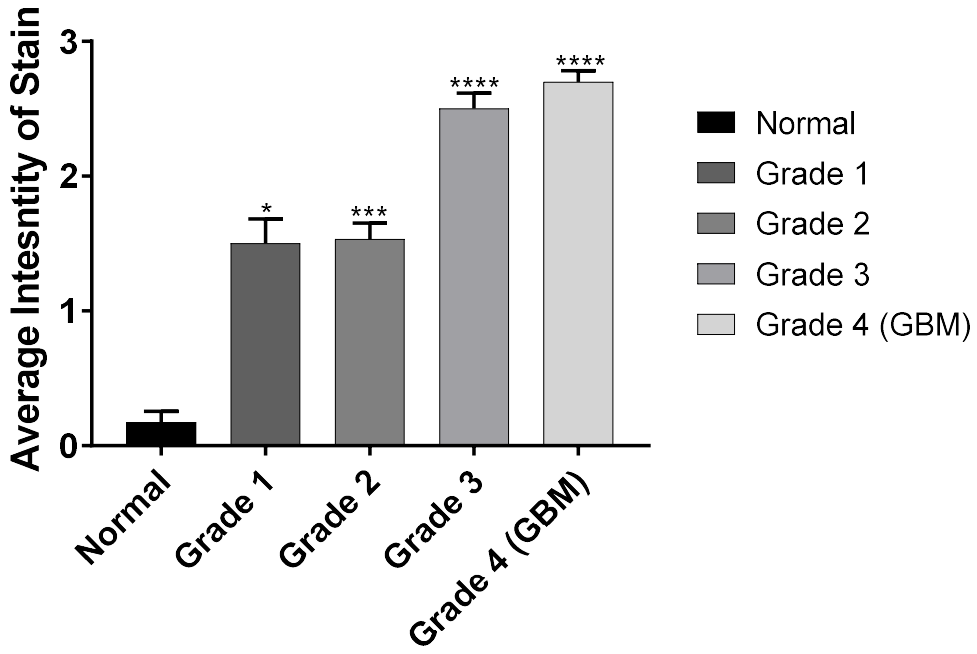

Figure 4.31: Average Intensity of ERK5 staining classified by tumour grade

All cores were given a value from 0 to 3. The sum of these values was averaged for each grade. Values for grades 1-4 were significantly different to normal brain, with grade 4 GBM having the highest average value. There was no significant difference between grade 1 and grade 2 or between grade 3 and grade 4 but these two groups were significantly different from each other.

**p=<0.05 ***p=<0.0005 ****p=<0.0001 using a Kruskal-Wallis H Test.*

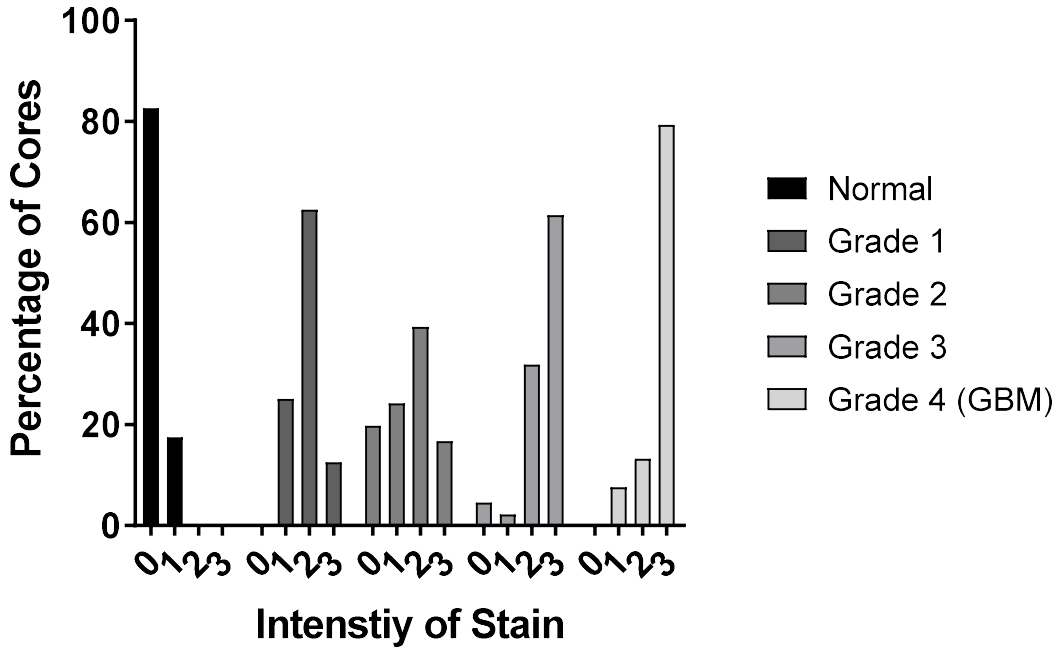

Figure 4.32: Intensity of ERK5 staining classified by tumour grade

All cores were given a value from 0 to 3 and the percentage of cores in each category is show (data shown is the same as in figure 4.29). Grade 4 (GBM) tumours have the highest percentage of cores classified as 3 intensity at 79%, followed by grade 3 with 61.4%, grade 2 with 16.7% and finally grade 1 with 12.5%. Normal brain tissue was mostly classified as 0 intensity (82.6%) with only 17.4% of cores being classified as 1 intensity.

4.9 Discussion

There are currently no MEK5 or ERK5 inhibitors in clinical trials; however, there have been 3 successful MEK1/2 inhibitors approved for treating patients with metastatic melanoma and non-small cell lung cancer (NSCLC) (table 4.3). These drugs are approved for treating patients with activating BRAF mutations, the upstream MAPKKK and activator of MEK1/2 (Roskoski Jr., 2018).

Table 4.3: FDA-approved MEK1/2 inhibitors			
Drug	**Target**	**Cancer**	**Approved**
Binimetinib	MEK1/2	Metastatic Melanoma	2018
Cobimetinib	MEK1/2		2015
Trametinib	MEK1/2		2013
		NSCLC	2017

Table 4.3 *- MEK1/2 inhibitors have recently been approved for treatment of both metastatic melanoma and NSCLC patients with BRAF mutations.*

ERK5 has been identified here as a target which is able to sensitise GBM cells to temozolomide treatment when depleted by siRNA and when inhibited by either

ERK5-in-1 or XMD8-92. This study has also shown significant over-expression of ERK5 mRNA and protein in brain tumours when compared to healthy brain tissue, further validating and strengthening EKR5 as a credible target in these tumours. Furthermore, inhibition of ERK5 using XMD8-92 has been shown to sensitise colon cancer cells in a xenograft model to chemotherapy and sensitise triple negative breast cancer cells to a combination of chemotherapeutic docetaxel and doxorubicin (Al-Ejeh et al., 2014, Pereira et al., 2016). Additionally, a study investigating differentially expressed genes involved in temozolomide resistance found enrichment of MAPK signalling (WNT signalling was also enriched) and upregulation of JNK1 (MAPK8) when temozolomide resistant cell lines were generated from long term temozolomide exposure (Xu et al., 2018b).

There were, however, some problems which have arisen during this study of ERK5. Firstly the inhibition of MEK5 and ERK5 by BIX02189 did not sensitise GBM cells to temozolomide treatment in either MTT or clonogenic survival assays. In the clonogenic assay this may be due to ineffective inhibition of MEK5 and ERK5 at the concentration used (1µM), as although decreased when compared to DMSO treated HeLa cells, the expression of phospho-ERK5 can clearly be seen by western blotting (figure 4.33). Treatment with BIX02189 also appears to upregulate phospho-ERK1/2 activity, an off-target effect which may have influenced sensitivity to temozolomide in our studies as it previously been shown that ERK1/2 activity is influenced in the presence of temozolomide, which may have been further enhanced by the addition of BIX02189, negating any sensitisation usually seen following ERK5 inhibition (Wang et al., 2016, Xu et al., 2018a). Sensitisation may therefore have been achieved if an increased dose of BIX02189 was used in combination with temozolomide in clonogenic survival assays, although, MTT assays which combined up to 10µM BIX02189 with temozolomide (50µM) showed no sensitisation. A higher dose of temozolomide may be needed to see any sensitisation; however, as both XMD8-92 and ERK5-in-1 have been developed to target ERK5 auto-phosphorylation, this may be the key to sensitisation of GBM cells to temozolomide (Deng et al., 2013, Yang et al., 2010). It would be important in future to assess the inhibition of ERK5 activity when using BIX02189, enabling an effective inhibitory dose to be selected to complete further studies. However, ERK5 inhibitors have been shown to generate different effects when compared to MEK5 inhibitors in chronic myeloid leukaemia (CML) cells. When cells were treated with either 10µM XMD8-92 or 10µM BIX02189 in hypoxic conditions (mimicking the bone marrow stem cell niche) differing results were generated regarding progenitor cell potential. When cells were returned to normal oxygen conditions post treatment, XMD8-92 abolished this progenitor potential whereas BIX02189 was only able to reduce it (Tusa et al., 2018a).

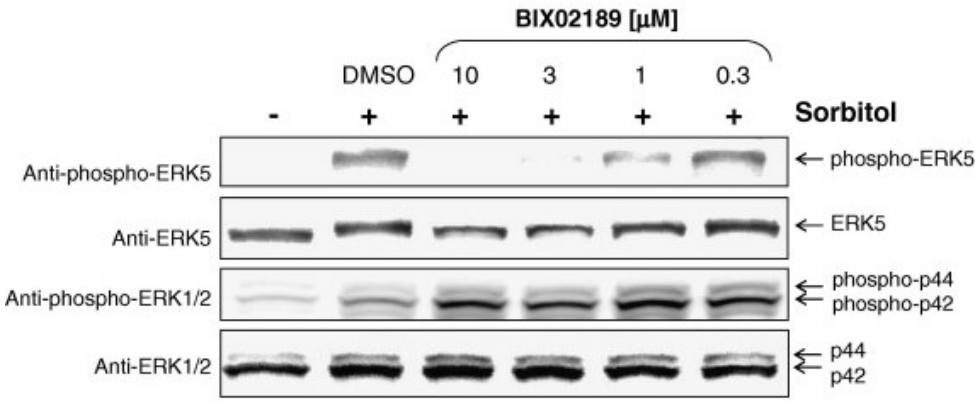

Figure 4.33: Inhibition of phospho-ERK5 following treatment with BIX02189
HeLa cells were treated with BIX02189 at varying concentrations for 90 minutes before sorbitol stimulation (0.4M). Phospho and total ERK5 were probed for along with phospho and total ERK1/2. ERK1/2 phosphorylation was increased as a result of BIX02189 treatment at all concentrations; however, total ERK1/2 remained relatively unchanged. ERK5 activity was almost totally abolished at 3μM and totally undetectable using 10μM BIX02189. Both 1 and 0.3μM BIX02189 had detectable phospho-ERK5 activity. Total ERK5 was decreased as a result of ≥3μM BIX02089 treatment. Untreated cells were used as a negative control; however, no loading control was shown.

Figure copied with permission from (Tatake et al., 2008)
Licence number: 4452461116168

Western blotting of primary and immortalised GBM cells showed ERK5 remains un-phosphorylated under normal conditions, which could indicate it is not inhibition of ERK5 phosphorylation and catalytic activity but total ERK5 protein levels which are upregulated and important in GBM. ERK5-in-1 is known to cause off-target inhibition of BRD4, a target which has been shown to decrease proliferation of GBM cells and also increase sensitivity to temozolomide in an additive manner following chemical inhibition (Lam et al., 2018, Pastori et al., 2014). These findings combined with the lack of sensitivity to temozolomide following MEK5 inhibition indicate a potential mechanism which is independent of ERK5 phosphorylation. Furthermore, XMD8-92 was only able to elicit an increase in temozolomide sensitivity when higher, BRD4 inhibiting, doses were used. However, as more than additive killing and DNA damaging effects were observed following ERK5 inhibition when combined with temozolomide, off-target effects on BRD4 do not completely explain this increase in temozolomide sensitivity.

Total ERK5 protein expression is upregulated in GBM tumours compared to normal brain, and was shown to be both nuclear and cytoplasmic in both cell lines and TMA cores and pan-ERK5 staining across whole cores was visible in those which were graded as intensities of 2 and 3. ERK5 is usually located in the cytoplasm, tethered by cdc37 and Hsp90, however, following activation ERK5 it is then shuttled to the nucleus where is can act as a transcription factor, independent of MEK5 phosphorylation and kinase activation (Erazo et al., 2013). siRNA depletion of ERK5

was able to sensitise GBM cells to temozolomide treatment which could indicate ERK5 protein loss, not catalytic activity, is key and therefore MEK5 inhibitors targeting ERK5 phosphorylation may never elicit temozolomide sensitisation. This may suggest that all the data generated using ERK5-in-1 to deplete cells of ERK5 activity is unrelated as effects could be due to BRD4 inhibition. However, ERK5-in-1 acts to inhibit ERK5 auto-phosphorylation which occurs in the C-terminus which also contains the NLS and the transcriptional activation domain, as well as sites for CDK1 phosphorylation important in mitosis (Deng et al., 2013, Simões et al., 2016). Targeting of these various motifs following ERK5-in-1 treatment could result in dysregulated nuclear localisation and transcription of target genes, as well as defective mitotic progression. As depletion of ERK5 following siRNA treatment showed localisation of ERK5 to be mainly cytoplasmic, it would have been interesting to investigate localisation following ERK5-in-1 treatment in order to determine if a similar loss of nuclear ERK5 occurred, which could be contributing to the more than additive increase in temozolomide sensitivity possibly in combination with off-target BRD4 inhibition.

Pan-ERK5 expression in both the nucleus and cytoplasm could be seen in TMA cores with very intense staining, similar to the staining seen in GBM cell line pellet sections transfected with control siRNA. Following ERK5 siRNA depletion, expression appeared to become absent from the nucleus. This loss of nuclear ERK5 could highlight a potential role for nuclear ERK5 protein in temozolomide resistance, as seen by an increase in sensitivity following ERK5 siRNA depletion. Pan-ERK5 staining was also observed in cores graded as 2 intensity; however, this was very clearly to a lesser degree. The progression from low to high ERK5 expression could be a result of tumour microenvironment changes which occur as the tumour grows, effecting signalling pathways which could induce ERK5 expression potentiating temozolomide resistance. It would have been interesting to know whether patients were resistant to temozolomide treatment in order to compare this with ERK5 expression levels.

The importance of FANCD2 in sensitising GBM cells to temozolomide using ERK5 inhibition is yet to be determined as the results from depletion of FANCD2 in LN-18 cells were variable. It is possible that the inconsistency seen in FANCD2 siRNA treated cells was due to the efficiency of FANCD2 knockdown, which could be investigated further using stable shRNA FANCD2 depleted GBM cells (Patil et al., 2014). The Fanconi Anaemia pathway is involved in several DNA damage pathways including homologous repair (HR), nucleotide excision repair (NER) and translesion synthesis (TLS). The FA pathway is the main mechanism which repairs DNA interstrand crosslinks (ICLs). The FANCM-FAAP24-MFH complex detects ICLs and recruits the core FA complex to these DNA damage lesions. Here the multi-subunit core complex ubiqutinates FANCD2-FANCI. Once ubiqutinated, the FANCD2-FANCI

complex recruits or interacts with other DNA damage proteins including BRCA1 and BRCA2 (Kee and D'Andrea, 2010). Depletion of FANCD1/BRCA2 or FANCD2 is known to sensitise GBM cells to temozolomide and FANCD2 has also been shown to be activated in response to temozolomide (Chen et al., 2007, Kondo et al., 2011, Patil et al., 2014). However, FANCC and FANCA, both part of the core complex, were shown to not have any effect on temozolomide sensitivity (Kondo et al., 2011). Furthermore, FANCD2 has been identified as a player in HR, acting in a role independent to the core FA complex. FANCD1/BRCA2-FANCD2-FANCG-XRCC complex is formed in response to phosphorylation of serine 7 on FANCG, which acts to initiate HR. It has therefore been speculated that both DNA damage proteins and FA proteins interact in order to repair temozolomide induced damage through pathways such as HR (Wilson et al., 2008). Importantly, previous work from the Collis laboratory has demonstrated that brain tumours re-activate and re-express high levels of FANCD2 compared to normal brain tissue (Patil et al., 2014). Therefore, although the data generated in U-138 cell is interesting, it is unlikely to be relevant or detrimental to the use of ERK5i as a temozolomide potentiating agent in GBM within the clinic.

Interestingly, an increase in the ability of cells to perform HR has been shown to confer resistance to temozolomide (del Alcazar et al., 2016). Methylation of O-6 guanine is the most toxic lesion caused by temozolomide and is either directly repaired by MGMT or if unrepaired, the methylated guanine is incorrectly paired with thymine. Mismatch repair (MMR) recognises this incorrect pairing and removes the newly paired base on the complementary strand so O-6-methylguanine remains on the parental strand of DNA. The methylated base is then re-paired with thymine and the futile cycle of MMR continues resulting in single strand gaps or breaks in DNA (Friedman et al., 2000). In the subsequent cycle of replication, replication fork collapse can causing double strand DNA breaks (DSBs) and eventually cell death. However, this damage at the replication fork can be repaired effectively by HR using sister chromatid exchange (SCE) (Kaina et al., 2007). RAD51 is used as a marker of HR and was shown to be unchanged in the combination of ERK5i and temozolomide when compared to untreated cells, unlike temozolomide alone cells which had a significant increase in RAD51 foci and subsequently HR. This reduction in cells ability to repair temozolomide induced damage by HR could a contributing factor to the sensitisation induced by the combination treatment. Furthermore, phosphorylation of CHK1 at serine 345 was also decreased in combination treatment when compared to temozolomide alone at 24 hours (figure 4.34). CHK1 is phosphorylated at serine 345 principally by ATR in response to DNA damage, and once activated will interact with and phosphorylate RAD51 which potentiates HR. This decrease in phospho-CHK1 further suggests reduced HR in cells treated with the combination treatment (Narayanaswamy et al.,

2016, Sørensen et al., 2005). Hypothetically, this could mean that FANCD2 is necessary for the sensitisation of GBM cells to this treatment combination as an intact HR response would be required. Furthermore, this could potentially explain why there is more phosphorylated DNA-PKcs, indicative of an increase in NHEJ to compensate. NHEJ in place of HR is known to cause chromosomal aberrations and cell death (Adamo et al., 2010, Pace et al., 2010).

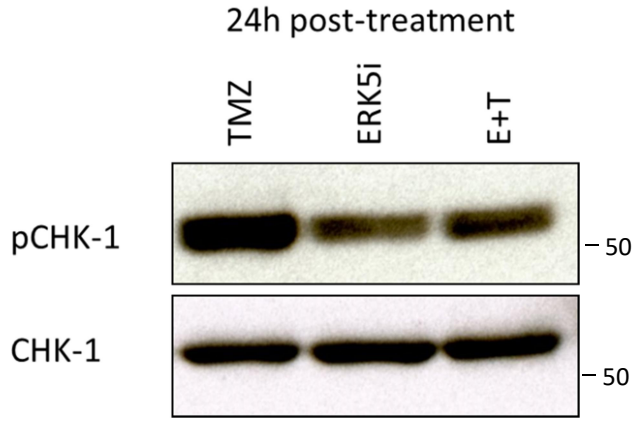

Figure 4.34: phospho-CHK1 (serine 345) following 24 hours treatment with ERK5i and TMZ
T98G cells were plated for 24 hours before being treated with ERK5i. Following 90 minutes incubation 200μM TMZ was added. Cells were incubated for 24 hours before harvesting for protein lysis 48 hours later. Cells were lysed, protein was quantified and samples were run on a western blot. Membranes were probed with phospho-CHK1 (serine 345) or total CHK1 primary antibodies.

Following treatment with the chemotherapeutic hydroxyurea, BRD4 inhibition has also been shown to downregulate CHK1 phosphorylation at both serine 317 and serine 345 (Zhang et al., 2018a), in a similar manner to that seen with the combination of ERK5i and temozolomide (figure 4.34). This resulted in a defective G2/M checkpoint and aberrant restarting of DNA replication, sensitising the cells to hydroxyurea (Zhang et al., 2018a). These findings highlight a role for BRD4 in the DNA damage response pathways which could be involved in temozolomide sensitisation; however, BRD4 has previously been shown to act as a repair complex adaptor in NHEJ. Following inhibition of BRD4, 53BP1 did not accumulate at site of double strand DNA breaks, subsequently resulting in defective NHEJ repair, an effect which was not observed during these studies where either ERK5i alone or in combination with temozolomide resulted in an increase in 53BP1 foci (Stanlie et al., 2014).

Nocodazole arrests cells in M-phase and was able to reduce DNA damage caused by combination treatment. HR is the main repair mechanism for replication fork DSBs, not only occurring in S-phase but also G2-phase of the cell cycle (Krejci et al., 2012). When cells are treated with nocodazole they are arrested in M-phase after damage is repaired by HR. This could explain the decrease in damage seen in the

combination treatment combined with nocodazole, as cells are arrested after damage is repaired and cannot be re-damaged as they are no longer cycling. However, if HR is reduced in the combination treatment and this is the mechanism by which cells are becoming sensitised then this hypothesis would not be true as the damage would be left unrepaired, suggesting that it is cycling through mitosis which is inducing more DNA breaks. When cells are in interphase, any double strand breaks that occur are repaired primarily by NHEJ (G1/S) over HR (G2). However, less is known about DNA breaks formed in mitosis as it is believed a full DNA repair response is supressed, with only partial activation of some components such as ATM, γH2AX and MDC1 (Giunta et al., 2010). ERK5 is an important survival factor during mitosis, interacting with pro-apoptotic BIM, where inhibition results in BIM-induced caspase activation and cell death (Gírio et al., 2007). Temozolomide is also known to induce BIM as part of the late pro-apoptotic response (Tomicic et al., 2015). Combining ERK5-in-1 with temozolomide could result in an increase in BIM activity and subsequent cell death, however, as ERK5 is only interacts with BIM in mitosis, this effect could be reduced following nocodazole treatment possibly explaining the decrease in DNA damage and subsequent cell death.

O-6-methylguanine damage was shown to be increased as a result of ERK5i and temozolomide combination and coupled with the reduction in RAD51 positive cells, this increase in damage and decrease in repair could be sensitising the cells to temozolomide treatment. Curiously, ERK5i only also appeared to increase O-6-methylguanine lesions, however, this was not significantly different to untreated control cells but a trend could be seen. Potentially ERK5i could be having off-target effects, somehow inhibiting the repair of these lesions whilst reducing a cell's ability to complete HR and repair the damage. To investigate whether this is an off-target effect of ERK5i, the ability of XMD8-92 to induce O-6-methylguanine could be investigated. However, this is unlikely because the effects of temozolomide and ERK5i were only seen after 96 hours or 120 hours post treatment and it is highly unlikely ERK5i would remain active exerting its inhibitory effects on repair for such a long time period. Not only this, ERK5i alone did not cause any significant increase in damage detected by immunofluorescence (53BP1 foci, DNA-PK or RAD51 positive cells) and alkaline comet assays, nor was there an increase in MNi. Inhibition of BRD4 has also been shown to cause aberrant chromosome segregation and therefore an increase in the presence of MNi, however, this was not observed following ERK5-in-1 treatment alone, only occurring as a result of combination treatment (You et al., 2009), indicating that BRD4 inhibition may not be toxic until combined with temozolomide or that BRD4 inhibition is not implicated here.

Not only was an increase in DNA damage visualised by comet assays, but both 53BP1 foci and DNA-PK phosphorylation, markers of DNA damage, were increased when cells were treated with ERK5i and temozolomide in combination. 53BP1 is a

promoter of NHEJ and is phosphorylated by CHK1, inhibiting its activity in mitosis and DNA-PK is a key regulator of NHEJ (Lieber, 2010, Orthwein et al., 2014). Both an increase in 53BP1 foci and DNA-PK phosphorylation suggest that combination treatment causes an increase in NHEJ (and a reduction in HR), which is activated as a result of an increase in DSBs. Further evidence of genomic instability is reflected by the increase in MNi in the combination treatment. By investigating co-expression of cyclin A, a cell cycle regulator which accumulates in S-phase and peaks in G2-phase, with DNA-PKcs which is active in G1, the presence of aberrant NHEJ could be explored further (Yam et al., 2002).

Crizotinib, an inhibitor of ALK, c-MET and ROS, has been shown to sensitise GBM cells to temozolomide. However, this increase in the potency of temozolomide was only effective in cells with mutant ROS1 fusion proteins (Das et al., 2015). Nevertheless, pleotrophin (PTN) is a growth factor which binds to and activates ALK and the associated cell proliferation pathways, has been shown to be over-expressed at both mRNA and protein levels, correlating with higher expression in higher grade gliomas (Kalamatianos et al., 2018). In neuroblastoma, ALK signalling has been shown to activate ERK5 via AKT signalling, which potentiates oncogenic signalling through activation of N-MYC. Inhibition of ERK5 using 5μM XMD8-92 resulted in a reduction of N-MYC protein expression that was almost undetectable by western blot (Umapathy et al., 2014). If ALK is over-expressed in GBM an increase in ERK5 signalling could be effecting cell proliferation, survival and apoptosis which may be targeted by ERK5i, potentiating the effect of temozolomide.

Further work to unravel the precise mechanism by which this occurs needs to be completed, focusing on the DNA damage response, as well as further validation in patient derived primary cells, 3D culture and orthotopic animal studies. However, the off-target effects of BRD4 inhibition using ERK5-in-1 and higher doses of XMD8-92 need to be investigated further. More selective ERK5 inhibitors, such as AX15836, are now available and do not show the anti-inflammatory or anti-proliferative effects which have previously been identified using earlier compounds such as XMD8-92 (Lin et al., 2016). It is believed that efficacy of the older inhibitors is mainly due to off-target BRD4 inhibition and that any phenotypes identified following ERK5 depletion or deletion are due to C-terminal function, not catalytic activity (Lin et al., 2016). Combining AX15836 with temozolomide in survival assays which are not reliant on metabolism, such as clonogenic survival assays or annexin V and PI staining, would clearly determine whether ERK5 inhibition is able to sensitise GBM cells to temozolomide. If confirmatory, use of this inhibitor with the various mechanistic studies would be important to further validate the findings using ERK5-in-1.

ERK5 is dysregulated in a vast array of cancers so once clinical trial testing of ERK5 inhibitors begins, the identification of a safe and efficacious drug could improve cancer treatment for a huge proportion of patients. However, adult mice with an inducible ERK5 knock out also died 2-4 weeks after ERK5 depletion due to increased endothelial cell death which caused their vasculature to become 'leaky' resulting in massive haemorrhage (Hayashi et al., 2004). The importance of ERK5 in maintaining vasculature integrity potentially highlights problems developers might face if ERK5 inhibitors are trialled in humans, but as ERK5 is over-expressed in GBM tumours there is a potentially exploitable therapeutic window which would allow for the selective targeting of tumour cells of the normal cell population. Furthermore, ERK5 inhibition did not cause significantly more DNA damage or cell death when used as an individual agent, which if combined with temozolomide targeted directly to the tumour cells using nanoparticles, combining the treatments may be less toxic to and therefore well tolerated by patients (Fang et al., 2015).

Chapter 5 – Fibroblast Growth Factor Receptor 4 is involved in Temozolomide resistance in GBM cells.

5.1 Introduction to Fibroblast Growth Factors and their Receptors

Fibroblast growth factors (FGF) were first identified in 1974 and were found to promote proliferation of fibroblasts that were extracted from pituitary tissue. The first FGF was named basic FGF and this is now known as FGF2 (Gospodarowicz, 1974). There are 18 secreted FGFs which bind to a family of 4 receptors (FGFR). These classic receptors (FGFR1-4) transduce ligand binding via an intracellular tyrosine kinase domain and a phosphorylation cascade that results in activation of signalling pathways. FGFs must bind to FGFRs in the presence of heparin sulphate or heparin sulphate proteoglycans in order to generate a signal cascade (Ornitz and Itoh, 2015). There is 1 receptor (FGFR5 or FGFRL1) which does not have a tyrosine kinase domain or an associated signalling pathway (Ornitz and Itoh, 2015, Sleeman et al., 2001). In addition to the 18 secreted FGFs, there are 4 which do not bind to an FGFR but instead act as co-factors for other proteins, such as voltage gated sodium channels (NaV) (Ornitz and Itoh, 2015). Table 5.1, adapted from Ornitz and Itoh, 2015, summarises FGFs, their subfamily, receptors and associated co-factors.

Table 5.1: Fibroblast Growth Factors, Receptors and Sub-families

Pathway	Subfamily	FGF	FGFR	Co-factor
Canonical	FGF1	1	All	Heparin/Heparin Sulphate
		2		
	FGF4	4	All	
		5		
		6		
	FGF7	3	2, 1	
		7		
		10		
		22		
	FGF8	8	All	
		17		
		18		
	FGF9	9	All	
		16		
		20		
Endocrine	FGF15/19	15/19	All	α/β Klotho
		21	1, 3	
		23	1,3,4	
Intracellular	FGF11	11		Co-factors for NaV Channels
		12		
		13		
		14		

Table 5.1 *- 18 secreted FGFs bind to a family of 4 receptors (FGFRs). 4 FGFs do not bind to FGFRs but instead act as co-factors for other proteins e.g. voltage gated sodium channels.*

FGFs have important roles in development, with some FGF and FGFR deletions leading to embryonic lethality in mice, e.g. FGF4, 8, 9, 10, 15, 18, 23 and FGFR1 and 2 null mice are not viable and die as early as embryonic day 4 or as late as the day of birth due to defects in various tissues (heart, CNS, lungs, limbs etc) (Ornitz and Itoh, 2015). Canonical FGFs (table 5.1) have many roles important in maintaining tissue homeostasis: survival, proliferation, differentiation, wound healing and angiogenesis. RAS-MAPK, PI3K-AKT, STAT and PLC*γ* are the signalling pathways which are activated in response to FGFs binding to their receptors (Ornitz and Itoh, 2015) (figure 5.1).

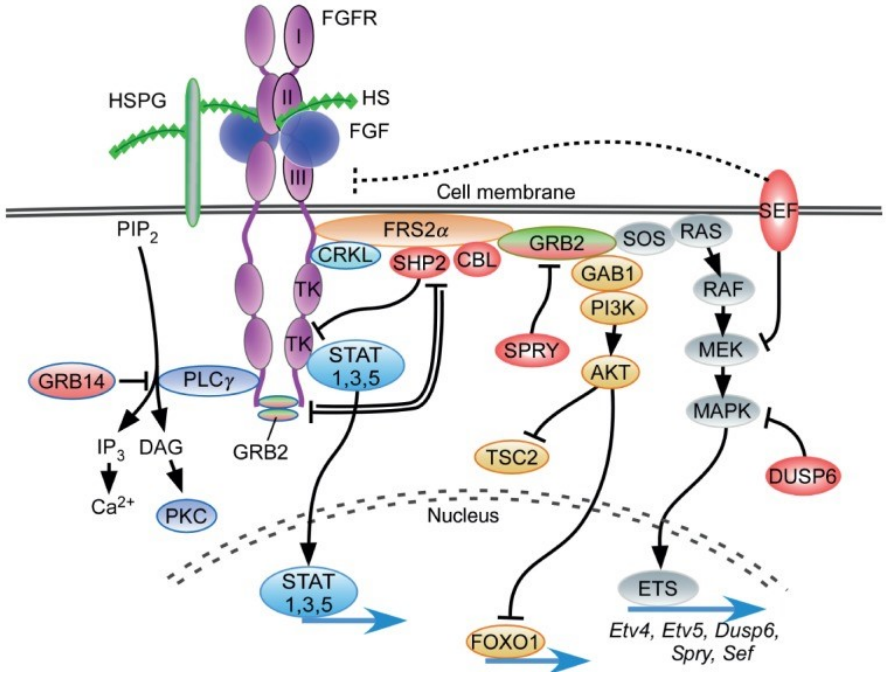

Figure 5.1: Canonical FGF Signalling

When FGF binds to the FGFR receptor along with heparin sulphate (HS) or heparin sulphate proteoglycan (HSPG), phosphorylation of the intracellular tyrosine kinase domains occurs. This activation causes various signalling cascades: RAS-MAPK (grey), PI3K-AKT (yellow), STAT (light blue) and PLCγ (dark blue).

RAS-MAPK – phosphorylation of the receptor results in an interaction between FRS2α and CRLK. FRS2α recruits GRB2 which in turn recruits SOS. SOS then activates the RAS/MAPK pathway.

PI3K/AKT – activated GRB2 recruits GAB1 alongside SOS. GAB1 then goes on to activate PI3K/AKT pathway.

PLCγ - activated PLCγ produces IP_3 which causes intracellular calcium to be released from endoplasmic reticulum stores. DAG is produced alongside IP_3 and activates the PKC pathway.

STAT – STAT 1,3 and 5 are transcription factors which relocate to the nucleus to control gene expression once they are active.

Legend adapted and image taken from (Ornitz and Itoh, 2015)

As FGFs and FGFRs are important in both development and homeostasis, dysregulation of them is often associated with a variety of diseases, including cancer.

5.2 Fibroblast Growth Factors and Receptors in Cancer

FGFs and FGFRs are thought to play a role in oncogenesis as dysregulation of the associated pathways (proliferation, survival, angiogenesis, epithelial-mesenchymal transition and migration) is associated with increased tumorigenicity. For example, driver mutations in the FGF and FGFR signalling pathways are present in over 90% of melanoma cases (Flippot et al., 2015).

In normal brain FGF2 (basic FGF) cannot be detected by immunohistochemistry, however, it has been shown that within glioma patients high FGF2 expression is associated with higher grade gliomas (IV) and increased malignancy, as well as increased vascular structures (Takahashi et al., 1992). However, it is not just FGFs that are dysregulated in cancer; FGFRs are also implicated in oncogenesis causing downstream pathways to become hyper activated (Babina and Turner, 2017). For example, gene amplification can result in increased protein expression leading to more FGFR receptors and an increase in growth signalling. Receptors can also undergo activation mutations which can result in a constitutively active receptor and increased signalling irrespective of ligand binding. Chromosomal rearrangement can occur resulting in fusion genes that result in an increase in the activation of receptors and their signalling pathways or an increase in receptor transcription via a more active promoter (Babina and Turner, 2017). FGFs produced by tumour cells or stromal cells of the tumour can also hyper-activate their respective receptors and this increase in FGF ligands can cause permanent changes to the receptor. FGFs also have a role in angiogenesis and epithelial-mesenchymal transition (where epithelial cells gain invasive properties), which can increase as a result of tumour secreted FGFs (Babina and Turner, 2017).

FGFR1 and FGFR2 amplifications have been implicated in breast cancer, FGFR3 translocation causing activation mutations in multiple myeloma and FGFR4 activating mutations in rhabdomyosarcoma (Chesi et al., 1997, Jacquemier et al., 1994, Meyer et al., 2008, Taylor VI et al., 2009). FGFR4 expression has also been shown to correlate with erlotinib resistance in GBM cell lines, potentially indicating a substitute role for FGFR4 in EGFR signalling pathways (Halatsch et al., 2009).

There have been and are currently many clinical trials investigating the inhibition of FGFs and FGFRs in cancers. However, there are no FDA approved FGF or FGFR inhibitors. There are currently four selective FGFR4 inhibitors in phase I and II clinical trials (table 5.2). The trials comprise a majority of hepatocellular carcinoma (HCC) patients; however, two trials include several other cancer types. FGFR4 is a target for patients with HCC as FGF19, which binds to FGFR4 in normal physiological conditions, is both amplified and over-expressed in these tumours (Sawey et al., 2011, Wu et al., 2011). The first inhibitor launched into clinical trials was NVP-

FGF401, a reversible inhibitor with an IC_{50} of 1.1nM. 6 months later a clinical trial involving BLU554, the FGFR4 inhibitor used in these studies, was opened (ClinicalTrials.gov, 2018). Although FGFR4 inhibition is not being investigated in relation to GBM, if future work is able to validate FGFR4 as a target, availability of FDA-approved drugs may speed up the process to clinical trials.

Table 5.2: FGFR4 inhibitors in clinical trials

Drug	IC_{50} (nM)	Trial Start	Disease	Phase
NVP-FGF401	1.1	Dec 2014	HCC	I & II
BLU554	5	July 2015	HCC	I
H3B-6527	1.2	March 2017	Advanced HCC (& others)	I
INCB062079	Not given	May 2017	HCC (& others)	I

Table 5.2 *– FGFR4 inhibitors are currently in phase I and II clinical trials, mainly targeting HCC. All these inhibitors target cysteine 552, a residue located in the tyrosine kinase domain of FGFR4, which is not conserved between the other family members.*

5.3 Depletion of FGFR4 using siRNA sensitises GBM cells to Temozolomide

As previously seen, FGFR4 pooled siRNA purchased from OTP did not cause an effective knock-down of FGFR4 achieving only a 65.71% depletion (figure 3.11, chapter 3). siPOOLS™ siRNA was used these to validate FGFR4 as a hit from the OTP kinase screen.

A range of 1nM to 10nM of siRNA was suggested by siTOOLS™ as the working concentrations to initially test for effective depletion of the target using siPOOLS™. From both qRT-PCR and western blotting an effective knock-down of more than 80% was achieved by 2.5nM or more (figure 5.2). Expression of FGFR4 was relatively low in GBM cell lines, with Ct values for qRT-PCR of around 28-30 when compared to 16-17 for GAPDH, therefore the use of another housekeeping gene, such as 18S, would further improve confidence in this qRT-PCR data. Such low expression levels resulted in difficulties in detection of FGFR4 protein via western blotting. As such, 30-60 minute exposures were required in order to detect FGFR4 bands, which also resulted to the appearance of various non-specific bands (figure 5.2).

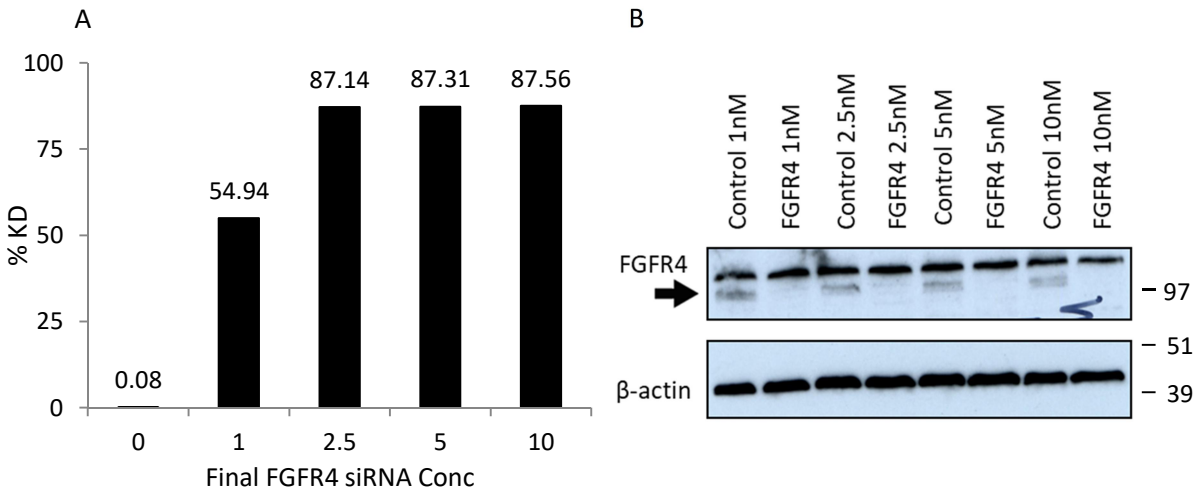

Figure 5.2: Expression of FGFR4 in T98G cells treated with FGFR4 siPOOLS siRNA for 48 hours

T98G cells were reverse transfected with siRNA at varying concentrations (1-10nM) before harvesting for RNA extraction or protein lysis 48 hours later. Following RNA extraction, cDNA was made and qRT-PCR was performed (A) or cells were lysed, protein was quantified and samples were run on a western blot (B).

siRNA concentration of 2.5nM or greater was able to generate sufficient knock down of FGFR4 (>85%). GAPDH was used as a house keeping gene to normalise samples for qRT-PCR and β-actin was used as a loading control for the western blot.

Fold change was calculated by $2^{-\Delta\Delta CT}$

% Knockdown was calculated by $(1-2^{-\Delta\Delta CT}) *100$

(n=1)

As a working concentration of 2.5nM, 5nM and 10nM siRNA all gave a similar percentage knock-down, 5nM was the concentration selected for future experiments. This was selected in order to attempt to minimise any toxicity to the cells caused by siRNA and transfection whilst maximising the efficacy of the knock-down.

In order to validate the result seen from the initial pooled siRNA OTP screen (chapter 3), the ability of FGFR4 depletion to sensitise GBM cells to temozolomide was investigated. T98G and U-87 cells were both reverse transfected for 48 hours in 96 well plates. Cells were treated with doses of temozolomide ranging from 0-400µM, and following 5 days incubation, an MTT assay was performed.

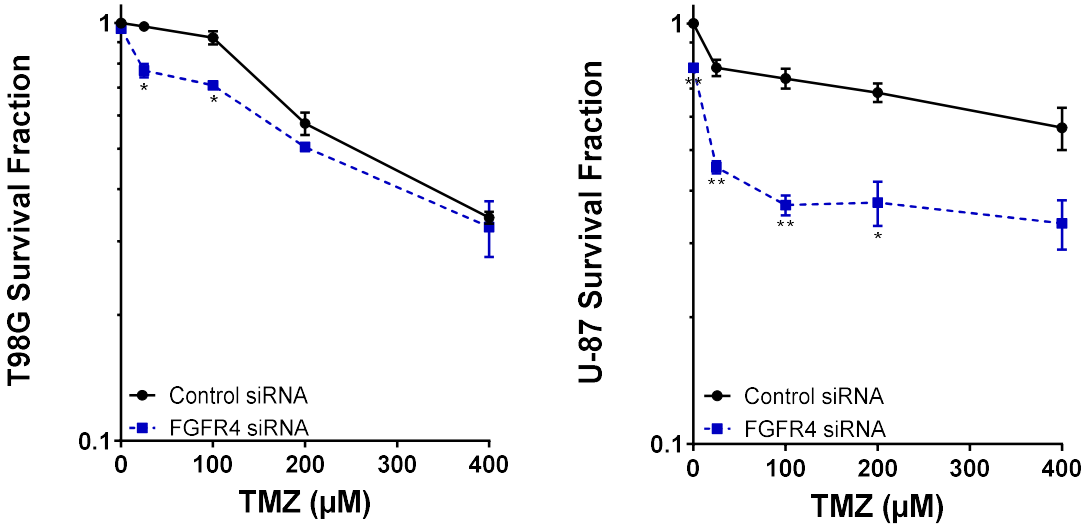

Figure 5.3: Cytotoxicity curves of GBM cells treated with Control or FGFR4 siRNA and TMZ

Cells were reverse transfected with siRNA and then treated with a range of TMZ (0-400µM) 48 hours later. Following 5 days incubation an MTT assay was performed. FGFR4 siRNA alone was relatively non-toxic in T98G cells, however, it caused around 20% cell death in U-87 cells (p=0.01). Both T98G and U-87 cells depleted of FGFR4 showed a reduced survival fraction when treated with TMZ in comparison to control cells, reflecting a modest increase in sensitivity to TMZ.

Data shown is the average surviving fraction (normalised to DMSO treated control siRNA) +/- standard deviation derived from two independent biological repeat experiments.

**=p<0.05 **=p<0.01 using Mann-Whitney U Test.*

Depletion of FGFR4 conferred a modest yet significant increase in sensitivity to temozolomide in both T98G and U-87 cells (figure 5.3), which further validates FGFR4 as a hit from the original kinome screen. In U-87 cells, FGFR4 siRNA alone caused significant decrease in survival fraction (p=0.01) As T98G cells are MGMT positive and U-87 cells are MGMT negative, this bodes well for pan-GBM clinical applicability of FGFR4 inhibition and does not select for one population of patients. However, as patients cannot be treated with siRNA, FGFR4 inhibitors were next investigated.

5.4 Inhibition of FGFR4 using BLU554 sensitised GBM cells to Temozolomide

As previously mentioned, in 2015 data from the first FGFR4 inhibitor was published. BLU9931, developed by Blueprint Medicines, is an FGFR4 inhibitor that was used to treat HCC patients whose tumours exhibited active FGFR pathways (Hagel et al., 2015). As the fibroblast growth factor receptor family has 3 other members which are highly homologous, there had been difficulty in developing inhibitors which target only one member of the family. BLU9931, however, was the first selective inhibitor developed to target only FGFR4, as it is binds to a cysteine molecule (cys552) which is not conserved between the other family members. BLU9931 covalently binds to the ATP binding motif of the kinase (Hagel et al., 2015). Blueprint Medicines have since developed another FGFR4 inhibitor, BLU554, which is currently being investigated in a Phase I trial (ClinicalTrials.gov, 2018). BLU554 also covalently binds to FGFR4 to inhibit the kinase activity in the same manner as BLU9931; however, BLU554 has higher selectivity for FGFR4 over FGFR 2 and 3 compared to BLU9931 (table 5.3) (Hagel et al., 2015, Hoeflich, 2015).

Table 5.3: IC_{50} (nM)of BLU inhibitors

FGF Receptor	BLU554	BLU9931
4	5	3
1	624	891
2	1202	552
3	2203	150

Table 5.3 *– IC_{50} of FGFR4 inhibitors BLU554 and BLU9931. BLU554 is currently in a phase I clinical trial and is more selective over FGFR2/3 compared to BLU9931.*

NVP-FGF401, made by Novartis, is an FGFR4 inhibitor currently in phase I and II clinical trials, however, there is little published data about how this inhibitor works (Graus Porta et al., 2017). When the current studies reported here were being conducted, BLU554 was the only other selective FGFR4 inhibitor in clinical trials (ClinicalTrials.gov, 2018). As there is more published data regarding the mechanism of action and IC_{50} values of BLU554, this was selected as an appropriate FGFR4 inhibitor to investigate as part of our studies.

Firstly, a range of doses of BLU554 were used in combination with two doses of temozolomide in two GBM cell lines (figure 5.4). T98G cells are resistant to temozolomide as they are MGMT positive and U-251 cells are sensitive to temozolomide as they are MGMT negative. Increasing doses of BLU554 significantly sensitised both T98G and U-251 cells to set doses of temozolomide (25μM, 50μM or 100μM) when used in combination. BLU554 did however become

slightly toxic to both cell lines when a dose of 5µM was reached. A set dose of BLU554 (0.5µM, 1µM or 5µM) also sensitised T98G cells to a range of temozolomide doses when used in combination (figure 5.5). Collectively, this data enables us to validate FGFR4 as a hit from the siRNA kinome screen.

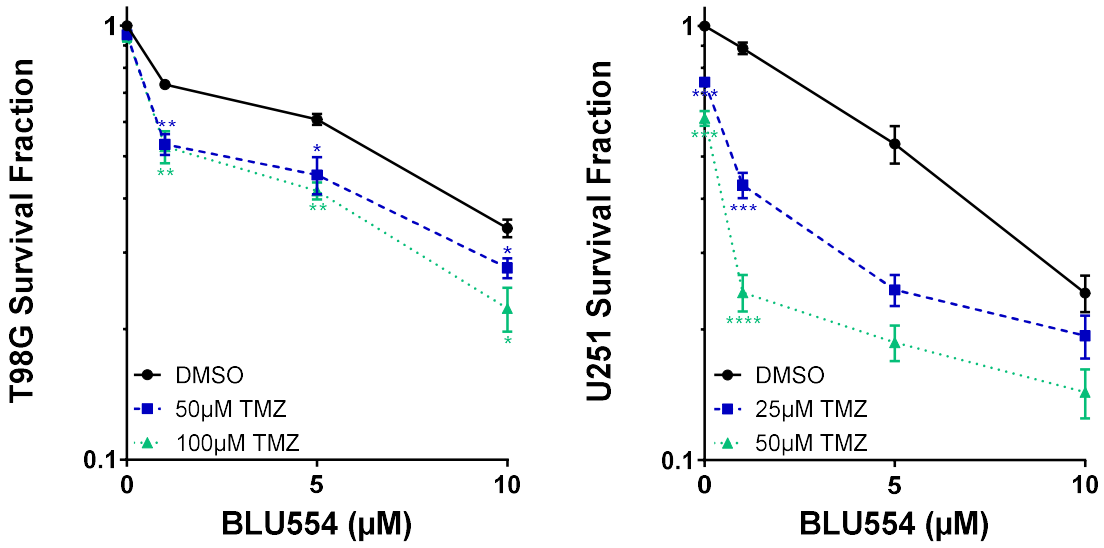

Figure 5.4: Cytotoxicity curves of GBM cells treated with FGRR4 inhibitor BLU554 and TMZ
Cells were plated and allowed to adhere for 24 hours. Cells were treated with a range of doses of BLU554 (0-10µM) before being treated with TMZ 2 hours later. Following 5 days incubation an MTT assay was performed. BLU554 alone caused an increase in toxicity at >5µM in both cell lines. Both T98G and U-251 cells treated with BLU554 showed a reduced survival fraction when treated in combination with TMZ as opposed to BLU554 alone.

Data shown is the average surviving fraction (normalised to DMSO treated controls) +/- standard deviation derived from three independent biological repeat experiments.
**=p<0.05 **=p<0.01 using a Mann-Whitney U Test.*

These experiments were completed by Connor McGarrity-Cottrell, 2nd Year Undergraduate Student from Sheffield Hallam University.

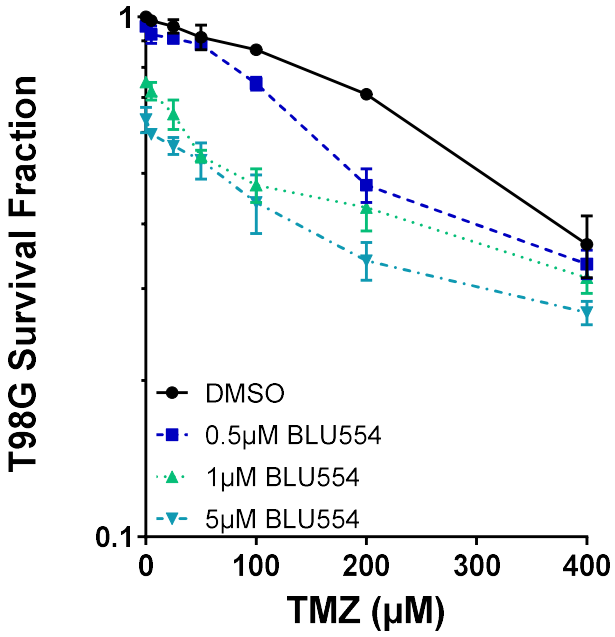

Figure 5.5: Cytotoxicity curves of GBM cells treated with FGRR4 inhibitor BLU554 and TMZ
Cells were plated and allowed to adhere for 24 hours. Cells were treated with a set dose of BLU554 (0-5μM) before being treated with increasing doses of TMZ (0-400μM) 2 hours later. Following 5 days incubation an MTT assay was performed. Combination treatment caused a reduced survival fraction; however, at the maximum dose of TMZ, there was little difference between TMZ alone and combinations. 1μM and 5μM BLU554 alone caused a significant reduction in survival fraction compared to DMSO treated cells (p=0.008 and 0.005).

Data shown is the average surviving fraction (normalised to DMSO treated controls) +/- standard deviation derived from two independent biological repeat experiments.

These experiments were completed by Connor McGarrity-Cottrell, 2nd Year Undergraduate Student from Sheffield Hallam University.

5.5 FGFR4 is expressed in Primary GBM Patient Cells

As FGFR4 expression is low in GBM cell lines, the expression in primary patient material was investigated using western blotting (figure 5.6A). Primary patient-derived GBM samples expressed FGFR4 and interestingly, lysates generated from cells grown in stem media had a higher expression of FGFR4 when compared to cells grown in normal media. Putative stem cell markers, nestin and CD133, were detected in primary cells grown in 3D scaffolds in stem-selecting media, validating their status as a stem-like population (figure 5.6B) (Singh et al., 2004). The primary cells were cultured and imaged Mr Ola Rominiyi (clinical PhD student in the Collis laboratory).

These preliminary findings validate FGFR4 as a potential target for treating GBM patients.

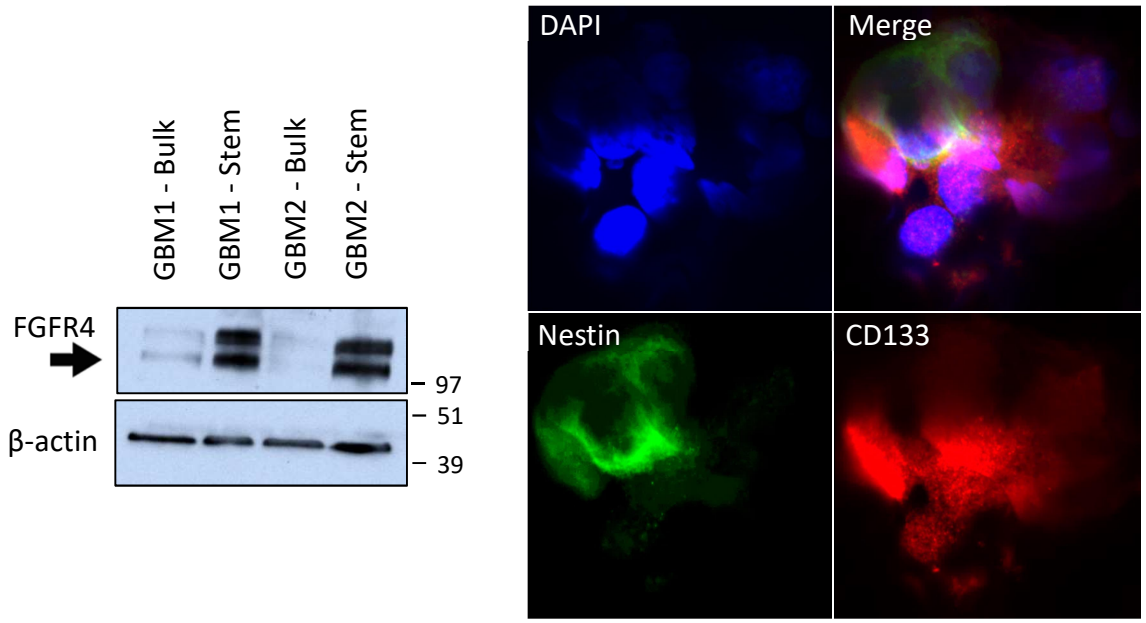

Figure 5.6: Expression of FGFR4 and stem cell markers in Patient Derived GBM Cells
Primary cells taken from GBM tumours during surgery were cultured in standard media ('bulk') or media supplemented to select for stem-like cells. After 6 weeks cells were harvested and lysed for western blotting. Samples were probed for FGFR4 expression and β-actin was used as a loading control for the western blot (A). Stem cells, cultured in 3D scaffolds, were identified by immunofluorescence detecting the expression of putative stem cell markers nestin and CD133. These images are courtesy of Mr Ola Rominiyi (B).

5.6 Future Work/Discussion

FGFR family members (FGFR1, 2 and 3) are targets in current GBM clinical trials (table 5.4) (ClinicalTrials.gov, 2018). Due to the homologous nature of FGFR1, 2 and 3, one drug to target all 3 receptors is being tested. The main focus of these two trials is the oncogenic fusion gene, FGFR-TACC (Transforming Acidic Coiled-Coil), which generates a constitutively active FGFR by combining the tyrosine kinase domain of FGFR with the coil-coil domain of TACC, altering the downstream regulation of ERK and STAT3 signalling pathways (Singh et al., 2012). In GBM patients, FGFR-TACC fusion genes are only present in a low proportion (3 out of 97 cases) and are found alongside wild-type IDH-1, which confers a worse prognosis than the mutant IDH-1 (Singh et al., 2012). This fusion gene has been shown in various other cancers, including lower grade glioma (3.5%) (Di Stefano et al., 2015), cervical squamous cell carcinoma (3%) (Carneiro et al., 2015) and paediatric low grade glioma (6-7%) (Zhang et al., 2013). However, pan-tyrosine kinase inhibitors, such as those used when treating chromic myeloid leukaemia, can have off target effects (anaemia, nausea, leukopenia) which cannot be tolerated in patients (Tsai et al., 2018).

Table 5.4: Pan-FGFR inhibitors in clinical trials for GBM			
Drug	**Trial Start**	**Disease**	**Phase**
NVP-BGJ398	Dec 2013	FGFR1/3-TACC1/3 fusion and/or FGFR1,2,3 activating mutation	II
AZD4547	Sept 2015	FGFR1/3-TACC1/3 fusion IDH wild type	I & II

Table 5.4 *– FGFR inhibitors which target the whole family of receptors are currently in phase I and II clinical trials in patients with recurrent GBM.*

Here, FGFR4 was identified as a potential target to sensitise GBM cells to temozolomide. By depleting cells of FGFR4 using siRNA or inhibiting the kinase activity using BLU554, GBM cells become more sensitive to temozolomide reflected by a decreased survival fraction when compared to temozolomide only treated cells. As two different methods have been shown to sensitise GBM cells to temozolomide, the strength of FGFR4 as a potential target has been increased. Positively, FGFR4 knock-out mice are viable with no apparent defects (Weinstein et al., 1998). However, future work would include western blotting to detect inhibition of FGFR4 activity by BLU554 at the range of doses used, in order to confirm the inhibitory activity of the drug in the cells used.

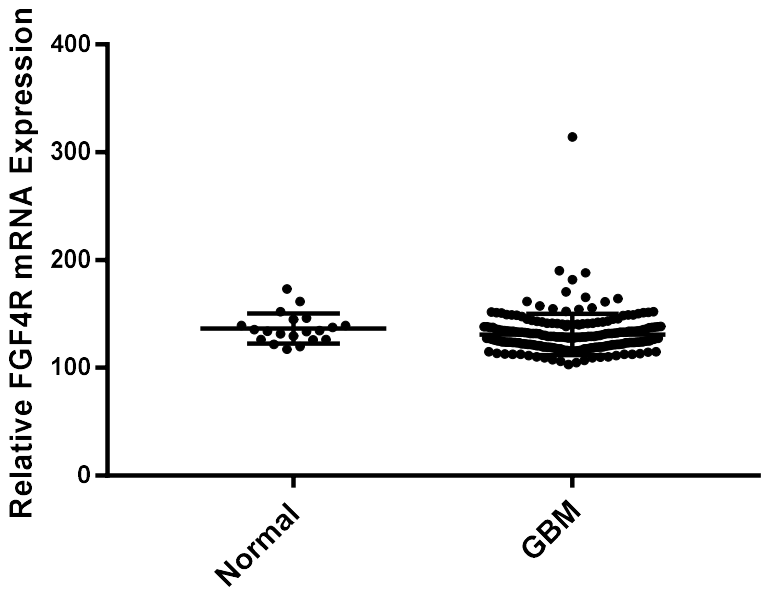

Figure 5.7: Relative FGFR4 mRNA Expression

Relative mRNA expression of FGFR4 was calculated using information from the REpository for Molecular BRAin Neoplasia DaTa (REMBRANT). There was a significant decrease in relative mRNA expression in GBM samples when compared to normal samples. The expression values were 136.5 for normal brain (n=20) and 130.5 for GBM (n=215), with a p-value of 0.03 using a Mann-Whitney U Test.

In the present study, FGFR4 protein has been detected in both GBM cell lines and primary patient GBM cells via western blotting; however, the expression of FGFR4 in non-cancerous and eloquent brain tissue has not been determined. An increased FGFR4 protein expression in GBM tumours could increase the potential of FGFR4 as a valid target. In order to explore this, immunohistochemistry investigating FGFR4 protein expression in both non-cancerous brain (normal) and GBM tissue would enable us to detect any changes in expression. Interestingly, FGFR4 mRNA expression in a cohort of GBM tumours is significantly less when compared to normal samples (figure 5.7) (Betastasis, 2018). This decrease in mRNA expression, also mirrored by a decrease in FGFR2 and FGFR3 mRNA expression in GBM tumours, although initially disappointing, needs to be investigated further as gene expression and protein function is not always co-dependent. For example, The Human Protein Atlas database does show FGFR4 expression to be low in brain tissue, however, IHC protein expression data has been shown to conflict with mRNA data (TheHumanProteinAtlas).

Although the over-expression of receptors is usually a therapeutic target, for example HER2 in breast cancer, in relation to mutant receptors, even a slight decrease in expression can result in hugely dysregulated downstream signalling e.g. mutations increasing receptor affinity for FGFs or chromosomal rearrangements causing fusion genes (Babina and Turner, 2017, Moasser and Krop, 2015). If FGFR4 is forming fusion genes similar to FGFR1/3-TACC1/3, seen in approximately 3.1% of GBM cases, there may be no increase in FGFR4 mRNA or protein expression but a

dysregulated signalling pathway which cannot be detected by qRT-PCR or immunohistochemistry (Di Stefano et al., 2015, Singh et al., 2012). A previous study has also identified FGFR4 activating mutations in a small number of GBM samples by using The Cancer Genome Atlas, which again may not confer an increase in protein expression (TGCA)(Masica and Karchin, 2011).

Rhabdomyosarcoma (RMS), a cancer of soft tissue (muscles, tendons, ligaments), has high FGFR4 expression in the tumours. Activating mutations in FGFR4 have been studied in RMS, and it was found that an increase in FGFR4 signalling (detected by an increase in phosphorylation), caused an increase in both total and phosphorylated STAT3 (Taylor VI et al., 2009). Similar findings have been shown in colorectal cancer where depleting cells of FGFR4 also decreased STAT3 activity (Turkington et al., 2014). Activating mutations in FGFR4 were found to increase tumour proliferation in RMS cell lines and xenografts transplanted into nude mice (Taylor VI et al., 2009). If similar mutations were present in the GBM cell lines used in this study, this could potentially have cause the chemo-sensitisation, however, as these mutations form a minor subset of all GBM tumours it is unlikely to have been present in all 3 GBM cell lines used.

Regarding chemo-resistance, it has previously been found that breast cancer cells which are resistant to the chemotherapy doxorubicin over express FGFR4. This overexpression has been shown to be responsible for chemo-resistance through upregulation of the anti-apoptotic pathways by the increased expression of BCL-xl (Roidl et al., 2009). FGFR4 dysregulation has also been shown to activate other anti-apoptotic pathways such as Protein Kinase B (PKB/AKT) in breast cancer (Tiong et al., 2016). These findings, although not specifically related to GBM, could potentially help us to understand why GBM stem cells (CD133+ve), which are a more chemo-resistant population, express more FGFR4 (Liu et al., 2006).

As this is preliminary data, it would be interesting to investigate the mechanism of action further. Similar assays used when exploring the mechanism of ERK5 in temozolomide resistance would be applied, particularly investigating the DNA damage response to the combination treatment. FGFR4 depletion and treatment with chemotherapeutics (5-fluorouracil and oxaliplatin) have shown synergistic effects in colon cancer and STAT3 depleted cells have been shown to have a reduced DNA damage response when treated with UV-light and oxaliplatin chemotherapy (Barry et al., 2010, Turkington et al., 2014). These findings may indicate a replication-associated mechanism of sensitisation, which potentially could be linked to temozolomide-mediated DNA lesions.

Chapter 6 – Small Molecule Screens in Temozolomide resistant GBM cells

6.1 Introduction

Treatment for GBM has remained unchanged for nearly 2 decades, since the approval of temozolomide for treating patients with recurrent glioblastoma in 2001 (Arney, 2013, NICE, 2001). Temozolomide has improved 2 year survival from 10.4% to 26.5% in a phase II clinical trial (Stupp et al., 2005), however, GBM still remains a death sentence with most patients passing away only 18 months from diagnosis (Di Carlo et al., 2017).

There are around 10,000 drugs currently in cancer clinical trials, however, the drop-out rate is extremely high with failure to get from phase 0 clinical trials to phase I clinical trials as high as 95% (ClinicalTrials.gov, 2018, Kola and Landis, 2004). For the compounds that are successful, it may have taken over 13 years before patients can receive this drug as part of their treatment regime (Paul et al., 2010). This process is extremely costly not only for the pharmaceutical industry but also health care providers, such as the NHS, as the cost of purchasing successful drugs is inflated to cover the financial loss of failures (Sleire et al., 2017). In order to target both poor productivity and expense of developing novel drugs, the Repurposing Drugs in Oncology (ReDO) Project has been developed. This project focuses on repurposing non-oncology low-cost drugs which have a well-developed and safe pharmacokinetic profile.

Studies investigating toxicity, absorption, distribution, metabolism and excretion are often available for drugs with the potential to be repurposed. Phase I trials to establish maximum tolerated doses are still likely to be required when repurposing a drug, however, the risk of the drug failing is reduced as the pharmacokinetics are more likely to be better understood (Pantziarka et al., 2014). A successful example of drug repurposing is sildenafil. This drug was initially developed to treat angina before being repurposed for treating erectile dysfunction and termed Viagra. It has now been further developed and is used to treat pulmonary hypertension (Ghofrani et al., 2006).

Collections of various pre-tested drugs have been compiled for high-throughput repurposing screens. Itraconazole, first developed as anti-fungal, is one drug which has been identified by such screens. Itraconazole was identified in a repurposing screen as an inhibitor of oncogenic hedgehog signalling in medulloblastoma (Kim et al., 2010). It is now being tested in clinical trials for various cancers, having also shown synergistic effects with chemotherapeutics (ClinicalTrials.gov, 2018, Kim et al., 2010, Pounds et al., 2017).

During this study we conducted a screen of over 2000 compounds with the aim of identifying novel small molecule inhibitors able to sensitise GBM cells to treatment with temozolomide. The compounds screened were from two libraries: a pharmacologically diverse selection of marketed drugs (Prestwick Chemical Library) and late phase clinical trial failures and natural compounds library targeted to CNS biology (Spectrum Collection Library).

6.2 Small Molecule Screen Optimisation – Positive Control

Seeding densities, which had been previously optimised for the siRNA screen (chapter 3), were used for the small molecule drug screen as the assays were to be carried out in the same 384-well format and duration. A positive control able to generate a z-prime of >0.5 was also required for this screen. O-6-benzylguanine (O6BG) is a small molecule inhibitor of MGMT, the enzyme responsible for repairing the most toxic lesion caused by temozolomide; methylation at the O6 position of guanine (Dolan et al., 1991). O-6-benzylguanine was tested in combination with temozolomide (50μM) as a potential positive control. DMSO was used as a negative control at the maximum concentration cells were exposed to in the positive control wells. Positive and negative controls were added to a 384 well plate in a checker-board fashion to mitigate any intra-plate localisation effects on cell growth (figure 6.1). On day 0 cells were plated, 24 hours later DMSO and O-6-benzylguanine were added to the wells, before DMSO and temozolomide were added following a further 24 hours incubation. The plates were then incubated for 5 days before processing, imaging and analysing in an identical manner to the siRNA screen plates (chapter 3).

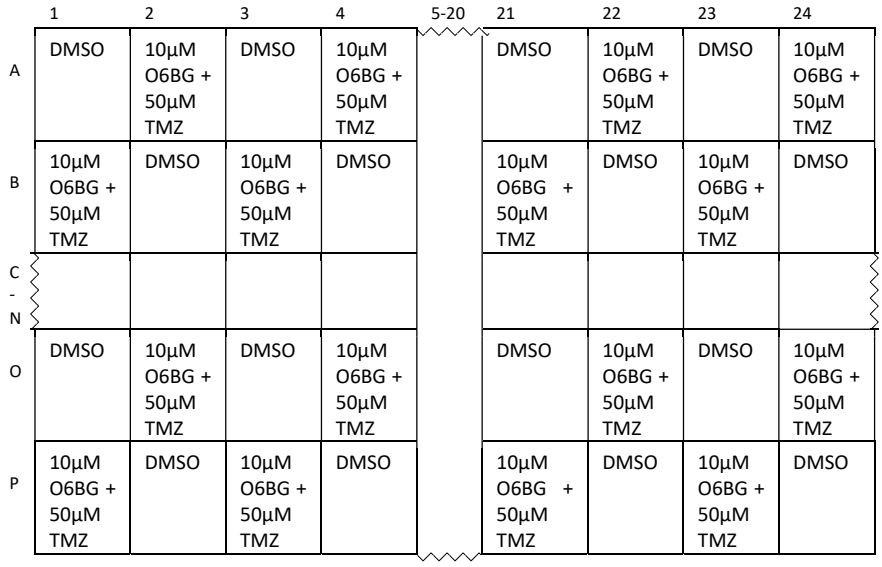

Figure 6.1: 384 well plate checker-board representation

24 hours after plating in a 384 well plate, T98G cells were treated with either DMSO or 10µM O6BG. Following a further 24 hours incubation, cells were treated with DMSO or 50µM TMZ. DMSO and drugs were added the wells using a Labcyte Echo 500. After 5 days, cells underwent staining, fixing and imaging and wells were analysed using a Multi Wavelength Cell Scoring application on MetaXpress which counted cells based on minimum and maximum microns and intensity above background.

10µM O-6-benzylguanine combined with 50µM temozolomide was able to generate significant cell death when compared to the negative DMSO control, giving a z-prime of 0.61 (as calculated in chapter 3). A score of >0.5 reflects a robust and reproducible assay (Bray and Carpenter, 2017). This drug combination therefore was used as a subsequent positive control in the outer columns of every plate for the small molecule drug screens.

6.3 Screen Optimisation – Negative Control

All compounds in the library were diluted in DMSO to a concentration of 10mM before being dispersed by the Labcyte Echo 500 at the volume required for the selected concentration (e.g. 1µM or 10µM). In order to ensure any effects on survival fractions were not due to increasing doses of DMSO, a DMSO dose response in T98G cells was conducted. Doses ranged from 1-100µM either alone or in combination with 50µM temozolomide (figure 6.2).

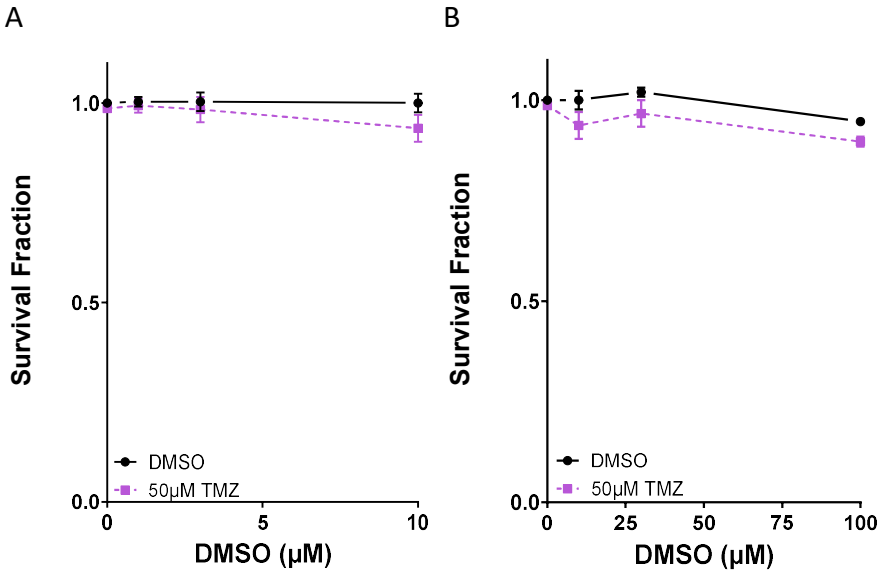

Figure 6.2: Fraction of GBM cells treated with DMSO

Cells were plated and allowed to adhere for 24 hours. Cells were treated with a range of volumes of DMSO equal to that dispersed for 0-100µM before being treated with 50µM TMZ 24 hours later. Drugs were added the wells using a Labcyte Echo 500. After 5 days, cells underwent staining, fixing and imaging and wells were analysed using a Multi Wavelength Cell Scoring application on MetaXpress which counted cells based on minimum and maximum microns and intensity above background. .

A and B show the same data plotted against a different x-axis.

Data shown is the surviving fraction +/- standard deviation from two independent biological repeat experiments.
Surviving fractions were normalised to untreated controls.

DMSO showed slightly toxicity (5-10%) at the highest concentration that would be used for dose responses of any potential hits. At 10µM, the highest screen concentration, there was very minimal toxicity. This was therefore deemed acceptable as a suitable negative control for the screen.

6.4 Prestwick Chemical Library

The Prestwick Chemical Library contains 1200 small molecule drugs, which form a diverse pharmacological collection. Both 1µM and 10µM were selected as standard doses to perform the screen at. Screening at 1µM did not highlight any particular compounds that sensitised the cells to temozolomide (data not shown). However, when the library was screened at 10µM, 9 compounds were identified as potential 'hits' (table 6.1). Hits were selected if they were able to reduce survival fraction by 20% or greater when compared to DMSO negative control.

Table 6.1: Prestwick Chemical Screen 'hits'- 10µM	
Compound	**Survival Fraction**
Metronidazole	0.74
Allantoin	0.75
Atracurium besylate	0.80
Dropropizine (R,S)	0.71
Midodrine hydrochloride	0.76
Perhexiline maleate	0.78
Thioridazine hydrochloride	0.78
Fluphenazine dihydrochloride	0.66
Butamben	0.68

Table 6.1 *– Small molecules identified as sensitisers of GBM cells to temozolomide following initial screening at 10µM. The compounds have a range of roles including: anti-bacterial, muscle relaxant, vasodilator, hypotensor and anti-psychotic.*

Increasing doses of the selected compounds (0-30µM) were then combined with 50µM of temozolomide. Out of all the compounds tested, only butamben was able to sensitise the cells to temozolomide (figure 6.3). Butamben is a voltage dependent calcium channel blocker and an ATP sensitive potassium channel antagonist; used as a local anaesthetic (Beekwilder et al., 2006, Winkelman et al., 2005). It is not immediately obvious how this drug may affect cellular responses to temozolomide; however, it was decided to validate it further as a potential temozolomide sensitising agent.

Thioridazine hydrochloride, an anti-psychotic agent which acts through inhibition of DRD2 receptors in the CNS, was subsequently identified as a sensitiser to temozolomide in GBM (Johannessen et al., 2018) (see section 6.6 for more detail).

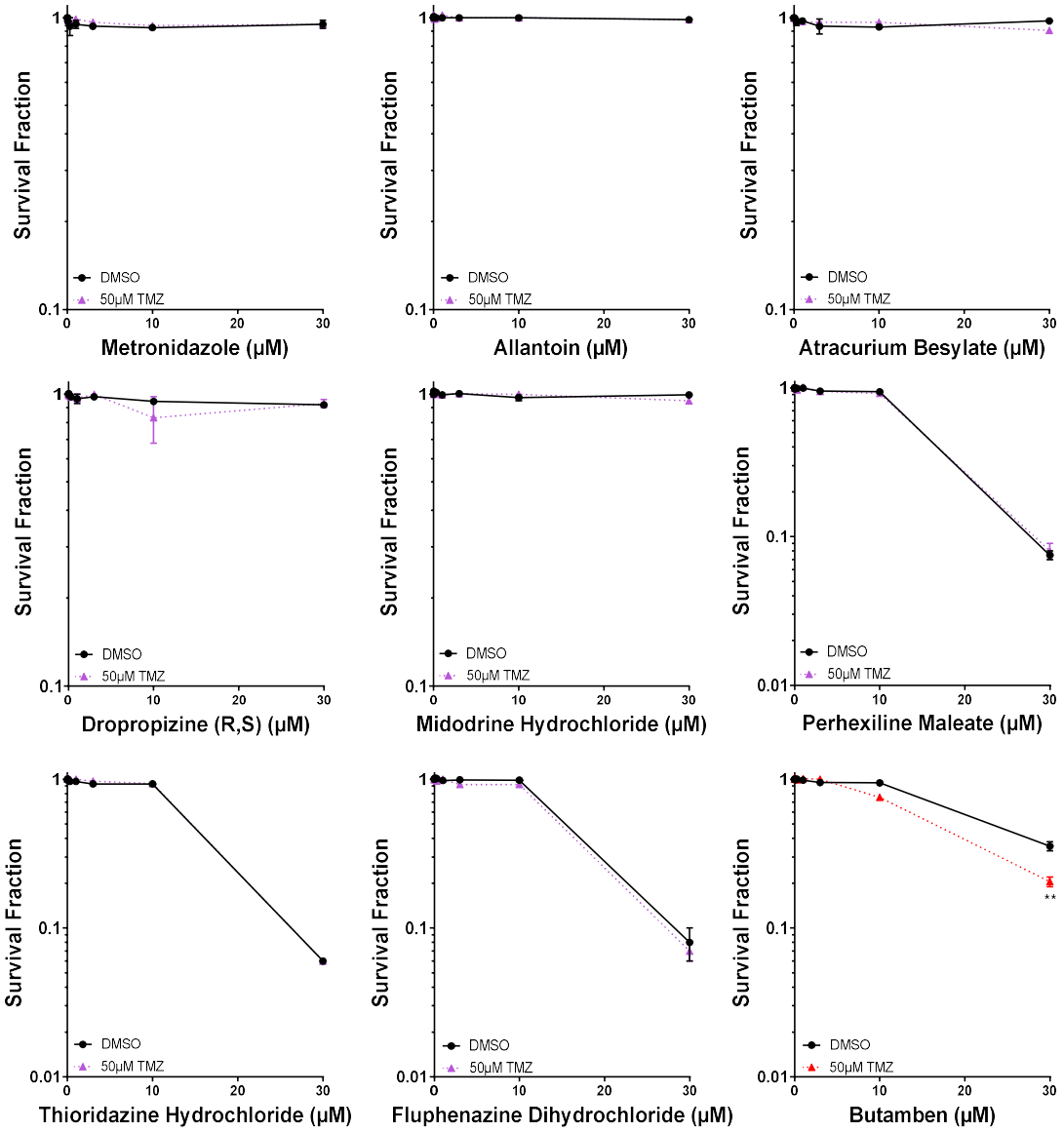

Figure 6.3: Cytotoxicity curves of GBM cells treated with Prestwick Chemical Screen 'hits' and TMZ

Cells were plated and allowed to adhere for 24 hours. Cells were treated with a range of doses of drugs (0-30μM) before being treated with TMZ 24 hours later. Following 5 days incubation an MTT assay was performed. Only T98G cells treated with butamben showed a reduced survival fraction when treated in combination with TMZ as opposed to drug alone, this reduction in survival was significant at 30μM (p=0.009).

Data shown is the average surviving fraction (normalised to DMSO treated control) +/- standard deviation from 3 independent biological repeat experiments.
***=P<0.005 using a Mann-Whitney U Test.*

6.4.1 Validation of Butamben as a Temozolomide sensitising agent

Fresh butamben was purchased from Selleck (S4583) and tested in increasing doses in T98G cells (0-30µM). This fresh drug was inherently more toxic when compared to the Prestwick library stocks (most likely due to age-mediated degradation) but it was still able to sensitise the cells to temozolomide (figure 6.4). Combinations of temozolomide and butamben ranging from 5µM to 17.5µM resulted in a significant decrease in survival fraction; however, this significance was lost when using ≥20µM of butamben due to increasing cytotoxicity of the drug alone.

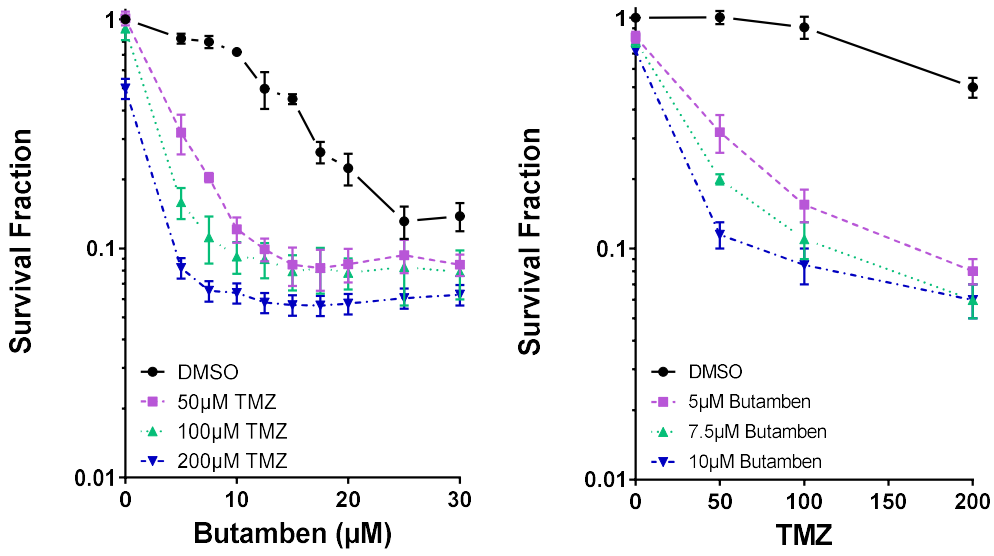

Figure 6.4: Cytotoxicity curves of GBM cells treated with Butamben and TMZ

Cells were plated and allowed to adhere for 24 hours. Cells were treated with a range of doses of butamben (0-30µM) before being treated with TMZ 24 hours later. Following 5 days incubation an MTT assay was performed. Butamben alone was slightly toxic at 7.5 µM and 10µM with a significantly reduced survival fraction of 0.80 and 0.72, however, this increased dramatically with increasing doses (p=0.05 and 0.01 respectively using a Mann-Whitney U Test). T98G cells treated with butamben showed a reduced survival fraction when treated in combination with TMZ as opposed to butamben alone.

A and B show the same data plotted against a different x-axis.
A x-axis Butamben B x-axis TMZ
Data shown is the average surviving fraction (normalised to DMSO treated control) +/- standard deviation from 3 independent biological repeat experiments.

In order to determine whether this was a cell line specific effect, butamben was tested in combination with temozolomide in several additional cell lines; including some non-GBM cells (figure 6.5). Butamben was also combined with temozolomide in clonogenic survival assays which are more sensitive than MTT assays (figure 6.6). The doses selected were between 0-10µM as these had a relatively low toxicity in T98G cells.

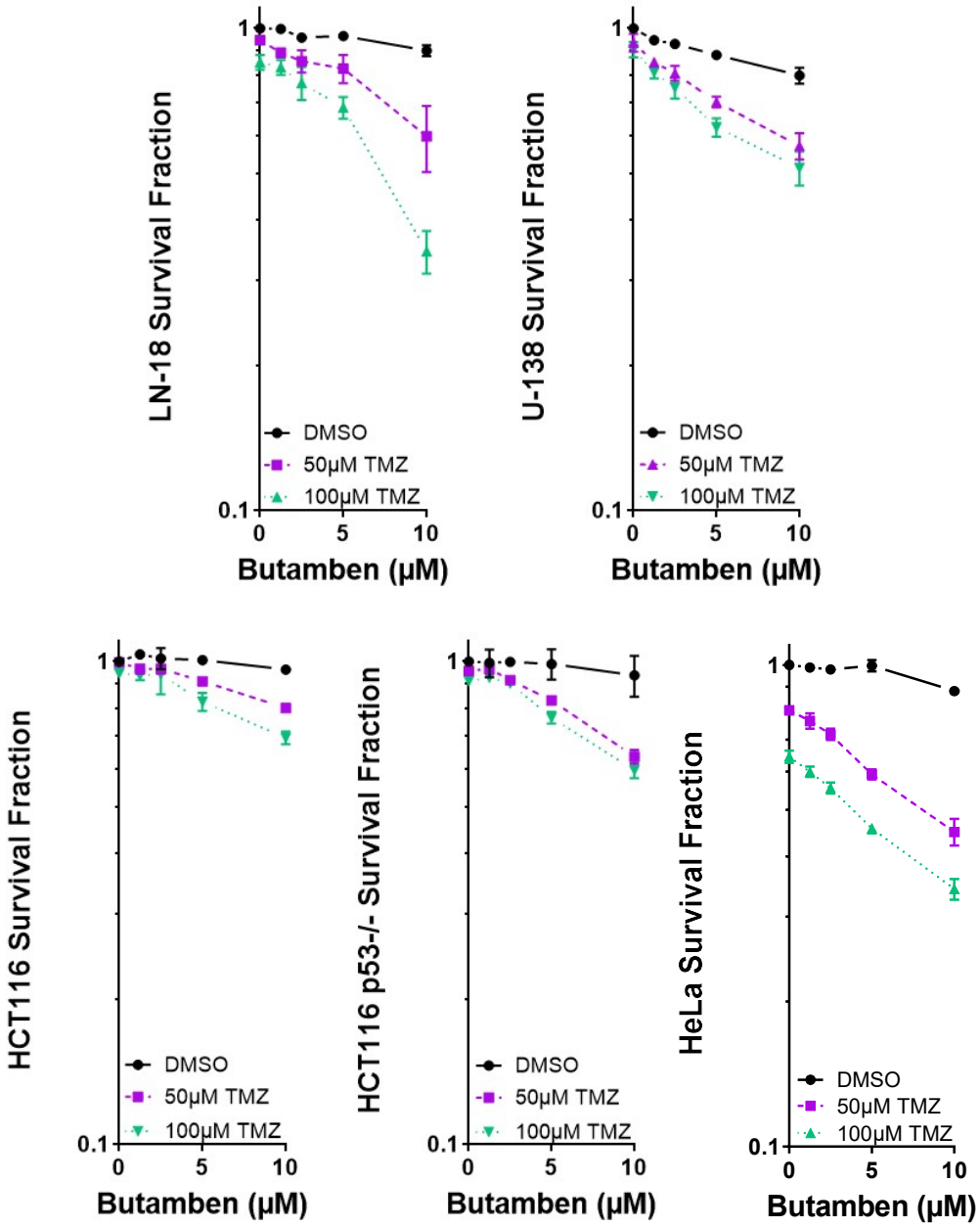

Figure 6.5: Cytotoxicity curves for a range of cancer cells treated with Butamben and TMZ

Cells were plated and allowed to adhere for 24 hours. Cells were treated with a range of doses of butamben (0-10µM) before being treated with TMZ 24 hours later. Following 5 days incubation an MTT assay was performed. All cells treated with butamben showed a reduced survival fraction when treated in combination with TMZ as opposed to butamben alone, however, this sensitivity varied between cell lines.

Data shown is the surviving fraction (normalised to DMSO treated controls) +/- standard deviation derived from 3 independent biological repeat experiments.

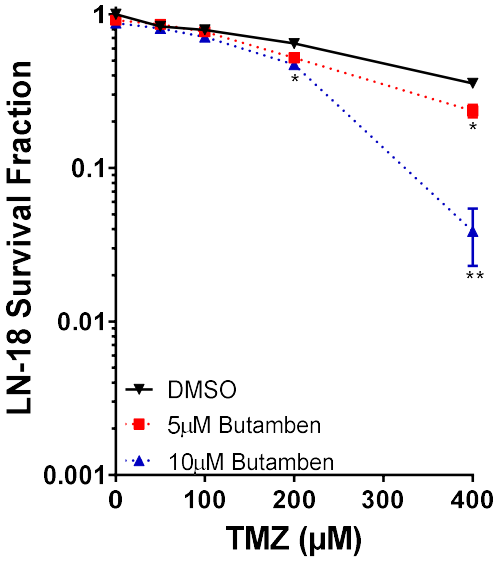

Figure 6.6: Clonogenic survival curves for LN-18 cells treated with Butamben and TMZ
Cells were plated and allowed to adhere for 24 hours. Cells were treated with DMSO, 5μM or 10μM butamben before being treated with a range of doses of TMZ (0-400μM) 24 hours later. Cells were incubated for 12 days allowing colonies to form. Cell colonies were fixed in 0.04% methylene blue in 100% ethanol for 30 minutes at room temperature. >50 cells were counted as a colony. Both 5μM and 10μM butamben combined with TMZ were more effective at killing cells when compared to TMZ alone The higher dose of butamben was more effective at sensitising cells to TMZ.

Data shown is the surviving fraction (normalised to DMSO treated controls) +/- standard deviation derived from two independent biological repeat experiments.
**=p<0.05 **=p<0.01 using a Mann-Whitney U Test.*

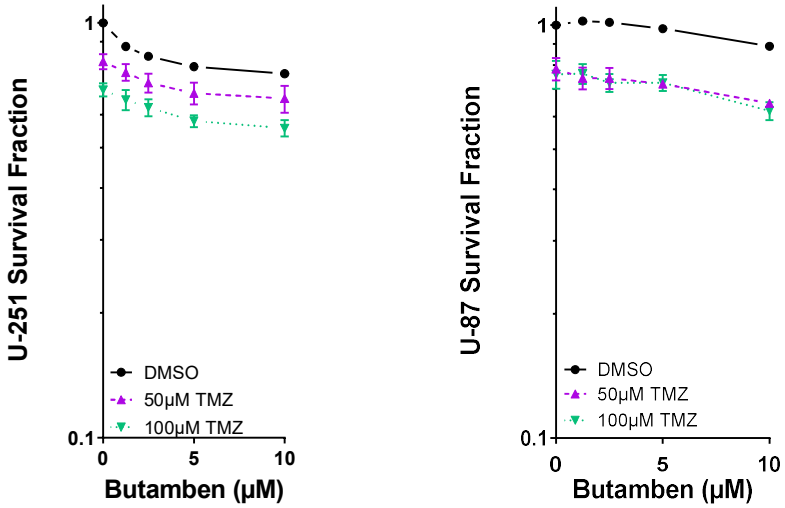

Figure 6.7: Cytotoxicity curves for a range of GBM cells treated with Butamben and TMZ
Cells were plated and allowed to adhere for 24 hours. Cells were treated with a range of doses of butamben (0-10μM) before being treated with TMZ 24 hours later. Following 5 days incubation an MTT assay was performed. All cells treated with butamben showed a reduced survival fraction when treated in combination with TMZ as opposed to butamben alone; however, this sensitivity is only due to initial death caused by TMZ treatment.

Data shown is the surviving fraction (normalised to DMSO treated controls) +/- standard deviation derived from 3 independent biological repeat experiments.

There were two GBM cell lines which did not sensitise to the combination of butamben and temozolomide (figure 6.7). These were U-87 and U-251 cells which are both MGMT negative (figure 3.1A). In order to test whether MGMT is required for butamben to sensitise cells to temozolomide, MGMT proficient cells were depleted using siRNA before being drug treated.

Both control and MGMT siRNA treated T98G cells were sensitive to the combination of butamben and temozolomide (figure 6.8). However, the combination treatment which caused a significant increase in cell death resulted in OD values near the sensitivity limit of the assay. MGMT depletion combined with temozolomide caused almost 50% cell death which resulted in a much less dramatic sensitisation when additionally combined with butamben. Expected values generated from combination treatment (B+T) were 0.38 for MGMT siRNA and 0.77 for control siRNA, compared to the observed values of 0.18 and 0.23 respectively. Additional clonogenic survival assays would therefore be a more accurate measure of whether MGMT proficiency is required for the combination to be effective.

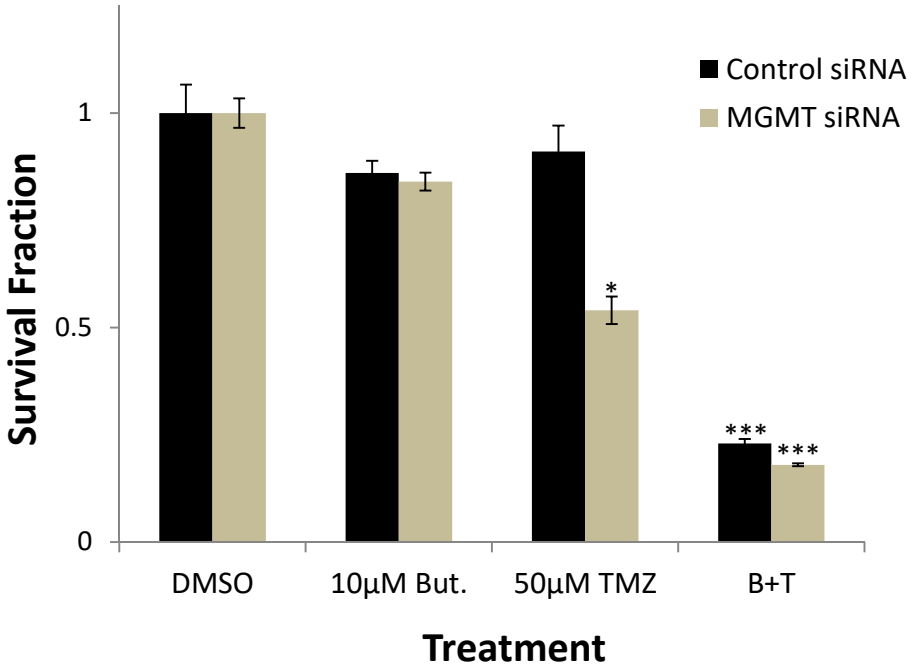

Figure 6.8: Survival Fraction of T98G cells treated with Butamben and siRNA

Cells were reverse transfected for 48 hours before being treated with 10µM butamben. 24 hours later cells were treated with 50µM TMZ. Following 5 days incubation an MTT assay was performed. Cells treated with MGMT siRNA were more sensitive to temozolomide treatment, a positive control for the assay. Both control and MGMT siRNA treated cells had a significant decrease in survival fraction when treated with the combination of butamben and temozolomide when compared to the respective DMSO control cells.

Data shown is the surviving fraction (normalised to DMSO treated controls for control or MGMT siRNA) +/- standard deviation derived from two independent biological repeat experiments,
**=p<0.05, ***=P<0.005 using a Mann-Whitney U Test.*

6.4.2 Butamben and DNA damage

In order to ascertain a potential mechanism by which butamben sensitised cells to temozolomide, comet assays were used to asses DNA damage caused by the combination of butamben and temozolomide. These assays were carried out both a responding GBM cell line (T98G) and a non-responding GBM cell line (U-251). The combination of butamben and temozolomide caused a modest, yet significant increase in tail moment (an established measure of DNA damage, see methods section for further details) in T98G cells when compared to temozolomide treated cells, however, this increase was not detected in non-responding U-251 cells (figure 6.9).

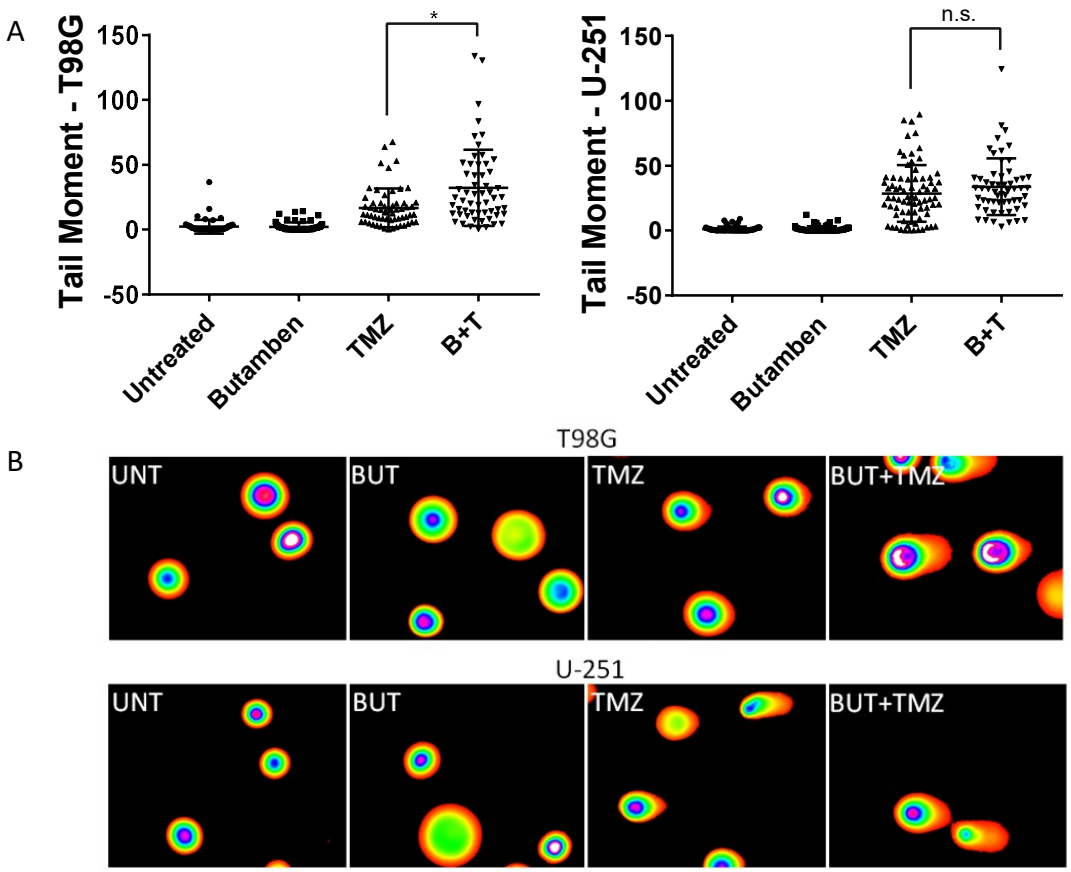

Figure 6.9: Assessing DNA damage using comet assays in GBM cells treated with butamben
Cells were plated before being treated with DMSO or 10µM butamben. 24 hours later 200µM TMZ was added. Cells were collected for comet assays 24 hours post TMZ treatment. Comets were imaged and then analysed using CometScore. 50 cells were imaged for each condition, example images seen in B. The combination of butamben and TMZ caused a significant increase in DNA damage in T98G cells (p=0.04) when compared to TMZ alone (A). U-251 cells did not exhibit a significant increase in DNA damage in the combination treatment when compared to TMZ alone (p=0.47) (A), consistent with butamben not sensitising these cells to treatment with TMZ (figure 6.6).

Data shown is the Tail Moment +/- standard deviation.
** = p < 0.05 using a Kruskal-Wallis H Test.*
(n=2)

Unfortunately, due to time constraints the mechanism by which butamben sensitises GBM cells to temozolomide was not further studied.

6.5 Spectrum Collection Library

The Spectrum Collection library contains 1040 compounds including failures from late phase clinical trials, FDA approved drugs and natural compounds. However, these have all been selected as compounds with the potential to target the CNS. The Spectrum Collection library was screened identically to the Prestwick Chemical Library, both at 1µM and 10µM. Screening at 1µM identified two compounds which sensitised T98G cells to temozolomide; thalidomide and deoxysappanone B trimethyl ether.

Thalidomide, which acts in as an anti-angiogenic, has previously been identified as a compound with the potential to sensitise GBM tumours to treatment with temozolomide and had a positive effect on survival in phase II clinical trials (Baumann et al., 2004). It has also been trialled in other cancers where temozolomide is given as a chemotherapeutic, including melanoma, leiomyosarcoma and neuroblastoma (ClinicalTrials.gov, 2018).

Deoxysappone B trimethyl ether is an inhibitor of TDP1, involved in the repair of DNA damage, and an inhibitor of CYP3A4 (National Center for Biotechnology Information, 2018a). TDP1 depleted GBM cells have been shown to be more sensitive to temozolomide when compared to TDP1 proficient cells (Alagoz et al., 2013).

As both of the compounds identified in the 1µM screen had been previously identified as known sensitisers of GBM cells to temozolomide, this was positive reinforcement that the screen was a valid approach by which to identify novel temozolomide sensitising agents. However, as these were the two targets identified from the screen at 1µM, an additional screen was carried out using 10µM of each compound within the library to try and identify initial hits.

Two compounds were identified from the 10µM screen. These were pyrvinium pamoate (PP) and d-penicillamine (D-pen). Both drugs were relatively non-toxic at 10µM with survival fractions of 0.97 and 0.71 respectively. When combined with temozolomide alone, survival fractions decreased to 0.05 and 0.16 respectively.

6.5.1 Pyrvinium Pamoate

Pyrvinium pamoate is an androgen receptor inhibitor. Androgen receptors are activated by testosterone and dihydrotestosterone (DHT). Pyrvinium pamoate has been investigated as a potential therapeutic in prostate cancer where androgen receptors are central to both the initial oncogenic development as well as progression into a more aggressive and advanced prostate cancer (Lim et al., 2014).

Pyrvinium pamoate was purchased for a dose response in T98G cells (Sigma-Aldrich 1592001). This fresh drug was extremely toxic and over 90 percent of cells were dead at a dose of 1µM. The combination of pyrvinium pamoate and temozolomide did not sensitise the GBM cells in a dose response (figure 6.10).

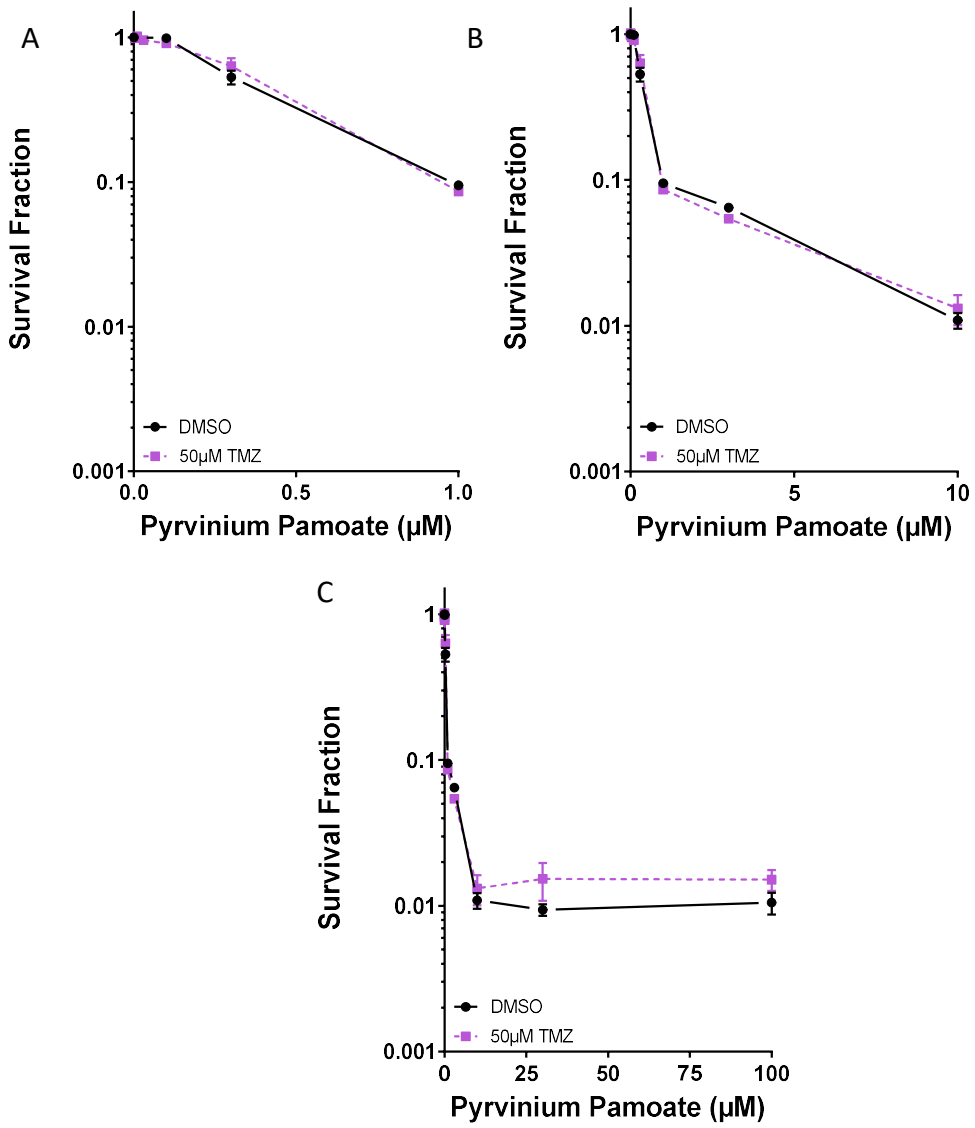

Figure 6.10: Cytotoxicity cruves of GBM cells treated with Pyrvinium Pamoate

T98G cells were plated and allowed to adhere for 24 hours. Cells were treated with a range of doses of PP (A: 0-1μM, B: 0-10μM and C: 0-100μM) before being treated with TMZ 24 hours later. Drugs were added the wells using a Labcyte Echo 500. After 5 days, cells underwent staining, fixing and imaging and wells were analysed using a Multi Wavelength Cell Scoring application on MetaXpress which counted cells based on minimum and maximum microns and intensity above background.

Survival fraction (A) shows T98G cells treated with a maximum dose of 1μM PP.
Survival fraction (B) shows T98G cells treated with a maximum dose of 10μM PP.
Survival fraction (C) shows T98G cells treated with a maximum dose of 100μM PP.
A, B and C show the same data plotted against a different x-axis.

Data shown is the average surviving fraction (normalised to DMSO treated controls) +/- standard deviation derived from 3 independent biological repeat experiments.

6.5.2 D-Penicillamine

Penicillamine is a chiral molecule which forms a mixture of both D- and L-penicillamine. These compounds are formed when penicillin degrades. Penicillamine is used as an anti-rheumatic and also as copper chelator in Wilson's disease, where a fatal level of copper builds up in organs such as the brain and liver (Finney et al., 2009, National Center for Biotechnology Information, 2018b). D-penicillamine was purchased for a dose response in T98G cells (Sigma-Aldrich P4875) to validate it as a novel temozolomide sensitising agent. This drug had a similar toxicity in both the library screen and dose response at 10µM, however, it was not able to sensitise T98G cells to temozolomide when used in combination (figure 6.11), suggesting that like pyrvinium pamoate, it too was a false positive hit from the screen.

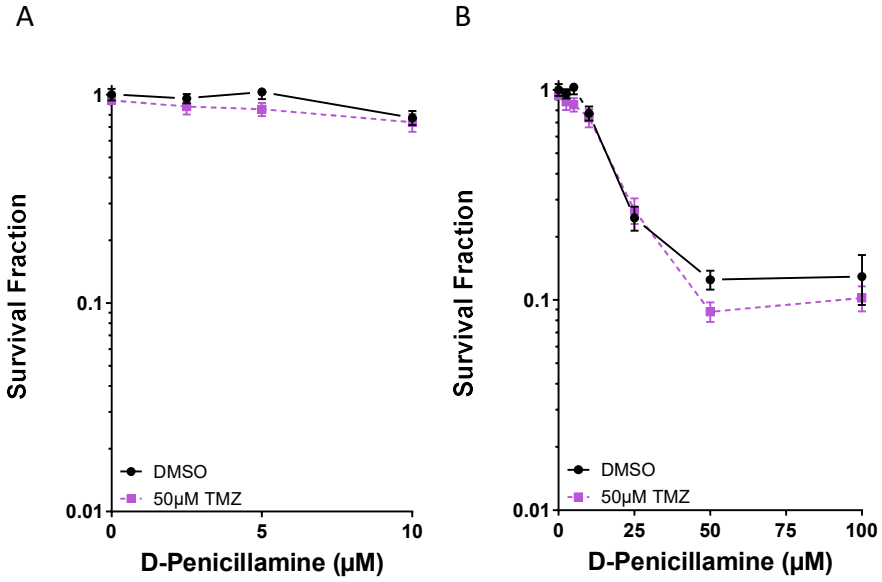

Figure 6.11: Cytotoxicity curves of GBM cells treated with D-Penicillamine

T98G cells were plated and allowed to adhere for 24 hours. Cells were treated with a range of doses of D-Pen (A: 0-10µM and B: 0-100µM) before being treated with TMZ 24 hours later. Drugs were added the wells using a Labcyte Echo 500. After 5 days, cells underwent staining, fixing and imaging and wells were analysed using a Multi Wavelength Cell Scoring application on MetaXpress which counted cells based on minimum and maximum microns and intensity above background. .

Survival fraction (A) shows T98G cells treated with a maximum dose of 10µM D-Pen.
Survival fraction (B) shows T98G cells treated with a maximum dose of 100µM D-Pen.
A and B show the same data plotted against a different x-axis.

Data shown is the average surviving fraction (normalised to DMSO treated controls) +/- standard deviation derived from 3 independent biological repeat experiments.

6.6 Discussion

Repurposing drugs has become an attractive approach in oncology as there has been a gradual decline in the number of drugs approved for treatment each year since the 1990s (Sleire et al., 2017). During this study we have identified butamben as a potential novel sensitiser of GBM cells to temozolomide. Butamben is used as a topical anaesthetic and as an epidural for chronic pain. Its anaesthetic properties are thought to be due to inhibition of voltage gated ion channels (sodium, calcium and potassium) linked to nociception (Beekwilder et al., 2006, Winkelman et al., 2005, Van den Berg et al., 1995).

Ion channels are known to be important in GBM as they help regulate proliferation via cell cycle checkpoints, and the sequencing of over 20,000 genes in 21 GBM patients revealed that over 90% had mutations in genes relating to transport of ions (Joshi et al., 2011).

ATP-sensitive voltage gated potassium channel inhibitors are able to reduced cell proliferation in GBM cell line U-87 both *in vitro* and *in vivo (*xenograft nude mouse models) (Ru et al., 2014). Furthermore, big conductance potassium channels (BK), which are activated by membrane potential changes and intracellular calcium, are over-expressed in GBM patients and are thought to contribute to the migratory properties of the tumour cells (Wondergem et al., 2008).

GBM patients with mutations in sodium ion channels have a reduced overall survival when compared to patients with potassium or calcium ion channel mutations. Additionally, patients with IDH1 mutations, which confers better survival, did not have any sodium ion channel mutations. However, this study included only a small cohort of patients (n=21) and did not reach statistical significance (Di Stefano et al., 2015, Joshi et al., 2011).

Mibefradil is an l-type and t-type (CaV 3.2) calcium channel blocker. The l-type inhibition targets hypertension and that was the original target, however, repurposing has shown t-type inhibition to slow growth of glioma stem cells (GSCs) (Keir et al., 2013). T-type channels are highly expressed in GSC population compared to the bulk tumour population, and under normal physiological conditions have important roles in cell cycle progression, cell growth and proliferation (Keir et al., 2013, Zhang et al., 2013). The combination of mibefradil and temozolomide was able to cause a decrease in both cell proliferation and increase in cell death detected by trypan blue (Zhang et al., 2017). These findings translated into an orthotopic GSC xenograft model in immunocompromised mice, where the combination of treatment reduced tumour growth in an additive manner (Keir et al., 2013). Butamben is also a t-type calcium channel inhibitor and may be acting in an identical manner to mibefradil, explaining the temozolomide

sensitisation seen (Beekwilder et al., 2006, Zhang et al., 2017), although at present the mechanism by which the two drugs interact is currently unknown. This effect has not only been seen in GSCs, as U-87 cells have also shown reduced proliferation and migration in response to inhibition of t-type calcium currents (Zhang et al., 2012). Mibefradil has been recently tested in two phase I trials in patients with recurrent GBM, in combination with either radiotherapy or temozolomide, however, the result have not yet been published (ClinicalTrials.gov, 2018). As butamben affects various ion channels, it would have been prudent to test sensitisation using alternative methods to MTT assays. One example would be to use trypan blue, as this does not rely on metabolism, but it can be used to identify a non-viable cell population through the uptake of the blue dye. Clonogenic survival assays which simply stain clonal cell colonies were used as an alternative measure of cell proliferation and were able to show similar temozolomide sensitisation seen using MTT assays.

One key issue with the use of butamben is the anaesthetic property of the drug. Even if butamben was given directly into the tumour cavity during surgery, the compromised blood brain barrier seen in GBM patients means the anaesthetic is likely to reach systemic circulation thereby effecting normal tissues, making the combination of butamben and temozolomide highly unlikely to ever reach clinical trials. This unfeasibility makes it difficult to see how such a drug would have been included in a small molecule library where compounds have been selected for repurposing. If the target which enables butamben to sensitise GBM cells to temozolomide could be identified, inhibition with an alternative small molecule compound which does not have anaesthetic properties may have the potential for success in clinical trials.

Not only have calcium channels been identified as potential targets for temozolomide sensitivity, one initial hit from the Prestwick Screen, fluphenazine dihydrochloride, is an anti-psychotic and an inhibitor of calcium-modulated protein (calmodulin) (Hait et al., 1987). Calmodulin is activated by the binding of calcium ions (Ca^{2+}) which enable it to act as a second messenger, binding to ion channels, enzymes and various other proteins relaying signalling information to pathways involved in apoptosis, smooth muscle contraction, metabolism and immunity (Chin and Means, 2000). Calmodulin has been shown to be important for the growth of rat glioblastoma cells (C6 cells), with increasing inhibition of calmodulin correlating with reduced tumour cell growth (Lee and Hait, 1985). Although the mechanism for this increased apoptosis is unclear, it may be via effects on calmodulin sensitive phosphodiesterases thus effecting cAMP and cGMP signalling (Lee and Hait, 1985). The degree of calmodulin inhibition does not completely explain the anti-proliferative effects, but further studies showed a similar correlation regarding inhibition of sigma receptors (bind to anti-psychotropic drugs e.g. Xanax) (Vilner

and Bowen, 1993). Calmodulin 3 (CALM3) and Calcium/Calmodulin Dependent Protein Kinase II Beta (CAMK2B), Calcium/Calmodulin-Dependent Protein Kinase Type 1B (PNCK) and two cAMP dependent kinases (PRKAR1A and PRKAR2B) were also initial hits in the primary OTP screen. However, these were not taken forward as potential hits as they did not sensitise cells to temozolomide when depleted by siGENOME siRNA, however, as this was much less effective than OTP they could still be potential targets (chapter 3). However, when a calmodulin inhibitor (trifluoperazine) was combined with chemotherapy (bleomycin) in 17 GBM patients in a Phase II trial, there was unfortunately no improvement with the combination. Although trifluoperazine is lipophilic and readily crosses the blood brain barrier, bleomycin is amphipathic and therefore potentially ineffective at treating GBM; possibly explaining why there was no sensitisation observed (Hait et al., 1990, Kristiansen et al., 1981).

Thioridazine hydrochloride, an anti-psychotic, was also identified as an initial hit in the Prestwick Chemical Screen, however, the combination of thioridazine hydrochloride and temozolomide was unable to sensitise GBM cells in a series of dose response experiments. Thioridazine hydrochloride has now been shown to sensitise GBM cells to temozolomide both *in vitro* and *in vivo* through inhibition of autophagy. This results in the accumulation of autophagosomes and eventually cell death (Johannessen et al., 2018). This publication, although strengthening the findings from the initial Prestwick Chemical Screen, highlights the difficulties in the reproducibility associated with screening such small drug volumes. Due to this subsequent publication it would be interesting to revisit the compounds initially identified and retest them in combination with temozolomide in a different format.

Both pyrvinium pamoate and d-penicillamine were identified as initial positive hits from the Spectrum Collection. Pyrvinium pamoate has anti-oncogenic properties through its ability to inhibit wingless (Wnt) signalling (Venerando et al., 2013) and it is able to reduce proliferation of both prostate and breast cancer cells *in vitro* (Jones et al., 2009, Xu et al., 2016). Wnt signalling is thought to increase chemo-resistance possibly through maintaining GSC populations but also by its indirect effect on MGMT, which may possibly explain any sensitisation effects initially seen (Suwala et al., 2018, Wickström et al., 2015). However, as the results were unable to be repeated, it is unknown if pyrvinium pamoate can sensitise GBM cells to temozolomide.

Penicillamine is known to have anti-angiogenic properties due to its ability to chelate copper, which is a required factor for angiogenesis, and the use of penicillamine as a cancer therapeutic has been investigated for a long time. In 1990, penicillamine was used to deplete cells of copper in glioblastoma rat xenografts. This depletion caused both a reduction in angiogenesis and a significant

reduction in tumour growth and size (Brem et al., 1990a, Brem et al., 1990b). Penicillamine was used in a phase II trial in combination with radiotherapy in patients with glioblastoma multiforme. Although the drug was well tolerated by the patients, there was no improvement in overall survival. Unfeasibly, it was suggested that penicillamine may be more beneficial before the onset of GBM occurs as the successful animal models were treated with penicillamine before the tumour cells were implanted (Brem et al., 2005). There are no trials that have investigated the use of penicillamine in combination with temozolomide, however, when penicillamine is prescribed, patients are warned not to take temozolomide due to the increased risk of haematological and renal toxicity (Prescribers' Digital Reference, 2018).

However, further validation of these compounds showed that both were unable to sensitise GBM cells to temozolomide in a dose-response. The initial sensitisation could potentially have been caused by activity of degradation products due to the age of the drugs in the screening library, however, the lack of sensitisation may simply have just been false positive hits generated. However, there was some difficulty during this screen as the positive control of O-6-benzylguanine in combination with temozolomide was not always able to generate significant cell death detectable by the assay. This may have been due to static charges preventing the drugs reaching the media/cells, causing the drugs to not be delivered by the Labcyte Echo 500 to the desired concentration. In an attempt to control for this possibility, plates were gently tapped after drugs were added before being centrifuged to bring all liquid into the well bottom. Additionally, drugs stocks were vortex thoroughly before being used and the dispensing report of the Labcyte Echo 500 was checked after every drug screen. Unfortunately, all of the above solutions were unable to rectify the issues of the positive control failing. This could have led to the false positive results, as the robustness and reproducibility of the assay was lost.

Chapter 7 – Conclusions

In the UK, brain cancer kills around 5,000 people every year, reducing life expectancy by 20 years (Burnet et al., 2005), and in 2014, brain cancer was classified as a cancer of unmet need by Cancer Research UK. This is because on average 50% of all patients diagnosed with cancer will achieve at least a 10 year survival, however, for patients with brain cancer, 10 year survival is only achieved by 13.5% (CancerResearchUK, 2011a, CancerResearchUK, 2011b). GBM, the most common high-grade glioma, accounts for around half of all primary adult brain tumours (Adamson et al., 2009, Kleihues et al., 2000).

Currently, the most aggressive treatment for GBM is de-bulking surgery followed by radiotherapy combined with both concomitant and adjuvant temozolomide (Stupp et al., 2009). Between 2007 and 2011, almost 11,000 people were diagnosed with GBM in England, with a median survival of just over 6 months and a 5 year survival of only 3.4% (Brodbelt et al., 2015). GBM tumours readily become resistant to temozolomide treatment and almost 90% of patients with recurrent GBM have tumours that have a complete lack of response to a second cycle of temozolomide (Oliva et al., 2010). The constantly mutating and evolving tumour genome results in massive intratumoural heterogeneity and consequently treatment failure and disease recurrence (Qazi et al., 2017). As such, GMB is currently an incurable disease.

Previous studies from several groups have aimed to develop treatments for GBM patients that augment the potency/cytotoxicity of temozolomide within cancer cells. MGMT is a DNA repair enzyme that is able to directly repair the toxic lesions caused by temozolomide, as such, the activity of MGMT was targeted by the use of a specific inhibitor called O-6-benzylguanine, which was tested in clinical trials. As MGMT is a suicide enzyme, once it has accepted a methyl group from DNA to repair the alkylation damage caused by temozolomide or accepted a benzyl group from O-6-benzylguanine, it will then be targeted for degradation. This means that DNA damage induced by temozolomide can accumulate if the levels of damage exceed the cellular levels of MGMT, which can be artificially reduced by O-6-benzylguanine. Unfortunately, there was no improvement in overall survival when patients received both O-6-benzylguanine and temozolomide, and haematological toxicity was a common side effect (Quinn et al., 2009), leading to the cessation of O-6-benzylguanine trials.

APNG, a BER protein, has also been investigated in relation to resistance to temozolomide in GBM; however, high expression has been shown to be both beneficial and detrimental to overall survival in patients (Agnihotri et al., 2012, Fosmark et al., 2017). Inhibition of the BER pathway has been targeted in order to

attempt to sensitise temozolomide resistant ovarian and CRC tumour cells to temozolomide. Methoxyamine, which binds to the abasic site inhibiting BER, did sensitise tumours cells to temozolomide alkylation damage (Fishel et al., 2007, Taverna et al., 2001). There is currently a phase II clinical trial investigating the use of methoxyamine in combination with temozolomide in patients with recurrent GBM, however, the trial is still active and the results are yet to be published (ClinicalTrials.gov, 2018). Inhibitors of PARP, a family of proteins also involved the BER pathway, are being investigated in clinical trials for patients with both recurrent (olaparib) and newly diagnosed GBM (veliparib), however, results have not yet been published as the recurrent GBM trial was only completed in July 2017 and the trial in newly diagnosed GBM patients is still actively recruiting (ClinicalTrials.gov, 2018, Morales et al., 2014). There are also various other targets which are currently in trials for patients with GBM. These include histone deacetylases, JAK1/2, PDGFR as well as pathways targeting survival, apoptosis and migration of tumour cells as well as improving the patient's immune response to specifically target tumour cells (ClinicalTrials.gov, 2018).

Nevertheless, there is still a desperate need to improve treatment and subsequently survival for GBM patients. The 'druggabiliy' of kinases combined with the possibility of targeting master regulator unlocks the potential to target subsequent downstream signalling pathways and networks which may be fundamental to the development and progression of cancer (Manning, 2009). Given previous success, as seen with imatinib in CML, and the potential to target complex signalling networks combined with the fact GBM patient survival has remained unchanged for decades (Manning, 2009, Stupp et al., 2005), it was hypothesised that yet to be identified targets and/or pathways within the kinome could sensitise GBM cells to standard of care temozolomide treatment and that inhibitors of these novel targets could be developed into future adjuvant therapies.

To investigate this hypothesis there were 5 aims, the first being carrying out an siRNA screen across the human kinome and completing two re-purposing small molecule drug screens in temozolomide resistant GBM cells. The experimental steps taken to achieve the aims of the project are shown for both the siRNA and small molecule re-purposing screens in figure 7.1. Both siRNA screens and re-purposing screens are well validated and established approaches to identify novel targets. Both screens had robust positive controls established which were known sensitisers of temozolomide: MGMT siRNA and O-6-benzylguanine (Agarwala and Kirkwood, 2000, Quinn et al., 2005). After optimisation, Z-prime values of >0.5 were established using these positive controls in both assays and the screens were carried out. There were no issues carrying out the siRNA kinome screen, with the positive control siRNA working well across all experimental repeats, resulting in a z-prime of >0.5 on each 384 well plate screened. However, the small molecule drug

screen positive control was not as successful and the assay robustness was lost. Attempts were made to rectify this loss including gently tapping plates to break any static charges, drugs stocks were vortex thoroughly before being used and the dispensing report of the Labcyte Echo 500 was checked after every drug screen. Unfortunately, all of the above solutions were unable to rectify the issues of the positive control failing.

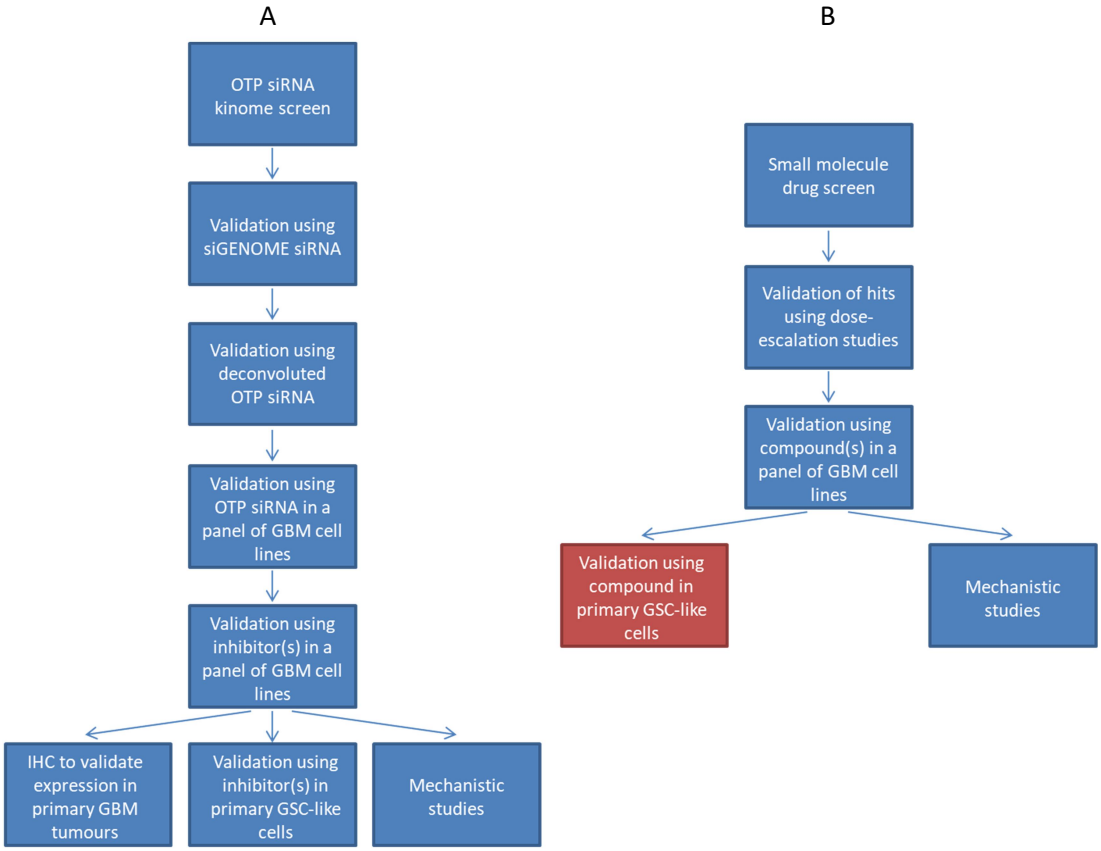

Figure 7.1: Flowchart Summary of Studies

The studies shown in blue were all completed in order to investigate the hypothesis 'inhibition of yet to be identified targets or pathways will enhance the cytotoxic effect of temozolomide in GBM'. Those in red were unfortunately not completed within the timeframe. Flowchart A shows the steps taken for the siRNA kinome screen as well as the subsequent validation and mechanistic steps. Flowchart B shows the steps taken for the small-molecule drug screens as well as the validation and mechanistic steps.

The second aim was to validate the results from the siRNA kinome screen. None of the hits from the initial kinome screen selected for validation using siGENOME siRNA were able to significantly sensitise GBM cells to temozolomide. However, even siGENOME siRNA targeting the well-established temozolomide sensitiser, MGMT, was unable to generate a significant increase in temozolomide sensitivity. ON-TARGETplus siRNA targeting MGMT was therefore used as a positive control to ensure the assay was working. This was less than ideal and consequently hits which

reduced survival to less than 90% when both siRNA and temozolomide were combined were selected for further validation. Validation using deconvoluted siRNA also resulted in some difficulties, with re-pooled siRNA in ineffectively depleting 4 out of 6 hits taken forward.

Of the two hits that were successfully depleted by siRNA, only one (MAP3K3) was able to sensitise GBM cells to temozolomide. MAP3K3 is over-expressed in almost two thirds of ovarian carcinomas (where expression is correlated with both grade and response to chemotherapy), and has also been shown to be amplified in up to 20% of breast cancers, with shRNA depletion increasing sensitivity to both doxorubicin and 5-FU (Fan et al., 2014, Jia et al., 2016). Although the inhibition of MAP3K3 would subsequently inhibit a whole pathway of downstream targets and signalling pathways, there are currently no specific MAP3K3 inhibitors reported. Therefore, downstream targets with inhibitors (MEK5/ERK5) were investigated further. ERK5 depletion using siRNA or small molecule inhibition sensitised a panel of MGMT positive and MGMT negative GBM cell to temozolomide, particularly evident by data shown from the clonogenic survival assays. Here, the LD_{10} for temozolomide alone was approximately 60μM in LN-18 cells; however, when combined with ERK5i, the LD_{10} was decreased to approximately 10μM, a 6 fold change temozolomide sensitivity. This is comparable to the data from clonogenic survival assays originally published in 1996, which showed fold changes for temozolomide sensitivity in GBM cells, ranging from 2.1 in T98G cells up to 19.5 in SF767 cells following the inhibition of MGMT activity using O-6-benzylguanine (Bobola et al., 1996), the target which was used as the positive control for both the siRNA and small molecule drug screen.

FGFR4 was the second hit which was selected following siGENOME validation as commercially inhibitors were available. FGFR4 was therefore validated using an alternative siRNA pool and an inhibitor, both showing an increase in temozolomide sensitivity in MGMT positive and MGMT negative GBM cell lines. However, it would be prudent to investigate FGFR4 protein levels in GBM tumour samples compared to normal brain tissue in order to establish whether a therapeutic window to specifically target the tumour cells is present. Pan-FGF inhibitors are currently undergoing clinical trials for HCC, however, pan-tyrosine kinase inhibitors, such as those used when treating CML, can have deleterious side effects such as anaemia, nausea, leukopenia and therefore may not be well tolerated by all patients (Tsai et al., 2018). However, if selective FGFR4 inhibitors are successfully approved for treating HCC it would speed up entry in to a GBM clinical trial, but there are currently very few reports investigating the dysregulation of FGFR4 signalling in GBM. As FGFR4 expression has been shown to correlate with erlotinib resistance in GBM cell lines it could indicate a substitute role for FGFR4 in oncogenic EGFR signalling pathways which are dysregulated in a high proportion of GBM patients

(Halatsch et al., 2009). Therefore, investigation into crosstalk between these pathways could identify novel therapeutic targets which could improve patient survival.

The third aim was to validate targets by investigating the mRNA and protein expression in brain tumours compared to healthy brain. Due to time constraints, the investigation into FGFR4 was minimal and mRNA expression was simply investigated using an online dataset. However, as FGFR family members are being investigated as potential therapeutic targets for a subset of GBM patients with activating fusion mutations and FGFR4 kinase activating mutations have also been identified in a subset of GBM patients, this increases the chances of a clinical trial, particularly if FGFR4 inhibitors become NICE approved for HCC (ClinicalTrials.gov, 2018, Masica and Karchin, 2011). However, GBM is very heterogeneous, both between patients and within tumours, it may have been unrealistically optimistic to hope to identify a therapeutic target which would sensitise all GBM patients across 4 subgroups to temozolomide treatment (Qazi et al., 2017, Verhaak et al., 2010).

The same dataset used to investigate FGFR4 mRNA expression in GBM was also used to investigate ERK5 mRNA expression, however, this which showed a significant increase in GBM tumours compared to normal brain. ERK5 protein expression was next investigated using IHC and TMAs. There was, again, a significant increase in ERK5 protein expression in GBM tumours compared to normal brain, with over-expression correlating with tumour grade, highlighting a potentially exploitable therapeutic window. However, although TMAs offer a large sample number which can all be processed identically, they only contain such small section of a tumour meaning intratumoural heterogeneity is readily lost which should be kept in mind when analysing results. One possible solution to this problem would be to take small sections from several locations within the tumour; however, this may not be feasible as it depends entirely on the resected tumour received for the initial TMA processing.

The fourth aim was to validate any hits identified in the small molecule drug screens. There was a high dropout rate for the initially identified compounds, with only 1 compound out of 9 (11%) sensitising GBM cells to temozolomide in dose-escalation studies. This may have been due to the loss of assay robustness highlighted by the failure of the positive control. The identified compound butamben was able to sensitise a panel of GBM and non-GBM cells to temozolomide but due to time constrains there was little mechanistic investigation carried out. However, as butamben is t-type calcium channel inhibitor, it was speculated that it may be acting in an identical manner to another t-type calcium channel inhibitor, mibefradil, which is a known sensitiser of GBM cells to temozolomide (Beekwilder et al., 2006, Zhang et al., 2017). A major issue

associated with the use of butamben is the anaesthetic property of the drug. This unfeasibility makes it difficult to see how such a drug would have been included in a small molecule library where compounds have been selected for repurposing. If the target which enables butamben to sensitise GBM cells to temozolomide could be identified, inhibition with an alternative small molecule compound which does not have anaesthetic properties may have the potential for success in clinical trials. In order to improve the outcomes of small molecule screening, compound library maintenance, particularly long term storage of plates, must be improved. This is highlighted by large changes in toxicity following the purchase of new compounds and subsequent irreproducibility of sensitisation, possibly due to the presence of degradation of compounds within the library.

The final aim was to investigate the mechanisms by which GBM cells are sensitised to temozolomide. Here the role of ERK5 inhibition and temozolomide sensitivity was mainly investigated, showing an increase in 53BP1 foci and DNA-PK phosphorylation suggesting that combination treatment causes an increase in NHEJ (and a reduction in HR), which is activated as a result of an increase in DSBs. Potential hypotheses could be 'ERK5 inhibition causes dysregulation of the DNA damage response pathways in GBM cells, sensitising them to temozolomide' or 'ERK5 inhibition sensitises GBM cells to temozolomide in a mitosis dependent manner, enhancing DNA damage and dysregulating the DNA damage response pathways'. However, ERK5-in-1 is now known to have off-target effects on BRD4, a protein which has been shown to decrease proliferation of GBM cells, dysregulate NHEJ and also increase sensitivity to temozolomide in GBM cells following inhibition, potentially contributing to the phenotype seen as a result of ERK5-in-1 inhibition and temozolomide treatment (Lam et al., 2018, Pastori et al., 2014, Wang et al., 2018a).

The sensitisation seen when combination treatment is used could also be TP53 dependent as ERK5 is known to down-regulate TP53 expression and a study investigating 5-FU chemo-sensitivity in HCT116 colon cancer cells showed TP53 null mutants were not sensitised following ERK5 inhibition, unlike their wild type counterpart (Lim and Woo, 2011, Pereira et al., 2016, Yang et al., 2013b). In these studies both wild-type and mutant TP53 GBM cell lines were used: LN-18 has both mutant and wild-type TP53, T98G and U-251 cells have TP53 mutations and U-87 cells are homozygous for TP53 which may suggest that the sensitisation seen is not TP53 dependent (Van Meir et al., 1994). U-138 cells which did not respond to combination treatment are TP53 wild-type (Van Meir et al., 1994). TP53 dependent ERK5 inhibition has also been shown to sensitise triple-negative breast cancer cells to the DNA cross-linking agent cisplatin (Ortiz-Ruiz et al., 2014). However, data investigating 5-FU sensitisation in CRC saw ERK5 inhibition resulted in minimal change to TP53 protein levels. Instead, an increase in p21, a CDK inhibitor and

negative regulator of cell cycle progression, and an increase in PUMA, a pro-apoptotic protein, both which are dependent on TP53 activity were identified as potential players in the increase in apoptosis and reduction in xenograft tumour size following ERK5 inhibition and 5-FU treatment (Pereira et al., 2016). Furthermore, a lack of cell cycle checkpoint regulation and dysregulated cell cycle progression through the G1 and G2 checkpoints could also be involved in chemotherapeutic sensitisation of cancer cells following ERK5 inhibition, potentially via NF-κB signalling (Cude et al., 2007, Pereira et al., 2016, Perez-Madrigal et al., 2012).

A potential mechanism may have been highlighted when the addition of nocodazole, which arrests cells in metaphase of mitosis, reduced the amount of DNA damage in combination treatment (Zieve et al., 1980). This suggests that the damage is mainly derived during mitotic progression, which is also consistent with the dramatic increase in MNi observed in cells treated with ERK5i and temozolomide. The damage generated also seems to primarily activate the NHEJ pathway, which is particularly active in the G1 phase of the cell cycle. However, it has also been reported by several groups that deleterious activity of the NHEJ pathway outside of G1 can lead to DNA damage and chromosomal aberrations (Adamo et al., 2010, Pace et al., 2010). This was coupled with a reduction in HR pathway activity, which is known to confer resistance to temozolomide when over-activated, and could therefore be further potentiating the sensitisation induced by the combination treatment (del Alcazar et al., 2016).

Further work to unravel the precise mechanism by which the increase in temozolomide sensitivity following ERK5 inhibition/depletion needs to be completed, potentially focusing on the increased DNA damage and the resulting cell death as a consequence of mitotic progression and the dysregulated DNA damage response, as well as further validation in patient derived primary cells, 3D culture and orthotopic animal studies. However, as adult mice with an inducible ERK5 knock out died 2-4 weeks after ERK5 depletion due to increased endothelial cell death which caused their vasculature to become 'leaky' resulting in massive haemorrhage (Hayashi et al., 2004), problems associated with vasculature may be an issue with ERK5 inhibitors in clinical trials. Although in GBM cells, ERK5 inhibition did not cause significantly more DNA damage or cell death when used as an individual agent, which if combined with temozolomide targeted directly to the tumour cells using nanoparticles, combining the treatments may be well tolerated by patients, with little normal tissue toxicity (Fang et al., 2015). However, off-target effect of BRD4 inhibition must be investigated further as new generation ERK5 specific inhibitors, such as AX 15836, have shown a dramatically reduce anti-inflammatory and anti-proliferative actions in cancer cells suggesting BRD4 or ERK5

kinase independent mechanisms are responsible for these phenotypes (Lin et al., 2016, Wang et al., 2018a).

If ERK5 inhibition is shown to increase temozolomide sensitivity in GBM cells following research using new generation ERK5 inhibitors, such inhibitors would need to undergo investigation in clinical trials before being approved for treating patients. As ERK5 was over-expressed in more than 93% of GBM patient cores and expression was significantly higher than normal brain tissue, it would most likely be a suitable drug target for all GBM patients. ERK5 inhibitors could therefore be used alongside radiotherapy and temozolomide which are given post-surgery, but also in combination with subsequent cycles of temozolomide. ERK5 inhibitors were able to sensitise both temozolomide resistant and non-resistant cell lines so by combining the treatments, the standard dose of temozolomide would be potentiated. Furthermore, as the combination of ERK5 inhibition and temozolomide induced more DNA damage in GBM cells, the effects of radiotherapy may also be enhanced, killing more tumour cells and improving the prospect of patient survival. However, even if the potentiation of temozolomide is shown to be purely due to BRD4 inhibition, ERK5 is still dysregulated in a vast array of cancers once clinical trial testing begins and both a safe and efficacious ERK5 inhibitor is identified, cancer treatment and survival could be improved for a huge number of patients.

Chapter 8 – References

ABRAHAM, B. K., FRITZ, P., MCCLELLAN, M., HAUPTVOGEL, P., ATHELOGOU, M. & BRAUCH, H. 2005. Prevalence of CD44+/CD24−/low cells in breast cancer may not be associated with clinical outcome but may favor distant metastasis. *Clinical cancer research,* 11**,** 1154-1159.

ADAMO, A., COLLIS, S. J., ADELMAN, C. A., SILVA, N., HOREJSI, Z., WARD, J. D., MARTINEZ-PEREZ, E., BOULTON, S. J. & LA VOLPE, A. 2010. Preventing nonhomologous end joining suppresses DNA repair defects of Fanconi anemia. *Molecular cell,* 39**,** 25-35.

ADAMSON, C., KANU, O. O., MEHTA, A. I., DI, C., LIN, N., MATTOX, A. K. & BIGNER, D. D. 2009. Glioblastoma multiforme: a review of where we have been and where we are going. *Expert Opin Investig Drugs***,** 1061-1083.

ADCREVIEW. *DEPATUXIZUMAB MAFODOTIN (ABT-414) DRUG DESCRIPTION* [Online]. Available: https://adcreview.com/abt-414-drug-description/ [Accessed 14/11/2018].

AGARWALA, S. S. & KIRKWOOD, J. M. 2000. Temozolomide, a novel alkylating agent with activity in the central nervous system, may improve the treatment of advanced metastatic melanoma. *The oncologist,* 5**,** 144-151.

AGNIHOTRI, S., GAJADHAR, A. S., TERNAMIAN, C., GORLIA, T., DIEFES, K. L., MISCHEL, P. S., KELLY, J., MCGOWN, G., THORNCROFT, M. & CARLSON, B. L. 2012. Alkylpurine–DNA–N-glycosylase confers resistance to temozolomide in xenograft models of glioblastoma multiforme and is associated with poor survival in patients. *The Journal of clinical investigation,* 122**,** 253-266.

AHMED, A. U., AUFFINGER, B. & LESNIAK, M. S. 2013. Understanding glioma stem cells: rationale, clinical relevance and therapeutic strategies. *Expert review of neurotherapeutics,* 13**,** 545-555.

AHMED, S. U., CARRUTHERS, R., GILMOUR, L., YILDIRIM, S., WATTS, C. & CHALMERS, A. J. 2015. Selective inhibition of parallel DNA damage response pathways optimizes radiosensitization of glioblastoma stem-like cells. *Cancer research,* 75**,** 4416-4428.

AKAO, Y., NAKAGAWA, Y. & NAOE, T. 2006. MicroRNAs 143 and 145 are possible common onco-microRNAs in human cancers. *Oncology reports,* 16**,** 845-850.

AL-EJEH, F., MIRANDA, M., SHI, W., SIMPSON, P. T., SONG, S., VARGAS, A. C., SAUNUS, J. M., SMART, C. E., MARIASEGARAM, M. & WIEGMANS, A. P. 2014. Kinome profiling reveals breast cancer heterogeneity and identifies targeted therapeutic opportunities for triple negative breast cancer. *Oncotarget,* 5**,** 3145.

AL-HAJJ, M., WICHA, M. S., BENITO-HERNANDEZ, A., MORRISON, S. J. & CLARKE, M. F. 2003. Prospective identification of tumorigenic breast cancer cells. *Proceedings of the National Academy of Sciences,* 100**,** 3983-3988.

ALAGOZ, M., WELLS, O. S. & EL-KHAMISY, S. F. 2013. TDP1 deficiency sensitizes human cells to base damage via distinct topoisomerase I and PARP mechanisms with potential applications for cancer therapy. *Nucleic acids research,* 42**,** 3089-3103.

ALDAPE, K., ZADEH, G., MANSOURI, S., REIFENBERGER, G. & VON DEIMLING, A. 2015. Glioblastoma: pathology, molecular mechanisms and markers. *Acta neuropathologica,* 129**,** 829-848.

ALMEIDA, K. H. & SOBOL, R. W. 2007. A unified view of base excision repair: lesion-dependent protein complexes regulated by post-translational modification. *DNA repair,* 6**,** 695-711.

ALVINO, E., PASSARELLI, F., CANNAVÒ, E., FORTES, C., MASTROENI, S., CAPORALI, S., JIRICNY, J., CAPPELLINI, G. C. A., SCOPPOLA, A. & MARCHETTI, P. 2014. High expression of the mismatch repair protein MSH6 is associated with poor patient survival in melanoma. *American journal of clinical pathology,* 142**,** 121-132.

AMSBIOTECHNOLOGY 2010. DNA Damage, PARP, and the Comet Assay.
ARMSTRONG, G. T., STOVALL, M. & ROBISON, L. L. 2010. Long-term effects of radiation exposure among adult survivors of childhood cancer: results from the childhood cancer survivor study. *Radiation research,* 174**,** 840-850.
ARNEY, K. 2013. *The Story of Temozolomide* [Online]. Available: https://scienceblog.cancerresearchuk.org/2013/07/18/the-story-of-temozolomide/ [Accessed 09/11/2018].
BABINA, I. S. & TURNER, N. C. 2017. Advances and challenges in targeting FGFR signalling in cancer. *Nature Reviews Cancer,* 17**,** 318.
BALLABH, P., BRAUN, A. & NEDERGAARD, M. 2004. The blood–brain barrier: an overview: structure, regulation, and clinical implications. *Neurobiology of disease,* 16**,** 1-13.
BAO, S., WU, Q., MCLENDON, R. E., HAO, Y., SHI, Q., HJELMELAND, A. B., DEWHIRST, M. W., BIGNER, D. D. & RICH, J. N. 2006. Glioma stem cells promote radioresistance by preferential activation of the DNA damage response. *nature,* 444**,** 756-760.
BARANI, I. J. & LARSON, D. A. 2015. Radiation therapy of glioblastoma. *Current Understanding and Treatment of Gliomas.* Springer.
BARRY, S. P., TOWNSEND, P. A., KNIGHT, R. A., SCARABELLI, T. M., LATCHMAN, D. S. & STEPHANOU, A. 2010. STAT3 modulates the DNA damage response pathway. *International journal of experimental pathology,* 91**,** 506-514.
BARTKOVA, J., HOŘEJŠÍ, Z., KOED, K., KRÄMER, A., TORT, F., ZIEGER, K., GULDBERG, P., SEHESTED, M., NESLAND, J. M. & LUKAS, C. 2005. DNA damage response as a candidate anti-cancer barrier in early human tumorigenesis. *Nature,* 434**,** 864.
BATCHELOR, T. T., GERSTNER, E. R., YE, X., DESIDERI, S., DUDA, D. G., PEEREBOOM, D., LESSER, G. J., CHOWDHARY, S., WEN, P. Y. & GROSSMAN, S. 2017. Feasibility, phase I, and phase II studies of tandutinib, an oral platelet-derived growth factor receptor-β tyrosine kinase inhibitor, in patients with recurrent glioblastoma. *Neuro-oncology,* 19**,** 567-575.
BAUMANN, F., BJELJAC, M., KOLLIAS, S. S., BAUMERT, B. G., BRANDNER, S., ROUSSON, V., YONEKAWA, Y. & BERNAYS, R. L. 2004. Combined thalidomide and temozolomide treatment in patients with glioblastoma multiforme. *Journal of neuro-oncology,* 67**,** 191-200.
BECKMAN, G., BECKMAN, L., PONTEN, J. & WESTERMARK, B. 1971. G-6-PD and PGM phenotypes of 16 continuous human tumor cell lines. *Human heredity,* 21**,** 238-241.
BEEKWILDER, J. P., VAN KEMPEN, G. T. H., VAN DEN BERG, R. J. & YPEY, D. L. 2006. The local anesthetic butamben inhibits and accelerates low-voltage activated T-type currents in small sensory neurons. *Anesthesia & Analgesia,* 102**,** 141-145.
BEIER, D., HAU, P., PROESCHOLDT, M., LOHMEIER, A., WISCHHUSEN, J., OEFNER, P. J., AIGNER, L., BRAWANSKI, A., BOGDAHN, U. & BEIER, C. P. 2007. CD133+ and CD133− glioblastoma-derived cancer stem cells show differential growth characteristics and molecular profiles. *Cancer research,* 67**,** 4010-4015.
BELKAHLA, S., KHAN, A. U. H., GITENAY, D., ALEXIA, C., GONDEAU, C., VO, D.-N., ORECCHIONI, S., TALARICO, G., BERTOLINI, F. & CARTRON, G. 2018. Changes in metabolism affect expression of ABC transporters through ERK5 and depending on p53 status. *Oncotarget,* 9**,** 1114.
BELLO, L., FRANCOLINI, M., MARTHYN, P., ZHANG, J., CARROLL, R. S., NIKAS, D. C., STRASSER, J. F., VILLANI, R., CHERESH, D. A. & BLACK, P. M. 2001. αvβ3 and αvβ5 integrin expression in glioma periphery. *Neurosurgery,* 49**,** 380-390.
BETASTASIS 2018. REpository for Molecular BRAin Neoplasia DaTa. *In:* BETASTASIS (ed.).
BHULLAR, K. S., LAGARÓN, N. O., MCGOWAN, E. M., PARMAR, I., JHA, A., HUBBARD, B. P. & RUPASINGHE, H. V. 2018. Kinase-targeted cancer therapies: progress, challenges and future directions. *Molecular cancer,* 17**,** 48.

BOBOLA, M. S., TSENG, S. H., BLANK, A., BERGER, M. S. & SILBER, J. R. 1996. Role of O6-methylguanine-DNA methyltransferase in resistance of human brain tumor cell lines to the clinically relevant methylating agents temozolomide and streptozotocin. *Clinical cancer research,* 2**,** 735-741.

BONDY, M. L., SCHEURER, M. E., MALMER, B., BARNHOLTZ-SLOAN, J. S., DAVIS, F. G., IL'YASOVA, D., KRUCHKO, C., MCCARTHY, B. J., RAJARAMAN, P., SCHWARTZBAUM, J. A., SADETZKI, S., SCHLEHOFER, B., TIHAN, T., WIEMELS, J. L., WRENSCH, M. & BUFFLER, P. A. 2008. Brain tumor epidemiology: consensus from the Brain Tumor Epidemiology Consortium. *Cancer,* 113**,** 1953-68.

BRADFORD, P. T., GOLDSTEIN, A. M., TAMURA, D., KHAN, S. G., UEDA, T., BOYLE, J., OH, K.-S., IMOTO, K., INUI, H. & MORIWAKI, S.-I. 2011. Cancer and neurologic degeneration in xeroderma pigmentosum: long term follow-up characterises the role of DNA repair. *Journal of medical genetics,* 48**,** 168-176.

BRANZEI, D. & FOIANI, M. 2008. Regulation of DNA repair throughout the cell cycle. *Nature reviews Molecular cell biology,* 9**,** 297.

BRAY, M.-A. & CARPENTER, A. 2017. Advanced assay development guidelines for image-based high content screening and analysis.

BREGY, A., SHAH, A. H., DIAZ, M. V., PIERCE, H. E., AMES, P. L., DIAZ, D. & KOMOTAR, R. J. 2013. The role of Gliadel wafers in the treatment of high-grade gliomas. *Expert review of anticancer therapy,* 13**,** 1453-1461.

BREM, S., GROSSMAN, S. A., CARSON, K. A., NEW, P., PHUPHANICH, S., ALAVI, J. B., MIKKELSEN, T. & FISHER, J. D. 2005. Phase 2 trial of copper depletion and penicillamine as antiangiogenesis therapy of glioblastoma. *Neuro-oncology,* 7**,** 246-253.

BREM, S., TSANACLIS, A. M. C. & ZAGZAG, D. 1990a. Anticopper treatment inhibits pseudopodial protrusion and the invasive spread of 9L gliosarcoma cells in the rat brain. *Neurosurgery,* 26**,** 391-396.

BREM, S. S., ZAGZAG, D., TSANACLIS, A., GATELY, S., ELKOUBY, M. & BRIEN, S. 1990b. Inhibition of angiogenesis and tumor growth in the brain. Suppression of endothelial cell turnover by penicillamine and the depletion of copper, an angiogenic cofactor. *The American journal of pathology,* 137**,** 1121.

BRENNAN, C. W., VERHAAK, R. G., MCKENNA, A., CAMPOS, B., NOUSHMEHR, H., SALAMA, S. R., ZHENG, S., CHAKRAVARTY, D., SANBORN, J. Z. & BERMAN, S. H. 2013. The somatic genomic landscape of glioblastoma. *Cell,* 155**,** 462-477.

BROCHIER, C. & LANGLEY, B. 2013. Chromatin modifications associated with DNA double-strand breaks repair as potential targets for neurological diseases. *Neurotherapeutics,* 10**,** 817-830.

BRODBELT, A., GREENBERG, D., WINTERS, T., WILLIAMS, M., VERNON, S. & COLLINS, V. P. 2015. Glioblastoma in England: 2007–2011. *European Journal of Cancer,* 51**,** 533-542.

BURNET, N., JEFFERIES, S., BENSON, R., HUNT, D. & TREASURE, F. 2005. Years of life lost (YLL) from cancer is an important measure of population burden—and should be considered when allocating research funds. *British journal of cancer,* 92**,** 241.

CAHILL, D. P., LEVINE, K. K., BETENSKY, R. A., CODD, P. J., ROMANY, C. A., REAVIE, L. B., BATCHELOR, T. T., FUTREAL, P. A., STRATTON, M. R. & CURRY, W. T. 2007. Loss of the mismatch repair protein MSH6 in human glioblastomas is associated with tumor progression during temozolomide treatment. *Clinical cancer research,* 13**,** 2038-2045.

CAMGOZ, A., PASZKOWSKI-ROGACZ, M., SATPATHY, S., WERMKE, M., HAMANN, M. V., VON BONIN, M., CHOUDHARY, C., KNAPP, S. & BUCHHOLZ, F. 2018. STK3 is a therapeutic target for a subset of acute myeloid leukemias. *Oncotarget,* 9**,** 25458.

CANCERGENOMEATLASRESEARCHNETWORK 2008. Comprehensive genomic characterization defines human glioblastoma genes and core pathways. *Nature,* 455**,** 1061.

CANCERRESEARCHUK. 2011a. *Brain, other CNS and intracranial tumours survival statistics* [Online]. Available: http://www.cancerresearchuk.org/health-professional/cancer-statistics/statistics-by-cancer-type/brain-other-cns-and-intracranial-tumours/survival#heading-Zero [Accessed 17 1 18 2018].

CANCERRESEARCHUK. 2011b. *Cancer Statistics for the UK* [Online]. Available: http://www.cancerresearchuk.org/health-professional/cancer-statistics [Accessed 18/04/2016 2016].

CANCERRESEARCHUK. 2015. *Cancer Statistics for the UK* [Online]. Available: https://www.cancerresearchuk.org/health-professional/cancer-statistics-for-the-uk#heading-Zero [Accessed 12/11/2018].

CARGNELLO, M. & ROUX, P. P. 2011. Activation and function of the MAPKs and their substrates, the MAPK-activated protein kinases. *Microbiology and molecular biology reviews,* 75**,** 50-83.

CARNEIRO, B. A., ELVIN, J. A., KAMATH, S. D., ALI, S. M., PAINTAL, A. S., RESTREPO, A., BERRY, E., GILES, F. J. & JOHNSON, M. L. 2015. FGFR3–TACC3: a novel gene fusion in cervical cancer. *Gynecologic oncology reports,* 13**,** 53-56.

CARVAJAL-VERGARA, X., TABERA, S., MONTERO, J. C., ESPARÍS-OGANDO, A., LÓPEZ-PÉREZ, R., MATEO, G., GUTIÉRREZ, N., PARMO-CABAÑAS, M., TEIXIDÓ, J. & SAN MIGUEL, J. F. 2005. Multifunctional role of Erk5 in multiple myeloma. *Blood,* 105**,** 4492-4499.

CASSIDY, J., BISSETT, D., SPENCE, R. A. J., PAYNE, M. & MORRIS-STIFF, G. 2015. *Oxford Handbook of Oncology,* New York, USA, Oxford University Press.

CAVANAUGH, J. E., HAM, J., HETMAN, M., POSER, S., YAN, C. & XIA, Z. 2001. Differential regulation of mitogen-activated protein kinases ERK1/2 and ERK5 by neurotrophins, neuronal activity, and cAMP in neurons. *Journal of Neuroscience,* 21**,** 434-443.

CHAO, T.-H., HAYASHI, M., TAPPING, R. I., KATO, Y. & LEE, J.-D. 1999. MEKK3 directly regulates MEK5 activity as part of the big mitogen-activated protein kinase 1 (BMK1) signaling pathway. *Journal of Biological Chemistry,* 274**,** 36035-36038.

CHARNI, S., DE BETTIGNIES, G., RATHORE, M. G., AGUILÓ, J. I., VAN DEN ELSEN, P. J., HAOUZI, D., HIPSKIND, R. A., ENRIQUEZ, J. A., SANCHEZ-BEATO, M. & PARDO, J. 2010. Oxidative phosphorylation induces de novo expression of the MHC class I in tumor cells through the ERK5 pathway. *The Journal of Immunology,* 185**,** 3498-3503.

CHE, X., ZHANG, G., ZHANG, X. & XUE, J. 2018. Overexpression of G Protein-Coupled Receptor Kinase 6 (GRK6) Is Associated with Progression and Poor Prognosis of Papillary Thyroid Carcinoma. *Medical science monitor: international medical journal of experimental and clinical research,* 24**,** 3540.

CHEN, C. C., TANIGUCHI, T. & D'ANDREA, A. 2007. The Fanconi anemia (FA) pathway confers glioma resistance to DNA alkylating agents. *Journal of molecular medicine,* 85**,** 497-509.

CHESI, M., NARDINI, E., BRENTS, L. A., SCHRÖCK, E., RIED, T., KUEHL, W. M. & BERGSAGEL, P. L. 1997. Frequent translocation t (4; 14)(p16. 3; q32. 3) in multiple myeloma is associated with increased expression and activating mutations of fibroblast growth factor receptor 3. *Nature genetics,* 16**,** 260.

CHIKH, A., FERRO, R., ABBOTT, J. J., PIÑEIRO, R., BUUS, R., IEZZI, M., RICCI, F., BERGAMASCHI, D., OSTANO, P. & CHIORINO, G. 2016. Class II phosphoinositide 3-kinase C2β regulates a novel signaling pathway involved in breast cancer progression. *Oncotarget,* 7**,** 18325.

CHIN, D. & MEANS, A. R. 2000. Calmodulin: a prototypical calcium sensor. *Trends in cell biology,* 10**,** 322-328.

CHINOT, O. L., WICK, W., MASON, W., HENRIKSSON, R., SARAN, F., NISHIKAWA, R., CARPENTIER, A. F., HOANG-XUAN, K., KAVAN, P. & CERNEA, D. 2014. Bevacizumab plus radiotherapy–temozolomide for newly diagnosed glioblastoma. *New England Journal of Medicine,* 370**,** 709-722.

CICENAS, J., KALYAN, K., SOROKINAS, A., STANKUNAS, E., LEVY, J., MESKINYTE, I., STANKEVICIUS, V., KAUPINIS, A. & VALIUS, M. 2015. Roscovitine in cancer and other diseases. *Annals of translational medicine,* 3.

CLINICALTRIALS.GOV. 2018. *Clinical Trials.gov Database* [Online]. Available: https://clinicaltrials.gov/ [Accessed 24/09/2018 2018].

COHEN, A. L., HOLMEN, S. L. & COLMAN, H. 2013. IDH1 and IDH2 mutations in gliomas. *Current neurology and neuroscience reports,* 13**,** 1-7.

CUDE, K., WANG, Y., CHOI, H.-J., HSUAN, S.-L., ZHANG, H., WANG, C.-Y. & XIA, Z. 2007. Regulation of the G2–M cell cycle progression by the ERK5–NFκB signaling pathway. *The Journal of cell biology,* 177**,** 253-264.

DAS, A., CHENG, R. R., HILBERT, M. L., DIXON-MOH, Y. N., DECANDIO, M., VANDERGRIFT WILLIAM III, A., BANIK, N. L., LINDHORST, S. M., CACHIA, D. & VARMA, A. K. 2015. Synergistic effects of crizotinib and temozolomide in experimental FIG-ROS1 fusion-positive glioblastoma. *Cancer growth and metastasis,* 8**,** CGM. S32801.

DE BONIS, P., ALBANESE, A., LOFRESE, G., DE WAURE, C., MANGIOLA, A., PETTORINI, B. L., POMPUCCI, A., BALDUCCI, M., FIORENTINO, A., LAURIOLA, L., ANILE, C. & MAIRA, G. 2011. Postoperative infection may influence survival in patients with glioblastoma: simply a myth? *Neurosurgery,* 69**,** 864-8; discussion 868-9.

DE GRASSI, A., SEGALA, C., IANNELLI, F., VOLORIO, S., BERTARIO, L., RADICE, P., BERNARD, L. & CICCARELLI, F. D. 2010. Ultradeep sequencing of a human ultraconserved region reveals somatic and constitutional genomic instability. *PLoS biology,* 8**,** e1000275.

DE KLEIN, A., VAN KESSEL, A. G., GROSVELD, G., BARTRAM, C. R., HAGEMEIJER, A., BOOTSMA, D., SPURR, N. K., HEISTERKAMP, N., GROFFEN, J. & STEPHENSON, J. R. 1982. A cellular oncogene is translocated to the Philadelphia chromosome in chronic myelocytic leukaemia. *Nature,* 300**,** 765.

DEL ALCAZAR, C. R. G., TODOROVA, P. K., HABIB, A. A., MUKHERJEE, B. & BURMA, S. 2016. Augmented HR Repair Mediates Acquired-temozolomide Resistance in Glioblastoma. *Molecular Cancer Research***,** molcanres. 0125.2016.

DENG, N., ZHOU, H., FAN, H. & YUAN, Y. 2017. Single nucleotide polymorphisms and cancer susceptibility. *Oncotarget,* 8**,** 110635-110649.

DENG, X., ELKINS, J. M., ZHANG, J., YANG, Q., ERAZO, T., GOMEZ, N., CHOI, H. G., WANG, J., DZAMKO, N. & LEE, J.-D. 2013. Structural determinants for ERK5 (MAPK7) and leucine rich repeat kinase 2 activities of benzo [e] pyrimido-[5, 4-b] diazepine-6 (11H)-ones. *European journal of medicinal chemistry,* 70**,** 758-767.

DHARMACON™. 2018. *ON-TARGETplus siRNA* [Online]. Available: https://dharmacon.horizondiscovery.com/rnai/sirna/on-targetplus/#all [Accessed 30/10/2018].

DHILLON, A. S., HAGAN, S., RATH, O. & KOLCH, W. 2007. MAP kinase signalling pathways in cancer. *Oncogene,* 26**,** 3279.

DI CARLO, D. T., CAGNAZZO, F., BENEDETTO, N., MORGANTI, R. & PERRINI, P. 2017. Multiple high-grade gliomas: Epidemiology, management, and outcome. A systematic review and meta-analysis. *Neurosurgical review***,** 1-13.

DI STEFANO, A. L., FUCCI, A., FRATTINI, V., LABUSSIERE, M., MOKHTARI, K., ZOPPOLI, P., MARIE, Y., BRUNO, A., BOISSELIER, B. & GIRY, M. 2015. Detection, characterization

and inhibition of FGFR-TACC fusions in IDH wild type glioma. *Clinical Cancer Research*, clincanres. 2199.2014.

DICK, D. 1997. Human acute myeloid leukemia is organized as a hierarchy that originates from a primitive hematopoietic cell. *Nature Med,* 3, 730-737.

DING, N. H., ZHANG, L., XIAO, Z., RONG, Z. X., LI, Z., HE, J., CHEN, L., OU, D. M., LIAO, W. H. & SUN, L. Q. 2018. NEK4 kinase regulates EMT to promote lung cancer metastasis. *Journal of cellular and molecular medicine*.

DISERENS, A., DE TRIBOLET, N., MARTIN-ACHARD, A., GAIDE, A., SCHNEGG, J. & CARREL, S. 1981. Characterization of an established human malignant glioma cell line: LN-18. *Acta neuropathologica,* 53, 21-28.

DOLAN, M. E., MITCHELL, R. B., MUMMERT, C., MOSCHEL, R. C. & PEGG, A. E. 1991. Effect of O6-benzylguanine analogues on sensitivity of human tumor cells to the cytotoxic effects of alkylating agents. *Cancer research,* 51, 3367-3372.

DREW, B. A., BUROW, M. E. & BECKMAN, B. S. 2012. MEK5/ERK5 pathway: the first fifteen years. *Biochimica et Biophysica Acta (BBA)-Reviews on Cancer,* 1825, 37-48.

ENGLISH, J. M., PEARSON, G., BAER, R. & COBB, M. H. 1998. Identification of substrates and regulators of the mitogen-activated protein kinase ERK5 using chimeric protein kinases. *Journal of Biological Chemistry,* 273, 3854-3860.

ERAZO, T., MORENO, A., RUIZ-BABOT, G., RODRÍGUEZ-ASIAIN, A., MORRICE, N. A., ESPADAMALA, J., BAYASCAS, J. R., GÓMEZ, N. & LIZCANO, J. M. 2013. Canonical and kinase activity-independent mechanisms for extracellular signal-regulated kinase 5 (ERK5) nuclear translocation require dissociation of Hsp90 from the ERK5-Cdc37 complex. *Molecular and cellular biology,* 33, 1671-1686.

FAN, Y., GE, N., WANG, X., SUN, W., MAO, R., BU, W., CREIGHTON, C. J., ZHENG, P., VASUDEVAN, S. & AN, L. 2014. Amplification and over-expression of MAP3K3 gene in human breast cancer promotes formation and survival of breast cancer cells. *The Journal of pathology,* 232, 75-86.

FANG, C., WANG, K., STEPHEN, Z. R., MU, Q., KIEVIT, F. M., CHIU, D. T., PRESS, O. W. & ZHANG, M. 2015. Temozolomide nanoparticles for targeted glioblastoma therapy. *ACS applied materials & interfaces,* 7, 6674-6682.

FELSBERG, J., THON, N., EIGENBROD, S., HENTSCHEL, B., SABEL, M. C., WESTPHAL, M., SCHACKERT, G., KRETH, F. W., PIETSCH, T. & LÖFFLER, M. 2011. Promoter methylation and expression of MGMT and the DNA mismatch repair genes MLH1, MSH2, MSH6 and PMS2 in paired primary and recurrent glioblastomas. *International journal of cancer,* 129, 659-670.

FENECH, M. 2000. The in vitro micronucleus technique. *Mutation Research/Fundamental and Molecular Mechanisms of Mutagenesis,* 455, 81-95.

FINEGAN, K. G., WANG, X., LEE, E.-J., ROBINSON, A. C. & TOURNIER, C. 2009. Regulation of neuronal survival by the extracellular signal-regulated protein kinase 5. *Cell death and differentiation,* 16, 674.

FINNEY, L., VOGT, S., FUKAI, T. & GLESNE, D. 2009. Copper and angiogenesis: unravelling a relationship key to cancer progression. *Clinical and Experimental Pharmacology and Physiology,* 36, 88-94.

FISHEL, M. L., HE, Y., SMITH, M. L. & KELLEY, M. R. 2007. Manipulation of base excision repair to sensitize ovarian cancer cells to alkylating agent temozolomide. *Clinical Cancer Research,* 13, 260-267.

FISHER, K. W., DAS, B., KIM, H. S., CLYMER, B. K., GEHRING, D., SMITH, D., COSTANZO-GARVEY, D., FERNANDEZ, M., BRATTAIN, M. G. & KELLY, D. 2015. AMPK promotes aberrant PGC1β expression to support human colon tumor cell survival. *Molecular and cellular biology*, MCB. 00528-15.

FLIPPOT, R., KONE, M., MAGNE, N. & VIGNOT, S. 2015. FGF/FGFR signalling: Implication in oncogenesis and perspectives. *Bulletin du cancer,* 102**,** 516-526.

FORSSTRÖM, L. M., SUMI, K., MÄKINEN, M. J., OH, J. E., HERVA, R., KLEIHUES, P., OHGAKI, H. & AALTONEN, L. A. 2017. Germline MSH6 Mutation in a Patient With Two Independent Primary Glioblastomas. *Journal of Neuropathology & Experimental Neurology,* 76**,** 848-853.

FOSMARK, S., HELLWEGE, S., DAHLROT, R. H., JENSEN, K. L., DERAND, H., LOHSE, J., SØRENSEN, M. D., HANSEN, S. & KRISTENSEN, B. W. 2017. APNG as a prognostic marker in patients with glioblastoma. *PloS one,* 12**,** e0178693.

FRIEDMAN, H. S., KERBY, T. & CALVERT, H. 2000. Temozolomide and treatment of malignant glioma. *Clinical cancer research,* 6**,** 2585-2597.

FRISCH, S. & TIMMERMANN, B. 2017. The evolving role of proton beam therapy for sarcomas. *Clinical Oncology,* 29**,** 500-506.

FU, D., CALVO, J. A. & SAMSON, L. D. 2012. Balancing repair and tolerance of DNA damage caused by alkylating agents. *Nature Reviews Cancer,* 12**,** 104.

FUTREAL, P. A., COIN, L., MARSHALL, M., DOWN, T., HUBBARD, T., WOOSTER, R., RAHMAN, N. & STRATTON, M. R. 2004. A census of human cancer genes. *Nature Reviews Cancer,* 4**,** 177.

GHOFRANI, H. A., OSTERLOH, I. H. & GRIMMINGER, F. 2006. Sildenafil: from angina to erectile dysfunction to pulmonary hypertension and beyond. *Nature Reviews Drug Discovery,* 5**,** 689.

GILBERT, M. R., DIGNAM, J. J., ARMSTRONG, T. S., WEFEL, J. S., BLUMENTHAL, D. T., VOGELBAUM, M. A., COLMAN, H., CHAKRAVARTI, A., PUGH, S. & WON, M. 2014. A randomized trial of bevacizumab for newly diagnosed glioblastoma. *New England Journal of Medicine,* 370**,** 699-708.

GIUNTA, S., BELOTSERKOVSKAYA, R. & JACKSON, S. P. 2010. DNA damage signaling in response to double-strand breaks during mitosis. *The Journal of cell biology,* 190**,** 197-207.

GMTGROUP 2002. Chemotherapy in adult high-grade glioma: a systematic review and meta-analysis of individual patient data from 12 randomised trials. *The Lancet,* 359**,** 1011-1018.

GOLDSMITH, Z. & DHANASEKARAN, D. 2007. G protein regulation of MAPK networks. *Oncogene,* 26**,** 3122.

GORGOULIS, V. G., VASSILIOU, L.-V. F., KARAKAIDOS, P., ZACHARATOS, P., KOTSINAS, A., LILOGLOU, T., VENERE, M., DITULLIO JR, R. A., KASTRINAKIS, N. G. & LEVY, B. 2005. Activation of the DNA damage checkpoint and genomic instability in human precancerous lesions. *Nature,* 434**,** 907.

GOSPODAROWICZ, D. 1974. Localisation of a fibroblast growth factor and its effect alone and with hydrocortisone on 3T3 cell growth. *Nature,* 249**,** 123.

GRABHER, C., VON BOEHMER, H. & LOOK, A. T. 2006. Notch 1 activation in the molecular pathogenesis of T-cell acute lymphoblastic leukaemia. *Nature Reviews Cancer,* 6**,** 347.

GRAUS PORTA, D., WEISS, A., FAIRHURST, R. A., WARTMANN, M., STAMM, C., REIMANN, F., BUHLES, A., KINYAMU-AKUNDA, J., STERKER, D., MURAKAMI, M., WANG, Y., ENGELMAN, J., HOFMANN, F. & SELLERS, W. R. 2017. NVP-FGF401, a first-in-class highly selective and potent FGFR4 inhibitor for the treatment of HCC. *American Association for Cancer Research Annual Meeting 2017.* Washington, DC.

GZELL, C., BACK, M., WHEELER, H., BAILEY, D. & FOOTE, M. 2017. Radiotherapy in Glioblastoma: the Past, the Present and the Future. *Clinical Oncology,* 29**,** 15-25.

GÍRIO, A., MONTERO, J. C., PANDIELLA, A. & CHATTERJEE, S. 2007. Erk5 is activated and acts as a survival factor in mitosis. *Cellular signalling,* 19**,** 1964-1972.

HAGEL, M., MIDUTURU, C., SHEETS, M., RUBIN, N., WENG, W., STRANSKY, N., BIFULCO, N., KIM, J. L., HODOUS, B. & BROOIJMANS, N. 2015. First selective small molecule inhibitor of FGFR4 for the treatment of hepatocellular carcinomas with an activated FGFR4 signaling pathway. *Cancer discovery*.

HAINSWORTH, J. D., ERVIN, T., FRIEDMAN, E., PRIEGO, V., MURPHY, P. B., CLARK, B. L. & LAMAR, R. E. 2010. Concurrent radiotherapy and temozolomide followed by temozolomide and sorafenib in the first-line treatment of patients with glioblastoma multiforme. *Cancer,* 116**,** 3663-3669.

HAIT, W., GLAZER, L., KAISER, C., CROSS, J. & KENNEDY, K. A. 1987. Pharmacological properties of fluphenazine-mustard, an irreversible calmodulin antagonist. *Molecular pharmacology,* 32**,** 404-409.

HAIT, W. N., BYRNE, T. N., PIEPMEIER, J., DURIVAGE, H. J., CHOUDHURY, S., DAVIS, C. A. & GATES, J. A. 1990. The effect of calmodulin inhibitors with bleomycin on the treatment of patients with high grade gliomas. *Cancer research,* 50**,** 6636-6640.

HALATSCH, M.-E., LÖW, S., MURSCH, K., HIELSCHER, T., SCHMIDT, U., UNTERBERG, A., VOUGIOUKAS, V. I. & FEUERHAKE, F. 2009. Candidate genes for sensitivity and resistance of human glioblastoma multiforme cell lines to erlotinib. *Journal of neurosurgery,* 111**,** 211-218.

HALE, V. L., JERALDO, P., CHEN, J., MUNDY, M., YAO, J., PRIYA, S., KEENEY, G., LYKE, K., RIDLON, J., WHITE, B. A., FRENCH, A. J., THIBODEAU, S. N., DIENER, C., RESENDIS-ANTONIO, O., GRANSEE, J., DUTTA, T., PETTERSON, X. M., SUNG, J., BLEKHMAN, R., BOARDMAN, L., LARSON, D., NELSON, H. & CHIA, N. 2018. Distinct microbes, metabolites, and ecologies define the microbiome in deficient and proficient mismatch repair colorectal cancers. *Genome Med,* 10**,** 78.

HANAHAN, D. & WEINBERG, R. A. 2000. The hallmarks of cancer. *Cell,* 100**,** 57-70.

HANAHAN, D. & WEINBERG, R. A. 2011. Hallmarks of cancer: the next generation. *cell,* 144**,** 646-674.

HANNUS, M., BEITZINGER, M., ENGELMANN, J. C., WEICKERT, M.-T., SPANG, R., HANNUS, S. & MEISTER, G. 2014. siPools: highly complex but accurately defined siRNA pools eliminate off-target effects. *Nucleic acids research,* 42**,** 8049-8061.

HARRIS, M. O., KALLENBERGER, L., BORÁN, M. A., ENOIU, M., COSTANZO, V. & JIRICNY, J. 2015. Mismatch repair-dependent metabolism of O 6-methylguanine-containing DNA in Xenopus laevis egg extracts. *DNA repair,* 28**,** 1-7.

HARTMANN, C., HENTSCHEL, B., SIMON, M., WESTPHAL, M., SCHACKERT, G., TONN, J. C., LOEFFLER, M., REIFENBERGER, G., PIETSCH, T. & VON DEIMLING, A. 2013. Long-term survival in primary glioblastoma with versus without isocitrate dehydrogenase mutations. *Clinical Cancer Research,* 19**,** 5146-5157.

HAYASHI, M., KIM, S.-W., IMANAKA-YOSHIDA, K., YOSHIDA, T., ABEL, E. D., ELICEIRI, B., YANG, Y., ULEVITCH, R. J. & LEE, J.-D. 2004. Targeted deletion of BMK1/ERK5 in adult mice perturbs vascular integrity and leads to endothelial failure. *The Journal of clinical investigation,* 113**,** 1138-1148.

HICKMAN, M. J. & SAMSON, L. D. 2004. Apoptotic signaling in response to a single type of DNA lesion, O6-methylguanine. *Molecular cell,* 14**,** 105-116.

HOANG, V. T., YAN, T. J., CAVANAUGH, J. E., FLAHERTY, P. T., BECKMAN, B. S. & BUROW, M. E. 2017. Oncogenic signaling of MEK5-ERK5. *Cancer letters,* 392**,** 51-59.

HOEFLICH, K. 2015. BLU-554, A Novel, Potent and Selective Inhibitor of FGFR4 for the Treatment of Liver Cancer. *50th International Liver Congress.* Vienna, Austria.

HONDA, T., OBARA, Y., YAMAUCHI, A., COUVILLON, A. D., MASON, J. J., ISHII, K. & NAKAHATA, N. 2015. Phosphorylation of ERK5 on Thr732 is associated with ERK5 nuclear localization and ERK5-dependent transcription. *PloS one,* 10**,** e0117914.

HONG, J. D., WANG, X., PENG, Y. P., PENG, J. H., WANG, J., DONG, Y. P., HE, D., PENG, Z. Z., TU, Q. S. & SHENG, L. F. 2017. Silencing platelet-derived growth factor receptor-β enhances the radiosensitivity of C6 glioma cells in vitro and in vivo. *Oncology letters,* 14**,** 329-336.

ILIOPOULOS, D., BIMPAKI, E. I., NESTEROVA, M. & STRATAKIS, C. A. 2009. MicroRNA signature of primary pigmented nodular adrenocortical disease: clinical correlations and regulation of Wnt signaling. *Cancer research,* 69**,** 3278-3282.

IÑESTA-VAQUERA, F. A., CAMPBELL, D. G., TOURNIER, C., GÓMEZ, N., LIZCANO, J. M. & CUENDA, A. 2010. Alternative ERK5 regulation by phosphorylation during the cell cycle. *Cellular signalling,* 22**,** 1829-1837.

JACKSON, S. P. & BARTEK, J. 2009. The DNA-damage response in human biology and disease. *Nature,* 461**,** 1071-8.

JACQUEMIER, J., ADELAIDE, J., PARC, P., PENAULT-LLORCA, F., PLANCHE, J., DELAPEYRIERE, O. & BIRNBAUM, D. 1994. Expression of the FGFR1 gene in human breast-carcinoma cells. *International journal of cancer,* 59**,** 373-378.

JANG, M. H., KANG, H. J., JANG, K. S., PAIK, S. S. & KIM, W. S. 2016. Clinicopathological analysis of CD44 and CD24 expression in invasive breast cancer. *Oncology letters,* 12**,** 2728-2733.

JENTZSCH, T., ROBL, B., HUSMANN, M., BODE-LESNIEWSKA, B. & FUCHS, B. 2014. Expression of MSH2 and MSH6 on a tissue microarray in patients with osteosarcoma. *Anticancer research,* 34**,** 6961-6972.

JEREMIC, B., GRUJICIC, D., ANTUNOVIC, V., DJURIC, L., STOJANOVIC, M. & SHIBAMOTO, Y. 1994. Influence of extent of surgery and tumor location on treatment outcome of patients with glioblastoma multiforme treated with combined modality approach. *Journal of neuro-oncology,* 21**,** 177-185.

JIA, W., DONG, Y., TAO, L., PANG, L., REN, Y., LIANG, W., JIANG, J., CHENG, G., ZHANG, W. J. & YUAN, X. 2016. MAP3K3 overexpression is associated with poor survival in ovarian carcinoma. *Human pathology,* 50**,** 162-169.

JIANG, W., JIN, G., CAI, F., CHEN, X., CAO, N., ZHANG, X., LIU, J., CHEN, F., WANG, F. & DONG, W. 2019. Extracellular signal-regulated kinase 5 increases radioresistance of lung cancer cells by enhancing the DNA damage response. *Experimental & Molecular Medicine,* 51**,** 19.

JOHANNESSEN, T. C., HASAN-OLIVE, M. M., ZHU, H., DENISOVA, O., GRUDIC, A., LATIF, M. A., SAED, H., VARUGHESE, J. K., RØSLAND, G. V. & YANG, N. 2018. Thioridazine inhibits autophagy and sensitizes glioblastoma cells to temozolomide. *International journal of cancer*.

JOHNSON, G. L. & LAPADAT, R. 2002. Mitogen-activated protein kinase pathways mediated by ERK, JNK, and p38 protein kinases. *Science,* 298**,** 1911-1912.

JONES, J. O., BOLTON, E. C., HUANG, Y., FEAU, C., GUY, R. K., YAMAMOTO, K. R., HANN, B. & DIAMOND, M. I. 2009. Non-competitive androgen receptor inhibition in vitro and in vivo. *Proceedings of the National Academy of Sciences,* 106**,** 7233-7238.

JOSHI, A. D., PARSONS, D. W., VELCULESCU, V. E. & RIGGINS, G. J. 2011. Sodium ion channel mutations in glioblastoma patients correlate with shorter survival. *Molecular cancer,* 10**,** 17.

JÄKEL, O. State of the art in hadron therapy. AIP Conference Proceedings, 2007. AIP, 70-77.

KAINA, B., CHRISTMANN, M., NAUMANN, S. & ROOS, W. P. 2007. MGMT: key node in the battle against genotoxicity, carcinogenicity and apoptosis induced by alkylating agents. *DNA repair,* 6**,** 1079-1099.

KALAMATIANOS, T., DENEKOU, D., STRANJALIS, G. & PAPADIMITRIOU, E. 2018. Anaplastic Lymphoma Kinase in Glioblastoma: Detection/Diagnostic Methods and Therapeutic Options. *Recent patents on anti-cancer drug discovery,* 13**,** 209-223.

KAMAKURA, S., MORIGUCHI, T. & NISHIDA, E. 1999. Activation of the protein kinase ERK5/BMK1 by receptor tyrosine kinases Identification and characterization of a signaling pathway to the nucleus. *Journal of Biological Chemistry,* 274**,** 26563-26571.

KANG, S., HONG, J., LEE, J. M., MOON, H. E., JEON, B., CHOI, J., YOON, N. A., PAEK, S. H., ROH, E. J. & LEE, C. J. 2017. Trifluoperazine, a well-known antipsychotic, inhibits glioblastoma invasion by binding to calmodulin and disinhibiting calcium release channel IP3R. *Molecular cancer therapeutics,* 16**,** 217-227.

KATO, Y., TAPPING, R. I., HUANG, S., WATSON, M. H., ULEVITCH, R. J. & LEE, J.-D. 1998. Bmk1/Erk5 is required for cell proliferation induced by epidermal growth factor. *Nature,* 395**,** 713.

KE, X. & SHEN, L. 2017. Molecular targeted therapy of cancer: The progress and future prospect. *Frontiers in Laboratory Medicine,* 1**,** 69-75.

KEE, Y. & D'ANDREA, A. D. 2010. Expanded roles of the Fanconi anemia pathway in preserving genomic stability. *Genes & development,* 24**,** 1680-1694.

KEIR, S. T., FRIEDMAN, H. S., REARDON, D. A., BIGNER, D. D. & GRAY, L. A. 2013. Mibefradil, a novel therapy for glioblastoma multiforme: cell cycle synchronization and interlaced therapy in a murine model. *Journal of neuro-oncology,* 111**,** 97-102.

KELLY, K., SACAPANO, M. R., PROSOLOVICH, K., ONG, J. & BLACK, K. 2005. Blood brain barrier permeability to temozolomide. AACR.

KIM, J., TANG, J. Y., GONG, R., KIM, J., LEE, J. J., CLEMONS, K. V., CHONG, C. R., CHANG, K. S., FERESHTEH, M. & GARDNER, D. 2010. Itraconazole, a commonly used antifungal that inhibits Hedgehog pathway activity and cancer growth. *Cancer cell,* 17**,** 388-399.

KIND, M., KLUKOWSKA-RÖTZLER, J., BEREZOWSKA, S., ARCARO, A. & CHARLES, R.-P. 2017. Questioning the role of selected somatic PIK3C2B mutations in squamous non-small cell lung cancer oncogenesis. *PloS one,* 12**,** e0187308.

KLEBER, S., SANCHO-MARTINEZ, I., WIESTLER, B., BEISEL, A., GIEFFERS, C., HILL, O., THIEMANN, M., MUELLER, W., SYKORA, J. & KUHN, A. 2008. Yes and PI3K bind CD95 to signal invasion of glioblastoma. *Cancer cell,* 13**,** 235-248.

KLEIHUES, P., CAVENEE, W. K. & INTERNATIONAL AGENCY FOR RESEARCH ON, C. 2000. *Pathology and genetics of tumours of the nervous system,* Lyon, Lyon : IARC Press, 2000.

KOLA, I. & LANDIS, J. 2004. Can the pharmaceutical industry reduce attrition rates? *Nature reviews Drug discovery,* 3**,** 711.

KONDO, N., TAKAHASHI, A., MORI, E., NODA, T., ZDZIENICKA, M. Z., THOMPSON, L. H., HELLEDAY, T., SUZUKI, M., KINASHI, Y. & MASUNAGA, S. 2011. FANCD1/BRCA2 plays predominant role in the repair of DNA damage induced by ACNU or TMZ. *PloS one,* 6**,** e19659.

KONDURI, S. D., TICKU, J., BOBUSTUC, G. C., SUTPHIN, R. M., COLON, J., ISLEY, B., BHAKAT, K. K., KALKUNTE, S. S. & BAKER, C. H. 2009. Blockade of MGMT expression by O6 benzyl guanine leads to inhibition of pancreatic cancer growth and induction of apoptosis. *Clinical Cancer Research,* 15**,** 6087-6095.

KREJCI, L., ALTMANNOVA, V., SPIREK, M. & ZHAO, X. 2012. Homologous recombination and its regulation. *Nucleic acids research,* 40**,** 5795-5818.

KRISTIANSEN, K., HAGEN, S., KOLLEVOLD, T., TORVIK, A., HOLME, I., STAT, M., NESBAKKEN, R., HATLEVOLL, R., LINDGREN, M. & BRUN, A. 1981. Combined modality therapy of operated astrocytomas grade III and IV. Confirmation of the value of postoperative irradiation and lack of potentiation of bleomycin on survival time: a prospective multicenter trial of the Scandinavian Glioblastoma Study Group. *Cancer,* 47**,** 649-652.

KUHNT, D., BECKER, A., GANSLANDT, O., BAUER, M., BUCHFELDER, M. & NIMSKY, C. 2011. Correlation of the extent of tumor volume resection and patient survival in surgery of glioblastoma multiforme with high-field intraoperative MRI guidance. *Neuro-oncology,* 13**,** 1339-1348.

KULKARNI, S., GOEL-BHATTACHARYA, S., SENGUPTA, S. & COCHRAN, B. H. 2018. A large-scale RNAi screen identifies SGK1 as a key survival kinase for GBM stem cells. *Molecular Cancer Research,* 16**,** 103-114.

KUNWAR, S., CHANG, S., WESTPHAL, M., VOGELBAUM, M., SAMPSON, J., BARNETT, G., SHAFFREY, M., RAM, Z., PIEPMEIER, J. & PRADOS, M. 2010. Phase III randomized trial of CED of IL13-PE38QQR vs Gliadel wafers for recurrent glioblastoma. *Neuro-oncology,* 12**,** 871-881.

LACROIX, M., ABI-SAID, D., FOURNEY, D. R., GOKASLAN, Z. L., SHI, W., DEMONTE, F., LANG, F. F., MCCUTCHEON, I. E., HASSENBUSCH, S. J. & HOLLAND, E. 2001. A multivariate analysis of 416 patients with glioblastoma multiforme: prognosis, extent of resection, and survival. *Journal of neurosurgery,* 95**,** 190-198.

LAM, F. C., MORTON, S. W., WYCKOFF, J., HAN, T.-L., HWANG, M. K., MAFFA, A., BALKANSKA-SINCLAIR, E., YAFFE, M. B., FLOYD, S. R. & HAMMOND, P. T. 2018. Enhanced efficacy of combined temozolomide and bromodomain inhibitor therapy for gliomas using targeted nanoparticles. *Nature communications,* 9**,** 1991.

LAN, T., ZHAO, Z., QU, Y., ZHANG, M., WANG, H., ZHANG, Z., ZHOU, W., FAN, X., YU, C. & ZHAN, Q. 2016. Targeting hyperactivated DNA-PKcs by KU0060648 inhibits glioma progression and enhances temozolomide therapy via suppression of AKT signaling. *Oncotarget,* 7**,** 55555.

LEE, G. L. & HAIT, W. N. 1985. Inhibition of growth of C6 astrocytoma cells by inhibitors of calmodulin. *Life sciences,* 36**,** 347-354.

LEE, J.-D., ULEVITCH, R. J. & HAN, J. 1995. Primary structure of BMK1: a new mammalian map kinase. *Biochemical and biophysical research communications,* 213**,** 715-724.

LEE, S. Y. 2016. Temozolomide resistance in glioblastoma multiforme. *Genes & Diseases,* 3**,** 198-210.

LENNARTSSON, J., BUROVIC, F., WITEK, B., JUREK, A. & HELDIN, C.-H. 2010. Erk 5 is necessary for sustained PDGF-induced Akt phosphorylation and inhibition of apoptosis. *Cellular signalling,* 22**,** 955-960.

LI, Y.-P. 2013a. GRK6 expression in patients with hepatocellular carcinoma. *Asian Pacific journal of tropical medicine,* 6**,** 220-223.

LI, Z. 2013b. CD133: a stem cell biomarker and beyond. *Experimental hematology & oncology,* 2**,** 17.

LIANG, A., ZHOU, B. & SUN, W. 2017. Integrated genomic characterization of cancer genes in glioma. *Cancer cell international,* 17**,** 90.

LIEBER, M. R. 2010. The mechanism of double-strand DNA break repair by the nonhomologous DNA end-joining pathway. *Annual review of biochemistry,* 79**,** 181-211.

LIM, J. H. & WOO, C.-H. 2011. Laminar flow activation of ERK5 leads to cytoprotective effect via CHIP-mediated p53 ubiquitination in endothelial cells. *Anatomy & cell biology,* 44**,** 265-273.

LIM, M., OTTO-DUESSEL, M., HE, M., SU, L., NGUYEN, D., CHIN, E., ALLISTON, T. & JONES, J. O. 2014. Ligand-independent and tissue-selective androgen receptor inhibition by pyrvinium. *ACS chemical biology,* 9**,** 692-702.

LIN, E. C., AMANTEA, C. M., NOMANBHOY, T. K., WEISSIG, H., ISHIYAMA, J., HU, Y., SIDIQUE, S., LI, B., KOZARICH, J. W. & ROSENBLUM, J. S. 2016. ERK5 kinase activity is dispensable for cellular immune response and proliferation. *Proceedings of the National Academy of Sciences,* 113**,** 11865-11870.

LIN, X., MORGAN-LAPPE, S., HUANG, X., LI, L., ZAKULA, D., VERNETTI, L., FESIK, S. & SHEN, Y. 2007. 'Seed'analysis of off-target siRNAs reveals an essential role of Mcl-1 in resistance to the small-molecule Bcl-2/Bcl-X L inhibitor ABT-737. *Oncogene,* 26**,** 3972.

LINOS, E., RAINE, T., ALONSO, A. & MICHAUD, D. 2007. Atopy and risk of brain tumors: a meta-analysis. *J Natl Cancer Inst,* 99**,** 1544-50.

LIU, F., WANG, J., YANG, X., LI, B., WU, H., QI, S., CHEN, C., LIU, X., YU, K. & WANG, W. 2016. Discovery of a Highly Selective STK16 Kinase Inhibitor. *ACS chemical biology,* 11**,** 1537-1543.

LIU, G., YUAN, X., ZENG, Z., TUNICI, P., NG, H., ABDULKADIR, I. R., LU, L., IRVIN, D., BLACK, K. L. & JOHN, S. Y. 2006. Analysis of gene expression and chemoresistance of CD133+ cancer stem cells in glioblastoma. *Molecular cancer,* 5**,** 67.

LIU, L. & GERSON, S. L. 2006. Targeted modulation of MGMT: clinical implications. *Clinical cancer research,* 12**,** 328-331.

LIU, X., SHI, Y., GUAN, R., DONAWHO, C., LUO, Y., PALMA, J., ZHU, G.-D., JOHNSON, E. F., RODRIGUEZ, L. E. & GHOREISHI-HAACK, N. 2008. Potentiation of temozolomide cytotoxicity by poly (ADP) ribose polymerase inhibitor ABT-888 requires a conversion of single-stranded DNA damages to double-stranded DNA breaks. *Molecular Cancer Research,* 6**,** 1621-1629.

LOEB, L. A. 2016. Human cancers express a mutator phenotype: hypothesis, origin, and consequences. *Cancer research,* 76**,** 2057-2059.

LOEB, L. A. & HARRIS, C. C. 2008. Advances in chemical carcinogenesis: a historical review and prospective. *Cancer research,* 68**,** 6863-6872.

LOEB, L. A., SPRINGGATE, C. F. & BATTULA, N. 1974. Errors in DNA replication as a basis of malignant changes. *Cancer research,* 34**,** 2311-2321.

LOEW, S., VOUGIOUKAS, V. I., HIELSCHER, T., SCHMIDT, U., UNTERBERG, A. & HALATSCH, M.-E. 2008. Pathogenetic pathways leading to glioblastoma multiforme: association between gene expressions and resistance to erlotinib. *Anticancer research,* 28**,** 3729-3732.

LOILOME, W., JUNTANA, S., NAMWAT, N., BHUDHISAWASDI, V., PUAPAIROJ, A., SRIPA, B., MIWA, M., SAYA, H., RIGGINS, G. J. & YONGVANIT, P. 2011. PRKAR1A is overexpressed and represents a possible therapeutic target in human cholangiocarcinoma. *International journal of cancer,* 129**,** 34-44.

LORD, C. J. & ASHWORTH, A. 2016. BRCAness revisited. *Nature Reviews Cancer,* 16**,** 110.

LU, Q. R., SUN, T., ZHU, Z., MA, N., GARCIA, M., STILES, C. D. & ROWITCH, D. H. 2002. Common developmental requirement for Olig function indicates a motor neuron/oligodendrocyte connection. *Cell,* 109**,** 75-86.

LU, S.-J., LI, F., VIDA, L. & HONIG, G. R. 2004. CD34+ CD38-hematopoietic precursors derived from human embryonic stem cells exhibit an embryonic gene expression pattern. *Blood,* 103**,** 4134-4141.

MANDAL, P. K., BLANPAIN, C. & ROSSI, D. J. 2011. DNA damage response in adult stem cells: pathways and consequences. *Nature Reviews Molecular Cell Biology,* 12**,** 198.

MANNING, B. D. 2009. Challenges and opportunities in defining the essential cancer kinome. *Science signaling,* 2**,** pe15-pe15.

MARSISCHKY, G. T., FILOSI, N., KANE, M. F. & KOLODNER, R. 1996. Redundancy of Saccharomyces cerevisiae MSH3 and MSH6 in MSH2-dependent mismatch repair. *Genes & development,* 10**,** 407-420.

MARTINCORENA, I., RAINE, K. M., GERSTUNG, M., DAWSON, K. J., HAASE, K., VAN LOO, P., DAVIES, H., STRATTON, M. R. & CAMPBELL, P. J. 2017. Universal patterns of selection in cancer and somatic tissues. *Cell,* 171**,** 1029-1041. e21.

MARUSYK, A. & POLYAK, K. 2010. Tumor heterogeneity: causes and consequences. *Biochimica et Biophysica Acta (BBA)-Reviews on Cancer,* 1805**,** 105-117.

MASICA, D. L. & KARCHIN, R. 2011. Correlation of somatic mutation and expression identifies genes important in human glioblastoma progression and survival. *Cancer research***,** canres. 0180.2011.

MAXWELL, J. A., JOHNSON, S. P., MCLENDON, R. E., LISTER, D. W., HORNE, K. S., RASHEED, A., QUINN, J. A., ALI-OSMAN, F., FRIEDMAN, A. H. & MODRICH, P. L. 2008. Mismatch repair deficiency does not mediate clinical resistance to temozolomide in malignant glioma. *Clinical Cancer Research,* 14**,** 4859-4868.

MEBRATU, Y. & TESFAIGZI, Y. 2009. How ERK1/2 activation controls cell proliferation and cell death: Is subcellular localization the answer? *Cell cycle,* 8**,** 1168-1175.

MEEK, K., DANG, V. & LEES-MILLER, S. P. 2008. DNA-PK: the means to justify the ends? *Advances in immunology,* 99**,** 33-58.

MEHTA, P., JENKINS, B., MCCARTHY, L., THILAK, L., ROBSON, C., NEAL, D. & LEUNG, H. 2003. MEK5 overexpression is associated with metastatic prostate cancer, and stimulates proliferation, MMP-9 expression and invasion. *Oncogene,* 22**,** 1381.

MEYER, K. B., MAIA, A.-T., O'REILLY, M., TESCHENDORFF, A. E., CHIN, S.-F., CALDAS, C. & PONDER, B. A. 2008. Allele-specific up-regulation of FGFR2 increases susceptibility to breast cancer. *PLoS biology,* 6**,** e108.

MINTZ, B. & ILLMENSEE, K. 1975. Normal genetically mosaic mice produced from malignant teratocarcinoma cells. *Proceedings of the National Academy of Sciences,* 72**,** 3585-3589.

MOASSER, M. M. & KROP, I. E. 2015. The evolving landscape of HER2 targeting in breast cancer. *JAMA oncology,* 1**,** 1154-1161.

MONTERO, J. C., OCANA, A., ABAD, M., ORTIZ-RUIZ, M. J., PANDIELLA, A. & ESPARÍS-OGANDO, A. 2009. Expression of Erk5 in early stage breast cancer and association with disease free survival identifies this kinase as a potential therapeutic target. *PloS one,* 4**,** e5565.

MORALES, J., LI, L., FATTAH, F. J., DONG, Y., BEY, E. A., PATEL, M., GAO, J. & BOOTHMAN, D. A. 2014. Review of poly (ADP-ribose) polymerase (PARP) mechanisms of action and rationale for targeting in cancer and other diseases. *Critical Reviews™ in Eukaryotic Gene Expression,* 24.

MOREIRA, M. P., DA CONCEIÇÃO BRAGA, L., CASSALI, G. D. & SILVA, L. M. 2018. STAT3 as a promising chemoresistance biomarker associated with the CD44+/high/CD24-/low/ALDH+ BCSCs-like subset of the triple-negative breast cancer (TNBC) cell line. *Experimental cell research,* 363**,** 283-290.

MOROISHI, T., HANSEN, C. G. & GUAN, K.-L. 2015. The emerging roles of YAP and TAZ in cancer. *Nature Reviews Cancer,* 15**,** 73.

MURAI, J., ZHANG, Y., MORRIS, J., JI, J., TAKEDA, S., DOROSHOW, J. H. & POMMIER, Y. 2014. Rationale for poly (ADP-ribose) polymerase (PARP) inhibitors in combination therapy with camptothecins or temozolomide based on PARP trapping versus catalytic inhibition. *Journal of Pharmacology and Experimental Therapeutics,* 349**,** 408-416.

NARAYANASWAMY, P. B., TKACHUK, S., HALLER, H., DUMLER, I. & KIYAN, Y. 2016. CHK1 and RAD51 activation after DNA damage is regulated via urokinase receptor/TLR4 signaling. *Cell death & disease,* 7**,** e2383.

NATIONAL CENTER FOR BIOTECHNOLOGY INFORMATION, P. C. D. 2018a. Deoxysappone B Trimethyl Ether.

NATIONAL CENTER FOR BIOTECHNOLOGY INFORMATION, P. C. D. 2018b. *Penicillamine* [Online]. Available: https://pubchem.ncbi.nlm.nih.gov/compound/D-Penicillamine#section=Top [Accessed 05/10/2018].

NATIONALCANCERINSTITUTE. 2015. *What Is Cancer?* [Online]. Available: https://www.cancer.gov/about-cancer/understanding/what-is-cancer [Accessed 12/11/2018].

NATIONALCANCERINSTITUTE. 2018. *Drugs Approved for Brain Tumours* [Online]. Available: https://www.cancer.gov/about-cancer/treatment/drugs/brain [Accessed 13/11/2018].

NEUMANN, F., GOURDAIN, S., ALBAC, C., DEKKER, A. D., BUI, L. C., DAIROU, J., SCHMITZ-AFONSO, I., HUE, N., RODRIGUES-LIMA, F. & DELABAR, J. M. 2018. DYRK1A inhibition and cognitive rescue in a Down syndrome mouse model are induced by new fluoro-DANDY derivatives. *Scientific reports,* 8**,** 2859.

NEWLANDS, E. S., STEVENS, M. F., WEDGE, S. R., WHEELHOUSE, R. T. & BROCK, C. 1997. Temozolomide: a review of its discovery, chemical properties, pre-clinical development and clinical trials. *CANCER TREAT REV,* 23**,** 35-61.

NGUYEN, C. L., POSSEMATO, R., BAUERLEIN, E. L., XIE, A., SCULLY, R. & HAHN, W. C. 2012. Nek4 regulates entry into replicative senescence and the response to DNA-damage in human fibroblasts. *Molecular and cellular biology***,** MCB. 00436-12.

NHSENGLAND. *Proton beam therapy* [Online]. Available: https://www.england.nhs.uk/commissioning/spec-services/highly-spec-services/pbt/ [Accessed 08/03/2019 2019].

NICE 2001. Guidance on the use of temozolomide for the treatment of recurrent malignant glioma (brain cancer).

NICE. 2007. *Carmustine implants and temozolomide for the treatment of newly diagnosed high-grade glioma* [Online]. Available: https://www.nice.org.uk/guidance/ta121/resources/carmustine-implants-and-temozolomide-for-the-treatment-of-newly-diagnosed-highgrade-glioma-pdf-373304989 [Accessed 12/11/2018].

NICE. 2016a. *DCVax-L for treating newly diagnosed glioblastoma multiforme [ID836]* [Online]. Available: https://www.nice.org.uk/guidance/indevelopment/gid-ta10143 [Accessed 14/11/2018].

NICE. 2016b. *Nivolumab for treating recurrent glioblastoma [ID998]* [Online]. Available: https://www.nice.org.uk/guidance/indevelopment/gid-ta10126 [Accessed 14/11/2018].

NICE. 2017a. *Asunercept for treating glioblastoma* [Online]. Available: https://www.nice.org.uk/guidance/indevelopment/gid-ta10227 [Accessed 14/11/2018].

NICE. 2017b. *Depatuxizumab mafodotin for treating recurrent EGFR-amplified glioblastoma [ID1244]* [Online]. Available: https://www.nice.org.uk/guidance/indevelopment/gid-ta10242 [Accessed].

NICE. 2018a. *Brain tumours (primary) and brain metastasis in adults. Rationale and Impact.* [Online]. Available: https://www.nice.org.uk/guidance/ng99/chapter/rationale-and-impact#management-of-glioma-grade-iv-glioma-following-surgery [Accessed 13/11/2018].

NICE. 2018b. *Brain tumours (primary) and brain metastasis in adults. Recommendations.* [Online]. Available: https://www.nice.org.uk/guidance/ng99/chapter/Recommendations#management-of-glioma [Accessed 13/11/2018].

NICOLAS, M., WOLFER, A., RAJ, K., KUMMER, J. A., MILL, P., VAN NOORT, M., HUI, C.-C., CLEVERS, H., DOTTO, G. P. & RADTKE, F. 2003. Notch1 functions as a tumor suppressor in mouse skin. *Nature genetics,* 33**,** 416.

NIK-ZAINAL, S. 2019. From genome integrity to cancer. *Genome Med,* 11**,** 4.

NIMESH, M., CAMPBELL, D. G., MORRICE, N., PEGGIE, M. & COHEN, P. 2003. An analysis of the phosphorylation and activation of extracellular-signal-regulated protein kinase 5 (ERK5) by mitogen-activated protein kinase kinase 5 (MKK5) in vitro. *Biochemical Journal,* 372**,** 567-575.

NITHIANANDARAJAH-JONES, G. N., WILM, B., GOLDRING, C. E., MÜLLER, J. & CROSS, M. J. 2012. ERK5: structure, regulation and function. *Cellular signalling,* 24**,** 2187-2196.

NOONAN, E. M., SHAH, D., YAFFE, M. B., LAUFFENBURGER, D. A. & SAMSON, L. D. 2012. O 6-Methylguanine DNA lesions induce an intra-S-phase arrest from which cells exit into apoptosis governed by early and late multi-pathway signaling network activation. *Integrative Biology,* 4**,** 1237-1255.

NORTHWESTBIOTHERAPEUTICS. 2018. *DCVax® – L* [Online]. Available: https://www.nwbio.com/dcvax-l/ [Accessed 14/11/2018].

OGDEN, A. T., WAZIRI, A. E., LOCHHEAD, R. A., FUSCO, D., LOPEZ, K., ELLIS, J. A., KANG, J., ASSANAH, M., MCKHANN, G. M. & SISTI, M. B. 2008. Identification of A2B5+ CD133− tumor-initiating cells in adult human gliomas. *Neurosurgery,* 62**,** 505-515.

OHGAKI, H. & KLEIHUES, P. 2013. The definition of primary and secondary glioblastoma. *Clinical cancer research,* 19**,** 764-772.

OLIVA, C. R., NOZELL, S. E., DIERS, A., MCCLUGAGE, S. G., SARKARIA, J. N., MARKERT, J. M., DARLEY-USMAR, V. M., BAILEY, S. M., GILLESPIE, G. Y. & LANDAR, A. 2010. Acquisition of temozolomide chemoresistance in gliomas leads to remodeling of mitochondrial electron transport chain. *Journal of Biological Chemistry***,** jbc. M110. 147504.

ORNITZ, D. M. & ITOH, N. 2015. The fibroblast growth factor signaling pathway. *Wiley Interdisciplinary Reviews: Developmental Biology,* 4**,** 215-266.

ORTHWEIN, A., FRADET-TURCOTTE, A., NOORDERMEER, S. M., CANNY, M. D., BRUN, C. M., STRECKER, J., ESCRIBANO-DIAZ, C. & DUROCHER, D. 2014. Mitosis inhibits DNA double-strand break repair to guard against telomere fusions. *Science,* 344**,** 189-193.

ORTIZ-RUIZ, M. J., ÁLVAREZ-FERNÁNDEZ, S., PARROTT, T., ZAKNOEN, S., BURROWS, F. J., OCAÑA, A., PANDIELLA, A. & ESPARÍS-OGANDO, A. 2014. Therapeutic potential of ERK5 targeting in triple negative breast cancer. *Oncotarget,* 5**,** 11308.

OSTLING, O. & JOHANSON, K. J. 1984. Microelectrophoretic study of radiation-induced DNA damages in individual mammalian cells. *Biochemical and biophysical research communications,* 123**,** 291-298.

PACE, P., MOSEDALE, G., HODSKINSON, M. R., ROSADO, I. V., SIVASUBRAMANIAM, M. & PATEL, K. J. 2010. Ku70 corrupts DNA repair in the absence of the Fanconi anemia pathway. *Science,* 329**,** 219-223.

PAGÈS, V. & FUCHS, R. P. P. 2002. How DNA lesions are turned into mutations within cells? *Oncogene,* 21**,** 8957.

PANTZIARKA, P., BOUCHE, G., MEHEUS, L., SUKHATME, V., SUKHATME, V. P. & VIKAS, P. 2014. The repurposing drugs in oncology (ReDO) project. *ecancermedicalscience,* 8.

PASTORI, C., DANIEL, M., PENAS, C., VOLMAR, C.-H., JOHNSTONE, A. L., BROTHERS, S. P., GRAHAM, R. M., ALLEN, B., SARKARIA, J. N. & KOMOTAR, R. J. 2014. BET bromodomain proteins are required for glioblastoma cell proliferation. *Epigenetics,* 9**,** 611-620.

PATEL, A. P., TIROSH, I., TROMBETTA, J. J., SHALEK, A. K., GILLESPIE, S. M., WAKIMOTO, H., CAHILL, D. P., NAHED, B. V., CURRY, W. T. & MARTUZA, R. L. 2014. Single-cell RNA-seq highlights intratumoral heterogeneity in primary glioblastoma. *Science,* 344**,** 1396-1401.

PATIL, A. A., SAYAL, P., DEPONDT, M.-L., BEVERIDGE, R. D., ROYLANCE, A., KRIPLANI, D. H., MYERS, K. N., COX, A., JELLINEK, D. & FERNANDO, M. 2014. FANCD2 re-expression

is associated with glioma grade and chemical inhibition of the Fanconi Anaemia pathway sensitises gliomas to chemotherapeutic agents. *Oncotarget,* 5**,** 6414-6424.

PAUL, S. M., MYTELKA, D. S., DUNWIDDIE, C. T., PERSINGER, C. C., MUNOS, B. H., LINDBORG, S. R. & SCHACHT, A. L. 2010. How to improve R&D productivity: the pharmaceutical industry's grand challenge. *Nature reviews Drug discovery,* 9**,** 203.

PAULINO, A. C., SIMON, J. H., ZHEN, W. & WEN, B.-C. 2000. Long-term effects in children treated with radiotherapy for head and neck rhabdomyosarcoma. *International Journal of Radiation Oncology* Biology* Physics,* 48**,** 1489-1495.

PAVAN, S., MEYER-SCHALLER, N., DIEPENBRUCK, M., KALATHUR, R. K. R., SAXENA, M. & CHRISTOFORI, G. 2018. A kinome-wide high-content siRNA screen identifies MEK5-ERK5 signaling as critical for breast cancer cell EMT and metastasis. *Oncogene,* 37**,** 4197-4213.

PEREIRA, D. M., SIMÕES, A. E., GOMES, S. E., CASTRO, R. E., CARVALHO, T., RODRIGUES, C. M. & BORRALHO, P. M. 2016. MEK5/ERK5 signaling inhibition increases colon cancer cell sensitivity to 5-fluorouracil through a p53-dependent mechanism. *Oncotarget,* 7**,** 34322.

PEREZ-MADRIGAL, D., FINEGAN, K. G., PARAMO, B. & TOURNIER, C. 2012. The extracellular-regulated protein kinase 5 (ERK5) promotes cell proliferation through the down-regulation of inhibitors of cyclin dependent protein kinases (CDKs). *Cellular signalling,* 24**,** 2360-2368.

PICCIRILLO, S., COMBI, R., CAJOLA, L., PATRIZI, A., REDAELLI, S., BENTIVEGNA, A., BARONCHELLI, S., MAIRA, G., POLLO, B. & MANGIOLA, A. 2009. Distinct pools of cancer stem-like cells coexist within human glioblastomas and display different tumorigenicity and independent genomic evolution. *Oncogene,* 28**,** 1807.

PICCIRILLO, S. G., COLMAN, S., POTTER, N. E., VAN DELFT, F. W., LILLIS, S., CARNICER, M.-J., KEARNEY, L., WATTS, C. & GREAVES, M. 2015. Genetic and functional diversity of propagating cells in glioblastoma. *Stem Cell Reports,* 4**,** 7-15.

POLLACK, A., BAE, K., KHOR, L.-Y., AL-SALEEM, T., HAMMOND, M. E., VENKATESAN, V., BYHARDT, R. W., ASBELL, S. O., SHIPLEY, W. U. & SANDLER, H. M. 2009. The importance of protein kinase A in prostate cancer: relationship to patient outcome in Radiation Therapy Oncology Group trial 92-02. *Clinical Cancer Research***,** 1078-0432. CCR-08-2704.

PONTEN, J. & MACINTYRE, E. 1968. Long term culture of normal and neoplastic human glia. *Acta Pathologica Microbiologica Scandinavica,* 74**,** 465-486.

POUNDS, R., LEONARD, S., DAWSON, C. & KEHOE, S. 2017. Repurposing itraconazole for the treatment of cancer. *Oncology letters,* 14**,** 2587-2597.

POZO, N., ZAHONERO, C., FERNÁNDEZ, P., LIÑARES, J. M., AYUSO, A., HAGIWARA, M., PÉREZ, A., RICOY, J. R., HERNÁNDEZ-LAÍN, A. & SEPÚLVEDA, J. M. 2013. Inhibition of DYRK1A destabilizes EGFR and reduces EGFR-dependent glioblastoma growth. *The Journal of clinical investigation,* 123**,** 2475-2487.

PRESCRIBERS' DIGITAL REFERENCE. 2018. *Penicillamine - Drug Summary* [Online]. Available: http://www.pdr.net/drug-summary/Cuprimine-penicillamine-1452 [Accessed 08/10/2018].

PRICE, S. & GILLARD, J. 2014. Imaging biomarkers of brain tumour margin and tumour invasion. *The British journal of radiology*.

QAZI, M., VORA, P., VENUGOPAL, C., SIDHU, S., MOFFAT, J., SWANTON, C. & SINGH, S. 2017. Intratumoral heterogeneity: pathways to treatment resistance and relapse in human glioblastoma. *Annals of Oncology,* 28**,** 1448-1456.

QUINN, J. A., DESJARDINS, A., WEINGART, J., BREM, H., DOLAN, M. E., DELANEY, S. M., VREDENBURGH, J., RICH, J., FRIEDMAN, A. H. & REARDON, D. A. 2005. Phase I trial

of temozolomide plus O6-benzylguanine for patients with recurrent or progressive malignant glioma. *J Clin Oncol,* 23**,** 7178-7187.

QUINN, J. A., JIANG, S. X., REARDON, D. A., DESJARDINS, A., VREDENBURGH, J. J., RICH, J. N., GURURANGAN, S., FRIEDMAN, A. H., BIGNER, D. D. & SAMPSON, J. H. 2009. Phase II trial of temozolomide plus o6-benzylguanine in adults with recurrent, temozolomide-resistant malignant glioma. *Journal of clinical oncology,* 27**,** 1262-1267.

RAZUMOVSKAYA, E., SUN, J. & RÖNNSTRAND, L. 2011. Inhibition of MEK5 by BIX02188 induces apoptosis in cells expressing the oncogenic mutant FLT3-ITD. *Biochemical and biophysical research communications,* 412**,** 307-312.

REGAN, C. P., LI, W., BOUCHER, D. M., SPATZ, S., SU, M. S. & KUIDA, K. 2002. Erk5 null mice display multiple extraembryonic vascular and embryonic cardiovascular defects. *Proceedings of the National Academy of Sciences,* 99**,** 9248-9253.

REIFENBERGER, G., WIRSCHING, H.-G., KNOBBE-THOMSEN, C. B. & WELLER, M. 2017. Advances in the molecular genetics of gliomas—implications for classification and therapy. *Nature Reviews Clinical Oncology,* 14**,** 434.

REITMAN, Z. J. & YAN, H. 2010. Isocitrate dehydrogenase 1 and 2 mutations in cancer: alterations at a crossroads of cellular metabolism. *Journal of the National Cancer Institute,* 102**,** 932-941.

RICH, J. N. & BAO, S. 2007. Chemotherapy and cancer stem cells. *Cell stem cell,* 1**,** 353-355.

ROBERTS, O. L., HOLMES, K., MÜLLER, J., CROSS, D. A. & CROSS, M. J. 2010. ERK5 is required for VEGF-mediated survival and tubular morphogenesis of primary human microvascular endothelial cells. *Journal of cell science***,** jcs. 072801.

ROIDL, A., BERGER, H.-J., KUMAR, S., BANGE, J., KNYAZEV, P. & ULLRICH, A. 2009. Resistance to chemotherapy is associated with fibroblast growth factor receptor 4 up-regulation. *Clinical Cancer Research,* 15**,** 2058-2066.

RONSON, G. E., PIBERGER, A. L., HIGGS, M. R., OLSEN, A. L., STEWART, G. S., MCHUGH, P. J., PETERMANN, E. & LAKIN, N. D. 2018. PARP1 and PARP2 stabilise replication forks at base excision repair intermediates through Fbh1-dependent Rad51 regulation. *Nature communications,* 9**,** 746.

ROSKOSKI JR., R. 2003. STI-571: an anticancer protein-tyrosine kinase inhibitor. *Biochemical and biophysical research communications,* 309**,** 709-717.

ROSKOSKI JR., R. 2018. *FDA-approved protein kinase inhibitors* [Online]. Available: http://www.brimr.org/PKI/PKIs.htm [Accessed].

ROUSE, J. & JACKSON, S. P. 2002. Interfaces between the detection, signaling, and repair of DNA damage. *Science,* 297**,** 547-51.

ROVIDA, E., DI MAIRA, G., TUSA, I., CANNITO, S., PATERNOSTRO, C., NAVARI, N., VIVOLI, E., DENG, X., GRAY, N. S. & ESPARÍS-OGANDO, A. 2015. The mitogen-activated protein kinase ERK5 regulates the development and growth of hepatocellular carcinoma. *Gut,* 64**,** 1454-1465.

ROZEN, E. J., ROEWENSTRUNK, J., BARALLOBRE, M. J., DI VONA, C., JUNG, C., FIGUEIREDO, A. F., LUNA, J., FILLAT, C., ARBONÉS, M. L. & GRAUPERA, M. 2018. DYRK1A kinase positively regulates angiogenic responses in endothelial cells. *Cell reports,* 23**,** 1867-1878.

RU, Q., TIAN, X., WU, Y.-X., WU, R.-H., PI, M.-S. & LI, C.-Y. 2014. Voltage-gated and ATP-sensitive K+ channels are associated with cell proliferation and tumorigenesis of human glioma. *Oncology reports,* 31**,** 842-848.

SAMANTA, A. K., HUANG, H. J., BAST, R. C. & LIAO, W. S.-L. 2004. Overexpression of MEKK3 confers resistance to apoptosis through activation of NFκB. *Journal of Biological Chemistry,* 279**,** 7576-7583.

SARKARIA, J. N., KITANGE, G. J., JAMES, C. D., PLUMMER, R., CALVERT, H., WELLER, M. & WICK, W. 2008. Mechanisms of chemoresistance to alkylating agents in malignant glioma. *Clinical Cancer Research,* 14**,** 2900-2908.

SASAKI, M., KNOBBE, C. B., ITSUMI, M., ELIA, A. J., HARRIS, I. S., CHIO, I. I. C., CAIRNS, R. A., MCCRACKEN, S., WAKEHAM, A. & HAIGHT, J. 2012. D-2-hydroxyglutarate produced by mutant IDH1 perturbs collagen maturation and basement membrane function. *Genes & development,* 26**,** 2038-2049.

SAWEY, E. T., CHANRION, M., CAI, C., WU, G., ZHANG, J., ZENDER, L., ZHAO, A., BUSUTTIL, R. W., YEE, H. & STEIN, L. 2011. Identification of a therapeutic strategy targeting amplified FGF19 in liver cancer by Oncogenomic screening. *Cancer cell,* 19**,** 347-358.

SCHABEL, J. F. 1976. Nitrosoureas: a review of experimental antitumor activity. *Cancer treatment reports,* 60**,** 665-698.

SCHULTZ, L. B., CHEHAB, N. H., MALIKZAY, A. & HALAZONETIS, T. D. 2000. p53 binding protein 1 (53BP1) is an early participant in the cellular response to DNA double-strand breaks. *The Journal of cell biology,* 151**,** 1381-1390.

SETO, K. K. & ANDRULIS, I. L. 2015. Atypical protein kinase C zeta: potential player in cell survival and cell migration of ovarian cancer. *PloS one,* 10**,** e0123528.

SHA, J., HAN, Q., CHI, C., ZHU, Y., PAN, J., DONG, B., HUANG, Y., XIA, W. & XUE, W. 2018. PRKAR2B promotes prostate cancer metastasis by activating Wnt/β-catenin and inducing epithelial-mesenchymal transition. *Journal of cellular biochemistry*.

SHELTON, P. M., DURAN, A., NAKANISHI, Y., REINA-CAMPOS, M., KASASHIMA, H., LLADO, V., MA, L., CAMPOS, A., GARCÍA-OLMO, D. & GARCÍA-ARRANZ, M. 2018. The Secretion of miR-200s by a PKCζ/ADAR2 Signaling Axis Promotes Liver Metastasis in Colorectal Cancer. *Cell reports,* 23**,** 1178-1191.

SIDNEY, L. E., BRANCH, M. J., DUNPHY, S. E., DUA, H. S. & HOPKINSON, A. 2014. Concise review: evidence for CD34 as a common marker for diverse progenitors. *Stem cells,* 32**,** 1380-1389.

SIEGAL, T., RUBINSTEIN, R., BOKSTEIN, F., SCHWARTZ, A., LOSSOS, A., SHALOM, E., CHISIN, R. & GOMORI, J. M. 2000. In vivo assessment of the window of barrier opening after osmotic blood-brain barrier disruption in humans. *Journal of neurosurgery,* 92**,** 599-605.

SIMÕES, A., PEREIRA, D., GOMES, S., BRITO, H., CARVALHO, T., FRENCH, A., CASTRO, R., STEER, C., THIBODEAU, S. & RODRIGUES, C. 2015. Aberrant MEK5/ERK5 signalling contributes to human colon cancer progression via NF-κB activation. *Cell death & disease,* 6**,** e1718.

SIMÕES, A. E., RODRIGUES, C. M. & BORRALHO, P. M. 2016. The MEK5/ERK5 signalling pathway in cancer: a promising novel therapeutic target. *Drug discovery today,* 21**,** 1654-1663.

SINGH, D., CHAN, J. M., ZOPPOLI, P., NIOLA, F., SULLIVAN, R., CASTANO, A., LIU, E. M., REICHEL, J., PORRATI, P. & PELLEGATTA, S. 2012. Transforming fusions of FGFR and TACC genes in human glioblastoma. *Science,* 337**,** 1231-1235.

SINGH, J., SHARMA, K. & PILLAI, P. P. 2018. PDGFR inhibition mediated intracellular signalling in C6 glioma growth and migration: role of ERK and ROCK pathway. *Cytotechnology,* 70**,** 465-477.

SINGH, S. K., CLARKE, I. D., TERASAKI, M., BONN, V. E., HAWKINS, C., SQUIRE, J. & DIRKS, P. B. 2003. Identification of a cancer stem cell in human brain tumors. *Cancer research,* 63**,** 5821-5828.

SINGH, S. K., HAWKINS, C., CLARKE, I. D., SQUIRE, J. A., BAYANI, J., HIDE, T., HENKELMAN, R. M., CUSIMANO, M. D. & DIRKS, P. B. 2004. Identification of human brain tumour initiating cells. *nature,* 432**,** 396.

SITOOLSBIOTECHGMBH. 2018. *siTOOLS Biotech ™* [Online]. Available: https://www.sitoolsbiotech.com/ [Accessed 19/09/2018 2018].

SLEEMAN, M., FRASER, J., MCDONALD, M., YUAN, S., WHITE, D., GRANDISON, P., KUMBLE, K., WATSON, J. D. & MURISON, J. G. 2001. Identification of a new fibroblast growth factor receptor, FGFR5. *Gene,* 271**,** 171-182.

SLEIRE, L., FØRDE-TISLEVOLL, H. E., NETLAND, I. A., LEISS, L., SKEIE, B. S. & ENGER, P. Ø. 2017. Drug repurposing in cancer. *Pharmacological research,* 124**,** 74-91.

SOHN, S. J., SARVIS, B. K., CADO, D. & WINOTO, A. 2002. ERK5 MAPK regulates embryonic angiogenesis and acts as a hypoxia-sensitive repressor of vascular endothelial growth factor expression. *Journal of Biological Chemistry,* 277**,** 43344-43351.

SONG, H., JIN, X. & LIN, J. 2004. Stat3 upregulates MEK5 expression in human breast cancer cells. *Oncogene,* 23**,** 8301.

SOTTORIVA, A., SPITERI, I., PICCIRILLO, S. G., TOULOUMIS, A., COLLINS, V. P., MARIONI, J. C., CURTIS, C., WATTS, C. & TAVARÉ, S. 2013. Intratumor heterogeneity in human glioblastoma reflects cancer evolutionary dynamics. *Proceedings of the National Academy of Sciences,* 110**,** 4009-4014.

STANLIE, A., YOUSIF, A. S., AKIYAMA, H., HONJO, T. & BEGUM, N. A. 2014. Chromatin reader Brd4 functions in Ig class switching as a repair complex adaptor of nonhomologous end-joining. *Molecular cell,* 55**,** 97-110.

STEIN, G. H. 1979. T98G: an anchorage-independent human tumor cell line that exhibits stationary phase G1 arrest in vitro. *Journal of cellular physiology,* 99**,** 43-54.

STENNING, S. P., FREEDMAN, L. S. & BLEEHEN, N. M. 1987. An overview of published results from randomized studies of nitrosoureas in primary high grade malignant glioma. *BRIT J CANCER,* 56**,** 89-90.

STICHEL, D., EBRAHIMI, A., REUSS, D., SCHRIMPF, D., ONO, T., SHIRAHATA, M., REIFENBERGER, G., WELLER, M., HÄNGGI, D. & WICK, W. 2018. Distribution of EGFR amplification, combined chromosome 7 gain and chromosome 10 loss, and TERT promoter mutation in brain tumors and their potential for the reclassification of IDHwt astrocytoma to glioblastoma. *Acta neuropathologica***,** 1-11.

STRATTON, M. R., CAMPBELL, P. J. & FUTREAL, P. A. 2009. The cancer genome. *Nature,* 458**,** 719.

STRITZELBERGER, J., DISTEL, L., BUSLEI, R., FIETKAU, R. & PUTZ, F. 2018. Acquired temozolomide resistance in human glioblastoma cell line U251 is caused by mismatch repair deficiency and can be overcome by lomustine. *Clinical and Translational Oncology,* 20**,** 508-516.

STUPP, R., HEGI, M. E., GORLIA, T., ERRIDGE, S. C., PERRY, J., HONG, Y.-K., ALDAPE, K. D., LHERMITTE, B., PIETSCH, T. & GRUJICIC, D. 2014. Cilengitide combined with standard treatment for patients with newly diagnosed glioblastoma with methylated MGMT promoter (CENTRIC EORTC 26071-22072 study): a multicentre, randomised, open-label, phase 3 trial. *The lancet oncology,* 15**,** 1100-1108.

STUPP, R., HEGI, M. E., MASON, W. P., VAN DEN BENT, M. J., TAPHOORN, M. J., JANZER, R. C., LUDWIN, S. K., ALLGEIER, A., FISHER, B. & BELANGER, K. 2009. Effects of radiotherapy with concomitant and adjuvant temozolomide versus radiotherapy alone on survival in glioblastoma in a randomised phase III study: 5-year analysis of the EORTC-NCIC trial. *The lancet oncology,* 10**,** 459-466.

STUPP, R., MASON, W. P., VAN DEN BENT, M. J., WELLER, M., FISHER, B., TAPHOORN, M. J. B., BELANGER, K., BRANDES, A. A., MAROSI, C., BOGDAHN, U., CURSCHMANN, J., JANZER, R. C., LUDWIN, S. K., GORLIA, T., ALLGEIER, A., LACOMBE, D., CAIRNCROSS, J. G., EISENHAUER, E. & MIRIMANOFF, R. O. 2005. Radiotherapy plus concomitant and adjuvant temozolomide for glioblastoma. *NEW ENGL J MED,* 352**,** 987-996.

STUPP, R., TAILLIBERT, S., KANNER, A., READ, W., STEINBERG, D. M., LHERMITTE, B., TOMS, S., IDBAIH, A., AHLUWALIA, M. S. & FINK, K. 2017. Effect of tumor-treating fields plus maintenance temozolomide vs maintenance temozolomide alone on survival in patients with glioblastoma: a randomized clinical trial. *Jama,* 318**,** 2306-2316.

SU, C., SUN, F., CUNNINGHAM, R. L., RYBALCHENKO, N. & SINGH, M. 2014. ERK5/KLF4 signaling as a common mediator of the neuroprotective effects of both nerve growth factor and hydrogen peroxide preconditioning. *Age,* 36**,** 9685.

SUN, Q., PEI, C., LI, Q., DONG, T., DONG, Y., XING, W., ZHOU, P., GONG, Y., ZHEN, Z. & GAO, Y. 2018. Up-regulation of MSH6 is associated with temozolomide resistance in human glioblastoma. *Biochemical and biophysical research communications,* 496**,** 1040-1046.

SUN, W., KESAVAN, K., SCHAEFER, B. C., GARRINGTON, T. P., WARE, M., JOHNSON, N. L., GELFAND, E. W. & JOHNSON, G. L. 2001. MEKK2 associates with the adapter protein Lad/RIBP and regulates the MEK5-BMK1/ERK5 pathway. *Journal of Biological Chemistry,* 276**,** 5093-5100.

SUREBAN, S. M., MAY, R., WEYGANT, N., QU, D., CHANDRAKESAN, P., BANNERMAN-MENSON, E., ALI, N., PANTAZIS, P., WESTPHALEN, C. B. & WANG, T. C. 2014. XMD8-92 inhibits pancreatic tumor xenograft growth via a DCLK1-dependent mechanism. *Cancer letters,* 351**,** 151-161.

SUWALA, A. K., KOCH, K., RIOS, D. H., ARETZ, P., UHLMANN, C., OGOREK, I., FELSBERG, J., REIFENBERGER, G., KÖHRER, K. & DEENEN, R. 2018. Inhibition of Wnt/beta-catenin signaling downregulates expression of aldehyde dehydrogenase isoform 3A1 (ALDH3A1) to reduce resistance against temozolomide in glioblastoma in vitro. *Oncotarget,* 9**,** 22703.

SUZUKI, S., NAMIKI, J., SHIBATA, S., MASTUZAKI, Y. & OKANO, H. 2010. The neural stem/progenitor cell marker nestin is expressed in proliferative endothelial cells, but not in mature vasculature. *Journal of Histochemistry & Cytochemistry,* 58**,** 721-730.

SVILAR, D., DYAVAIAH, M., BROWN, A. R., TANG, J.-B., LI, J., MCDONALD, P. R., SHUN, T. Y., BRAGANZA, A., WANG, X.-H. & MANIAR, S. 2012. Alkylation sensitivity screens reveal a conserved cross-species functionome. *Molecular Cancer Research,* 10**,** 1580-1596.

SØRENSEN, C. S., HANSEN, L. T., DZIEGIELEWSKI, J., SYLJUÅSEN, R. G., LUNDIN, C., BARTEK, J. & HELLEDAY, T. 2005. The cell-cycle checkpoint kinase Chk1 is required for mammalian homologous recombination repair. *Nature cell biology,* 7**,** 195.

TAKAHASHI, J. A., FUKUMOTO, M., IGARASHI, K., ODA, Y., KIKUCHI, H. & HATANAKA, M. 1992. Correlation of basic fibroblast growth factor expression levels with the degree of malignancy and vascularity in human gliomas. *Journal of neurosurgery,* 76**,** 792-798.

TANDLE, A. T., KRAMP, T., KIL, W. J., HALTHORE, A., GEHLHAUS, K., SHANKAVARAM, U., TOFILON, P. J., CAPLEN, N. J. & CAMPHAUSEN, K. 2013. Inhibition of polo-like kinase 1 in glioblastoma multiforme induces mitotic catastrophe and enhances radiosensitisation. *European journal of cancer,* 49**,** 3020-3028.

TAO, R., LI, Q., GAO, X. & MA, L. 2018. Overexpression of GRK6 associates with the progression and prognosis of colorectal carcinoma. *Oncology letters,* 15**,** 5879-5886.

TATAKE, R. J., O'NEILL, M. M., KENNEDY, C. A., WAYNE, A. L., JAKES, S., WU, D., KUGLER JR, S. Z., KASHEM, M. A., KAPLITA, P. & SNOW, R. J. 2008. Identification of pharmacological inhibitors of the MEK5/ERK5 pathway. *Biochemical and biophysical research communications,* 377**,** 120-125.

TAVERNA, P., LIU, L., HWANG, H.-S., HANSON, A. J., KINSELLA, T. J. & GERSON, S. L. 2001. Methoxyamine potentiates DNA single strand breaks and double strand breaks induced by temozolomide in colon cancer cells. *Mutation Research/DNA Repair,* 485**,** 269-281.

TAYLOR VI, J. G., CHEUK, A. T., TSANG, P. S., CHUNG, J.-Y., SONG, Y. K., DESAI, K., YU, Y., CHEN, Q.-R., SHAH, K. & YOUNGBLOOD, V. 2009. Identification of FGFR4-activating mutations in human rhabdomyosarcomas that promote metastasis in xenotransplanted models. *The Journal of clinical investigation,* 119**,** 3395-3407.

TEIXIDOR, P., ARRÁEZ, M. Á., VILLALBA, G., GARCIA, R., TARDÁGUILA, M., GONZÁLEZ, J. J., RIMBAU, J., VIDAL, X. & MONTANÉ, E. 2016. Safety and efficacy of 5-aminolevulinic acid for high grade glioma in usual clinical practice: a prospective cohort study. *PloS one,* 11**,** e0149244.

TESSER-GAMBA, F., PETRILLI, A. S., DE SEIXAS ALVES, M. T., GARCIA FILHO, R. J., JULIANO, Y. & TOLEDO, S. R. C. 2012. MAPK7 and MAP2K4 as prognostic markers in osteosarcoma. *Human pathology,* 43**,** 994-1002.

THAKER, N., ZHANG, F., MCDONALD, P. R., SHUN, T. Y., LEWEN, M. D., POLLACK, I. F. & LAZO, J. S. 2009. Identification of Survival Genes in Human Glioblastoma Cells Using siRNA Screening. *Molecular pharmacology***,** mol. 109.058024.

THE GENOMES PROJECT, C., AUTON, A., ABECASIS, G. R., ALTSHULER, D. M., DURBIN, R. M., BENTLEY, D. R., CHAKRAVARTI, A., CLARK, A. G., DONNELLY, P., EICHLER, E. E., FLICEK, P., GABRIEL, S. B., GIBBS, R. A., GREEN, E. D., HURLES, M. E., KNOPPERS, B. M., KORBEL, J. O., LANDER, E. S., LEE, C., LEHRACH, H., MARDIS, E. R., MARTH, G. T., MCVEAN, G. A., NICKERSON, D. A., SCHMIDT, J. P., SHERRY, S. T., WANG, J., WILSON, R. K., BOERWINKLE, E., DODDAPANENI, H., HAN, Y., KORCHINA, V., KOVAR, C., LEE, S., MUZNY, D., REID, J. G., ZHU, Y., CHANG, Y., FENG, Q., FANG, X., GUO, X., JIAN, M., JIANG, H., JIN, X., LAN, T., LI, G., LI, J., LI, Y., LIU, S., LIU, X., LU, Y., MA, X., TANG, M., WANG, B., WANG, G., WU, H., WU, R., XU, X., YIN, Y., ZHANG, D., ZHANG, W., ZHAO, J., ZHAO, M., ZHENG, X., GUPTA, N., GHARANI, N., TOJI, L. H., GERRY, N. P., RESCH, A. M., BARKER, J., CLARKE, L., GIL, L., HUNT, S. E., KELMAN, G., KULESHA, E., LEINONEN, R., MCLAREN, W. M., RADHAKRISHNAN, R., ROA, A., SMIRNOV, D., SMITH, R. E., STREETER, I., THORMANN, A., TONEVA, I., VAUGHAN, B., ZHENG-BRADLEY, X., GROCOCK, R., HUMPHRAY, S., JAMES, T., KINGSBURY, Z., SUDBRAK, R., ALBRECHT, M. W., AMSTISLAVSKIY, V. S., BORODINA, T. A., LIENHARD, M., MERTES, F., SULTAN, M., TIMMERMANN, B., YASPO, M.-L., FULTON, L., et al. 2015. A global reference for human genetic variation. *Nature,* 526**,** 68.

THEHUMANPROTEINATLAS. *The Human Protein Atlas* [Online]. Available: https://www.proteinatlas.org/ [Accessed 25/09/2018].

THERMOFISHERSCIENTIFIC. 2018. *Alexa Fluor® 488 Annexin V/Dead Cell Apoptosis Kit* [Online]. Available: https://www.thermofisher.com/uk/en/home/references/protocols/cell-and-tissue-analysis/flow-cytometry-protocol/apoptosis/alexa-fluor-488-annexin-v-dead-cell-apoptosis-kit.html#prot2 [Accessed 15/10/2018 2018].

THEROYALMARSDEN. 2017. *The UK's first MR Linac Scan* [Online]. Available: https://www.royalmarsden.nhs.uk/news-and-events/news/uks-first-mr-linac-scan [Accessed 20/11/2018].

THON, N., KRETH, S. & KRETH, F.-W. 2013. Personalized treatment strategies in glioblastoma: MGMT promoter methylation status. *Onco Targets Ther,* 6**,** 1363-1372.

TIONG, K. H., TAN, B. S., CHOO, H. L., CHUNG, F. F.-L., HII, L.-W., TAN, S. H., KHOR, N. T. W., WONG, S. F., SEE, S.-J. & TAN, Y.-F. 2016. Fibroblast growth factor receptor 4

(FGFR4) and fibroblast growth factor 19 (FGF19) autocrine enhance breast cancer cells survival. *Oncotarget,* 7**,** 57633.

TOMICIC, M. T., MEISE, R., AASLAND, D., BERTE, N., KITZINGER, R., KRÄMER, O. H., KAINA, B. & CHRISTMANN, M. 2015. Apoptosis induced by temozolomide and nimustine in glioblastoma cells is supported by JNK/c-Jun-mediated induction of the BH3-only protein BIM. *Oncotarget,* 6**,** 33755.

TRIVEDI, R. N., WANG, X.-H., JELEZCOVA, E., GOELLNER, E. M., TANG, J. & SOBOL, R. W. 2008. Human methyl purine DNA glycosylase and DNA polymerase β expression collectively predict sensitivity to temozolomide. *Molecular pharmacology*.

TSAI, Y.-F., HUANG, W.-C., CHO, S.-F., HSIAO, H.-H., LIU, Y.-C., LIN, S.-F., LIU, T.-C. & CHANG, C.-S. 2018. Side effects and medication adherence of tyrosine kinase inhibitors for patients with chronic myeloid leukemia in Taiwan. *Medicine,* 97.

TSIGELNY, I. F., KOUZNETSOVA, V. L., LIAN, N. & KESARI, S. 2016. Molecular mechanisms of OLIG2 transcription factor in brain cancer. *Oncotarget,* 7**,** 53074.

TURKINGTON, R., LONGLEY, D., ALLEN, W., STEVENSON, L., MCLAUGHLIN, K., DUNNE, P., BLAYNEY, J., SALTO-TELLEZ, M., VAN SCHAEYBROECK, S. & JOHNSTON, P. 2014. Fibroblast growth factor receptor 4 (FGFR4): a targetable regulator of drug resistance in colorectal cancer. *Cell death & disease,* 5**,** e1046.

TUSA, I., CHELONI, G., POTETI, M., GOZZINI, A., DESOUZA, N. H., SHAN, Y., DENG, X., GRAY, N. S., LI, S. & ROVIDA, E. 2018a. Targeting the Extracellular Signal-Regulated Kinase 5 Pathway to Suppress Human Chronic Myeloid Leukemia Stem Cells. *Stem cell reports*.

TUSA, I., GAGLIARDI, S., TUBITA, A., PANDOLFI, S., URSO, C., BORGOGNONI, L., WANG, J., DENG, X., GRAY, N. S. & STECCA, B. 2018b. ERK5 is activated by oncogenic BRAF and promotes melanoma growth. *Oncogene,* 37**,** 2601.

UMAPATHY, G., EL WAKIL, A., WITEK, B., CHESLER, L., DANIELSON, L., DENG, X., GRAY, N. S., JOHANSSON, M., KVARNBRINK, S. & RUUTH, K. 2014. The kinase ALK stimulates the kinase ERK5 to promote the expression of the oncogene MYCN in neuroblastoma. *Sci. Signal.,* 7**,** ra102-ra102.

VAN DEN BERG, R., VAN SOEST, P., WANG, Z., GROULS, R. & KORSTEN, H. 1995. The local anesthetic n-butyl-p-aminobenzoate selectively affects inactivation of fast sodium currents in cultured rat sensory neurons. *Anesthesiology: The Journal of the American Society of Anesthesiologists,* 82**,** 1463-1473.

VAN MEIR, E. G., KIKUCHI, T., TADA, M., LI, H., DISERENS, A.-C., WOJCIK, B. E., HUANG, H. S., FRIEDMANN, T., DE TRIBOLET, N. & CAVENEE, W. K. 1994. Analysis of the p53 gene and its expression in human glioblastoma cells. *Cancer Research,* 54**,** 649-652.

VAN TELLINGEN, O., YETKIN-ARIK, B., DE GOOIJER, M., WESSELING, P., WURDINGER, T. & DE VRIES, H. 2015. Overcoming the blood–brain tumor barrier for effective glioblastoma treatment. *Drug Resistance Updates,* 19**,** 1-12.

VARGHESE, R. T., LIANG, Y., GUAN, T., FRANCK, C. T., KELLY, D. F. & SHENG, Z. 2016. Survival kinase genes present prognostic significance in glioblastoma. *Oncotarget,* 7**,** 20140.

VENERANDO, A., GIRARDI, C., RUZZENE, M. & PINNA, L. A. 2013. Pyrvinium pamoate does not activate protein kinase CK1, but promotes Akt/PKB down-regulation and GSK3 activation. *Biochemical Journal,* 452**,** 131-137.

VERHAAK, R. G., HOADLEY, K. A., PURDOM, E., WANG, V., QI, Y., WILKERSON, M. D., MILLER, C. R., DING, L., GOLUB, T. & MESIROV, J. P. 2010. Integrated genomic analysis identifies clinically relevant subtypes of glioblastoma characterized by abnormalities in PDGFRA, IDH1, EGFR, and NF1. *Cancer cell,* 17**,** 98-110.

VILNER, B. J. & BOWEN, W. D. 1993. σ receptor-active neuroleptics are cytotoxic to C6 glioma cells in culture. *European Journal of Pharmacology: Molecular Pharmacology,* 244**,** 199-201.

VINJAMURI, M., ADUMALA, R. R., ALTAHA, R., HOBBS, G. R. & CROWELL, E. B. 2009. Comparative analysis of temozolomide (TMZ) versus 1,3-bis (2-chloroethyl)-1 nitrosourea (BCNU) in newly diagnosed glioblastoma multiforme (GBM) patients. *J NEURO-ONCOL,* 91**,** 221-225.

VO, V., LEE, J., LEE, H., CHUN, W., LIM, S. & KIM, S. 2014. Inhibition of JNK potentiates temozolomide-induced cytotoxicity in U87MG glioblastoma cells via suppression of Akt phosphorylation. *Anticancer research,* 34**,** 5509-5515.

WALKER, M. D., GREEN, S. B., BYAR, D. P., ALEXANDER JR, E., BATZDORF, U., BROOKS, W. H., HUNT, W. E., MACCARTY, C. S., MAHALEY JR, M. S. & MEALEY JR, J. 1980. Randomized comparisons of radiotherapy and nitrosoureas for the treatment of malignant glioma after surgery. *New England Journal of Medicine,* 303**,** 1323-1329.

WANG, J., ERAZO, T., FERGUSON, F. M., BUCKLEY, D. L., GOMEZ, N., MUÑOZ-GUARDIOLA, P., DIÉGUEZ-MARTÍNEZ, N., DENG, X., HAO, M. & MASSEFSKI, W. 2018a. Structural and atropisomeric factors governing the selectivity of pyrimido-benzodiazipinones as inhibitors of kinases and bromodomains. *ACS chemical biology,* 13**,** 2438-2448.

WANG, J., LEI, K. & HAN, F. 2018b. Tumor microenvironment: recent advances in various cancer treatments. *European review for medical and pharmacological sciences,* 22**,** 3855-3864.

WANG, X., GHAREEB, W. M., LU, X., HUANG, Y., HUANG, S. & CHI, P. 2018c. Coexpression network analysis linked H2AFJ to chemoradiation resistance in colorectal cancer. *Journal of cellular biochemistry*.

WANG, X. & TOURNIER, C. 2006. Regulation of cellular functions by the ERK5 signalling pathway. *Cellular signalling,* 18**,** 753-760.

WANG, Y., GAO, S., WANG, W. & LIANG, J. 2016. Temozolomide inhibits cellular growth and motility via targeting ERK signaling in glioma C6 cells. *Molecular medicine reports,* 14**,** 5732-5738.

WEINSTEIN, M., XU, X., OHYAMA, K. & DENG, C.-X. 1998. FGFR-3 and FGFR-4 function cooperatively to direct alveogenesis in the murine lung. *Development,* 125**,** 3615-3623.

WEISS, W. A., TAYLOR, S. S. & SHOKAT, K. M. 2007. Recognizing and exploiting differences between RNAi and small-molecule inhibitors. *Nature chemical biology,* 3**,** 739.

WELLER, M., WICK, W., ALDAPE, K., BRADA, M., BERGER, M., PFISTER, S. M., NISHIKAWA, R., ROSENTHAL, M., WEN, P. Y. & STUPP, R. 2015. Glioma. *Nature reviews Disease primers,* 1**,** 15017.

WICK, W., FRICKE, H., JUNGE, K., KOBYAKOV, G., MARTENS, T., HEESE, O., WIESTLER, B., SCHLIESSER, M. G., VON DEIMLING, A. & PICHLER, J. 2014. A phase II, randomized, study of weekly APG101+ reirradiation versus reirradiation in progressive glioblastoma. *Clinical Cancer Research*.

WICKSTRÖM, M., DYBERG, C., MILOSEVIC, J., EINVIK, C., CALERO, R., SVEINBJÖRNSSON, B., SANDÉN, E., DARABI, A., SIESJÖ, P. & KOOL, M. 2015. Wnt/β-catenin pathway regulates MGMT gene expression in cancer and inhibition of Wnt signalling prevents chemoresistance. *Nature communications,* 6**,** 8904.

WILSON, J., YAMAMOTO, K., MARRIOTT, A., HUSSAIN, S., SUNG, P., HOATLIN, M., MATHEW, C., TAKATA, M., THOMPSON, L. & KUPFER, G. 2008. FANCG promotes formation of a newly identified protein complex containing BRCA2, FANCD2 and XRCC3. *Oncogene,* 27**,** 3641.

WINKELMAN, D., BECK, C., YPEY, D. & O'LEARY, M. 2005. Inhibition of the A-type K+ channels of dorsal root ganglion neurons by the long-duration anesthetic butamben. *Journal of Pharmacology and Experimental Therapeutics,* 314**,** 1177-1186.

WONDERGEM, R., ECAY, T. W., MAHIEU, F., OWSIANIK, G. & NILIUS, B. 2008. HGF/SF and menthol increase human glioblastoma cell calcium and migration. *Biochemical and biophysical research communications,* 372**,** 210-215.

WORLDHEALTHORGANISATION. 2018a. *Cancer* [Online]. Available: https://www.who.int/news-room/fact-sheets/detail/cancer [Accessed 05/03/2019].

WORLDHEALTHORGANISATION. 2018b. *The Top 10 Causes of Death* [Online]. Available: http://www.who.int/news-room/fact-sheets/detail/the-top-10-causes-of-death [Accessed 12/11/2018].

WU, A.-L., COULTER, S., LIDDLE, C., WONG, A., EASTHAM-ANDERSON, J., FRENCH, D. M., PETERSON, A. S. & SONODA, J. 2011. FGF19 regulates cell proliferation, glucose and bile acid metabolism via FGFR4-dependent and independent pathways. *PloS one,* 6**,** e17868.

XIE, C., SHENG, H., ZHANG, N., LI, S., WEI, X. & ZHENG, X. 2016. Association of MSH6 mutation with glioma susceptibility, drug resistance and progression. *Molecular and clinical oncology,* 5**,** 236-240.

XU, J., ZHANG, Y., GUO, X. & SUN, T. 2018a. Glycogenolysis in Acquired Glioma Resistance to Temozolomide: A Role for the [Ca2+] i-dependent Activation of Na, K-ATPase/ERK1/2 Signaling. *Frontiers in pharmacology,* 9**,** 873.

XU, L., ZHANG, L., HU, C., LIANG, S., FEI, X., YAN, N., ZHANG, Y. & ZHANG, F. 2016. WNT pathway inhibitor pyrvinium pamoate inhibits the self-renewal and metastasis of breast cancer stem cells. *International journal of oncology,* 48**,** 1175-1186.

XU, L.-Q., TAN, S.-B., HUANG, S., DING, H.-Y., LI, W.-G., ZHANG, Y., LI, S.-Q. & WANG, T. 2017. G protein-coupled receptor kinase 6 is overexpressed in glioma and promotes glioma cell proliferation. *Oncotarget,* 8**,** 54227.

XU, P., ZHANG, G., HOU, S. & SHA, L.-G. 2018b. MAPK8 mediates resistance to temozolomide and apoptosis of glioblastoma cells through MAPK signaling pathway. *Biomedicine & Pharmacotherapy,* 106**,** 1419-1427.

YAM, C., FUNG, T. & POON, R. 2002. Cyclin A in cell cycle control and cancer. *Cellular and Molecular Life Sciences CMLS,* 59**,** 1317-1326.

YAN, H., YANG, K., XIAO, H., ZOU, Y. J., ZHANG, W. B. & LIU, H. Y. 2012. Over-Expression of Cofilin-1 and Phosphoglycerate Kinase 1 in Astrocytomas Involved in Pathogenesis of Radioresistance. *CNS neuroscience & therapeutics,* 18**,** 729-736.

YAN, L., CARR, J., ASHBY, P. R., MURRY-TAIT, V., THOMPSON, C. & ARTHUR, J. S. C. 2003. Knockout of ERK5 causes multiple defects in placental and embryonic development. *BMC developmental biology,* 3**,** 11.

YANG, C.-C., ORNATSKY, O. I., MCDERMOTT, J. C., CRUZ, T. F. & PRODY, C. A. 1998. Interaction of myocyte enhancer factor 2 (MEF2) with a mitogen-activated protein kinase, ERK5/BMK1. *Nucleic acids research,* 26**,** 4771-4777.

YANG, J., FAN, J., LI, Y., LI, F., CHEN, P., FAN, Y., XIA, X. & WONG, S. T. 2013a. Genome-wide RNAi screening identifies genes inhibiting the migration of glioblastoma cells. *PloS one,* 8**,** e61915.

YANG, J., LIN, Y., GUO, Z., CHENG, J., HUANG, J., DENG, L., LIAO, W., CHEN, Z., LIU, Z.-G. & SU, B. 2001. The essential role of MEKK3 in TNF-induced NF-κB activation. *Nature immunology,* 2**,** 620.

YANG, Q., DENG, X., LU, B., CAMERON, M., FEARNS, C., PATRICELLI, M. P., YATES III, J. R., GRAY, N. S. & LEE, J.-D. 2010. Pharmacological inhibition of BMK1 suppresses tumor growth through promyelocytic leukemia protein. *Cancer cell,* 18**,** 258-267.

YANG, Q., LIAO, L., DENG, X., CHEN, R., GRAY, N., YATES III, J. & LEE, J. 2013b. BMK1 is involved in the regulation of p53 through disrupting the PML–MDM2 interaction. *Oncogene,* 32**,** 3156.

YAO, S., ZHONG, L., LIU, J., FENG, J., BIAN, T., ZHANG, Q., CHEN, J., LV, X., CHEN, J. & LIU, Y. 2016. Prognostic value of decreased GRK6 expression in lung adenocarcinoma. *Journal of cancer research and clinical oncology,* 142**,** 2541-2549.

YOU, J., LI, Q., WU, C., KIM, J., OTTINGER, M. & HOWLEY, P. M. 2009. Regulation of aurora B expression by the bromodomain protein Brd4. *Molecular and cellular biology,* 29**,** 5094-5103.

ZEPPERNICK, F., AHMADI, R., CAMPOS, B., DICTUS, C., HELMKE, B. M., BECKER, N., LICHTER, P., UNTERBERG, A., RADLWIMMER, B. & HEROLD-MENDE, C. C. 2008. Stem cell marker CD133 affects clinical outcome in glioma patients. *Clinical Cancer Research,* 14**,** 123-129.

ZHANG, J., DULAK, A. M., HATTERSLEY, M. M., WILLIS, B. S., NIKKILÄ, J., WANG, A., LAU, A., REIMER, C., ZINDA, M. & FAWELL, S. E. 2018a. BRD4 facilitates replication stress-induced DNA damage response. *Oncogene***,** 1.

ZHANG, J., SU, G., TANG, Z., WANG, L., FU, W., ZHAO, S., BA, Y., BAI, B., YUE, P. & LIN, Y. 2018b. Curcumol Exerts Anticancer Effect in Cholangiocarcinoma Cells via Down-Regulating CDKL3. *Frontiers in physiology,* 9**,** 234.

ZHANG, J., WU, G., MILLER, C. P., TATEVOSSIAN, R. G., DALTON, J. D., TANG, B., ORISME, W., PUNCHIHEWA, C., PARKER, M. & QADDOUMI, I. 2013. Whole-genome sequencing identifies genetic alterations in pediatric low-grade gliomas. *Nature genetics,* 45**,** 602.

ZHANG, W.-B., WANG, Z., SHU, F., JIN, Y.-H., LIU, H.-Y., WANG, Q.-J. & YANG, Y. 2010. Activation of AMP-activated protein kinase by temozolomide contributes to apoptosis in glioblastoma cells via p53 activation and mTORC1 inhibition. *Journal of biological chemistry,* 285**,** 40461-40471.

ZHANG, Y., CRUICKSHANKS, N., YUAN, F., WANG, B., PAHUSKI, M., WULFKUHLE, J., GALLAGHER, I., KOEPPEL, A. F., HATEF, S. & PAPANICOLAS, C. 2017. Targetable T-type calcium channels drive glioblastoma. *Cancer research*.

ZHANG, Y., YU, G., CHU, H., WANG, X., XIONG, L., CAI, G., LIU, R., GAO, H., TAO, B. & LI, W. 2018c. Macrophage-Associated PGK1 Phosphorylation Promotes Aerobic Glycolysis and Tumorigenesis. *Molecular cell,* 71**,** 201-215. e7.

ZHANG, Y., ZHANG, J., JIANG, D., ZHANG, D., QIAN, Z., LIU, C. & TAO, J. 2012. Inhibition of T-type Ca2+ channels by endostatin attenuates human glioblastoma cell proliferation and migration. *British journal of pharmacology,* 166**,** 1247-1260.

ZHOU, J., ATSINA, K.-B., HIMES, B. T., STROHBEHN, G. W. & SALTZMAN, W. M. 2012. Novel delivery strategies for glioblastoma. *Cancer journal (Sudbury, Mass.),* 18.

ZHU, Y. & PARADA, L. F. 2002. The molecular and genetic basis of neurological tumours. *Nature Reviews Cancer,* 2**,** 616.

ZIEVE, G. W., TURNBULL, D., MULLINS, J. M. & MCINTOSH, J. R. 1980. Production of large numbers of mitotic mammalian cells by use of the reversible microtubule inhibitor Nocodazole: Nocodazole accumulated mitotic cells. *Experimental cell research,* 126**,** 397-405.